

STRUCTURAL SAFETY OF CRACKED CONCRETE DAMS

REPORT 2019:623



Structural Safety of Cracked Concrete Dams

ERIK NORDSTRÖM
MANOUCHEHR HASSANZADEH
RICHARD MALM
TOMAS EKSTRÖM
MÅRTEN JANZ

ISBN 978-91-7673-623-4 | © Energiforsk October 2019

Energiforsk AB | Phone: 08-677 25 30 | E-mail: kontakt@energiforsk.se | www.energiforsk.se

Foreword

The question regarding how state assessments of cracked concrete structures should be performed has since long been very interesting for the Dam Safety R&D program at Energiforsk. This report builds upon the project “Investigating the structural safety of cracked concrete dams” which was conducted by CEATI’s Dam Safety Interest Group (DSIG) in 2015, a project that the program proposed and supported.

This study aims to develop a Swedish guideline for assessing status as well as current and future security levels on a cracked concrete dam but can also function as a knowledge base for the area and contains several reference projects where the cause and effect of cracks have been studied. It is a comprehensive study conducted as a collaboration between SWECO and ÅF. Carl-Oscar Nilsson (Uniper), Mats Persson (Vattenfall) and Anders Sjödin (Statkraft) have participated in the reference group that followed the project.

The report was translated to English in 2019.

These are the results and conclusions of a project, which is part of the Dam Safety R&D program run by Energiforsk. The authors are responsible for the content.

Sammanfattning

Sprickor eller sprickbildning i betongdammar ger behov av att bestämma aktuellt tillstånd ur dammsäkerhetssynpunkt och en bedömning av kvarvarande livslängd med sprickbildningen i beaktande. Jämförelsen görs mellan rådande krav och aktuellt tillstånd i förhållande till dessa. Tillståndskontroll används för att ge svar på aktuellt tillstånd och framtida utveckling och då behövs kunskap om vilka typer av sprickor som uppstått och vad som orsakat dessa. Därför behövs en kombination av observationer, mätningar och teoretiska modeller/analyser. I ett tidigare projekt inom ramen för Dam Safety Interest Group (DSIG) skapades en justegsmetod för hantering av spruckna betongdammar [1] och föreliggande arbete bygger vidare på detta och gör nödvändiga anpassningar för svenska förhållanden.

Målsättningen har varit att utveckla en svensk riktlinje för att bedöma status och nuvarande, samt framtida, säkerhetsnivå för en sprucken betongdamm. Syfte har varit att skapa en enhetlig och tillförlitlig metodik för tillståndsbedömning av spruckna betongdammar samt en bra vägledning för planering av åtgärder.

Rapportens upplägg avspeglar en förvaltningsprocess med delarna KRAV-UNDERSÖKNINGAR-ANALYS -ÅTGÄRD och i rapporten exemplifierat med REFERENSPROJEKT som visar tillämpning av de rekommendationer som rapporten omfattar.

Rekommenderade krav för betongdammar återfinns generellt i kraftbranschens gemensamma vägledning RIDAS [3], [4], med fokus på täthet, stabilitet, bärförmåga och begränsade deformationer.

Undersökningar utförs lämpligen stegvis från en visuell inspektion till mer eller mindre detaljerade undersökningar med provtagning beroende på hur oklara förhållandena är för t.ex. de mekaniska egenskaperna, utbredning av sprickor, orsak till uppsprickning etc. Resultatet används ofta senare när analyser utförs och därför utförs de lämpligen i samråd med personen som utför analyserna i ett senare skede.

Analysen kan vara allt ifrån enkla tankemodeller via analytiska beräkningar till avancerade numeriska analyser. Syftet med dessa är att besvara hur väl dammen uppfyller ställda krav. Resultatet kan även användas för att föreslå ev. vidare undersökningar, instrumentering eller förstärkningsåtgärder.

Åtgärder utförs då avvikelser från ställda krav (nu eller i framtiden) inte kan accepteras. Ofta handlar det om att sänka lasten, bromsa utveckling eller att höja/återställa prestanda. Ibland väljs övervakning, t.ex. med planenliga inspektioner eller med fast instrumentering, som utvärderas för att följa ev. utveckling av sprickbildning istället för en fysisk åtgärd.

Referensprojekten som sammanställts visar att en vanlig orsak till kritiska sprickor ofta är säsongsmässiga temperaturvariationer. Värmeisolering av dammkroppen för att utjämna temperaturspanningar är där en effektiv åtgärd. Vid inomhusförhållanden kan uttorkningskrympning ge sprickbildning. I många fall var även konstruktionerna skadade av frost och/eller ASR. Generellt sett är det inte ovanligt med sprickbildning som har sitt ursprung från byggtiden och som inte utvecklas mer.

Summary

Cracks and cracking in concrete dams can give a need to determine the current status from a dam safety perspective and an estimation on remaining service-life taking the cracks in to consideration. A comparison between the current status and the formal requirements should be made. Condition control is a prerequisite to define the current status and future development and to do this there is a need for knowledge on what type of cracks has occurred and the reason for cracking. To do this there is a need to combine observations, sampling, measurements and theoretical models/ analysis. A previous project within Dam Safety Interest Group (DSIG) resulted in a seven- step-method to analyse cracked concrete dams [1] and the current work is taking this forward to adapt the methodology to Swedish conditions.

The goal has been to develop a Swedish guideline to define status and both current and future safety level for a cracked concrete dam with the purpose to create a uniform and reliable methodology for condition control and guidance for planning of measures.

The disposition of the report is based on a management process with the parts REQUIREMENTS-INVESTIGATIONS-ANALYSIS-MEASURES and in the report also with REFERENCE PROJECTS exemplifying the recommendations given in the report.

Recommended requirements for concrete dams can be found in the Swedish power industry guideline RIDAS [3], [4], with focus on water-tightness, stability, load-bearing capacity and limited deformations.

Investigations is best performed stepwise from a visual inspection to a more or less detailed investigation with sampling depending on how unclear the conditions are regarding mechanical properties, crack extent, reason for cracks etc. The results are commonly used later when analysis is performed and therefore it is preferred to plan them in cooperation with the person that will do the analysis later.

Analysis can be anything from simple behavior models via analytical calculations to advanced numerical simulations. The purpose with the analysis is to investigate if the dam fulfills the requirements. The results can also be used to suggest further investigations, monitoring or strengthening measures.

Measures are taken when the deviation from the requirements are not acceptable (now or in the future). It is often a matter of reducing the load, slow down the development or increase/restore the performance. Surveillance with planned inspections, or monitoring, can be used for evaluating any crack propagation and is sometimes selected instead of a physical measure.

The compilation of reference projects shows that a common reason for critical cracks often origins from movement due to seasonal temperature variations. Insulation of the dam body to minimize the impact from this is effective. Indoors also cracking from shrinkage is common. Many of the cases have the cause for cracking and damages from frost or ASR. Generally, it is also common with cracks from the time of construction that will not develop further.

List of content

1	Introduction	10
1.1	Background	10
1.2	Purpose and Objectives	10
1.3	Implementation of Project	10
1.4	Disposition of the Report	12
1.5	Requirements for Load-Bearing and Non-Load-Bearing Parts	13
2	Investigations	15
2.1	Visual inspection	15
2.1.1	Definition and purpose	15
2.1.2	Preparation and planning	17
2.1.3	Implementation	19
2.1.4	Evaluation	32
2.1.5	Reporting	33
2.2	In-depth inspection and condition assessment	36
2.2.1	Definition and purpose	36
2.2.2	Preparation and planning	37
2.2.3	Implementation	37
2.2.4	Evaluation	49
2.2.5	Reporting	50
2.3	Measurements, methods and instruments	52
2.3.1	Temperature and moisture	52
2.3.2	Cracks and crack widths	55
2.3.3	Frost damage	56
2.3.4	ASR damage	60
2.3.5	Leaching	70
2.3.6	Components damaged by corrosion	75
2.3.7	Evaluation of core samples and boreholes	80
2.4	Specimens, sampling methods, laboratory methods	84
2.4.1	Sampling through core drilling	84
2.4.2	Density and porosity	85
2.4.3	Moisture, moisture content and degree of saturation	85
2.4.4	Chloride content in concrete	85
2.4.5	Determination of carbonation depth	85
2.4.6	Leaching	85
2.4.7	Strength	85
2.4.8	Elastic modulus	86
2.4.9	Concrete shrinkage	86
2.5	Underwater inspection, diving inspection, ROV	86
2.5.1	Diving inspections	86

2.5.2	ROV inspections	87
3	Analysis	89
3.1	Introduction	89
3.2	Methods of analysis	89
3.2.1	Conceptual model	89
3.2.2	Analytical calculations	89
3.2.3	Finite element calculations	91
3.2.4	Non-linear finite element calculations	92
3.2.5	Other types of calculation methods	94
3.3	Choice of method of analysis	95
3.4	Simulation of different phenomena	97
3.4.1	New concrete	98
3.4.2	Long term effects	98
3.4.3	Cracking, crushing	99
3.4.4	Degradation	99
3.4.5	Seasonal variation in temperature	103
3.4.6	Reinforcement measures	105
3.4.7	Stability failure	105
3.4.8	Potential failure modes (PFMA)	107
3.5	Modelling aspects	108
3.5.1	Material models	108
3.5.2	Delimitations	112
3.5.3	Boundary conditions, interactions and contact conditions	113
3.5.4	Loads	114
3.5.5	Crack propagation vs. existing cracks/damages	115
3.5.6	Safety format and non-linear analyses	117
3.6	Material Data	119
3.6.1	Uncertainty in material data	119
3.7	Validation of calculation model	125
3.7.1	Validation of material model	125
3.7.2	Validation of structural model	126
3.7.3	Validation of convergence of results and equilibrium	127
3.7.4	Validation with simpler analyses	127
3.7.5	Validation against measurements	128
3.8	Methodology for evaluation of the impact of cracking	130
3.9	Acceptance Criteria	133
4	Measures	137
4.1	Introduction	137
4.2	Emergency measures	137
4.3	Monitoring Development	139
4.3.1	Prerequisites	139
4.3.2	Strategy for systematic design of a monitoring system	139

4.3.3	Selection of equipment	140
4.3.4	Optimisation and installation	144
4.4	Mitigating measures	146
4.4.1	Surface protection measures	146
4.4.2	Climate protection	147
4.5	Repair	147
5	Reference projects	160
5.1	Introduction	160
5.2	Summary	164
5.3	Spillway dam 1 (Temp/gate loading)	166
5.3.1	Brief description of plant	166
5.3.2	Assessment of stability and the load capacity of the gate shafts	166
5.4	Spillway dam 2 (Concrete Lifts/temp)	168
5.4.1	Brief description of plant	168
5.4.2	Assessment of the stability of the spillway	169
5.5	Spillway dam 3 (ASR/frost/temp)	170
5.5.1	Brief description of plant	170
5.5.2	Assessment of stability of the middle pier of the spillway	171
5.6	Power house 1 (Drying/temperature)	172
5.6.1	Brief description of plant	172
5.6.2	Assessment of widened joints and cracks in the station	173
5.7	Arch dam 1 (Frost/temp/ice load)	177
5.7.1	Brief description of plant	177
5.7.2	Assessment of arch	178
5.8	Spillway dam 4 (ASR/frost/temperature)	183
5.8.1	Brief description of plant	183
5.8.2	Assessment of floodgate	184
5.9	Buttress dam 1 (Temp)	186
5.9.1	Brief description of plant	186
5.9.2	Assessment of stability	186
5.10	Spillway dam 5 (Temp)	190
5.10.1	Brief description of facility	190
5.10.2	Assessment of stability	190
5.11	Spillway dam 6 (Temp)	195
5.11.1	Brief description of plant	195
5.11.2	Assessment	195
5.12	Buttress dam 2 (Temp)	200
5.12.1	Brief description of plant	200
5.12.2	Assessment	201
5.13	Arch dam 2 (Temp)	211
5.13.1	Brief description of plant	211
5.13.2	Assessment	211

5.14	Buttress dam (temperature)	212
5.14.1	Brief description of plant	212
5.14.2	Assessments	214
5.15	Discussion	221
5.15.1	Conclusion of discussion	230
APPENDIX A – TEMPERATURE AND MOISTURE MEASUREMENT		238
	Temperature measurement – Choice of sensor	238
	Moisture measurement	239
	Background theory	239
	Types of sensors and measuring principle	240
	References	241
APPENDIX B – FROST DEGRADATION		242
	Central terms and parameters	242
	The mode of action of frost attacks	243
APPENDIX C – ALKALI-SILICA REACTIONS		244
	Mechanism	244
	Expansion and cracking	246
	References	248
APPENDIX D – SPILLWAY DAM 2 (CONCRETE LAYERS/TEMP)		249
	Description of structure	249
	Assessment	249
	Calculating pore water pressure	250
	Calculation of temperatures in the dam:	251
	Calculation of mechanical stresses:	252
	Calculations:	254
	Conclusions:	257
APPENDIX E – BUTTRESS DAM 2 (IN-DEPTH)		258
	Description of dam	258
	Assessment	259
APPENDIX F – NON-LINEAR MATERIAL MODELS USED IN THE REFERENCE PROJECTS		279
	Concrete	279
	Reinforcement	282
	Plastic material models for concrete	283
	References:	290

1 Introduction

1.1 BACKGROUND

Many Swedish concrete dams have significant cracks or extensive crack formations where the condition and remaining service life need to be determined. In order to assess the condition of a cracked concrete structure, knowledge of which types of cracks have arisen and what caused them is needed. To obtain this basic information, extensive investigations are often required. The observed cracks may have been caused by many things, but may also be a result of several interacting effects where a mechanism causes crack initiation e.g. when the concrete is new, and as the structure ages another degradation mechanism dominates instead. It can also be that observed damages occur due to several mechanisms acting simultaneously, where the extent of the combined effects far exceeds the sum of the individual degradation mechanisms.

It is therefore essential to combine observations, measurements and theoretical models/analyses in the condition assessment of cracked concrete structures in order to be able to make predictions about the future status of the structure. In a previous project within the framework of the Dam Safety Interest Group (DSIG), a seven step method was created for handling cracked concrete dams [1]. The present work is based on this method and makes necessary adjustments for Swedish conditions and commonly occurring dam types.

1.2 PURPOSE AND OBJECTIVES

In the present project, the aim has been to develop a Swedish guideline for assessing the status as well as present and future safety level of a cracked concrete dam.

The purpose has been to create a uniform and reliable methodology for the condition assessment of cracked concrete dams. This, in turn, in order to provide dam owners and other professionals within the hydropower industry with a better basis for evaluation and prioritisation of possible measures of enhancement and maintenance of aging concrete plants.

1.3 IMPLEMENTATION OF PROJECT

The work has been carried out by a project group manned jointly by SWECO and ÅF with funding from Energiforsk's dam safety program. The project group has consisted of:

Manouchehr Hassanzadeh, SWECO (project manager)
Erik Nordström, SWECO
Richard Malm, SWECO
Tomas Ekström, ÅF
Mårten Janz, ÅF

The work in the project was divided into different themes which also reflect the disposition of the report. It is based on a management process that is commonly

used for existing plant structures. See Figure 1-1 from [2], which presents a process that starts with requirements on the plant or the structural part and this is dealt with briefly in section 1.5 below.

In order to assess whether the requirements are met, INVESTIGATIONS and ANALYSES must be carried out so that the current status can be assessed in relation to the requirements set. It is dealt with in the respective sections described below.

Investigations - describes reliable methods for conducting inspections, field measurements, and laboratory investigations. This also includes e.g. which indicators to look for, type of equipment, examination methods, types of test samples and how these should be taken out from the structure etc. The section "Investigations" constitutes chapter 2 of the report.

Analysis - defines methods useful for determining the cause and structural impact of cracks on concrete dams (including their impact over time). This also includes giving recommendations on situations where analytical methods are sufficient and when it is justified to apply more advanced numerical methods. This section also presents simpler methods that for instance can be used for quick verification or validation. The section "Analysis" constitutes chapter 3 of the report.

If, through investigations and analyses, it is found that the requirements set are not met, then MEASURES must be taken.

Measures - provides a review of methods for risk reduction (temporary and permanent measures), methods for assessing the impact that existing cracks have on dam safety and how these affect the stability over time. In addition, strategies for developing monitoring programs for cracked concrete dams are included. In addition to this, the section also includes strategies for how a systematic approach can be applied for instrumentation on larger plants based on potential failure modes (PFMA). The section "Measures" constitutes chapter 4 of the report.

Reference projects - reproduces the work process/methodology in some selected reference projects from observation of damage to reinforcement, instrumentation/monitoring etc. Chapter 5 presents a number of projects that exemplify the methodologies and work procedures described in chapters 2-4.

Guidelines - constitutes coordination and editorial work in joining the results from all themes to a uniform guideline. Has no chapter of its own in the report, but partly forms chapter 1 and is then woven into the other chapters.

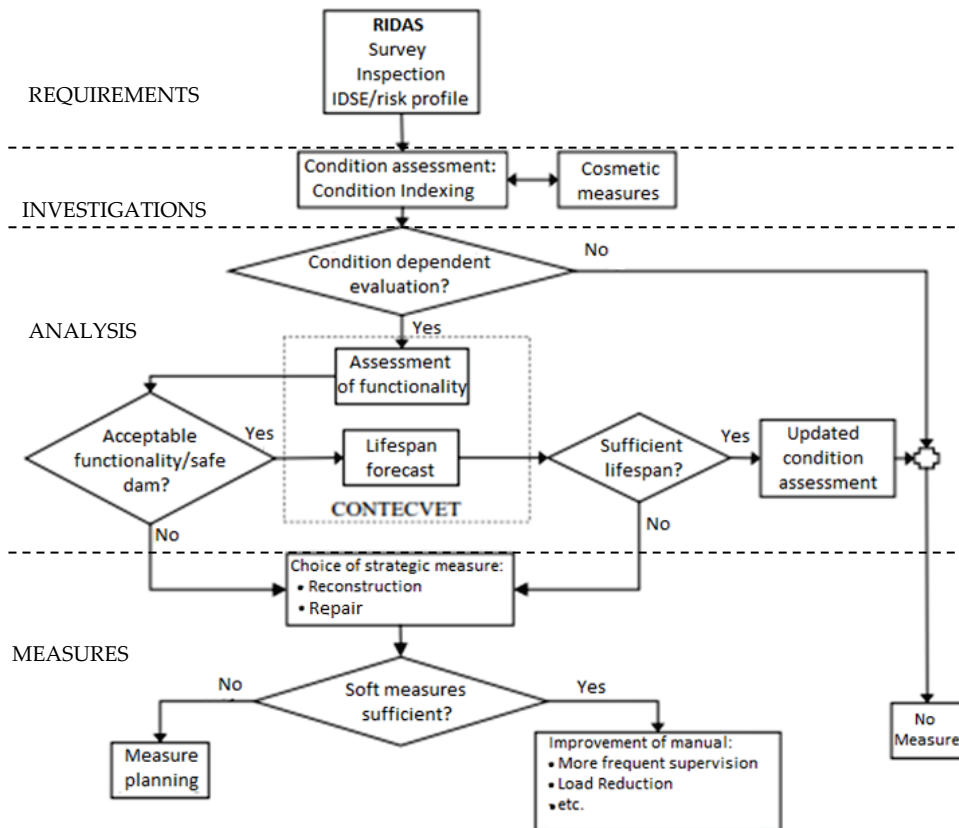


Figure 1-1 – Workflow according to management system based on [2].

1.4 DISPOSITION OF THE REPORT

The theme areas for the work presented in the previous section are reflected each in separate chapters. Several sections contain in-depth material found in the appendices.

In the previously implemented DSIG project [1], a seven step method was defined for handling cracked concrete dams. The seven step method connects to the present report and the current chapter as follows:

1. **Detection of cracks** - Chapter 2 provides a methodology for inspection and condition assessment of dam structures with respect to cracks. Different types of cracks are described on the basis of their configuration, location on the structure, underlying cause, time for initiation and propagation in relation to the age of the structure, and their current and future impact on the load-bearing capacity and durability of the structure. Suitable testing and analysis methods for determining the cause of crack and their impact on the structure are provided.
2. **Crack mapping** - Chapters 2 and 3 points out the importance of systematic crack mapping and theoretical analyses being combined for a safe assessment of the current and future impact of the cracks on the structure, as well as the selection of suitable and durable repair methods (chapter 4).

3. **Dam type and construction methods** - Causes of cracking is often connected to dam type and design (boundary conditions, loads and exposure environment), construction methods (inherent and initial stresses, cracks that are formed during the construction period). The real practical cases e.g. a new/old dam, a repaired dam structure etc., constitute valuable knowledge and experience which is presented in chapter 5. Examples of common and extensive cracking in Swedish dams are given here. The entire chain from the discovery of the crack, condition assessment (cause and impact), proposals for measures, measures taken and follow-up are presented. The chapter summarizes the links between the previous chapters 2, 3 and 4.
4. **Definition of cause of cracking and risk for propagation/increased extent** - The report presents methods for defining cracking, risk of propagation and increased extent. Chapters 2 and 3 provide the practical and theoretical tools, while chapter 5 outlines experiences from the practical and integrated approaches.
5. Comparison with similar practical cases - See points 3 and 4 above.
6. **Failure mode analysis** - Chapter 3 provides the theoretical analysis methods if connection to dam safety is considered to exist. It also lists the parameters that are necessary for the analyses. Chapter 2 describes methods of measurement for determining the current values of the parameters and their future development.
7. **Handling of cracking** - measures, assessment, monitoring and/or observing any changes. Chapter 4 presents measures for the monitoring of cracks, as well as measures to remedy negative impact on the stability and durability of the structure.

The methodology points to all important elements in the analysis of cracks and their importance for concrete structures and concrete dams. The present work provides an in-depth study in the sections *investigation* of cracks and their causes, *analysis* of the importance of cracks and suitable measures to solve potential problems that have arisen or are likely to arise due to cracking.

1.5 REQUIREMENTS FOR LOAD-BEARING AND NON-LOAD-BEARING PARTS

According to the Swedish Dam Safety Guidelines, RIDAS [3] and [4], the following general requirements for dam safety apply:

The prerequisites for a high level dam safety are to design and construct the plants with suitable safety margins, operate and maintain these in a safe manner as well as maintaining a preparedness to handle emerging situations.

The general requirements of dam and power plant owners for hydraulic concrete structures are somewhat more concrete than for dams, it should be ensured that the structures provide the possibility of safely retaining and discharging water. If an examined part has a function linked to hydropower production, the highest possible accessibility for uninterrupted electricity production is also usually desirable. More specifically regarding the technical requirements for concrete that can be compromised due to cracking is that the structure must be:

- Water tight against prevailing water pressure
- Have acceptable stability and act monolithically.
- Meet requirements for load-bearing capacity and stiffness.

The requirements apply both at the moment the check-up is performed, but usually also for a long time to come.

2 Investigations

Generally in RIDAS [3] & [4] it is stated about condition control that:

"The purpose of the dam owner's condition control is to continuously monitor and check the current status of a dam in relation to its original status or functional requirements and any changes in laws and guidelines."

Furthermore, RIDAS [3] & [4] recommends that changes or deviations from the above should be:

"... carry out suitable analyses on how the change can affect the dam safety irrespective of the type of condition control during which the change is noted. The purpose of these analyses is that the dam owner must obtain a basis for what measures should be taken from a dam safety point of view. These dam safety analyses can also be used to find the weak spots of the dam and provide a basis for increasing the dam safety in relation to its original level. "

The following sections present methods for identifying cracking and possible in depth investigations to further study deficiencies and determine their cause and possible potential development.

2.1 VISUAL INSPECTION

2.1.1 Definition and purpose

Within the Swedish Transport Administration's management system, there are four types of inspection with different purposes, scope and time intervals [5].

1. **Overview inspection** aims at verifying that the requirements set in the maintenance contracts are fulfilled. The inspection refers to the structural parts and elements for which requirements for properties and measures have been set. Inspections are performed by a maintenance contractor at least once a year.
2. **General inspection** aims to follow up the assessments of damages that have not been remedied, as well as detecting and assessing damages that would could have given unsatisfactory load-bearing capacity or road safety, in connection with the previous main inspection. All structural elements except elements under water are inspected. Visual inspection methods can be used. The inspections are then carried out as required, in order to follow up the deficiencies found at the main inspection.
3. **Main inspection** aims at detecting and assessing deficiencies that can affect the function or traffic safety of the structure within a ten-year period. The purpose is also to detect deficiencies, which, if not remedied within the time period, can lead to increased management costs. All elements in the structure are inspected. Visual inspection methods that provide the same accuracy as a hand-held inspection can be used. Inspections should be carried out with a maximum interval of six years.
4. **Special inspection** is done when required, in order to investigate or follow up the shortcomings identified or assumed at the regular inspections. The purpose

may be to do some specific measurement, carry out an underwater inspection, a follow-up of damages, etc. The inspection relates to a single element of the structure. The timing is determined at regular inspections.

Main inspections and special inspections are in turn divided into sub-variants. These should be used to specify, if necessary, the type of inspection that is intended. The above division is reproduced here as indicated in [5]. The Swedish Transport Administration is currently reviewing the division and definitions.

By definition, the above list covers the recommendations in RIDAS [3], [4], according to the introduction, and in the case of concrete structures, the following types of condition checks are specified in RIDAS [3], [4]:

1. Operational assessment (continuous condition control)
2. Dam measurements
3. Functional testing
4. Inspection (twice a year)
5. In-depth inspection (normally every three years)
6. In-depth dam safety evaluation (with the longest interval being 9 - 18 years)

In the case of concrete structures, the Swedish Transport Administration's objectives generally coincide with the objectives stated by RIDAS within *Operational Assessment, Inspection, In-depth Inspection and in-depth dam safety evaluation (IDSE)*. New concepts will be introduced in the next version of RIDAS [3], [4], which is planned to be issued in 2019, but in the present report the current concepts are being used.

The technical content of performing the various inspections can be roughly divided into the following groups:

- I. Only observations, notes, photography and protocols
- II. Single measurements of dimensions, relative distance, crack width, temperature, humidity, etc.
- III. Single samples such as core samples, leakage water samples, determination of carbonation depth, etc.
- IV. Systematic sampling including simplified theoretical evaluation
- V. Systematic sampling including advanced theoretical evaluation

Combining the above list with the different types of inspections/condition assessments can be complicated and time consuming. Therefore, in this section, the following simplification is chosen:

- Type of inspection
- Visual inspection is performed in order to
 - × discover changes and damages as well as carrying out a preliminary technical assessment of their impact on the load-bearing capacity, stability and service life of the structure.
 - × confirm whether previous remarks have been remedied.

- × verify whether the measures implemented meet the prescribed requirements and fulfill their function.
- Detailed inspection is the continuation of the visual inspection, which includes far-reaching and advanced investigations with field-wise/laboratory work as well as theoretical content. Both in-depth inspections and IDSE may contain detailed inspection.
- Technical content
 - × Observations, single measurements and sampling (combination of points I - III above) - combined with Visual inspection
 - × Systematic sampling including theoretical evaluation (combination of points I - III above) - combined with Detailed inspection

A visual inspection is performed with simple aids and without any major impact on the concrete structure to be inspected. The purpose is to detect damages and changes. It can also include checking the outcome and the effect of the measures implemented. By damage the following things are referred to:

- Discolouration
- Cracking
- Splitting
- Delamination
- Corrosion
- Relative movements and settlements
- Leakage

Early detection of damages through visual inspection sometimes also provides an opportunity to put in mitigating measures to mitigate the consequences of damage that has occurred. It is often cheaper to make an alleviating measure at an early stage instead of allowing the damage to grow and to perform a more comprehensive measure.

2.1.2 Preparation and planning

In order to obtain useful results, the inspection should be carefully planned. The performer should form an idea of the structure prior to the field visit. The following should be prepared as far as possible. The description below is general and not fully adapted to just dam structures but also applies to other types of structures:

Previous inspection reports

Previous reports on inspections, condition assessments and repairs should be collected and studied. A list of the structures or structural parts that have been annotated, treated or repaired should be established. The work is greatly facilitated if these are marked on drawings.

Drawings and other documents

The drawings and other documents of the structure should be brought out if available. The following list, which is based on *section 1.4.2* of BBK04 [6], gives

advice on the details that as far as possible, and where applicable, should be taken into account. E.g. by providing information about:

- rules applied to the design during the time of construction as well as information on safety classes.
- load-bearing and non-load-bearing parts
- the functional requirements from the owner
- load conditions
- the concrete properties regarding
 - × strength class
 - × exposure class
 - × expected service life
 - × performance class
 - × composition, e.g. cement type, cement class and cement quantity, w/c ratio, air content, aggregate type and maximum aggregate size.
- the reinforcement regarding
 - × type
 - × strength properties
 - × relaxation properties of pre-stressed or post-tensioned reinforcement as well as any anchoring devices and other things that may be required in special cases
- design of concrete and detailed dimensions and locations for regular and pre-stressed reinforcement, joints, recesses and slots.
- reinforcement arrangement and placement
 - × number of bars
 - × dimension
 - × length
 - × height and position
 - × placement of any grouting and aeration tubes

Microclimate and associated exposure classes

Estimate with the help of Table 1 in SS-EN 206-2013 + A1: 2016 [7], the microclimate and exposure environment to which the structure and its parts are exposed. In the table, the exposure environment is categorized according to the risk of:

- corrosion from carbonation
- corrosion due to chlorides (not from seawater)
- corrosion due to chlorides from seawater
- freezing with or without the presence of de-icing salts
- chemical attacks

Access permit and accessibility

The person responsible for the structure must be contacted for obtaining an access permit. The responsible safety representative must also be contacted for any protective measures. HSE-regulations (Health, Safety & Environment) usually apply, which means that work certificates are sometimes required in order to carry

out inspections downstream of the spillway gates. A risk analysis is usually conducted to identify potential risks associated with the inspection.

Some structural parts can be difficult to access. Therefore, a list of the parts that are difficult to access should be established. The list should also contain suggestions on the equipment that is needed to access the structural part.

Tools and measuring equipment

The tools and measuring equipment that should be included depends on the purpose of the inspection and may vary between cases. Below some basic equipment is mentioned [5]. (Highlighted bold is the author's recommended minimum level)

- **Flashlight** and/or cord lamp
- **Camera, binoculars** and compass
- **Tape measure**, folding rule, caliper, **crack width gauge**
- Thermometer and humidity meter
- **Hammer**, sledge hammer, **chisel** and knife
- Equipment for locating the reinforcement and measuring the thickness of the covering concrete

2.1.3 Implementation

In addition to preparations according to the previous section, it is crucial that the inspector has the right attitude with a watchful and committed eye in the field. It is not uncommon for an inspector to get stuck in details and forget about putting the details in a context and looking at any large-scale impact of identified cracking. Below is a guide for interpretation of deviations of importance in the field.

Inspection of discolouration

The surface of the concrete can be discoloured for various reasons. Discolouration can itself be harmless, but it can from a persistence perspective be a sign of favorable conditions for different degradation processes.

Discolouration can be caused by:

- **Solution, transport and precipitation of salts** on the concrete surface. The precipitated salt affects the color of the surface.
 - × Lime (calcium hydroxide/portlandite), which is a product of the hydration of the cement, is dissolved in water, which transports it to the surface of the concrete. At the surface, the water evaporates and leaves the lime which causes a brightening (whiter shade) of the surface of the concrete. Later, the lime reacts with the carbon dioxide of the air and is converted to calcium carbonate (calcite, "limestone") which is white and insoluble in water. The calcium carbonate forms a lasting discolouration on the concrete surface. The process is slow and often involves easily soluble salts in the concrete. The water can also dissolve reinforcement corrosion and bring it to the surface. The same applies to easily soluble salts/products in the aggregate. If the watercourses and the rock that are in contact with the concrete easily soluble salts can also be transported. But it should be noted that some of the moisture transport (especially in thick structures) takes place via diffusion, which cannot carry salts. In the layers located near the surface, the moisture condenses again due to the cold, dissolves salts and transports them to the surface.
 - × Water flowing through cracks leaches the lime of the cement and transports it to the downstream side of the crack. The water flows off or drops on the downstream side of the concrete surface and in this way the dissolved limestone spreads. When the water evaporates, it leaves the lime, which hardens by reacting with the carbon dioxide of the air, forming calcium carbonate (calcite), which is white and insoluble in water. The calcium carbonate eventually seals the crack and impedes water flow. The water starts to drip from the crack. The process causes substances contained in the watercourse, the rock or within the concrete to be transported to the surface and accumulate when the water evaporates. Accumulation of the transported substances changes the color of the calcium carbonate. Corrosion products cause light to dark brown color. Bedrock that is in contact with the concrete structure can also affect the color. Red and yellow colors occur. Note the difference between structures with cracks and those that do not have cracks. The penetration is considerably more difficult in the latter case.
 - × Salts found in the surroundings of the concrete structure, e.g. in soil and rock can be sucked in through capillary forces and transported to the surface where evaporation of water takes place. In this way, salts accumulate on the surface of the concrete and can discolour the surface. However, the process requires leaking concrete and heavy evaporation of water from the concrete surface.
- **Minerals in aggregate reacting with the cement** that leads to spalling and discolouration. Alkali Silica Reactions (ASR) are one example. Another example is aggregate materials containing sulphides, which, through reactions with the cement, leads to the formation of iron oxide and sulfate ions. Iron oxides give the concrete surface a light to dark brown shade if they are transported to the surface of the concrete. The sulfate ions can form swelling reaction products that cracks the concrete and facilitate the iron oxide transport

to the surface. Sulfur pyrite, or iron disulfide (FeS_2), is a mineral that can occur in the aggregate. Pyrite is oxidized in the presence of moisture and oxygen and forms rust that discolour the concrete surface [8].

- **Corrosion products (on reinforcement bars)** can be dissolved in the water in the pores and transport to the surface. Rust formed on reinforcing bars can spall the concrete cover. It should be noted that in the case of slow corrosion processes, thick concrete covers and high moisture content, the corrosion products have enough time to dissolve in the water and be transported to the surface without cracking of the concrete cover. Corrosion of reinforcement before casting can also lead to discolouration. Reinforcements corrodes while waiting for mounting and casting. In some cases, traces of corroded reinforcement can be observed on the surface of the concrete. Rain can wash the rust and store it on the bottom of the mould, which can be observed after removal of formwork. Reinforcement for piers can discolour the previously cast concrete slab [8].
- **Metals (copper, zinc, etc.)** that are outside the concrete can corrode and discolour the surface of the concrete.
- **Biological growth (algae, fungi, bacteria, etc.)** discolours concrete surfaces. Soon after the hardening, the pH of the concrete surface is about 13, which is unfavourable for biological cultivation. When concrete is carbonated, the pH of the concrete surface decreases, which can facilitate biological growth [8]. However, this requires that the concrete surface is moist. The colour depends on the biological growth.

Inspection of cracks, splitting and delamination

When conducting a visual inspection of cracks, one should be able to distinguish between the following three categories of cracks:

- I. Cracks initiated **BEFORE** hardening, but they are revealed during or shortly after hardening.
- II. Cracks initiated **AFTER** hardening due to any chemical or physical process. The process governs the rate of the crack development and can act simultaneously with other degradation processes, see definition of non-mechanical load below in this section.
- III. Cracks initiated by **MECHANICAL LOADS** that exceed the load levels assumed for design, see the definition of mechanical load below in this section.

In the case of visual inspection, it may be difficult to recognize category III, since it is not normally possible to analyse load and load-bearing systems during the inspection. Such an analysis normally requires deeper studies of loads and drawings and perhaps calculations. This deficiency can be compensated for by experience and by ruling out certain options. Although it is not possible to account for the mechanisms which may have caused the cracks, the inspection can distinguish between structural cracks (originating from mechanical stress) and non-structural cracks (derived from influences other than mechanical stress). Pictures and sketches are good tools for recognizing non-structural cracks.

It is necessary to distinguish between "*structural cracks*" and "*non-structural cracks*". The term *structural* refers to the load bearing properties of the system, and refers to the cracks that have been caused by overload and directly affect the load-bearing capacity of the structure. The term *non-structural* concerns the properties of the system that are not related to load bearing. The cracks have not been caused by mechanical overload and do not directly affect the load-bearing capacity of the structure. Some types of non-structural cracks can in the long term affect the load bearing properties of the structure. E.g. cracking caused by internal frost attacks, ASR attacks and thermal mechanisms can be mentioned.

Figure 2-1 shows grouping of common mechanical and non-mechanical crack types. According to the figure, "*Types of cracks Before hardening*" corresponds to the Category I cracks mentioned above. "*Physical*", "*Chemical*" and "*Thermal*" are cracks that occur after hardening and are non-structural as shown in the figure, i.e. they correspond to Category II as described above. Structural cracks include cracks that are caused e.g. by accidental loads, creep and design loads. *Structural cracks* correspond to Category III above.

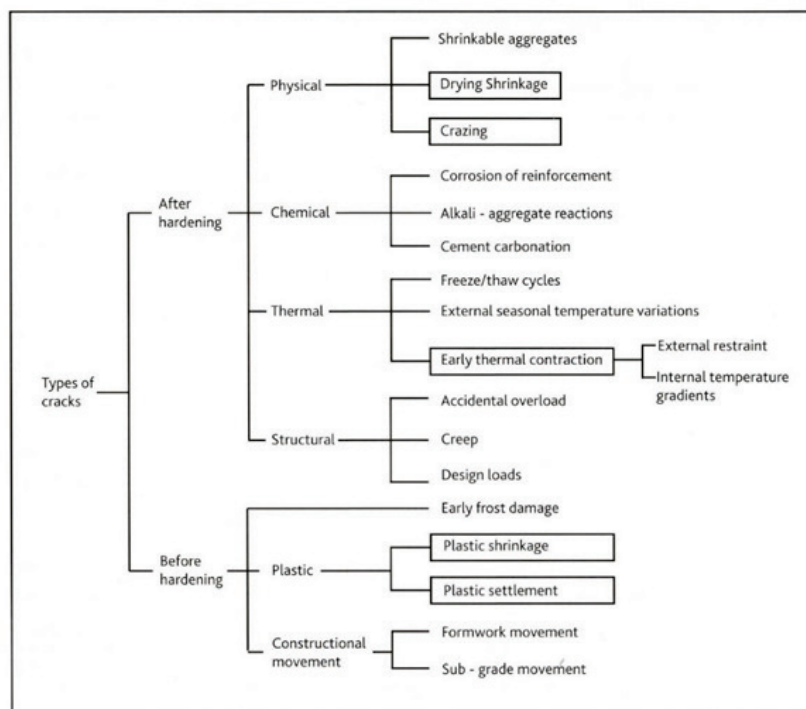


Figure 2-1 – Common types of cracks according to Concrete Society [9].

Figure 2-2 shows a summary of common causes of degradation according to SS-EN 1504-9: 2008 [10], which is largely reminiscent of the categorization presented by Concrete Society [9] for cracking after the hardening of the concrete.

Table 2-1 contains references to figures illustrating the crack types. Due to space limitations, this report does not present pictures/sketches for every single type of crack. For hydropower plants, however, reference is made to [11] and [12], where images are presented on different crack types.

Most degradation mechanisms presented in Figure 2-2 in addition to abrasion, biological impact, erosion and wear - sooner or later cause cracks in concrete structures. Certain mechanisms such as frost attacks and ASR can work in different ways and thus induce various types of degradation. Frost attacks can lead to internal frost attacks with great strength reduction and cracking. Frost attacks can also lead to peeling and erosion of the concrete surface if it occurs in the presence of de-icing salts or if it occurs at the water-line of hydraulic structures. ASR attacks can cause pop-outs, bursting of craters from the surface of the concrete, or causing expansion with subsequent crazing and cracking.

Aggressive substances such as sulphates convert the components of the hardened cement into less durable and expansive substances. The expansion can lead to cracking or a weak surface that easily erodes. Table 23.8:1 in the "Concrete Handbook – Materials" (*Swedish: "Betonghandbok – Material"*) [13] presents the effects that various chemical substances have on concrete. The table presents the substances that can cause expansion and cracking on concrete.

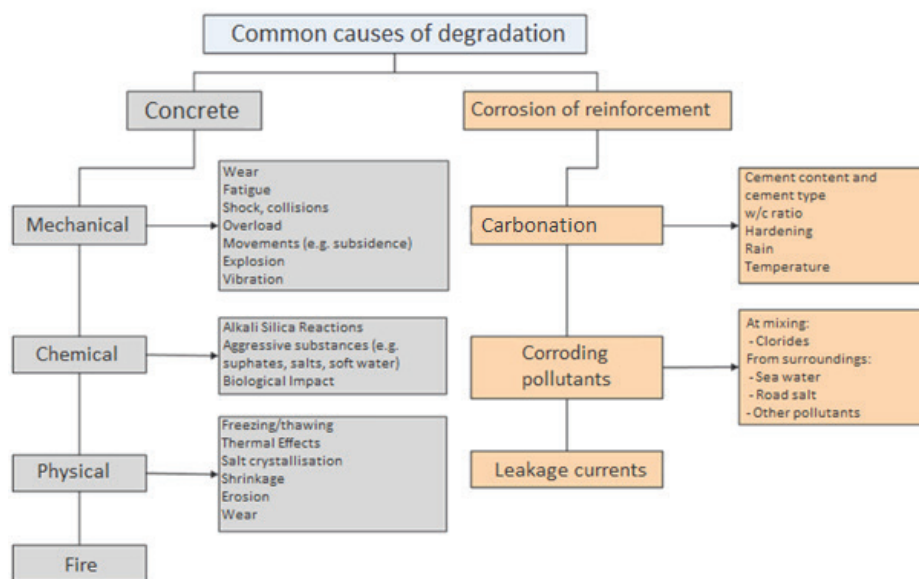


Figure 2-2 Common causes of degradation, (from SS-EN 1504-9:2008) [10].

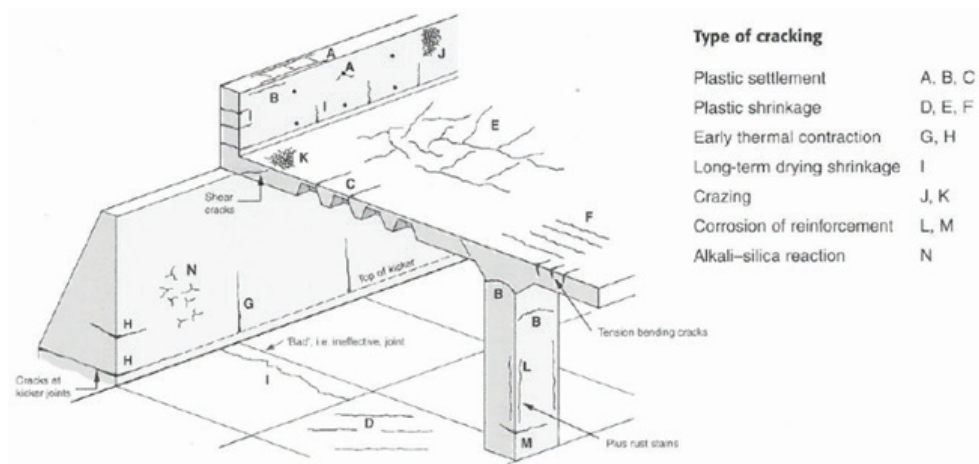


Figure 2-3 – Example of cracks and crack patterns in a hypothetical concrete structure [9].

Table 2-1 – Classification of cracks. In the table sources for figures illustrating each type of crack can be found. (Due to space limitations, this report does not present pictures / sketches for every single type of crack. For hydropower plants, see [11] [12] for more information)

Type of crack	Figure ref.	Sub category	Structural element	Main cause	Secondary cause	Time of occurrence
Plastic settlement crack	A – Fig. 2-3, 2-4	Over reinforcement	Deep sections	Water separation	Fast drying	Half an hour to a few hours
	B – Fig. 2-3, 2-4	Arching	Top of pier			
	C – Fig. 2-3, 2-4	Change in thickness	Hole- and waffle slab			
	Fig. 2-4	Settlement of mould	Arches	Bad staging structure		During moulding
Plastic shrinkage crack	D - Fig. 2-5	Diagonal	Walls and slabs	Fast drying at an early age	Slow water separation	Half an hour to a few hours
	E - Fig. 2-5	Irregular	Reinforced slabs			
	F - Fig. 2-5	Over reinforcement	Reinforced slabs	As above, incl. reinforcement close to surface		
Thermal cracking, early cooling after hardening of concrete	G - Fig. 2-7	Outer restraint, through-going crack	Thick walls	Heat development	Fast cooling	A few days up to three weeks
	H - Fig. 2-7	Inner restraint, surface crack	Thick slabs	Temperature gradient		
Thermal cracking, seasonal		Outer restraint, through-going crack	Walls and slabs	Temperature variations at the structure boundaries	Change in boundary conditions, section	Determined by external factors

Type of crack	Figure ref.	Sub category	Structural element	Main cause	Secondary cause	Time of occurrence
variation in temperature		Inner restraint, surface crack	Walls and slabs		changes etc.	
Shrinkage cracks (autogenous)		Outer restraint		Concrete with low w/c ratio		A few hours to a few days
		Inner restraint				
Shrinkage cracks (drying)	I		Thin slabs and walls	Insufficient relaxation	Large shrinkage	Several weeks
Shrinkage cracks (carbonation)			Structure surfaces	Carbonation of concrete		Several years
Crazing	J - Fig. 2-6	Against sheathing	Untreated cast concrete surface	Tight mould	High cement content. Bad curing	One day to a week, sometimes much later
		Steel glazed surface	Slab	Machine glazing	Drying	Days to months
Reinforcement corrosion	L	Carbonation and external chlorides	Reinforced concrete structures	Insufficiently concrete coating, carbonation, chloride penetration	Low quality concrete	More than two years
	M	Calcium chloride	Concrete element	Surplus of calcium chloride		
Alkali Silica Reactions	N	Inner expansion and crazing	Moist parts	Reactive aggregate plus cement with high alkali content		More than five years
		Pop-outs				
Sulfate attacks			Parts in contact with groundwater and soil	Increase in volume due to reaction between cement and sulfates	Cement non-resistant to sulfates	A few years
Frost-attacks		Inner expansion	Parts in contact with liquid water during freezing and thawing	Expansion due to hydraulic pressure in the concrete pore system	Lack of air pores	A few years
		Surface Peeling	As above as well as parts exposed to de-icing salts			

Type of crack	Figure ref.	Sub category	Structural element	Main cause	Secondary cause	Time of occurrence
Fire		Inner cracking		Temperature gradient, differentiated expansion of elements, steam pressure		In case of fire
		Surface crack				
		Movement cracks				
External load – Short term		Tensile crack	May occur in many structural elements	When the tensile force exceeds the tensile strength of the material		During time of use
		Bending crack				
		Shear crack				
		Torsion crack				
External load – Long term		Flexural	Occurs in structures that are subjected to creep and shrinkage	Creep and shrinkage		During time of use
Dynamic load		Fatigue	Can occur in many elements			During time of use
		Hits, impact and collision				
Forced deformation		Settlement in ground	Ground structures, slabs, walls and supporting structures	Changed load and stress concentrations		During time of use

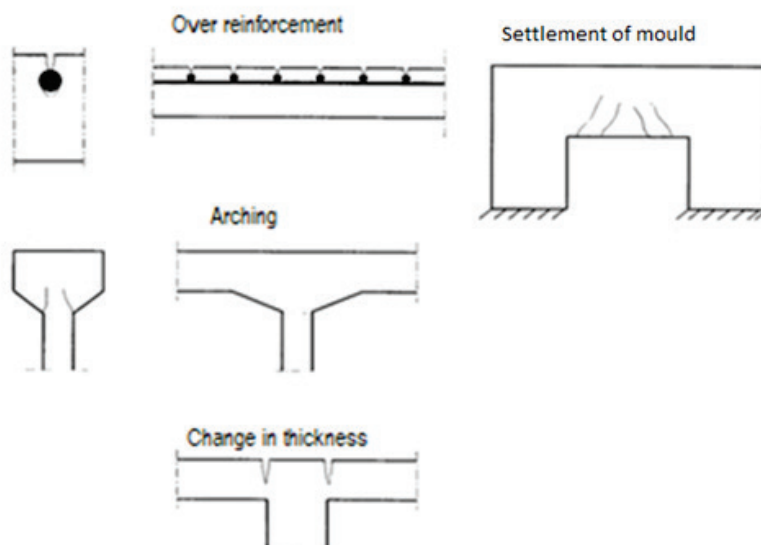


Figure 2-4 – Sketch of plastic cracking [14].

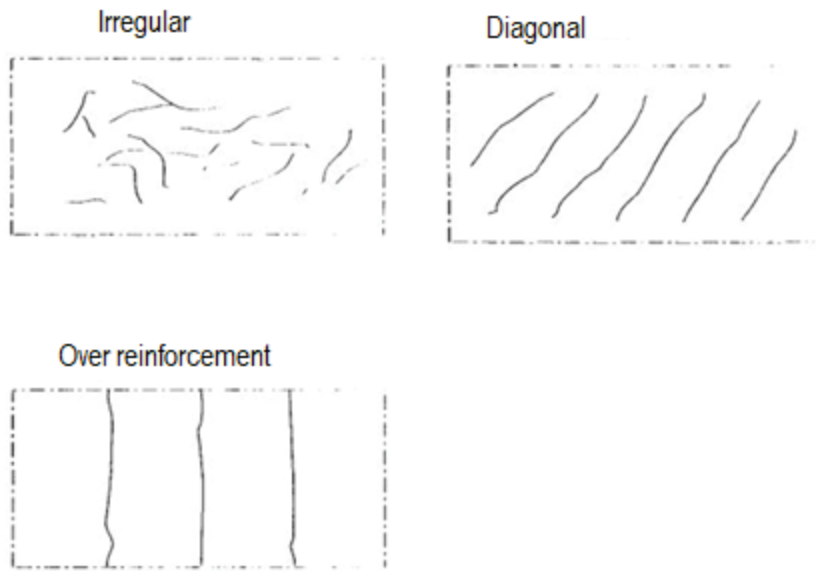


Figure 2-5 – Sketch of plastic shrinkage [14].

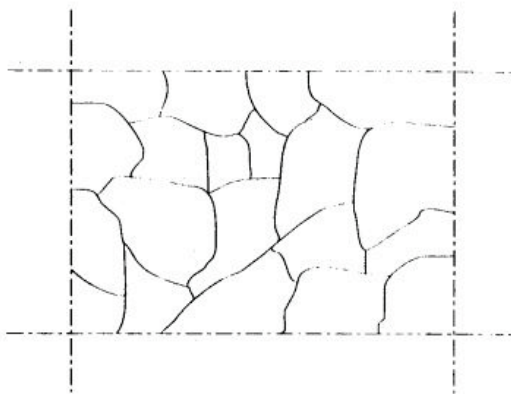


Figure 2-6 – Sketch of crazing caused by a tight mould or fast drying of a fresh concrete surface [14].

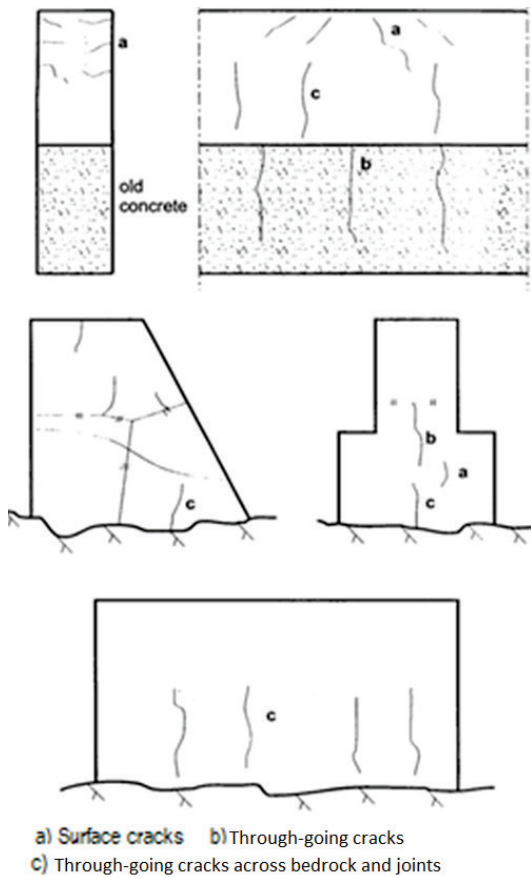
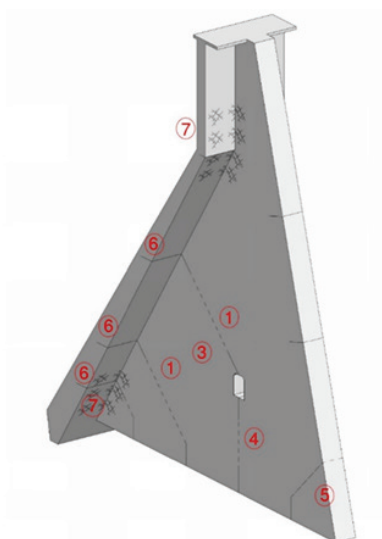


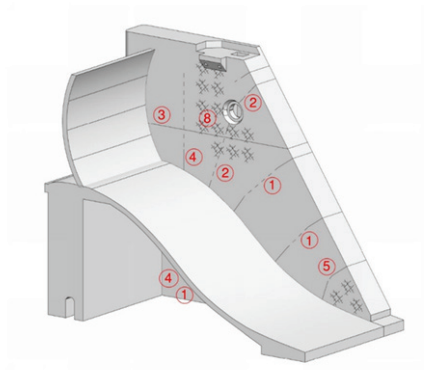
Figure 2-7 – Sketch of cracks caused by thermal stress [14].

Sketches of common cracks that occur in the concrete structures of hydropower are given in Figure 2-8 - Figure 2-10.



- 1) Oblique cracks in pier
- 2) Cracks along gates, see the next figure
- 3) Horizontal cracks in pier
- 4) Vertical cracks in pier
- 5) Oblique cracks in the downstream side of the pier
- 6) Horizontal cracks in the front slab
- 7) Frost damage and ice layers in the front slab
- 8) Frost damage/ASR around gates, see the next figure

Figure 2-8 – Typical cracks in a monolith in a buttress dam (type I), [11].



- 1) Oblique cracks in pier
- 2) Cracks around gate
- 3) Horizontal cracks in pier
- 4) Vertical cracks in pier
- 5) Oblique cracks in the downstream side of the pier
- 6) Horizontal cracks in the front slab, see the previous figure
- 7) Frost damage and ice layers in the front slab
- 8) Frost damage/ASR around gates
- 9) Frost damage/ASR in gear rack, see the next figure

Figure 2-9 – Typical cracks in a spillway pier (type II), [11].

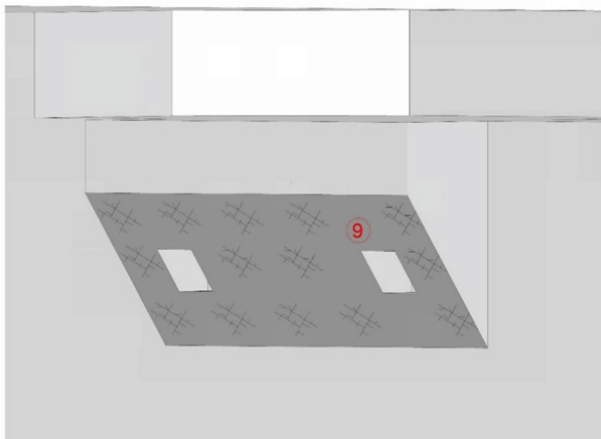


Figure 2-10 – Typical cracks in gate winch console (type III), [11].

Documentation of cracks

Documentation of cracks during visual inspection shall indicate the layout, main dimension (length, depth and width), location, orientation, etc. of the cracks. It is assumed that the inspector is familiar with the commonly occurring degradation processes that can cause cracking in the type of structure being inspected.

The visual inspection of cracks must not be confused with crack measurements performed for monitoring the stability or growth of cracks and for calibration and verification of calculation models since they are discovered and their causes are already known. In carrying out the visual inspections, the cause of damage is often unknown, which is why an in-depth mapping of the cracks can be a waste of time and resources. Furthermore, the crack widths are governed by the temperature and humidity of the structure which both change with the seasons. Visual inspection carried out at irregular intervals regarding season is not suitable for accurate mapping of the cracks but can be an aid for a systematic characterization and documentation of cracks.

Table 2-2 – Instruction for characterisation and documentation of cracks [1].

Applicable to a crack visible along the face of a non-reinforced concrete mass

Localization	Code	Comments
isolated in the concrete mass	I	
along a construction joint	J	
ending on a block side / joint	S	
ending at a block angle	A	

General shape	Units	Comments
developed length	m	
straight / curved shape	I, C, S	straight, curve one side, S-shape
maximum opening	mm	
opening variation	mmmm	indicates a virtual rotation center
orthotropy	%	in % from 0 (straight) to 100% (stepped)
small scale shape, amplitude	mm	first sinusoidal shape approximation
small scale shape, period	mm	second sinusoidal shape approximation
smoothness		use Barton models (<i>at right</i>)

Local shape parameters at each point	Units	Comments
opening	mm	
orientation / surface	°	not easily detected - 90° if perpendicular
orientation / vertical or reference	°	azimuth degrees
offset inside face	mm	provide orientation (clockwise / counter-CW)
offset perpendicular to face	mm	provide orientation (up out / up in)
depth	mm	possible only through interception borehole

Environment features	Units	Comments
oxydation		change in colour versus depth / distance
cuts or debonds aggregates		age of concrete when crack occurred
humidity / water flow		
infilling		ca lite, mud, ...

Development of hardware and software in the fields of photography and image processing has facilitated mapping of cracks in concrete structures, see Figure 2-11. Nowadays, with image processing of a photo, it is possible to identify cracks; determine their coordinates (location on the structure); measure the length, direction and width of the cracks and present them in the manner prescribed by the user. E.g. if desired, it can be stipulated that only cracks of a fixed length, width and orientation are presented. The characterizations that can be seen can be carried out with existing technology. It should be noted in this context that the costs of performing an advanced and automatic mapping can be high. The costs are governed by the processing and presentation required by the mapping results. Accuracy and precision are two parameters that can have a major impact on costs.

The following characteristics should be considered at least when you want to map cracks with advanced technology:

- The smallest crack width that you want to measure including the accuracy of the method of measurement.
- The smallest crack length you want to measure.
- Type of cracks that you want to measure.
- The orientations and dimensions (2D or 3D) that you want to measure, e.g. if a crack is to be presented on all sides of a buttress/support.

The above-mentioned properties give high demands on both the photography technique and the work method.

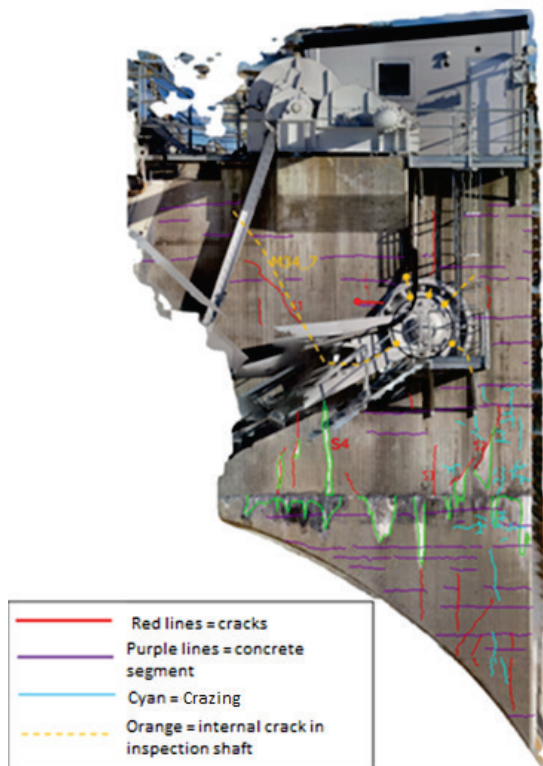


Figure 2-11 - Identified cracks on a spillway pier. About 500 photos were taken with drones about 1.5 m away from the pier side, after which they were put together into an "orthophoto", which was then lifted into a CAD program. The CAD program could be zoomed in so that cracks down to about 0.2 mm could be identified and marked out as shown in the figure. It was also seen that some crack was through to the inspection shaft in the pier and also to the other side.

Photography / scanning can be done as follows:

- Fixed camera that is moved manually
- Camera mounted on a frame that scans a surface
- Drone
- Laser Scanner

The accuracy/resolution of the camera is determined, apart from the price, by the way the photographing is performed. Fixed and one-frame cameras have better accuracy and resolution compared to the cameras mounted on a drone. A drone, on the other hand, has a better opportunity to get close to the subject in hard-to-reach parts of the structure. There is no need for scaffolding or use of a lift when the drone can reach all the structural parts.

The measuring objects (the reference points on a photographed surface) are localised either by total station measurement or by GPS. It should be noted that the GPS method is not easy to use in inspection galleries.

Inspection of relative movements and settlements

Relative movements and settlements are caused by the fact that the foundation or structure of the structural element is not stable and gets deformed. The movements can lead to cracks in the different parts of the structure. The cracks often occur in parts with stress concentrations, i.e. at corners and passages and places where there is a slight change in cross section. In a visual inspection, it can be difficult to determine if a crack is caused by relative movements and settlements, especially when the foundation cannot be inspected. It is therefore important to carefully map the cracks and draw them on the drawing surface, as they appear on the structure. In this way one can determine whether relative movements and settlements are the cause of the crack formation.

Inspection of leakage

Leakage in dam structures is a relatively common phenomenon. Leakage occurs in the following forms:

- i. Leakage through the foundation, water leaks in through the foundation into the inspection galleries of the dam structure.
- ii. Leakage in the interface between the foundation and the concrete structure.
- iii. Leakage in the interface between two structural elements of concrete or between two cast stages/cast sections.
- iv. Leakage through structure- and expansion joints.
- v. Leakage through cracks in a fully cast concrete structure.

All leakage types are important and should be noticed. In a visual inspection, it is important to note the location of the leakage in the structure and document it with clear photographs showing the position, size and details of the leakage. It is important to place a measuring stick next to the leakage when photographing. The time and date of the observation should be recorded in the photo and/or in the text of the report.

It is difficult to measure the amount of leakage during a visual inspection. However, one should estimate/describe the amount of leakage in some way. In the case of type v in the list above, it is important to be able to make a connection between the crack and some crack type(s) as previously described in this section. Furthermore, it is important to note whether the crack contains precipitations or not, and whether it is dry or moist.

2.1.4 Evaluation

The condition of the structure should be assessed on the basis of the requirements imposed on the structure and the damage observed. The inspection must lead to concrete results as follows:

1. No damage has been detected. Time for the next inspection. Inspection completed.

2. Minor damages have been discovered. Minor maintenance work must be performed. List of measures that need to be taken. Time for the next inspection. Inspection completed.
3. Comprehensive damage has been discovered. In-depth inspection /condition assessment is recommended.

The evaluation is carried out by the inspector.

When evaluating cracks, Table 2-3 can be used to assist in assessing the resulting damage. The table is prepared by RILEM TC 104 but is obtained from [8].

Table 2-3 – Exempel på klassificering av skador/sprickor enligt RILEM TC 104 [8].

Damage	Severity				
	1 (very mild)	2 (mild)	3 (moderate)	4 (severe)	5 (very severe)
Cracks in pre-stressed concrete due to overload	Crack width < 0.05 mm	Crack width 0.05 – 0.1 mm	Crack width 0.1 – 0.3 mm	Crack width 0.3 – 1 mm	Crack width 1 – 3 mm with limited splitting
Cracks in reinforced concrete due to overload	Crack width < 0.1 mm	Crack width < 0.1 – 0.3 mm	Crack width 0.3 – 1 mm	Crack width 1 – 3 mm with limited splitting	Crack width > 5 mm with widespread splitting
Cracks in non-reinforced concrete	Crack width < 1 mm	Crack width 1 - 10 mm	Crack width 10 – 20 mm	Crack width 20 – 25 mm	Crack width > 5 mm with limited splitting
Shrinkage or settlement cracks	One narrow crack	Several narrow cracks	Many narrow cracks	Some isolated wider cracks	Many wider cracks
Cracks due to reinforcement corrosion	Barely noticeable	Light rust stain	Thick rust stain	Thick rust stain and cracking along reinforcement	Thick rust stain and splitting along reinforcement
Pop-outs	Barely noticeable	Noticeable	Hole up to 10 mm in diameter	Hole between 10 and 50 mm in diameter	Hole > 50 mm in diameter
Splitting	Barely noticeable	Clearly noticeable	Larger than coarse aggregate grains	Surfaces up to 150 mm crack edge size	Surfaces larger than 150 mm crack edge

2.1.5 Reporting

The report should reflect the observations made during the inspection. One should keep in mind that the purpose of visual inspection is to detect and document the cracks. The documentation should state the layout of the cracks, main dimension (length, depth and width), location, orientation, etc. This rule should also be used for other types of damage that have been noted during the visual inspection. The

result is used partly for preliminary assessment of the underlying causes of the cracks/damages and partly to determine whether they constitute any immediate threat to the load-bearing capacity and stability of the structure or its durability.

The report shall describe the investigations carried out, including history, data, methodology and equipment, and state the provider. As a support, a simplified version of the report content presented in section 2.2.5 can be used. The focus of the report should be on the reporting of observations, overall evaluation with proposals for future inspections and measures. The following template can be used for registration and classification of the observed damages.

Template for the reporting of damages, revised template from [8].

Structure: Part of structure: Date:	Severity					
	0 None	1 Mild*	2 Mild	3 Moderate	4 Severe	5 Severe*
Discolouration	<input type="radio"/>	<input type="radio"/>	<input type="radio"/>	<input type="radio"/>	<input type="radio"/>	<input type="radio"/>
	<input type="radio"/>	<input type="radio"/>	<input type="radio"/>	<input type="radio"/>	<input type="radio"/>	<input type="radio"/>
	<input type="radio"/>	<input type="radio"/>	<input type="radio"/>	<input type="radio"/>	<input type="radio"/>	<input type="radio"/>
Cracking	<input type="radio"/>	<input type="radio"/>	<input type="radio"/>	<input type="radio"/>	<input type="radio"/>	<input type="radio"/>
	<input type="radio"/>	<input type="radio"/>	<input type="radio"/>	<input type="radio"/>	<input type="radio"/>	<input type="radio"/>
	<input type="radio"/>	<input type="radio"/>	<input type="radio"/>	<input type="radio"/>	<input type="radio"/>	<input type="radio"/>
	<input type="radio"/>	<input type="radio"/>	<input type="radio"/>	<input type="radio"/>	<input type="radio"/>	<input type="radio"/>
Splitting and delamination	<input type="radio"/>	<input type="radio"/>	<input type="radio"/>	<input type="radio"/>	<input type="radio"/>	<input type="radio"/>
	<input type="radio"/>	<input type="radio"/>	<input type="radio"/>	<input type="radio"/>	<input type="radio"/>	<input type="radio"/>
Corrosion	<input type="radio"/>	<input type="radio"/>	<input type="radio"/>	<input type="radio"/>	<input type="radio"/>	<input type="radio"/>
	<input type="radio"/>	<input type="radio"/>	<input type="radio"/>	<input type="radio"/>	<input type="radio"/>	<input type="radio"/>
Relative movements and settlements	<input type="radio"/>	<input type="radio"/>	<input type="radio"/>	<input type="radio"/>	<input type="radio"/>	<input type="radio"/>
	<input type="radio"/>	<input type="radio"/>	<input type="radio"/>	<input type="radio"/>	<input type="radio"/>	<input type="radio"/>
Leakage and precipitation	<input type="radio"/>	<input type="radio"/>	<input type="radio"/>	<input type="radio"/>	<input type="radio"/>	<input type="radio"/>
	<input type="radio"/>	<input type="radio"/>	<input type="radio"/>	<input type="radio"/>	<input type="radio"/>	<input type="radio"/>
	<input type="radio"/>	<input type="radio"/>	<input type="radio"/>	<input type="radio"/>	<input type="radio"/>	<input type="radio"/>
Existing reparation	<input type="radio"/>	<input type="radio"/>	<input type="radio"/>	<input type="radio"/>	<input type="radio"/>	<input type="radio"/>
Delamination/bond failure	<input type="radio"/>	<input type="radio"/>	<input type="radio"/>	<input type="radio"/>	<input type="radio"/>	<input type="radio"/>
Cracking	<input type="radio"/>	<input type="radio"/>	<input type="radio"/>	<input type="radio"/>	<input type="radio"/>	<input type="radio"/>
Other	<input type="radio"/>	<input type="radio"/>	<input type="radio"/>	<input type="radio"/>	<input type="radio"/>	<input type="radio"/>
Additional documents Drawings Photographs Other	Detailed information (including reference number etc)					
Additional comments (general condition, exposure conditions, etc.)						
Photograph			Photograph			

2.2 IN-DEPTH INSPECTION AND CONDITION ASSESSMENT

2.2.1 Definition and purpose

The in-depth inspection is the continuation of the visual inspection which is initiated if any of the damages are judged to be "Extensive damage", see alternative 3 in section 2.1.4. The inspection is carried out to produce data for condition- and service life assessment, as well as a basis for the assessment of repair needs and possibly the choice of repair method and planning of repair works. The included inspection can be initiated e.g. due to the following reasons:

Reason	Example
1 Damage has been discovered but the cause is not known or has to be established.	<ul style="list-style-type: none"> • Cracking caused both by frost attacks and ASR • Cracking caused by settlement, restraint (internal and external) or other types of attack.
2 The cause is known but its development stage/rate is not known.	<ul style="list-style-type: none"> • Carbonation and chloride penetration of the concrete cover which can lead to corrosion of reinforcement. • Expansion due to ASR. The remaining expansion is not known. • Development of the frost attack • Leaching of the concrete cover. Leaching of cracks. • Stability of cracks or changes over time.
3 The consequences of the damage is to be estimated	<ul style="list-style-type: none"> • Effect on stability and/or load-bearing capacity. • Effect on water-tightness. • Effect on durability.
4 Quality control, monitoring and follow-up	<ul style="list-style-type: none"> • Control of the result from a specific preventive measure or repair.

The in-depth inspection may include sampling, on-site measurements and calculations. By determining the development process of the damage, its extent and its impact on the physical and mechanical properties of the material, one can assess the current and future conditions of the structure. The result is the basis for the selection of measure. The measures that should be taken depend on parameters like the type of structure, type of damage and its cause as well as the requirements on the structure.

It should be noted that in-depth inspections and condition assessment can be quite complicated and may therefore require several subsequent investigations and that different methods are used. In order to be able to assess the condition of the structure and future changes with a reasonable degree of certainty, it may be necessary for the results of various investigations (measurements, monitoring and calculations) to be combined. This makes the inspection more difficult and sets high requirements on the operator and the evaluator. It is necessary that in-depth inspections are carried out by qualified personnel.

2.2.2 Preparation and planning

The content of the in-depth inspection depends primarily on the type of damage and its cause and the purpose of the inspection. An in-depth inspection may include core drilling for the preparation of test samples for various tests, installation of sensors and instruments for the measuring/monitoring of different changes etc., all of which should be taken into account during the planning stage, like the preparations described in section 2.1.2. In addition to the tools specified in section 2.1.2, special measuring equipment, tools and machines will be required at an in-depth inspection. Therefore, a specific list of equipment should be established for each type of measurement. Likewise, the extent and positions of measurements and samplings should be established.

The preparations should be summarized in a test program that is distributed to all who will be present at the in-depth inspection.

2.2.3 Implementation

For the purposes of this section, "damage" refers to individual cracks, crack systems (several cracks with distinctive directions, propagation, reinforcement spacing, etc.) as well as crack formations such as crazing, splitting and delamination.

The cause of damage is not known

Here it is assumed that the damage has developed but the cause is not established. The determination process can become complex and require detailed description of the analytical methods - which includes both theoretical and experimental tools – which is outside the current framework. Therefore, in this section, processes for determination are dealt with only briefly and detailed method descriptions are omitted. Furthermore, it is assumed that the readers are familiar with, and have general knowledge of, the different phenomena that can cause cracking in concrete structures. Section 2.4, 2.5, 3 and 5 provide more detailed descriptions of the phenomena and methods of analysis, as well as references to in-depth descriptions of different phenomena and methods of analysis.

With the help of sections 2.1.3 and 2.4, one can either determine the causes of the cracks or exclude any suspected causes. The following is a brief guide to determining the crack types listed in Table 2-1, Figure 2-7 - Figure 2-10.

I - Plastic Settlement crack

It should be possible to identify cracks of this type on site by visual inspection and with the help of images showing the shape, location and extent of the cracks, see section 2.1.3. The cracks occur at an early age. Therefore, it is valuable to start from previous inspections and archived images. Most durability damage that can be confused with this type of damage occurs between 5 to 10 years, perhaps even longer, after the construction is complete. The cracks that belong to this category are shallow, show no signs of leaching and can be without precipitates and other reaction products. In cases where it is difficult to assign the cause of cracking to plastic settlement cracks, core samples should be sampled. A person who has experience in microscopy of

concrete and cement samples can, through visual inspection and microscopy of a surface ground crack planes/cross sections, determine whether plastic settlement is the cause of the crack formation or not.

II - Plastic shrinkage crack

See "Plastic settlement crack"

III – Thermal cracking, early cooling after hardening of the concrete

It should be possible to identify cracks of this type on site by visual inspection and with the guidance of the images in section 2.1.3 which show the shape, location and extent of the cracks. The cracks occur at an early age about a couple of days up to three weeks after casting. When it comes to relatively thick structures, it may take even longer. A review of previous inspection reports and archived images facilitates the determination of the cause of cracking, since most durability damages that can be confused with this type of damage occurs between 5 and 10 years, perhaps even longer, after construction is complete. It is important to determine the boundary conditions of the part of the structure with respect to load transfer and exposure environment (moisture and temperature load).

If the cracks begin at the boundaries and pass through the cross section, it is a sign of external restraint forces caused by prevented cooling movements, Figure 2-7. The cracks in the lower part of the pier of Figure 2-8 may also be caused by external restraint (the rock causes the restraint). The cracks can be confused with the cracks caused by seasonal temperature changes and in certain contexts with prevented shrinkage. Archived images can be of great help in determining the causes. Cracks from restraint forces start perpendicular to the boundary and continue in the structural part. The crack can change direction when it has advanced a bit into the structure. The reason for the change of direction is the change of the stress field and the geometry of the structure. There may be a single crack in a structural part or several "parallel" cracks of varying width and length.

If the cracks occur in places far enough from the boundaries, i.e. places where one can ignore the boundary effects, internal restraint (strain gradient) can be the cause of cracking. Like cracks caused by external restraint, internal restraint cracks can be confused with the cracks caused by seasonal thermal movements and in some cases with prevented shrinkage. Archived image files can be very helpful in determining the causes.

An experienced inspector can through visual inspection determine whether a crack is caused by early cooling or not. Examination of temperature development during hardening, with possible measurement of cooling, can facilitate the assessment. Theoretical analyses with the help of analytical and numerical models can improve the accuracy of the assessment.

An experienced petrographer can, with the aid of a surface ground crack plane and crack cross-sections, as well as a thin section, distinguish between cracks from restraint and other cracks such as those caused by plastic settlement,

plastic shrinkage as well as cracks caused by other long-term degradation processes.

IV - Thermal cracking, seasonal variation in temperature

Thermal cracks caused by seasonal variation in temperature are in many respects similar to the thermal cracks caused by early cooling, but their location and extent may differ from the latter type. Cracks caused by seasonal temperature variations arise from internal restraint, i.e. the strain gradient that occurs due to temperature variations in the structure. It can sometimes be difficult to distinguish between cracks caused by seasonal temperature variations and those caused by early cooling. Previous inspection reports and archive images as well as monitoring through measurements of deformation and temperature can facilitate the determination of what caused the crack. Analysis of the behaviour of the structure with numerical models is also a good tool for determining the cause of the crack and distinguishing between different thermal effects that cause the cracks.

V - Shrinkage cracks (autogenous)

Autogenous shrinkage is caused by the hydration of the cement. Therefore, most of the autogenous shrinkage occurs within the first few weeks after casting, and often before formwork removal of the structure. The autogenous shrinkage is equal everywhere in a structure because the cement reactions take place at the same speed everywhere in the structure, provided the structure is cast without interruption. No strain gradients arise due to the autogenous shrinkage. When it comes to thick structures, there is a risk that

- the casting is performed in stages and the structure contains concrete layers with different degrees of hydration and
- there are temperature gradients that cause different cement reaction rates.

The autogenous shrinkage share of the total shrinkage of the concrete increases with reduced w/c ratio and an increased amount of cement. The autogenous shrinkage share of the total shrinkage is negligible for conventional concrete with a w/c ratio exceeding 0.50.

Any potential cracking caused by autogenous shrinkage may be visible shortly after formwork removal. The cracks appear more clearly if the concrete surface is reasonably dry while the cracks are still moist. It is difficult to distinguish between autogenous shrinkage and free drying shrinkage. Autogenous shrinkage is added to drying shrinkage, but the following aspects should be noted:

- Drying shrinkage may occur long time after the autogenous shrinkage. It can take a long time for a thick concrete structure to dry out. Therefore, it is not certain that one can add the stresses that arise due to prevented autogenous shrinkage to the stresses caused by prevented drying shrinkage. The creep of the material can cause the stresses that arise due to autogenous shrinkage to decrease or completely disappear before the drying shrinkage starts. However, the drying shrinkage can

drive further the cracks caused by autogenous shrinkage and increase their length and width.

- Due to the fact that the outer parts of the structure dry faster than the inner parts, shrinkage gradients can occur in the structure. This must be considered when determining the overall effect of the autogenous shrinkage and drying shrinkage.

Autogenous shrinkage can interact with the cooling of a concrete structure at an early age. When it comes to external restraint, the effects of the phenomena can be summed. If the cooling causes temperature gradients to occur, this should also be considered when determining the interaction between autogenous shrinkage and cooling of a concrete structure at an early age.

Interaction between autogenous shrinkage and seasonal temperature variations can become more complicated than the above cases due to strain gradients and require in-depth analyses, see sections 3 and 5.

VI - Shrinkage cracks (drying)

Drying shrinkage is caused by the drying out of the concrete. The boundary conditions of the structure (humidity and temperature in the surrounding environment), the diffusion properties and the geometry (the ratio of the volume of the structure to the area of the exposure surfaces of the structure) of the concrete determine the rate of drying out. If drying shrinkage is prevented by external factors such as adjacent structures and layers, external restraints can occur. The moisture gradient in the structure leads to a strain gradient arising in the structure which leads to internal restraint.

It is difficult to determine the drying shrinkage in a structure through testing. The safest way is to manufacture test specimens of the same type of concrete and subject them to the same drying as the structure is exposed to. This type of test can lead to inaccurate estimates when assessing the shrinkage of thick structures, as it may take several years for a thick structure to reach moisture equilibrium with its environment, whereas a test specimen manufactured with the same concrete as the structure dries relatively quickly. The thick structure can be exposed to ageing phenomena, the cement reactions can finish, the material creeps, and the material can be exposed to various chemical and physical attacks.

In order to reduce the miscalculation that may occur due to the cement hydration, the test specimens should be insulated from moisture for a sufficient amount of time in order for most of the cement reactions to take place. Subsequently, the specimens may be subjected to relatively slow drying. The change in length of the specimens shall be measured from the early stage to the moisture equilibrium with the surroundings of the structure. The specimen temperature and relative humidity are measured with RH sensors, see section 2.3.1. Alternatively, the specimens are gradually moved to different rooms/boxes with lower humidity. The purpose is that the specimens come into equilibrium with the room/box climate and their shrinkage at equilibrium with the current climate is determined. In this way one can obtain a connection

between the shrinkage of the concrete and its moisture. By measuring the humidity of the structure, see section 2.3.1, one can determine its free shrinkage at the point in question. Guidance for determining the shrinkage of the concrete can be found in [84].

It should be noted that the term "free shrinkage" refers to the shrinkage which is not affected by either the inner or outer restraint. It is not possible to determine the free shrinkage in a structure. One can only calculate the effect that the free shrinkage might have in a structure. The free shrinkage can lead to strains, deformations, displacements and cracks in a structure. Stresses can be determined by recalculating the strains into stresses.

The method mentioned above is not feasible for old structures. One can, however, use the connections between drying and shrinkage as stated in norms and standards, e.g. in SS-EN 1992-1-1: 2005 [32]. One can either measure the moisture distribution of the structure or calculate it or combine measurement and calculation, and then use the relationships specified in norms and standards to determine the current free shrinkage in the structure.

By numerical methods, and sometimes analytical methods, one can calculate the development of shrinkage and its effect on a structure. The methods basically correspond to the methods used for calculating temperature distribution in a structure and its effect on stresses and strains in the structure. Interaction between the mentioned phenomena is governed by time and the geometry of the structure, as well as the boundary conditions, see also section 3.

VII - Shrinkage cracks (carbonation)

When the calcium hydroxide of the concrete reacts with the carbon dioxide of the air, it is converted to calcium carbonate with a smaller volume than before. The concrete contracts because of the carbonation. The phenomenon acts from the surface and is slow.

Carbonation extends the drying shrinkage [83]. On-site testing shows that if the concrete is carbonated while drying, the final shrinkage increases by about 50%, provided that the concrete is dried from 100% RH to moisture levels corresponding to 80 - 50% RH [83]. Furthermore, the results show that the effect of carbonation on the shrinkage of the concrete becomes even greater if the concrete first dries out to a given moisture level and then is subjected to carbonation. The final shrinkage increases by about 100% within the specified range. This effect is one of the reasons for the rough surface cracks that are visible on old concrete structures.

In the case of conventional and water tight structural concrete, it may take several decades before the carbonation front reaches the level of reinforcement. Therefore, carbonation shrinkage causes only shallow cracks. The cracks can reach all the way to the reinforcement. The carbonation of the concrete cover can lead to corrosion of the reinforcement. Reinforcement expansion due to corrosion can lead to crack formation in the concrete cover. Carbonation shrinkage and reinforcement corrosion can interact to crack the concrete cover.

The depth of carbonation is determined by SS-EN 14630: 2005 [85]

VIII - Crazeing at formwork surface and steel trowelled surface

Crazeing on the formwork surface and the steel-trowelled surface should be identifiable on the spot by visual inspection and with the guidance of the images showing the shape, location and extent of the cracks, see section 2.1.3. The cracks occur at an early age, therefore it is valuable to start with previous inspections and archive images. Most of the durability damages that can be confused with this type of damage occur between 5 to 10 years, perhaps even longer, after the structure is complete. The cracks that belong to this category are shallow, show no signs of leaching and can be without precipitates and other reaction products. In cases where it is difficult to determine the cause of the crack, core samples should be taken from the structure. An experienced petrographer can, by visual inspection and microscopy of a ground crack surface/cross section, determine the cause of the crack.

IX - Reinforcement corrosion

Cracks caused by reinforcement corrosion appear relatively late in the corrosion process. The time for when cracks appear is governed by the composition of the concrete (w/c ratio, cement type and cement content), the thickness of the concrete layer and the exposure environment. It can take several years before the cracks appear. In some cases, cracking may be preceded by discolouration of the concrete surface. The surface of the concrete can get a brownish colour due to ongoing corrosion. The corrosion process and crack formation are described in section 2.3.6. Reinforcement corrosion can cause three types of cracks. Type CC1 is when cracks are oriented along the reinforcement through the concrete cover. Type CC2 causes spalling of the concrete cover, which are oriented along the reinforcement. Type CC3 causes delamination of the concrete cover. It should be noted that the cracks can contain corrosion products, which are brownish, or be completely empty. The cracks may also contain lime/calcite which are leaching products. In hydropower structures, the aggregate can discolour the water, which in turn discolours the lime/calcite and leads to the leaching products getting confused with corrosion products.

X – Alkali Silica Reactions

ASR damages can be both local and global cracking, pop-outs (craters formed on the concrete surface due to the expanding aggregate close to the surface pushing out materials) and discolouration.

Cracks caused by ASR occurs after relatively long time and it can take up to 20 years before they appear. Once the damage has developed, it is not difficult to determine if the cause of the crack is ASR or another mechanism. The local cracks formed on the concrete surface are crazeing, cracks (often three) that originate from the same point and pop-outs. If it is not possible to determine whether ASR is the root cause of the cracking, core samples should be taken for more accurate and in-depth laboratory analyses. One can, by means of petrographic studies on specimens prepared with surface grinding, determine whether ASR is the cause of the observed damages, see section 2.3.4. For further

uncertainties, SEM and EPMA analyses can be performed. Using the included lab performed analyses, one can detect ASR even if the cracks are not visible on the concrete surface.

The local crack formation is affected by the local stress condition. The direction of cracking is affected by the stress level. High compressive stress in a certain direction prevents expansion in the direction of the stress. Therefore, cracks are thin or hard to find in compressed structures such as piers. In pre-stressed structures, the crack width grows perpendicular to the direction in which the structure was pre-stressed.

The expansion of the concrete leads to stress- and strain gradients occurring in the structure, which in turn causes the structure to crack and global cracks are formed. The stress conditions and the global cracking is also affected by the shape of the structure and type of reinforcement (untensioned or pre-stressed reinforcement) and the support conditions. In the same way as in the case of prevented thermal and moisture movements, the crack geometry is affected by prevented ASR expansions and expansion gradients.

In hydropower structures, ASR often interacts with internal frost attacks. It is often difficult to determine which mechanism has initiated the cracking.

XI - Frost attacks

Frost attacks can lead to internal expansion and crack formation as well as external peeling, see section 2.3.3. The internal expansion and crack formation occur due to the pore system of the cement paste being filled with water, which expands during freezing. The expansion damages the cement paste and it loses its strength. Heavy reduction of the tensile strength of the concrete in combination with high water saturation degree (above 0.85) and exposure in a cold environment can indicate internal frost attacks, see section 2.3.3.

Sometimes, internal frost attacks can be confused with ASR attacks. But through petrographic investigation one can distinguish between the attacks. During internal frost attacks, the aggregate grains are often undamaged. Furthermore, the cement paste is weak, very moist and crumbly. In the case of ASR attacks, the crack/cracks (often three of them) start from an aggregate grain. In a concrete damaged by ASR, the cement paste retains its strength and is usually not as moist as one of frost-damaged cement paste.

In those cases where the frost and ASR attacks interact, the concrete cracks. The cracks are often rough and moist. The moisture and water saturation of the damaged concrete is high. The cracks pass through the aggregate while the cement paste is weak.

Frost attacks can also be confused with sulphate attacks, see sulphate attacks

XII - Sulphate attacks

Sulphate attacks are unusual in hydropower structures in Sweden, but can cause damage to concrete structures as water-soluble sulphates derived from sodium, potassium, ammonium and magnesium sulphate penetrate the concrete and react with the calcium hydroxide of the cement and tricalcium

aluminate. In connection with sulphate attacks, two reactions occur, the first of which leads to the formation of gypsum while the other leads to ettringite formation. Both reaction products are swelling and may cause cracking. The gypsum formation causes the cement paste to lose its cohesion and its strength decreases. The ettringite formation causes the concrete to rupture due to internal stresses caused by the swelling. The influence of the ettringite can be compared to internal frost attacks, which are a form of physical attack. By studying the exposure environment and supplementing the study with petrographic analysis, one can determine what caused the damage.

XIII - External loads - short term loading

External loading leads to cracking when the stresses caused by the load exceed the tensile strength of the concrete. To determine whether the cracks were caused by the load, one should study the mechanical properties of the structure and its behaviour at different loads. External loads that cause cracks do not affect the material outside of the cracks. External loads can lead to deformations, which can sometimes be large if the reason has been incorrect assumptions at the design stage.

XIV - External loads - long term loading

External loads that act for a long time can, in the same way as short-term loading, lead to cracking and deformation. The difference is that long-term load leads to cracks whose length and width are not stable, but rather they grow over time. E.g. the strength of the materials decreases with increased loading time. If this phenomenon has not been taken into account at the design stage, a heavily loaded structure may crack after a long time. Creep of material leads to increased deflection which can lead to increased length and width of bending cracks.

XV - Dynamic loading

Dynamic loads can lead to cracking through

- 1) fatigue (the strength of the material decreases)
- 2) overload/resonance (the strength of the material is exceeded) and
- 3) punches and explosions (overload and change of the geometry of the structure)

XVI - Forced deformation

Settlement is an example of forced deformation which successively increases the load in one or several sections of the structure which eventually leads to crack formation. The length and width of the cracks may increase as a result of the settlement increasing over time.

The process/cause of damage is known but its stage/rate is not known

Here it is assumed that the damage has developed and the cause has been established. The questions are:

- Are the damages increasing in extent, i.e. if the crack grows or do they stop?
- How does the damage affect the load-bearing capacity, stability and service life of the structure?
- How should the development of the damage and its impact on the structure be analysed?

The issues can become complex and require a detailed description of the methods of analysis (theoretical and experimental) that is outside the scope of the present directive. In this section, the issues are dealt with only briefly and detailed descriptions of methods are omitted. Furthermore, it is assumed that the reader is familiar with and has general knowledge of the various phenomena that can cause cracking in concrete structures. Section 2.3 and 2.4, 3 and 5 describe various phenomena that lead to damage and cracking and associated analysis methods. References to deeper studies of the various phenomena and methods of analysis are given in the sections mentioned.

I - Plastic Settlement crack

Plastic cracks are stable when they have developed, but they deteriorate

- the durability properties of the concrete surface,
- the bond between reinforcement and concrete,
- the durability of the concrete cover against carbonation, chloride penetration, leaching and frost attack etc.

In case of comprehensive damage, the concrete cover cannot meet the requirements set during the prescribed period of use. Various degradation mechanisms and overloads can impair the stability of the cracks. Due to the deterioration of concrete durability to various degradation mechanisms, plastic settlement cracks can shorten the service life of the structure.

In order to analyse the future of the structure with respect to plastic settlement cracks, the development of the settlement cracks over time and its impact on the mechanical and physical properties of the concrete must be studied in the context in which different loads and degradation mechanisms affect the area that is subjected to plastic settlement. The reason is that plastic settlement cracks are inherently stable and do not pose any danger to either the concrete or the reinforcement if the exposure environment is such that it does not subject the materials to various attacks.

II - Plastic shrinkage crack

See "Plastic settlement crack", point I.

III – Thermal cracking, early cooling after hardening of the concrete

The cracks are normally stable and do not develop over time, provided

- the load does not increase,

- the structure is not exposed to large internal and external restraint forces caused by different temperature fluctuations, autogenous shrinkage and drying shrinkage as well as
- the structure not being exposed to degradation mechanisms - such as leaching, carbonation, chlorine penetration, etc. - whose degrading effect is facilitated by the cracks.

The cracks can affect the mode of failure, stiffness, dynamic properties and durability of the structure.

The development of the cracks over time can be followed by monitoring and periodic measurements of crack width and crack length. If the cracks are stable, they do not pose any danger to the future of the structure, provided they have not already changed the mode of failure, load-bearing capacity or the stability of the structure. Furthermore, it is assumed that the cracks have not degraded the durability of the structure to various degradation mechanisms.

In those cases where prevented cooling deformations have not led to any cracks, the stresses remain, so their impact cannot be fully depreciated. If the cooling deformations are prevented, stresses arise in the structure which can be combined with the effects of other mechanical, physical and chemical phenomena. The combination of the effects can result in increased stresses and stress concentrations. Cracks are formed when the stresses exceed the tensile strength of the material. The cooling deformations can increase the effects of the autogenous shrinkage. Furthermore, the cooling interacts with the seasonal temperature changes.

However, it should be noted that the stresses that occur due to of the prevented drying deformations decrease over time due to relaxation of the material.

The future development of the cracks can be assessed using numerical models in combination with monitoring and measurements, provided that the properties of the structure and exposure environment as well as the load conditions are known, see also sections 3 and 5.

IV - Thermal cracking, seasonal variation in temperature

The cracks can be unstable and grow over time. Growth is triggered and affected by changes in load, structure design (repairs, reinforcements etc.), exposure environment and boundary conditions.

The cracks can be stable and not develop over time, provided

- the load does not increase,
- the effect of the seasonal temperature variation is dampened. It should be noted that it is not sufficient to maintain the range of variation constant, but it is necessary to reduce the absolute value of the interval limits,
- the structure is not subjected to large internal and external restraints caused by drying shrinkage, as well as

- the structure not being exposed to degradation mechanisms whose degrading effect is facilitated by the cracks.

The cracks can affect the mode of failure, stiffness, dynamic properties and durability of the structure.

The future development of the cracks can be assessed by means of numerical modelling in combination with monitoring and measurements, provided that the properties of the structure, the exposure environment and the load conditions are known, see also sections 3 and 5.

V - Shrinkage cracks (autogenous)

Most of the autogenous shrinkage occurs in connection with the hardening of the concrete and is negligible after a few weeks/months. The cracks caused by prevented autogenous shrinkage occur at a relatively early age. After formation, the cracks can remain stable provided that they are not combined with other effects such as thermal cracks, loading, drying shrinkage cracks, etc.

Cracks caused by autogenous shrinkage can have the same effect on the structure and the same development as thermal cracks at early cooling after the concrete has hardened, see point III above.

Autogenous shrinkage can interact with the seasonal temperature changes and drying shrinkage. It should, however, be noted that the stresses arising due to prevented autogenous shrinkage decrease over time due to relaxation of the material.

VI - Shrinkage cracks (drying)

Drying shrinkage occurs as the structure dries out. The process can be lengthy if the structure is thick. Therefore, it may take a long time before the cracks are formed. In addition, the cracking of the material is affected by its creep and relaxation. Creep/relaxation means that the stresses caused by prevented shrinkage deformations may decrease during slow drying processes.

Shrinkage cracks may have the same effect as thermal cracks on the properties of the structure, see points III and IV above.

Development of cracks caused by drying shrinkage can be determined in basically the same way as the cracks caused by seasonal temperature variations. In terms of shrinkage analysis, one must first determine the moisture distribution/drying distribution of the structure, which should be the basis for determining the corresponding strain/shrinkage distribution prevailing in the structure, see point IV above.

VII - Shrinkage cracks (carbonation)

Shrinkage caused by the carbonation of the concrete is a surface effect and occurs relatively slowly. Carbonation shrinkage expands the existing crack widths at the surface of the structure and a few centimetres below the surface.

The shrinkage cracks do not affect the load-bearing capacity and stability of the structure. Shrinkage cracks can affect the durability of the concrete.

Development of shrinkage cracks caused by carbonation can be determined by analytical models in combination with field measurements, see section 3.

VIII - Cracking at formwork surfaces and steel trowelled surfaces

See "I - Plastic settlement crack", point I.

IX - Reinforcement corrosion

Cracks caused by reinforcement corrosion affect the load-bearing capacity and durability of the structure. The corroded reinforcement should, if deemed necessary, be replaced with new reinforcement and the concrete surface restored. No analyses of crack development are required in this case.

Ongoing reinforcement corrosion may sooner or later lead to cracking. The reader is referred to section 2.3.6 for guidance for inspection and condition assessment of structures subjected to reinforcement corrosion.

Service life assessment of structures exposed to reinforcement corrosion is performed by measurements and calculations. The reader is referred to [34] for guidance.

X – Alkali Silica Reactions

The cracks caused by ASR are not stable, but they grow over time. The cracks "open" the material and make it susceptible to various attacks, such as frost attacks and leaching. ASR can pose a serious threat to the load-bearing capacity and stability of the structure. The strength and stiffness of the material decrease. Interaction between reinforcement and concrete deteriorates. The expansion of the material may lead to increased stress levels in the reinforcement, the structure being deformed and previously unloaded parts being loaded.

In order to assess the service life of the structure, the current and remaining expansion of the concrete should be determined. The current expansion together with calculation models indicate the current status of the structure with respect to load level and load-bearing capacity. The behaviour and load-bearing capacity of the structure with respect to future expansions are assessed by means of calculation models based on the current state and the future material expansions. For the assessment of the load-bearing capacity of simple structural elements such as reinforced beams and piers, there are hand calculation models, see section 2.3.4 and references given in the section. For analysis of coarse and relatively complex structure geometries, advanced numerical models should be used, see section 3.

XI - Frost attacks

Shallow frost damage does not affect the load-bearing capacity of the structure in the short term. Shallow frost damage slowly wears down the concrete cover, which after a few years leads to reinforcement corrosion and poorer interaction between concrete and reinforcement.

The internal frost damage that leads to internal (even external) cracking affects the load-bearing capacity of the structure. In case of internal frost damage, the

concrete is severely damaged with great decreases in strength and stiffness as a result. The tensile strength of the concrete is considerably reduced. The damage process of internal frost attacks can be considered as instantaneous, i.e. when the conditions for frost damage, see section 2.3.3, are met, the concrete is deemed to be damaged. Subsequently, the material deteriorates gradually without much change in the material properties, and the crack widths grow.

The load-bearing capacity of a frost-damaged structure should be analysed with great care. It is important to map and identify structural parts that have been damaged by internal frost attacks. Numerical modelling of frost attacks is dealt with in section 3.

XII - Sulphate attacks

Sulphate attack is a chemical process, but the effect on the load-bearing capacity and stability of the structure is treated in the same way as internal frost attacks.

XIII - External loads - short term loading

Cracks caused by external loads can be treated with conventional calculation and design methods. One may also use advanced calculation models, see sections 3 and 5.

XIV - External loads - long term loading

Cracks caused by external loads can be treated with conventional calculation and design methods. Advanced calculation models can also be used, see sections 3 and 5.

XV - Dynamic loading

Cracks caused by dynamic loads can be treated with conventional calculation and design methods. Advanced calculation models can also be used, see sections 3 and 5.

XVI - Forced deformation

Cracks caused by forced deformation can be treated with conventional calculation and design methods. Advanced calculation models can also be used, see sections 3 and 5.

2.2.4 Evaluation

The condition of the structure must be assessed on the basis of the requirements imposed on the structure and the damages that have been observed. The inspection must lead to concrete results as follows:

1. The damage that has been discovered has no effect on the load-bearing capacity and stability or durability of the structure.
 - a. Time for the next inspection
 - b. Completed inspection
2. The damage that has been discovered has no impact on the load-bearing capacity and stability of the structure, but affects its durability.

- a. The investigator should propose one or more measures with a latest implementation date.
- 3. The damage that has been discovered affects the load-bearing capacity and stability of the structure in the long term.
 - a. The investigator must propose one or more measures with a latest implementation date.
- 4. The damage that has been discovered has an immediate impact on the load-bearing capacity and stability of the structure.
 - a. The investigator must propose one or more measures that should be implemented immediately.

The evaluation is carried out by qualified personnel. It should be noted that the in-depth inspection may involve people with different skills.

2.2.5 Reporting

The report can have different dispositions but it should at least contain the following tasks:

1. **Introduction**
The background to the in-depth inspection should be described. It should be clear if the in-depth inspection is carried out as a result of a routine visual inspection or if it has been initiated for another reason. The set-up, methodology, scope, organization and competence requirements of the inspection should be stated.
2. **Purpose and goals**
This part of the report should describe the purpose and goal of the inspection in accordance with the agreement with the owner, including any changes made during the implementation.
3. **Existing drawings and documentation**
A summary of information on the structure, including structural details, size, location, and previously performed inspections and repairs, etc., should be included in this section. The results of the documentation review must be summarized and supplemented with photographs, sketches and any other relevant information that is suitable. A list of all documents collected and their sources included.
4. **Results of visual inspection and associated examinations**
The results of inspection and condition assessments for all parts of the structure, including those parts that affect the structure such as facade, cladding and foundation structure, should be included. The report should briefly describe methods and equipment used, results from quality control and verifications during construction, including all non conformance issues, major deficiencies that required corrective work and changes in the structure. The results should describe deviations between drawings and the as-built structure.
5. **Completed sampling and testing**
The test and sampling sites, methods and results of the non-destructive and destructive tests performed during the in-depth inspection should be summarized. The results can be supplemented with photographs and copies of

the laboratory test reports. If the tests were intended to deliver input data to calculation models for the assessment of the load-bearing capacity, stability and service life of the structure, it should be described.

6. The section should describe the methods that have been used to process the measurement results. The report should include the physical as well as the statistical aspects of the sampling and tests.
7. The results should clearly indicate whether the sampling and tests are sufficient to assess the load-bearing capacity, stability and service life of the structure.
8. **Completed calculations**
The purpose of the calculation must be clearly presented. It should be stated in the report if the method is used to identify the cause of damage, assess the current state or the future development. The theoretical background, assumptions and limitations of the calculation models should be described. It should be clear if the methods follow all or part of the instructions according to standards and norms, or are completely independent. The model inputs must be presented clearly. It should be clear how the material parameters produced in the inspection have been used in the models. The calculations should be presented in such a way that it can, if necessary, also be carried out by an outside party.
9. **Evaluation of the condition of the structure**
The report shall summarize the results of the in-depth inspection. All assumptions and methods used in the evaluation process must be stated and commented clearly. The damage, the cause of damage and its impact on the load-bearing capacity, stability and durability of the structure shall be described. The evaluation must be carried out in such a way that it can form the basis for the decision making and recommendations for possible measures.
10. Suggestions for various remedial (preventive or repair) measures are briefly presented in this section if the task is included in the order. The proposals are evaluated in general terms using the results of the tests and calculations. It should be noted that in-depth evaluation of the measures may be required if one wishes to produce a basis for selecting remedial measures.
11. **Results and recommendations**
The results of the previous sections should be summarized in this section if not previously done. This section should include a discussion of the condition of the structure and if any measure is needed. One should also specify the time frame within which the measure should be implemented. If one chooses to take any measures, the selection of measure should be supported by a thorough analysis of the effect of the measure on the future load-bearing capacity, stability and durability. The recommendations made here must address the following areas: Course of Action, Cost Calculation, Scheduling, Restrictions and Feasibility.

2.3 MEASUREMENTS, METHODS AND INSTRUMENTS

2.3.1 Temperature and moisture

Knowledge of the prevailing temperature and moisture conditions can be crucial in order to be able to interpret the current condition of a structure and possible causes for cracking. Methods for measuring temperature and moisture are described below. In-depth material can be found in Appendix A.

Measurement of air and concrete temperature

The temperature of the structure and the temperature on its boundaries can be valuable to determine. The temperature in the structure boundaries is governed by the surrounding air and water, as well as by other structures that are in contact with the structure considered. In order to measure the temperature, the following main methods are available [15]:

- Air/insertion/immersion measurements
- Surface Temperature Measurements

The first method is used to determine the temperature of the air and water, as well as measuring the temperature in the cavities (boreholes, cracks, gaps etc.) inside or between material layers and between different materials. The cavities can be filled with air, water or other substances. If the volume of the cavity is small in relation to the concrete surrounding it and that the circulation of the substance that fills the cavity is low, the temperature of the substance can be assumed to be equal to the temperature of the concrete. Therefore, inserting a thermometer can be a way to determine the temperature of the concrete.

The concrete temperature can also be determined by measuring the surface temperature. By putting the thermometer close to the surface of the concrete (a surface can be external or internal e.g. inside a gap) one can determine the temperature of the concrete. However, one should be aware that the circulation of water and air around the thermometer or heat radiation can affect the temperature. When measuring surface temperatures in the air, one can protect the thermometer against the influence of the air by placing a piece of insulation material over the thermometer a few minutes before readout.

The temperatures that apply during inspection of the concrete structures of hydropower plants can vary between $-40\text{ }^{\circ}\text{C}$ (extremely cold winter) and about $+50\text{ }^{\circ}\text{C}$ (sunlit surface during warm summer). The accuracy required for measurements depends on the purpose of the measurement. For inspection/monitoring of cracks, according to section 4.3.3, an accuracy of $0.1\text{ }^{\circ}\text{C}$ is required.

Measurement of air and concrete moisture

The humidity of the air is usually determined by means of equipment that determines the relative humidity of the air (RH). For background theory on relative humidity in air and measurement principles for this, see Appendix A. In the case of inspections, all humidity sensors should preferably be calibrated shortly before the inspection. It is relatively complicated to carry out moisture

measurements and it is generally recommended that experts/humidity consultants be involved for this.

The moisture of the concrete is expressed by different quantities, two of which are the most common sizes are the relative humidity (ϕ) and the moisture content (w) [kg/m^3]. The moisture content indicates the amount of physically bound water present in the concrete. The physically bound water is defined as the amount of water leaving the concrete when heated to 105°C . The moisture content is determined by drying out a concrete specimen with a known volume at $+105^\circ\text{C}$. The weight difference between the non-dried specimen and the dried specimen is the amount of moisture that the concrete contains. The moisture content is determined by dividing the amount of moisture by the sample body volume:

$$w = \frac{m_e}{V} \quad [\text{kg}/\text{m}^3] \quad (2-1)$$

m_e = the weight of the evaporable water [kg]

V = the volume of the specimen [m^3]

If a piece of concrete is placed in air with constant temperature and RH the moisture content of the concrete is set to an equilibrium position, called equilibrium moisture content (w_e , kg/m^3). The equilibrium moisture content is a function of the RH of the air and temperature ($w_e(\phi, \theta)$). At a constant temperature, w_e increases with the RH, and at a constant RH, w_e increases if the temperature decreases. Figure 2-12 shows the relationship between the moisture content of the concrete and the RH of the air. This relation is also called the sorption curve. The moisture content of the concrete at a given RH depends on whether the concrete is absorbing or emitting moisture, i.e. the appearance of the sorption curve is governed by the moisture exchange process. The adsorption and desorption curve are distinguished from each other. The adsorption curve (humidification) is below the desorption curve (drying).

The moisture that concrete adsorbs from the air is called hygroscopic moisture. The RH of the air can be as high as 100%. At this humidity level, the water vapour of the air condenses on material surfaces. If a piece of concrete is surrounded by air with RH just below 100%, it adsorbs moisture until it equilibrates with the air humidity. The moisture content reached by the concrete is the maximum moisture content that the concrete can reach when in contact with air. If the moist piece of concrete is placed in water, it will absorb more water. This moisture content is called over-hygroscopic moisture content.

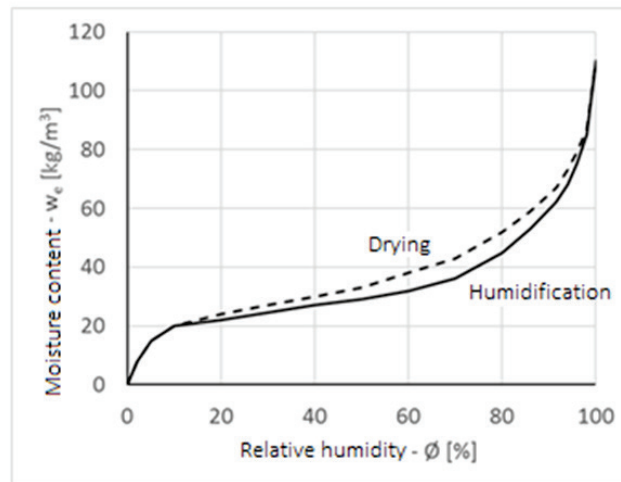


Figure 2-12 – Relation between the moisture content of the concrete and the RH of the air.

If a moist piece of concrete is placed in a container, see Figure 2-13, with dry air, the moisture is emitted to the air. Eventually, an equilibrium is reached in the container, where the moisture content of the concrete and the air are in equilibrium with each other. By measuring the moisture of the air, one can determine the RH that the concrete is in equilibrium with. The air moisture can be determined with an RH meter, usually a capacitive sensor, see Appendix A. The moisture content of the concrete can then be determined by the sorption curve or by weighing the concrete before and after drying at 105 °C. If the moisture content of the concrete is greater than the moisture content corresponding to the hygroscopic limit, the RH meters cannot be used to determine the RH of the concrete, but the moisture content of the concrete must be determined by weighing before and after drying at 105 °C.

If a hole in the concrete is drilled and closed so that moisture exchange between the air in the hole and the air outside the hole is prevented, a moisture equilibrium position eventually occurs, where the RH of the entrapped air will correspond to the RH that the surrounding concrete is in equilibrium with. By mounting an RH meter in the hole, see Figure 2-14, one can determine the RH of the entrapped air, and thus the RH that the surrounding concrete is in equilibrium with.

Two methods for determining the RH of the concrete are presented below.

1. Obtained sample

Samples are taken from the depth of the structure at which the relative humidity of the concrete is to be determined. In the case of deep sampling, a core is first drilled out and then samples are taken at different locations on the core sample corresponding to the desired depths. The test pieces are then placed in individual test tubes, which are sealed with a rubber plug through which the RH meter passes, see Figure 2-13. The disadvantage of this method is that the core sample becomes wet during the drilling. If the concrete is dry, it will absorb water during the drilling, which may lead to incorrect measurement results. According to [16], RH measurement through taking samples leads to uncertain results. The method is

no longer recommended by RBK (the Swedish Council for Construction Competence, Swedish: "Rådet för ByggKompetens") [17].



Figure 2-13 – Measurement of RH from samples obtained from the structure. The samples are placed in a test tube and a capacitive RH meter it placed into the tube [16].

2. Borehole measurements

The RH meter is placed in a borehole, whose endpoint corresponds to the position in the object where the RH is to be determined, see Figure 2-14. The measurements can be performed according to [17] or [18]. One of the difficulties with this method of measurement is to drill a relatively deep but at the same time narrow hole in a concrete wall and to place the sensor deep inside the hole and seal the measuring area.



Figure 2-14 – Measurement of borehole, [16]. The RH meter is placed in a drilled hole, where its endpoint corresponds to the position of the object in which the RH is to be determined

2.3.2 Cracks and crack widths

Measurement of cracks is described in section 4.3.3.

2.3.3 Frost damage

If it is suspected that the cause of cracking may be related to effects from frost, then determination of porosity, current degree of water saturation and possibly specific spacing factor (mean distance between air pores) is important. Explanations of basic concepts regarding frost degradation are given in Appendix B.

A frost-resistant cement paste contains well-distributed air pores that are not far from each other. The spacing factor indicates the average distance between the air pores. According to Fagerlund [19], the spacing factor is about 0.22 mm and 0.18 mm for frost-resistant cement paste in pure water and an environment with de-icing salts respectively. The minimum air content of a frost-resistant concrete is about 4%, which requires an air content of about 5% in the fresh concrete to compensate for possible variations.

The natural air pores are too large and are far apart. Therefore, air is added with air entraining agents to provide many small pores with short distances to each other. At a given air content, the spacing factor decreases with reduced pore diameter.

Frost attacks can give damages as follows:

- i. Internal cracking
- ii. Surface peeling
- iii. Combination of i and ii

Internal cracking

The internal cracking occurs due to internal expansion when the degree of saturation exceeds the critical degree in a big part of the concrete volume. When the water content in the pores of the concrete freezes, it expands. If there is not enough space for the water to expand in and/or if there is a large distance between the spaces, the air pores, internal pressure arises in the pores. The internal pressure exposes the cement paste structure to large tensile stresses, which causes the cement paste, the concrete, to expand. The concrete cracks if the stresses are sufficiently high.

Internal expansion caused by frost occurs when concrete is in contact with water for a long time. It can take several decades before any damage caused by internal expansion can be seen. However, the process can be shortened considerably if the structure is exposed to ASR, leaching as well as if the structure is in contact with non-frozen water in cold climates.

Figure 2-15 shows concrete structures in contact with water. Due to the location of the structure, the concrete is in contact with unfrozen water in winter time [11]. The heat transfer from the water (which is warmer than the air) via the concrete brings moisture into the concrete. Eventually, the critical degree of saturation of the concrete is achieved and the concrete freezes.



a) Internal frost damage of a structural part above the water-line



b) Internal frost damage at the intake of a power plant.



c) Internal frost damage above the water-line, as well as surface damage and leaching under water-line in a guide wall



d) Damages like in picture c) but at the intake

Figure 2-15 – Internal frost attacks [11].

Surface peeling

Surface peeling may occur in an environment with de-icing salt, e.g. bridge roadways and bridge piers, and in the hydropower plants where cold concrete structures are in contact with unfrozen water, e.g. at the waterline in winter.

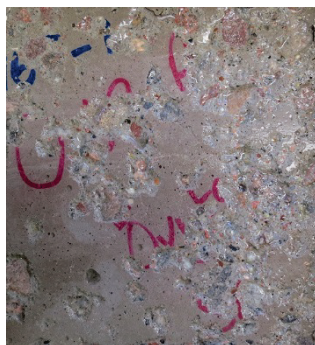
In salted environments, the salt prevents the water collected on the concrete surface from freezing. Thus, the concrete has access to water during freezing and thawing. If the concrete is not frost resistant, the condition for frost attack is relatively quickly fulfilled, i.e. that in an outer layer a few mm thick, the degree of saturation exceeds the critical degree. The surface layer expands due to freezing, leading to peeling off the outer layer, see Figure 2-16a. In this case, the material is damaged/peeled layer-wise. The inner parts of the material cannot reach the critical degree of saturation, the process only takes place within a layer close to the aggressive environment.

Peeling of concrete at the waterline is not uncommon on Swedish dams, see Figure 2-16b. Peeling occurs in contact with clean water without the presence of salts. The reason for this is that the concrete is in contact with unfrozen water during freezing and thawing. The damages at the water-line are the results of synergy effects with at least two mechanisms involved: leaching and frost, [20] and [21].

Erosion may also be involved. The phenomenon can be compared to salt frost attacks. Salt lowers the freezing temperature of the water and supplies concrete with non-frozen water during freezing and thawing. The same type of process occurs in dam structures, where the cold concrete (concrete with sub-zero temperatures) is in contact with unfrozen water. At relatively cold air temperatures, the surface of the concrete freezes even if the water is not frozen. Ice is formed on the concrete surface even a few decimetres below the water surface. The air pores located near the concrete surface are filled with water and freeze to the point of rupture. In this way, layers of the concrete are eroded one after the other at the water-line. In very cold areas, the development of damage can reach up to 1 mm/year [11].

Leaching accelerates the process. The river water has low calcium content, which means that the calcium of the concrete - primarily from the calcium hydroxide - migrates outwards, and is replaced by water. The leaching makes the surface layer more porous and weaker, as well as opening its pore structure, which facilitates water uptake the pores.

Erosion caused by water flow and mechanical erosion (e.g. friction between ice and the surface) can accelerate the process by removing weak layers and loose aggregate grains which speeds up the leaching process.



a) Surface peeling caused by frost attacks in the presence of de-icing salts, [21].



b) Surface peeling at the water-line, [11].

Figure 2-16 – Surface peeling of the concrete due to salt frost.

Measurements

It is not difficult to detect a fully developed frost attack during a visual inspection. However, it is difficult or almost impossible to detect a frost attack in the initiation phase. Often, it may be difficult to distinguish internal frost attacks from ASR attacks. In some structures, frost and ASR attacks interact. The following visual methods can be used to determine whether the damage has been caused by a frost attack:

1. Internal frost attacks appear as crazing on the concrete surface. The difference between crackles caused by internal frost attack and plastic shrinkage, tight formwork or rapid drying of fresh concrete surface is that the cracks associated with internal frost attacks are considerably deeper than in the other cases, and

that the cement paste loses its cohesion and can sometimes easily be scraped with a knife.

2. The difference between crazing caused by internal frost attacks and crazing caused by ASR is that the cracks in frost damaged structures are either empty or partially/fully filled with leaching products, while cracks in an ASR damaged structure may contain a slightly yellow gel. However, it should be noted that the colour is affected in both cases by the water, the bedrock and the constituents of the concrete, e.g. corroded reinforcement.
3. Unlike frost damaged concrete, the material between the cracks in an ASR damaged concrete is often undamaged and may, despite the damage, have a high strength.
4. In ASR damaged concrete, the cracks often pass through certain aggregate grains, while in frost damaged concrete the aggregate grains are often undamaged.
5. Sulphate attacks can also lead to crazing and weakening of the material. It can be difficult to distinguish between sulphate attacks and frost attacks if the damage occurs in an environment where conditions for both types of attack exist. In the case of Swedish dams, there are no prerequisites for the type of sulphate attack that can be confused with frost attacks.

When difficult to determine by visual inspection whether the damage has occurred due to internal frost attacks, one should take core samples. An experienced petrographer can determine whether the concrete is frost damaged or not by examining surface grinded specimens or via thin sections.

The current state and its development

If the concrete is undamaged but there still is a need to determine its future status regarding frost attacks, the following tests are available.

In order to determine the resistance the concrete has to internal frost attacks, the porosity and the spacing factor must be determined, which can be done by surface grinding (see description under methods connected to detection of ASR in section 2.3.4). If the porosity of the concrete is greater than 4% and the spacing factor is less than 0.22 mm, the concrete is probably resistant to internal frost attacks. The stated limit values should be considered as characteristic values. To be sure of the durability of the concrete, the mean value of the tests should be at least one standard deviation greater (for porosity) and less (for the spacing factor) than the limit values. One can also use SIS-CEN/TR Testing of frost resistance in concrete - Internal degradation.

In the case of older structures that have been in operation for a few decades and where the above tests show no frost resistance, one can examine the risk of future internal frost damage by determining the degree of saturation in the most exposed parts of the structure. The measured degree of saturation can then be compared to the critical degree. However, it is expensive and time-consuming to determine the critical degree of saturation of the concrete, and it is therefore not recommended. It is possible to find the critical degree of saturation for similar types of concrete in literature. One can also make a risk assessment as follows:

- If the most exposed part of the structure after long-term exposure has not reached a degree of saturation above 80%, and if the w/c ratio of the concrete is less than 0.55, the risk of internal frost damage is small.
- If, after prolonged exposure, the most exposed part of the structure has reached a degree of saturation above 80%, there is a risk of internal frost damage.

Surface damages caused by frost attacks in the presence of de-icing salts are relatively easy to identify. First, the cement paste is damaged around the aggregate grains and after a while the aggregate is loosened. In this way, the material layers are eroded. If one is unsure of identifying the underlying mechanism, it can be determined by petrographic analysis. Test method A according to SS 13 72 44: 2005 [22] can be used to determine whether the object is frost-resistant in the presence of de-icing salts. The purpose of the method is to ensure that recently produced concrete is frost resistant and it is therefore conservative. If it is used in the condition assessment, it is highly probable that the concrete is frost resistant in the presence of de-icing salts if the results are approved, but even concrete that failed the test may in reality have satisfactory frost resistance.

Surface damage in the waterline area of dam structures is relatively easy to identify and relate to frost attacks. Using test method B according to SS 13 72 44: 2005 [22], it is possible to determine whether the concrete is frost resistant in environments such as the waterline of dam structures. One can assume that a type of concrete that is frost resistant according to method B [22] is also frost resistant with respect to internal frost attacks. However, it should be noted that it is a somewhat conservative test method when it comes to internal frost attacks, see the reasoning in the previous paragraph.

2.3.4 ASR damage

General

Alkali Silica Reactions (ASR) is a damage mechanism that leads to cracking in concrete structures. In order for ASR to occur, access to reactive aggregate, sufficiently high alkali content (mainly from cement) and moisture is required. A swelling reaction occurs when the gel that is formed expands when absorbing moisture. Further details on the mechanism can be found in Appendix C.

The damage that occurs can roughly be divided into two categories:

1. local damage
2. global damage

The local damage is caused by the expansion of the reaction products which impair the mechanical and physical properties of the concrete, which in turn eventually leads to local cracks. The local crack formation is affected by the local stress condition. High compression stresses prevents expansion in the direction of the compressive stress. The expansion of the concrete leads to stress and strain gradients being formed in the structure, which in turn causes the structure to crack and global cracks are formed. The stress condition and the global crack formation are also affected by the shape and type of reinforcement (regular or pre-stressed

reinforcement) and the support conditions. In the same way as in the case of prevented thermal and moisture movements, the crack geometry is affected by prevented ASR expansions and expansion gradients.

Expansion and crack formation

The expansion of the concrete is governed by the expansion of the ASR gel. The reaction products may appear on the surface of an aggregate grain or inside an aggregate grain. The crack formation in the concrete depends to a large extent on what boundary conditions exist in the form of possible restraints for the structure in question.

Figure 2-17 shows a homogeneous concrete wall on bedrock. The wall movements in the x and y directions, respectively, are prevented along the boundary towards the bedrock. The concrete wall is assumed to be homogeneous and lacks reinforcement or is lightly reinforced with an evenly distributed reinforcement effect. No temperature or humidity gradient is assumed to occur. ASR causes the concrete to expand and micro-cracks to form. The supporting slab prevents the expansion of the wall, which leads to compressive stresses occurring in the lower part of the wall. The upper edge of the wall is relatively free to expand. The difference between the stress conditions in the lower and upper part, respectively, affects the micro- and macro-cracking. Cracks occur earlier in the upper edge compared to the lower edge. In addition to stress caused by ASR, stress arises due to restraints. The bearing slab prevents the lower edge movement, which means that "shear stresses" (τ , MPa) occur between the concrete wall and the supporting slab. The moment M [Nm] and the force F [N], respectively, are the resultant moment or axial force caused by τ . As shown in the figure, the moment causes tensile stresses in the top of the wall. The tensile stresses cause cracks that penetrate into the structure from the surface. The rough cracks - the crack width can be several millimetres - which are observed on the surfaces of the structures are caused by this mechanism among others. The cracks are further expanded due to thermal effects, drying shrinkage and frost attacks, see Figure 2-18.

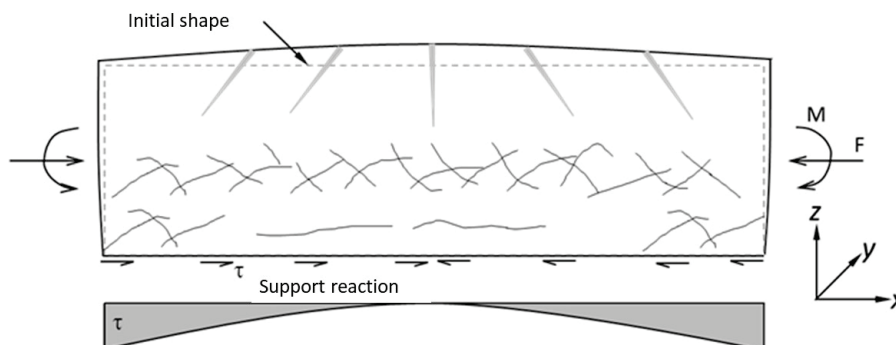


Figure 2-17 – How the supporting slab affects the crack formation in a homogenous concrete wall



Figure 2-18 – Structure damaged by ASR with a varying crack pattern.

It should be noted that the forces that occur due to the constraint caused by the supports also can be caused by other structural designs. Geometry and asymmetrical reinforcement can cause variation in crack pattern in the structure. The rough cracks seen in Figure 2-19 are the result of ASR expansion and unevenly distributed deformation in the structure.



Figure 2-19 – Flow splitter damaged by ASR [23].

Figure 2-20 shows a concrete element with longitudinal untensioned reinforcement and stirrups. At high reinforcement parts, the expansion is inhibited, especially if the structure is a pier. Axial expansion is counteracted by reinforcement and the compressive stress to which the pier is exposed and the lateral expansion counteracted by the stirrups. As stated above, the volume expansion at loading is smaller compared to the case where the concrete is free to expand. The result is that the structure surface cracks, while the inner parts can remain unaffected. The degree of damage is determined by the stress level, the amount of reinforcement and the geometry of the structure.

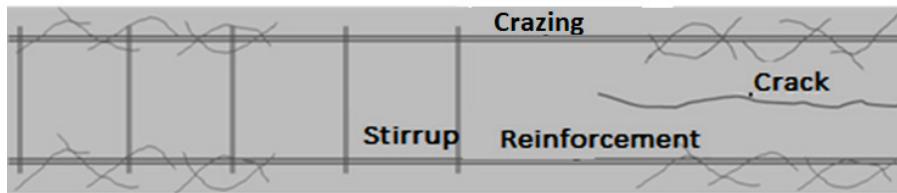


Figure 2-20 – How crack the crack formation is affected in a reinforced concrete beam damaged by ASR.

The ASR damage can be greater if the amount of reinforcement is low and if the structural element lacks stirrups. As can be seen from the right-hand part of the structural element in Figure 2-20, cracks parallel to the reinforcement can occur, see Figure 2-21. In pre-stressed bridge roadway beams, similar cracking can occur.



Figure 2-21 – Structure damaged by ASR with a cracking plane parallel to the main reinforcement.

Both temperature and humidity gradients can have a large impact on the crack formation. The mechanism affects in two ways. The reaction rate increases with both temperature and humidity. The part that is warmer and more moist expands faster, which causes the part that expands more slowly to try to obstruct (inhibit) the part that expands faster. An internal restraint arises like the case illustrated in Figure 2-17. The influence of the temperature and humidity gradient can, in adverse cases, be added to the ASR expansion. Figure 2-22 shows the influence that the moisture and temperature gradient has on the expansion of the concrete element, which can be added to the ASR expansion.

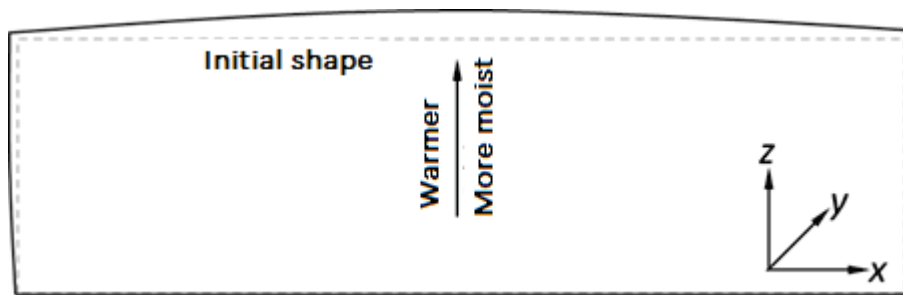


Figure 2-22 – Effect from the temperature and moisture gradient on deformations caused by ASR in a structure.

Diagnosis – Determination of ASR in structures

The determination of ASR through visual inspection can be done by the following observations:

1. Crack formation

The position and pattern of cracks as well as content of precipitation should be noted and photographed. Cracks arising from ASR are governed by restraining forces and stresses. The cracks orient themselves parallel to restraining forces. In the absence of restraining forces or when the restraining forces are large and operate from several directions, crazing (map cracks) is formed. It should be noted that other phenomena, such as plastic creep, also may cause crazing on the concrete surface [24]. ASR cracks develop later than most cracks. The time for the crack detection can be of great help in determining the underlying cause of the cracking. Therefore, it is important that the information presented in the previously produced inspection reports is taken into account when the causes of cracking are taken into account.

Depending on the type of reactive aggregate, the cracks are initiated from the aggregate periphery or from the inside of the aggregate. The crack width is at its maximum around the aggregate or inside the aggregate and decreases with increased distance from the initiation point. The cracks (often three of them) are symmetrically placed around the point of reaction according to Dyer [25]. The cracks may contain gel (the reaction product), which may also have been pressed out towards the surface of the concrete. The presence of gel filled cracks is a sign that ASR is the cause of cracking. The reaction product (gel) can react with substances in the concrete and change character, e.g. become more rigid. As described above, the gel may react with calcium to form calcium silicate hydrate which is more rigid than ASR gel. The gel that comes out to the surface can react with the carbon dioxide of the air to form a white precipitate [26]. This is evident from older cracked hydraulic structures. The appearance of the damage is similar to the damage caused by combined frost and leaching attacks.

A crack caused by ASR can be without gel or precipitation. It is possible that the gel is washed away or diffuses away from the crack. In some types of ASR attacks, the reaction between gels on the various substances of the concrete can produce new substances that block the migration of the gel to the crack and the surface of the concrete. Therefore, the absence of gel is not a reliable evidence that the cracking has not been caused by ASR [25].

2. Pop-out
When the reactive aggregate is close to the concrete surface, it spalls the concrete and forms a crater on the concrete surface, and pieces of concrete pop out of the concrete.
3. Discoloration
Sometimes ASR leads to discoloration of the concrete surface, especially in places where several cracks coincide [24]. The crack formation causes the various components of the concrete to dissolve and migrate towards the surface of the concrete, where they precipitate or react with the carbon dioxide in the air and discolour the surface.
4. Movements and deformations
All signs of expansion such as the joining of joints, movement relative to adjacent concrete sections, bulging of previously flat surfaces, closure of bending cracks and deflection of beams should be noted [24].

If visual inspection is not sufficient to determine or dismiss ASR as the cause of the crack formation, core samples should be taken from the structure, i.e. an in-depth inspection should be performed. The diameter of the core sample should be at least three times the maximum aggregate size. The length of the core sample should be at least twice as large as the diameter. Somerville [24] suggests core samples with a diameter of 100 mm and a length of 300 mm. If the structure contains tightly placed reinforcement bars and there is a risk of cutting the reinforcement while drilling, core samples of a smaller diameter, e.g. 75 mm, could be taken from the structure. It is important to mark the orientation of the core sample in relation to the orientation of the structure. RILEM presents a systematic description of the factors that should be taken into account during a visual inspection [27]. Review of the RILEM report is recommended for anyone who inspects structures damaged by ASR.

The drilled specimen can be examined in various ways:

1. Surface grinding
A disc is sawn/cut out from the core sample, preferably through two parallel cuts in the same direction as the longitudinal axis of the core sample. The disc is surface ground with abrasive to the desired flatness. If the concrete is weak, it is impregnated with epoxy to stabilize the cracks. If the epoxy contains fluorescent dyes, it becomes easier to observe the cracks when the flat surface is illuminated with ultraviolet light (UV light). If the concrete is treated with uranyl acetate, it reacts with the gel containing sodium and creates a yellowy fluorescent product which can be observed when exposed to UV light [24]. Through visual inspection and/or with a stereomicroscope (between 10 x and 100 x magnification) the surface is examined. ASR cracks occur around or inside the aggregate. The cracks in aggregates are connected with cracks in the cement paste. If the surface ground specimen shows a deep profile from the concrete surface, any delamination of the outer concrete surface layer can be observed.
2. Thin section
The sawn disc can be used to produce thin sections. Thin sections can be examined with a light microscope with polarized illumination and with SEM

(scanning electron microscope) [25]. The methods enable identification of the gel that is formed. Because ASR gel is amorphous, it does not let through polarized light and looks black if observed from the non-illuminated side. The scanning electron microscope enables the identification of various substances present in the crack. With the help of this information it is possible to determine whether the crack contains ASR products or not.

3. SEM and EPMA analyses

With SEM (1000 - 5000 x magnification) one can observe the boundary between very small reactive minerals and reaction products. Furthermore, ASR gel can be identified in small cracks in the concrete. If the SEM is equipped with EPMA (electron-probe micro-analyser), a semi-quantitative chemical analysis can be performed [27].

The current state and its development

The concrete expands and cracks due to ASR. The expansion and cracking are not in themselves the central issues, but their impact on the ability of the structure to meet the functional requirements imposed on it, is of central interest. Expansion and cracking affect the water-tightness and the transport properties (heat, moisture and leaching), strength and stiffness of the concrete, as well as interaction with adjacent structures (joints) and materials (reinforcement). It is difficult to assess a structure that is affected by ASR without being able to assess the impact of the ASR on the specified properties. In order to be able to make a systematic assessment, one must quantify the expansion and its future development as well as mapping the current crack formation and its future development with respect to the extent, spread, location and the width and orientation of the cracks.

The mechanical and physical properties of the concrete are governed by its expansion caused by ASR. The expansion/unit of time is a measure of the reaction rate and expansion at a time is a measure of the reactions that have taken place. The expansion is also a measure of the damage that has occurred in the concrete. In order to be able to perform a systematic state and lifetime assessment, the connections between the material properties and the current and future expansion should be known.

Expansion is usually expressed as strain (deformation per unit length, m/m). Units other than m/m occur as % ($100 \times m / m$) and ‰ ($1000 \times m/m$). The expansion can also be expressed as relative volume change (m^3/m^3). The expansion caused by ASR can be determined in a specimen (free expansion) or in a structure (supported, restrained expansion). With free expansion is meant that a concrete specimen that is exposed to ASR can expand freely without any counter-force. The expansion that takes place in a structure is not free. In a structure there are restraining forces from e.g. support, reinforcement and loads. Somerville [24], among others, indicates the relationship between the compressive and tensile strength of the concrete, its elastic modulus, and its free expansion caused by ASR. There are also empirical correlations between free expansion and restrained expansion for different counterbalancing stresses and the amount of reinforcement, [24]. Although the amount of data given in [24] is limited, it constitutes a good basis for analysis of a structure damaged by ASR.

The free expansion is measured on specimens in a laboratory environment, where they are subjected to accelerated tests. However, the expansion in a structure is more difficult to measure. The reason for this is that it may take a long time before the expansion starts and it is difficult to assess the time of when the expansion starts. Furthermore, it is difficult to assess in advance the location and direction of the expansion. Therefore, it is difficult to monitor expansion in a structure before the damage becomes visible. Instrumentation for monitoring is therefore usually performed when the cracks become visible. The monitoring provides good information about the development of the expansion. In combination with appropriate modelling tools, the measurements can provide good information about the current and future conditions of the structure.

To assess the current expansion of the concrete in a structure that has not been monitored, the average crack width per unit of length should be measured, provided that all expansion takes place in the cracks. Due to the fact that the expansion takes place in a structure, it is not free, but it is a restrained expansion. Below is a method for determining the restrained expansion, also known as the expansion index [24].

The restrained expansion is determined in the main and secondary direction of the structure. The main direction often coincides with the main principal stress directions, main reinforcement directions, pre-stressed reinforcement directions, direction of gravity, etc. The secondary directions correspond to the directions perpendicular to the main direction. Expansion caused by ASR occurs more easily in the direction coinciding with the secondary direction, i.e. the direction that makes the least resistance to expansion.

Five parallel lines of 1 m with a c-c distance of at least 0.25 m are drawn in both directions, see Figure 2-23. The crack width is measured at each intersection between the lines and the cracks. The average expansion for each direction is calculated as follows:

$$\bar{\varepsilon} = \frac{\sum \varepsilon_i}{n} \quad (2-2)$$

where

$$\varepsilon_i = \frac{\alpha \sum w \cdot \sin \theta}{L} + \beta \quad (2-3)$$

where

n = the number of points in each direction

w = crack width

θ = the angle between the reference line and the crack

L = the length of the reference lines

α = constant between 1 and 1.5

β = constant between $500 \cdot 10^{-6}$ and $1500 \cdot 10^{-6}$

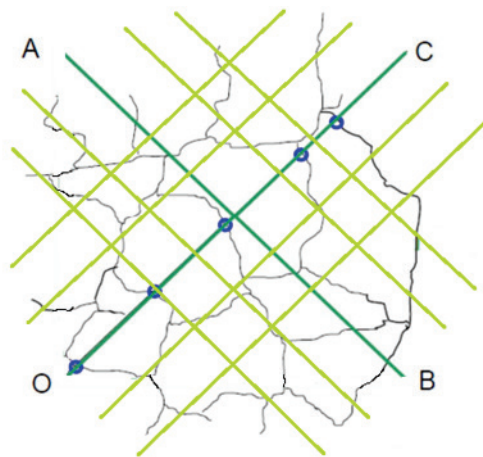


Figure 2-23 – Placement of five lines in the main (OC) and secondary (AB) directions respectively. The crack widths as the intersection between the lines (e.g. the line OC) and the cracks is measured.

It should be noted that there are other methods/procedures used for determining the expansion index, than the one presented above. The LCP cracking index can be mentioned among other things [28].

It is also important to determine the future development of the expansion, i.e. the remaining expansion. The task is important for the service life assessment of the structure and constitutes a basis for preventive and mitigating measures, repair and evaluation of the load-bearing capacity and stability of the structure. The remaining expansion is outlined below.

Figure 2-24 shows normalized expansion of concrete as a function of time. The curve applies to laboratory tests, but is applicable to the modelling of practical cases if the effect of moisture and temperature on the reaction rate are taken into account. As shown in the figure, the expansion consists of three phases: initial phase, acceleration phase and end-phase. It should be noted that the terms are not established. The expansion rate is greatest during the acceleration phase, where the cracks also become visible. Consequently, when ASR damage becomes visible, some of the total expansion may have occurred while some remains. Exactly when the cracks become visible and how much of the expansion remains is difficult to state, since both parameters are governed by the structure, the amount of reinforcement and the boundary conditions.

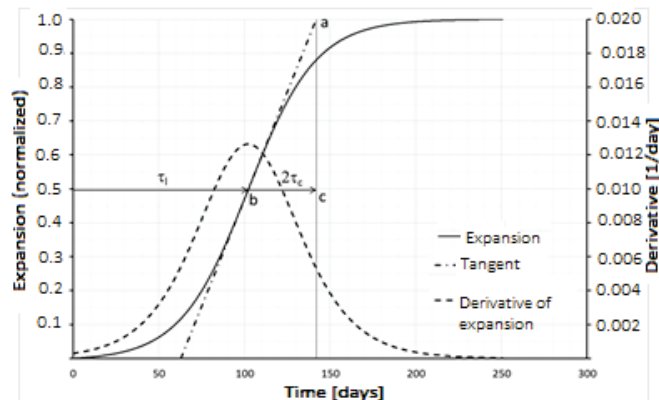


Figure 2-24 – Normalized expansion of concrete as a function of time.

The residual expansion is determined in the laboratory using core samples that are taken out of the structure. There is currently no standardized method for determining the residual expansion. There are some methods that are used in different laboratories. The methods are based on a cored specimen that is conditioned in different environments while their expansion is measured. All methods have both advantages and disadvantages. No methods will be described here, but the reader is referred to the relevant texts for the subject, e.g. [27].

Furthermore, some of the more or less well known methods include:

1. CBI method no. 1
2. LPC N ° 44
3. Swiss method
4. Toulouse method
5. Quebec method (Laval University) / U.S. Department of Transportation

When a core sample is taken out of a structure, it is released from confining forces. Therefore, the cored specimens are first conditioned in a humid chamber at 20 °C, while their change in length and possibly diameter are being measured. Once the deformations have stabilized, they are moved to different exposure environments to determine the residual expansion. The exposure environments can vary between different test methods. Below, general differences between the methods are described with regard to the conditioning and exposure environment of the test specimens. The following variations in the test methods occur:

1. Storage at 100% RH, 38 °C or 20 °C.
2. Sealed (protected from drying) specimen with 10 g water per kg specimen, 38 °C or 20 °C.
3. Storage in 1 mole of sodium hydroxide solution or saturated sodium chloride solution, 38 °C or 20 °C.

Storage at 100% RH can cause alkalis (particularly sodium ions) to be leached from the concrete, which can affect the reaction rate and the total expansion. Also, 100% RH may not reflect the actual humidity conditions of the structure. A sealed specimen with water addition can prevent alkali leaching. Water addition can lead to expansion of cement paste and gel as well as continued ASR. It is difficult to

distinguish between the effects, but the method can specify an upper limit for the residual reaction/expansion. It should be noted, however, that the supplemental water may affect the texture of the gel and change the stress conditions in the specimen.

Storage in sodium hydroxide and sodium chloride adds sodium ions (alkali) to the concrete and thus has an accelerating effect. Sodium hydroxide acts much faster than sodium chloride. The disadvantage of the method is that alkalis are supplied to the concrete which can give misleading results for those cases where the alkali content is limited in the concrete.

Temperature has a great impact on the reactions. Increased temperature increases the diffusion and reaction rate of the ions.

It is difficult to recommend a test method for determining the residual expansion. Unfortunately, it is often the distance to the laboratory, the contacts as well as the time and costs that determine the choice of test method. Therefore, the test results should be handled with caution and experts in the field should be consulted. If it is desired to use the results for analysis of load-bearing capacity, stability and service-life, the analysis should be supplemented with sensitivity analysis and risk assessment. If time and resources allow, larger numbers of specimens (which is often limited for economic reasons) should be used. Furthermore, alternative methods should be used if possible. It is important that the ASR expert and the expert conducting the structure analyses agree on the choice of method and the implementation.

2.3.5 Leaching

Type and effect

Decomposition of concrete caused by leaching occurs when water dissolves the cement paste constituents such as portlandite (CH), $\text{Ca}(\text{OH})_2$, calcium silicate hydrate, CSH, and calcium carbonate, CaCO_3 [29], [13]. Among the components, the portlandite is the most soluble in water and the calcium carbonate is the least. Concrete can be leached in five different ways [29]:

1. Solely leaching of the concrete surface
2. Leaching of the concrete surface in combination with mechanical erosion
3. Homogeneous leaching throughout the structure
4. Semi-homogenous leaching throughout the structure
5. Leaching through cracks and defective areas

Leaching can be powerful if the water is clean and soft, which e.g. occurs in the process industry (deionized water) and is naturally occurring in the Swedish mountain area. The leaching increases if the temperature decreases. Leaking, e.g. cracked and/or porous, concrete, increases the risk and rate of leaching. For concrete with high quality, especially with high water tightness, leaching takes a long time despite access to soft clean water.

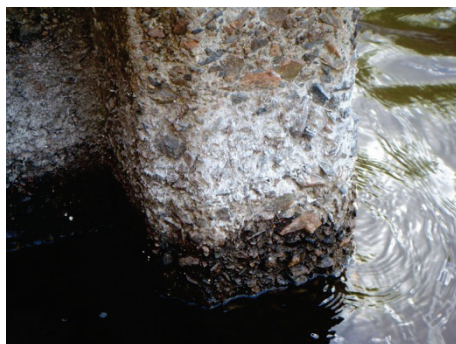
Leaching and similar processes can indirectly lead to cracking through an erosion process which causes weak zones with reduced strength to form in the structure,

which rupture due to other mechanical and physical processes. Leaching can expand existing cracks and lead to crack growth [11].

In order for homogeneous leaching throughout the structure to occur, a relatively large pressure gradient and concrete with relatively large permeability are required. Old concrete walls with a high w/c-ratio are an example of structures where homogeneous leaching can occur if the structure is subjected to one-sided water pressure. This phenomenon is unlikely for modern concrete with w/c ratios below 0.50. Furthermore, the phenomenon is theoretically impossible when the w/c ratio falls below 0.40, since the concrete then lacks capillary pores. Semi-homogenous leaching occurs in concrete with lower permeability. In this case, some channels are leached faster and govern the leaching process.

Examples of leaching

Figure 2-25a shows uniform leaching in combination with frost attacks at the waterline. The damage probably firstly occurs due water-saturation and leaching of the surface layer of the concrete first. Subsequently, the surface layer that has been weakened and saturated due to leaching is damaged by frost attacks and gets eroded. The decomposition process occurs due to layer-wise peeling, the speed of which is determined by the temperature of the air; the speed, temperature and composition of the water; and by the properties of the concrete such as w/c ratio the added pore volume.



a) Even leaching combined with frost attacks at the water line.



b) Leaching through cracks is common in old structures.



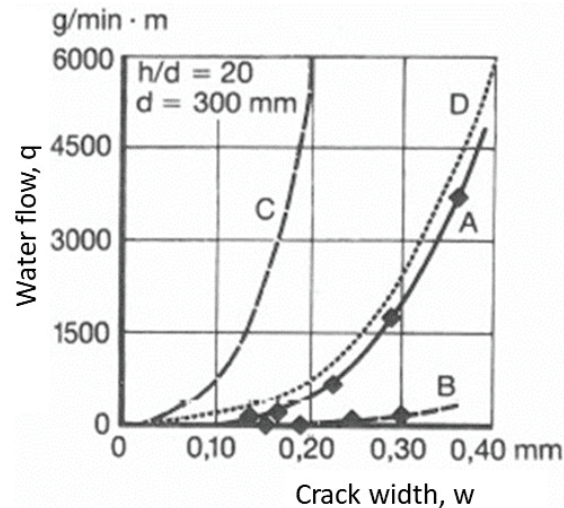
c) Leaching through a crack, which most likely occurred due to prevented thermal movement.

Figure 2-25 – Structures subjected to leaching [11].

In old structures where the concrete was compacted by ramming, joints often formed with incomplete bond between the concrete layers. The joints let water through which initially leaches the joint. If the water flow is limited, the joint is sealed by itself due to the leached calcium hydroxide having time to react with the carbon dioxide in the air to form calcium carbonate. Calcium carbonate that is not soluble by water clogs the joint, see Figure 2-25b. Dam structures constructed with high quality concrete, modern compaction technology and sealed joints exhibit good resistance to leaching. In such structures leaching occurs where the casting has failed or in cracked areas. Thermal cracks caused by restraint during hardening or by seasonal temperature variations are subject to leaching, Figure 2-25c, especially when the cracks occur on the upstream side of a dam structure.

Effects the crack width has on leaching

Figure 2-26 shows the water throughput as a function of crack width. Curve A is the measured flow after a short time and curve B is measured flow after 7 days (self-sealing). The curves C and D are calculated using Equation (19.8: 1) in Petersson [30]. As can be seen from curves A and B, the flow increases with increased crack width and the ability of the crack to self-seal decreases with increased crack width. According to curve B, the water flow is not stopped due to self-sealing when the crack width exceeds 0.30 mm. It should be noted that the age of the structure has a major impact on its self-sealing. The ability to self-seal decreases with the age of the structure.



A = Measured water flow after a short amount of time.

C = Calculated according to Equation (19.8:1) in Petersson 1994.

B = Measured water flow after 7 days of self sealing

D = Calculated with the same equation as in the case of C, but with crack widths as half crack widths. .

Figure 2-26 – Calculated and measured water flow [30].

The current state and its development

The current state of leaching can be determined visually or through laboratory analyses.

The visual assessment may only be done superficially on the surface of the structure or on drilled specimens. Lime depositions on surfaces and in cracks are signs of leaching. In cases where the precipitates are dry and no water drainage is observed on surfaces and cracks, it can be assumed that the process is slow or has stopped. The surface properties can be examined using a knife or chisel. If it is easy to scrape away parts of the surface and/or the area around the cracks, this indicates that the area is leached. The scraped-off depth can be the first estimate of the depth of the leaching. It should be noted that frost attacks and leaching can interact with one another. A surface (both on the uppermost layer of the structure and inside a crack) loses its strength and becomes more easily water-saturated due to leaching which increases the risk of surface frost attacks. Frost attacks have an accelerating effect on leaching and vice versa.

Laboratory analysis is performed on cored specimens. The test is performed to determine the extent and depth of the leaching. The analysis is about determining how much of the components important for cement have been leached out. The important substances are sodium, potassium, calcium, silicon, iron and aluminium. Leaching of sodium and potassium does not affect the strength of the concrete, but the pH of the concrete is lowered due to leaching. In concrete with only CEM I binder, the pH is lowered to about 12.5 when all of the sodium and potassium have been leached out. It is the calcium that maintains the pH value of 12.5 in the pore solution of the concrete.

The leaching of calcium lowers the calcium hydroxide (lime) content of the concrete. When the concrete is emptied of calcium hydroxide, calcium is leached from calcium silicate hydrate which gives the cement glue its strength, which results in a gradual reduction of the strength of the cement/concrete. Due to leaching of calcium from calcium silicate hydrate, silicon also begins to get leached from the cement which is followed by the leaching of iron and aluminium, which are also important constituents.

In a normal type of water-tight hydraulic structure concrete, the process is very slow. This also applies to surfaces inside cracks. Leaching can expand the cracks but the process is relatively slow. As mentioned above, the process can be accelerated if the concrete is exposed to frost attacks.

The laboratory analyses involve studying the content of the various substances at different layers parallel to the surface. The test also applies to the layers that are parallel or perpendicular to the crack plane, in case you want to study the leaching through a crack. The following test methods are available [31]:

1. Acid digestion with content determination using ICP-AES

“When dissolving concrete through acidification, concrete pieces are lowered into an acid bath consisting of distilled water with hydrochloric or nitric acid. The size of the concrete pieces can vary between a few hundredths of a gram to several hundred grams. The chosen size of the pieces is determined by the purpose of the test. The

dissolved concrete is diluted and analysed by means of atomic emission spectrometry with inductively coupled plasma (ICP-AES). Sometimes the abbreviation ICP-OES also occurs where OES stands for optical emission spectrometry. ” [31].

The method specifies the content of the various elements in the analysed sample. The accuracy of the method is governed by various factors. The cement type and cement content of the concrete should be known. The properties of the aggregate also affect the result. If the aggregate contains calcium, silicon, iron and aluminium it can affect the result. It is difficult to distinguish between the contributions from aggregate and cement. The tests should be supplemented with separate analysis of aggregate and analysis of concrete from an unaffected part of the structure to determine the cement content and the content of the various elements in an unaffected part of the structure. With this method, it is difficult to specify a fairly accurate leaching depth, since the tests are performed on a test piece which may be a few centimetres thick.

2. Scanning electron microscope (SEM)

“In a SEM, a high energy electron beam is swept across the surface of the sample. The electrons are generated in an electron source so as to be accelerated and focused into a beam of small diameter (1-2 μm). When the sample is hit by the electron beam, a plurality of signals are generated due to different physical mechanisms. Of greatest interest in the examination of concrete samples is the detection of secondary electrons (SE), back scattered electrons (BSE) and characteristic X-rays.” [31]

The method can be used for quantitative analysis of chemical composition at comparisons to standard samples with known content and/or an untested sample from another part of the structure. The method then reveals changes in the affected sample piece and enables determination of the leaching rate, reduction of e.g. calcium and the leaching depth. Compared to the acid digestion method, SEM is easier and more accurate when it comes to determining the leaching front. In order to perform the tests, well-made surface-ground test specimens are required.

3. Electron Probe Micro-Analyser (EPMA)

“An EPMA instrument is similar in some respects to the scanning electron microscope (SEM), which means that an accelerated and concentrated electron beam is used to bombard the sample surface. The instruments, on the other hand, differ on the point that the EPMA instrument is mainly used for quantitative analysis of chemical composition in materials. ” [31]

As stated above, EPMA analysis offers the same analysis possibilities as SEM, but with somewhat better results in terms of quantification of the composition of the material.

Preventive measures

During new construction, one should strive to select a concrete composition that is water tight and dimension the structure so that through-going cracks are avoided.

When it comes to leaching in existing structure, one should strive to stop the process as quickly as possible.

- Through-going cracks should be sealed to stop the water flow.
- The structural parts subjected to homogeneous and semi-homogeneous leaching should be sealed either on the upstream or downstream side in such a way that will stop the process.
- The structures subjected to leaching from the surface should be repaired (surface treated) before the damage reaches deeper into the concrete cover. The following limit values can be used for parameters that trigger the repair work.

The concrete cover should be at least equal to the largest of the values below:

1. Requirements according to SS-EN_1992-1-12005 [32] for the environment to which the structure is exposed.
2. The diameter of the main reinforcement (bonding requirements according to SS-EN_1992-1-12005 [32]).
3. Maximum aggregate size. If the erosion is allowed to continue further than this, it leads to greater intervention for repair with increased costs as a result.

2.3.6 Components damaged by corrosion

Corrosion process

Reinforcement in concrete is located in a highly alkaline environment ($\text{pH} > 12.5$). The alkaline environment protects the reinforcement against corrosion. The protection consists of a passivating oxide layer formed on the surface of the steel in an alkaline environment. The passivating oxide layer slows down the continued oxidation. The protection provided by the passivating layer may disappear for two reasons:

1. The carbon dioxide of the air can penetrate and react with the components that increase the pH of the concrete, thus carbonating the concrete ($\text{pH} < 9$). When the carbonation reaches the reinforcement, the passivating oxide layer disappears and the corrosion of the reinforcement begins.
2. Chlorides from sea water and de-icing salts penetrate into the concrete and eventually reach the reinforcement. At sufficiently high chloride concentrations, the chloride threshold level, the passivating oxide layer on the steel surface will pointwise get broken through, leading to local corrosion starting at these points, so called pitting corrosion.

When the protection provided by the concrete disappears, the reinforcement corrodes. Corrosion is an electrochemical process that takes place through the action of galvanic cells. A galvanic cell consists of an anode (positive pole) and a cathode (negative pole). The metal corrodes at the anode. There are different types of galvanic cells, i.e. corrosion cells [33]:

1. Corrosion cells with distinguishable anode and cathode surfaces; e.g. aluminium plate with brass fastening screw, where aluminium and brass make

up the anode and the cathode respectively. Another example is galvanized steel, where zinc is the anode while steel is the cathode.

2. Corrosion cells without a distinguishable anode and cathode; the entire metal surface serves as both anode and cathode; this can be done by the anode and cathode surfaces being small and numerous, whereby they change places with short time intervals.

In terms of reinforcement corrosion in concrete, it is also distinguished between micro- and macro-corrosion cells. Micro-corrosion cells are defined in the same way as Case 2 above. Macro-cells arise when the anode and cathode are located far apart from each other. This happens e.g. in connection with chloride-induced corrosion, as a part of the concrete structure is below the water surface. The part of the structure which lies above the water surface forms a cathode while the anode, i.e. the part that corrodes is located just below the water surface or at the splash-zone. Chloride-induced corrosion occurs locally in the form of pitting. Macro-cell corrosion may be similar to Case 1, i.e. the case where anode and cathode surfaces are distinguishable. In this case, the anode is located in the group while the cathode is made up by the surrounding surfaces.

Micro-corrosion cells lead to even corrosion or general corrosion. This is the case when e.g. the reinforcement corrosion is caused by the carbonation of the concrete. Macro-cell corrosion leads to pitting and point corrosion.

In concrete structures having cast-in reinforcement, galvanic corrosion may occur if the reinforcement is in contact with a more noble metal outside the concrete. If the reinforcement is in contact with turbines, pumps and generators containing more noble metals, the reinforcement (anode) can corrode. The corrosion can occur as point-corrosion or include a major part of the reinforcement. It should be noted that reinforcement does not corrode if it is in contact with a more noble metal that is cast-in.

The corrosion environment has a decisive influence on the properties of the corrosion products (rust) that are formed. E.g. red rust is formed if the oxygen supply is good at the anode. If the oxygen supply is limited, e.g. if the corrosion is under the water surface, black or green rust is formed. The red rust is porous and occupies considerably larger volume than the iron from which it comes. Consequently, the rust can induce spalling of the concrete. E.g. will corroding reinforcement be able to spall off the concrete cover layer when enough rust is formed. The black rust is considerably less bulky and therefore less "expanding". The black rust is dangerous in reinforced concrete because it can cause all of the reinforcing steel to dissolve without this showing on the concrete surface.

The process of corrosion of a non-cracked reinforced concrete structure is divided into two stages. During the first stage, which is also called the initiation stage, the passivating oxide layer disappears, see Figure 2-27. As noted above, carbonation of the concrete cover and penetration of chlorides are two causes which can cause the passivating oxide layer to disappear. During the initiation stage, the corrosion rate is very slow. Therefore, the corrosion that occurs can be ignored, i.e. it is assumed the reinforcement does not corrode. After the initiation stage, the propagation stage occurs during which the reinforcement corrodes. The corrosion rate is

governed by the environment surrounding the structure and the electrolytic conductivity of the concrete.

During the propagation stage, the area of the reinforcement is reduced. Bulky corrosion products can also spall off the concrete cover. Theoretically, the service life of the structure is surpassed when the covering layer is disintegrated or when the reinforcing area is reduced to such an extent that the load-bearing capacity of the structure becomes unacceptably low. The theoretical service life includes both the initiation and propagation stages [34]. The service life therefore depends on the duration of the initiation stage and the rate of corrosion. There are many factors that influence the service life of the structure. Which these factors are and what impact they have depends on, inter alia, the underlying mechanism, the corrosion stage and the environment in which the structure is located, as well as the properties of the structure and the constituent materials. For in-depth studies on corrosion theory, corrosion process and protection, as well as service life design of concrete structures with regard to corrosion, the reader is referred to [33], [34] and [35].

A concrete structure that is subject to corrosion attack can be protected or repaired to obtain a longer service life. The measures that can be taken are governed, inter alia, by the type and design of the structure, the corrosion mechanism, the corrosion stage and the shape and extent of the damage.

Inspection of a concrete structure damaged by corrosion

The corrosion process must have been going on for a long time before it can reveal itself and be discovered during a visual inspection. The corrosion process must have propagated far into the propagation stage before it can be detected visually.

Figure 2-27 shows a schematic view of the corrosion process. The horizontal axis shows the time [years] and the vertical axis presents the degree of corrosion, which here refers to the thickness [mm] of the corroded layer. When the reinforcement corrodes, corrosion products are formed. The properties of the corrosion products are governed by the access to oxygen and moisture. Increased amount of oxygen leads to greater volume of the corrosion product and increased humidity leads to the corrosion product being dissolved and transported away. Dense concrete makes transport of the dissolved corrosion products difficult. Interaction between the three mentioned effects governs the pressure that the corrosion products exert on the concrete cover. If the concrete is high strength and the concrete cover is thick, the concrete does not crack. The products are dissolved and transported away to the surface or any other place. After some time, the iron can disappear completely without the process being detected visually. If the concrete is weak and/or the concrete cover is small, the concrete spalls and the process becomes visible. The two mentioned cases are extreme cases of the damage that the corrosion process causes on the concrete cover. There are different variations between these two extreme cases.

Figure 2-27 shows three levels of “degree of corrosion”.

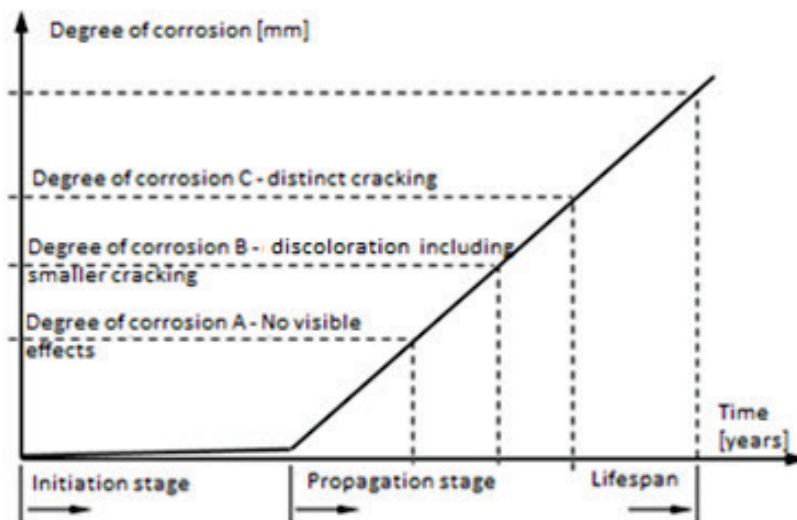


Figure 2-27 – Schematic image of the different stages of the corrosion process.

Degree of corrosion A characterizes a stage where there are no signs of ongoing corrosion that are detectable by visual inspection. Corrosion can be detected by testing. The following methods are available:

1. Sampling - for the determination of the
 - Chloride content at reinforcement level, section 2.4.4 and
 - Carbonation depth, section 2.4.5.

The fact that the concrete cover is carbonated or that a theoretical threshold value (e.g. 0.3% of the cement weight) is achieved does not mean that the degree of corrosion A is achieved. The concrete can e.g. be very dry or very wet so that electrolyte or oxygen are lacking to such an extent that the corrosion fails or is negligible. The methods only indicate that there is a risk of reinforcement corrosion.

2. Electrochemical methods - to determine
 - the resistivity of the concrete
 - mapping of the corrosion potential of the reinforcement
 - linear polarization resistance (LPR)

The methods are described in [35] with reference to deeper studies. Resistivity measurement as well as chloride measurement and measurement of depth of carbonation do not detect ongoing corrosion, but assess the risk of corrosion. Low resistance indicates conductive and continuous electrolyte in the concrete that facilitates the electron current and the corrosion process. The resistance of the concrete is affected by its moisture content. The resistance of the concrete decreases with increased moisture. The chloride content and the composition of the pore

system also affect the resistance of the concrete. Increased chloride content leads to lower resistance.

The potential of the reinforcement (the voltage) relative to a reference electrode, e.g. a $Cu/CuSO_4^-$, copper/copper sulphate electrode, is used to assess the probability of ongoing corrosion risk. Negative potential relative to the reference electrode indicates a corrosion risk. The greater the negative potential, the greater the probability of ongoing corrosion. The following evaluation is stated in the American standard ASTM [35].

Table 2-4 – Evaluation of probability of ongoing corrosion of steel in concrete structures in the atmosphere with the help of measured corrosion potential, according to American standard ASTM C876-09, [35].

Measured potential to $Cu/CuSO_4^-$ - reference electrode	Probability of ongoing corrosion
-200 mV and more positive	Low (10 %)
-200 mV to -350 mV	Uncertain assessment ("grey area")
-350 and more negative	High (90 %)

The LPR method is used to assess the instantaneous value of the corrosion rate. The method involves feeding in current to change the potential of the steel. There is a connection between the fed current and the rate of the corrosion in progress. By measuring the rate one can judge whether and where the corrosion takes place. The method is influenced by the size of the corrosive surface. It does not require much current to polarize a point corrosion, and therefore the method can lead to incorrect conclusions if the size of the corrosive surface is not known. The reader is referred to [35] for deeper studies.

3. Opening of a "window" in the structure

In order to check the presence of corrosion, the reinforcement can be dug out and exposed in selected surfaces, "windows", which after inspection are re-cast. Location of the windows and their size are selected from where corrosion is suspected to take place. When constructing windows and repairing them, the load-bearing capacity of the structure must be taken into account.

Degree of corrosion B refers to a stage where different signs of corrosion occur but which requires extra attention by the inspector. Discoloration and thin cracks may occur. Furthermore, the "drumminess" of the area when struck with a hammer may indicate ongoing corrosion. As described above, cracking and diffusion of corrosion products against the concrete surface depend on the properties of the concrete, the thickness of the concrete cover and the moisture content of the concrete. It should be noted that the conditions may be such that the surface is not discoloured at all, or the corrosion products are mixed with calcium hydroxide which is leached and transported to the surface. If the concrete surface is contaminated then the discoloration and cracks are not visible. Fortunately, the human ear is very sensitive to the mentioned drumminess sound and can detect relatively small areas with delamination of debonding.

Degree of corrosion C is a stage of visible cracking. Figure 2-28 shows different types of cracks caused by reinforcement corrosion. Type CC1 is cracks that run along the reinforcement through the concrete cover layer. Type CC2 results in decomposition of the cover layer, which runs along the reinforcement. Type CC3 results in delamination of the concrete cover. It should be noted that the cracks may contain corrosion products, which are brown, or be completely empty. The latter case may lead to incorrect conclusions when determining the cause of cracking. The cracks may also contain lime/calcite which are leaching products. In hydropower structures, the rock can discolour the water, which in turn discolours the lime/calcite and causes the leaching products to be confused with corrosion products.

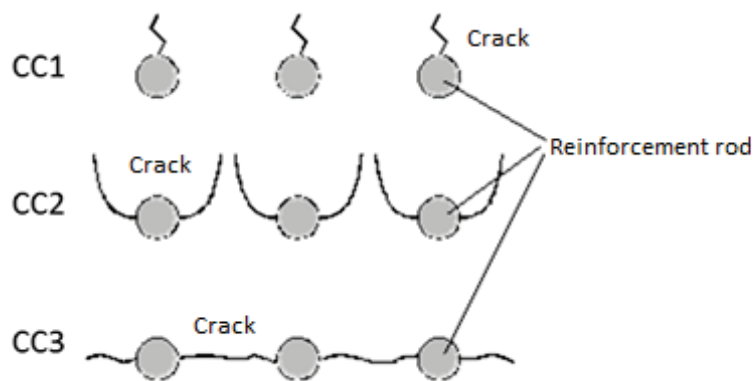


Figure 2-28 – Cracking patterns that occur when reinforcement corrodes, [8].

2.3.7 Evaluation of core samples and boreholes

General

Core samples are taken in order to

1. determine or verify a certain property of the material. The best way to evaluate a core sample is therefore to check whether it meets the requirements of a test specimen for carrying out the planned test or controls.
2. determine the quality of the concrete by visual evaluation. The quality of the concrete is determined according to a scale consisting of six classes according to the so-called. BETUT system (Concrete core evaluation, *Swedish: "BETongkärnUTvärdering"*) [36].
3. examine the presence of zones with cracking and zones subject to degradation processes.

For purpose 1 above, the sampling is performed to determine material properties by testing. The evaluation methods are therefore often prescribed by standards or specific regulations, see section 2.4. For purposes 2 and 3, the evaluation is discussed in detail in [36]. Here is a brief description of the methodology.

Evaluation of core sample

This section is based on [36].

During evaluation, a visual inspection is performed to classify the concrete quality of a core. The classification is done according to a scale in six steps where Class 1 corresponds to very good concrete and Class 6 corresponds to very poor concrete.

Table 2-5 –Explanation of the six different quality classes used at Vattenfall’s classification of the concrete quality of concrete cores. The presence of cobbles and core loss will be placed in Class 1 and Class 6 respectively, [36].

Class	Description
1	Vary good concrete. It is homogenous and free of cavities and pores.
2	Good concrete. It is relatively homogenous and free of cavities. Some occasional pores can be found. The concrete is not completely smooth.
3	Average concrete. Pores are more abundant. The pores have no connection to each other. Some cavities occur. Material is missing in the surface between the larger stones in the concrete.
4	Below average concrete. Traces of leakage of water are common. Many pores are connected to each other and form systems of pores. Larger cavities occur.
5	Poor and very permeable concrete. Large, coherent pore systems and deep cavities occur.
6	Very poor concrete. It barely keeps together. The core often consists of pieces of concrete.

In addition, special features are noted such as the presence of reinforcing bars, lime precipitate, browning, old grout etc.

This system is based on the fact that the quality of the concrete can be divided into six clearly distinguishable quality classes, see Table 2-5. As a core is reviewed, it is noted in a protocol how its quality class varies with its length. During the classification, which is made visual, the cohesion of the concrete, "number" of pores and the connection between them, the amount of cracks and cavities are studied. Class 1 corresponds to a very good concrete and Class 6 corresponds to a very poor concrete. The photograph in Figure 2-29 shows examples of how cores from each class can look [36]. Water tight concrete is equivalent to Class 3 or better. Since the classification is carried out visually, the classification to a certain extent becomes subjective, and especially on the borderline between two different classes different surveyors can classify the concrete differently.



Figure 2-29 – Example of what cores from their respective quality class may look like [36].

An evaluation also makes observations of up to seven different characteristics in the concrete: plums, core loss, brown colour, lime leaching, reinforcement bars, old grout and crack occurrence. The information is useful for assessment of ongoing degradation processes. These properties are further described in Table 2-6.

Table 2-6 – Explanation of the properties that should be examined when evaluating a concrete core, [36].

Properties	Description
Plums	Plums are large stones that have been used to save concrete. The limit for what can be considered as a plums should go at size > 64 mm since this is the largest aggregate size that has been used fairly widely (1950s). Although there are even larger aggregate stones (128 mm) in concrete structures from the 1930's, it is generally difficult to assess whether it is plum or aggregate. The transition surface between the concrete and the plum should be checked for traces of leakage.
Core loss	Core loss is the part(s) of the core sample that has been lost during drilling. If quantities with sludge and gravel are found, there is a risk that the material will be flushed away with the flushing water. A core loss can also be caused by cavities in a structure.
Brown colour	The occurrence of brown discolorations may mean that the concrete is leaking. A brown discoloration occurs when humus rich water is transported through the structure. Thus, the concrete is leaking, i.e. of quality class 4 or worse.
Lime leaching	Leaching happens due to the fact that the relatively soluble calcium hydroxide contained in hardened cement paste is dissolved by water flowing past or through a pervious paste, resulting in a calcium hydroxide deficit. Leaching causes lime to precipitate on the concrete. Thus, the concrete is leaky, i.e. of quality class 4 or worse.
Reinforcement bars	Core drilling can lead to the reinforcement of the structure being drilled or damaged. In some cases, the drilling work is required not to damage existing reinforcement. All occurrence of reinforcement should be noted (dimension and depth). It may also be interesting to

Properties	Description
	note if the reinforcement exhibits corrosion damage. Surface rust, however, may have occurred after the core was drilled out.
Occurrence of grout	Concrete from older structures may contain residues from previously performed grouting. For cores that are obtained in order to verify the results of a grouting, the main purpose of an investigation can be to see how large amount of new grout there is. At times grout is pigmented to facilitate these verifications.
Occurrence of cracks	It is not uncommon for cracks to occur in concrete structures. Cracking is a warning sign that something may not be right with the structure, especially if the cracks are rough. To determine the importance of cracking for load-bearing capacity, all the dimensions of the cracks are of importance, as is the system to which they are bound.

Instructions according to SS-EN 12504-1: 2009 "Testing of concrete in finished structures - Part 1: Core samples - Withdrawal, examination and pressure testing" [37] can be used to determine the compressive strength and compressive strength class of the concrete.

The result of compressive strength measurements can be used to verify a quality classification. The starting point is that low compressive strength results in poor concrete quality. If the result from the compressive strength measurements and from the concrete quality classification are dotted into a diagram, the dots should be approximately collected along one line, see Figure 2-30. If the deviation from that line is large, the quality classification should be checked [36]. Class 6 concrete is usually very difficult to test.

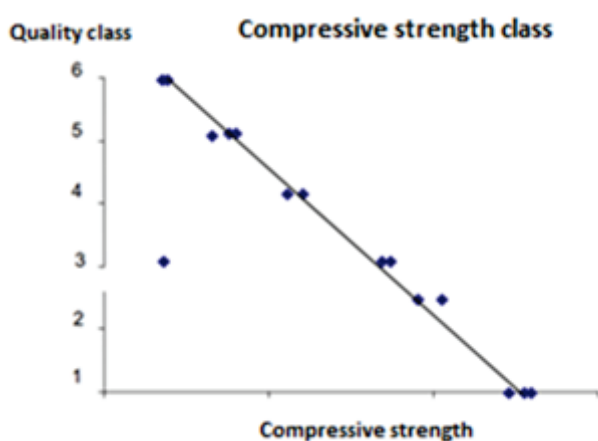


Figure 2-30 –Results from a quality classification and from a compressive strength test can be set against each other to check that the classification is correct. The diagram above illustrates an example of good agreement, [36].

Evaluation of boreholes

Concrete water-tightness, cracking and other defects are investigated with water loss measurement and borehole image scanning. Scanning of boreholes to detect cracking, degradation processes, cavities in casting and grouting can be done with equipment with varying capabilities from simple cameras to advanced equipment that scans the borehole with video cameras, ultrasonic equipment and equipment that measures electrical resistivity. There are various data processing systems that map cracks with respect to location and orientation, material boundaries, cavities, water leakage, etc. The advanced methods are gathered under the term BIPS (Borehole Image Processing System). Video footage is described in detail in [36]. The reader is referred to literature and performers for detailed method descriptions.

Lugeon tests are made to determine whether the concrete adjacent to the borehole is tight or not. During the measurement, the amount of water which can be pressed into the concrete at a certain time and with a certain pressure is registered while the opening of the hole is sealed by means of plugs. The water loss is stated in Lu (Lugeon, after Maurice Lugeon). 1 Lu corresponds to 1 liter of water per meter of borehole and minute at water pressure 1 MPa (10 bar) [1 Lu = 1 l/(min·m·MPa)]. If the plug(s) are placed at different depths in the hole, the permeability of the concrete can be mapped at different depths [36]. Lugeon tests are also used to determine the conductivity of the rock, (Eriksson and Stille 2005). Lugeon tests are also used for planning of grouting and verification of completed grouting, see also [36], [38] and [39]. For Lugeon tests, it is important to adapt the pressures applied to the current structural design and general status so that there is no risk of hydraulic fracturing of the concrete.

2.4 SPECIMENS, SAMPLING METHODS, LABORATORY METHODS

Below, different standards are referred to. It should be noted that standards are constantly revised and changed. If it is important that the test is performed according to the current standard, it is important to find out the contents of the latest version and that the date of the edition used is always specified.

2.4.1 Sampling through core drilling

Sampling and core drilling for hydropower plants is described in detail in [36]. Furthermore, the following standards should be considered:

- SS-EN 12504-1: 2009 - Testing concrete in structures - Part 1: Cored specimens - Taking, examining and testing in compression
- SS-EN 13791: 2007 - Assessment of in-situ compressive strength in structures and precast concrete components
- SS-EN 12390-1: 2012 - Testing hardened concrete - Part 1: Shape, dimensions and other requirements for specimens and moulds

2.4.2 Density and porosity

The following standard can be used to determine the density of the concrete:

- SS-EN 12390-7: 2009 - Testing hardened concrete - Part 7: Density of hardened concrete

There is no SS-EN standard for determining the porosity of the concrete. Here it is suggested to use the same specimen used to determine the density of the concrete, but use the procedure specified in:

- SS-EN 1936: 2006 - Natural stone test methods - Determination of real density and apparent density, and of total and open porosity
- SS-EN ISO 12570: 2000 - Hygrothermal performance of building materials and products - Determination of moisture content by drying at elevated temperature - Amendment 1 (ISO 12570:2000/Amd 1:2013)

It should be noted that drying of a specimen should occur at 105 °C.

2.4.3 Moisture, moisture content and degree of saturation

There is no SS-EN standard for determining the air humidity or the moisture content of the concrete, see section 2.3.1.

- EN ISO 12570 Hygrothermal performance of building materials and products.
- Determination of moisture content by drying at elevated temperature (ISO / FDIS 12570: 1999).

2.4.4 Chloride content in concrete

- SS-EN 14629: 2007 Products and systems for the protection and repair of concrete structures - Test methods - Determination of chloride content in hardened concrete

2.4.5 Determination of carbonation depth

- SS-EN 14630: 2005 Products and systems for the protection and repair of concrete structures - Test methods - Determination of carbonation depth in hardened concrete by the phenolphthalein method

2.4.6 Leaching

There is no SS-EN standard for determining the air humidity and the moisture content of the concrete, see section 2.3.5.

2.4.7 Strength

- SS 137231: 2005 Concrete testing - Hardened concrete - Tensile strength of test specimens.
- SS-EN 12390-6: 2009 Testing hardened concrete - Part 6: Tensile splitting strength of test specimens
- SS-EN 12390-3: 2009/AC: 2011 Testing of hardened concrete - Part 3: Compressive strength of test specimens

- SS-EN 13791: 2007 Assessment of in-situ compressive strength in structures and precast concrete components

2.4.8 Elastic modulus

- SS-EN 12390-13: 2013 Testing hardened concrete - Part 13: Determination of secant modulus of elasticity in compression

2.4.9 Concrete shrinkage

- SS 137215: 2000 Concrete testing – Hardened concrete - Shrinkage.

2.5 UNDERWATER INSPECTION, DIVING INSPECTION, ROV

Sometimes structures below the surface of the water also have to be inspected in order to check for the existence of damage or cracking. E.g. there may be an interest in inspecting the upstream side of a front slab where there is leakage or cracking on the downstream side in order to examine whether the crack is continuous all the way to the upstream side.

Underwater inspections usually take place either with divers or with some form of equipment for driving around and photographing underwater. In the latter case, the collective name is usually the ROV (Remotely Operated Vehicle). If the purpose is to detect cracks, there are some parameters that strongly influence the possibilities of doing so. The first is the visibility in the water. In some watercourses, the visibility is often very poor due to large amounts of organic material or fine-grained sediment. In most mountain rivers, however, the visibility is very good. The other parameter that has a large impact is potential coatings on structures that have been under water for long times. Sometimes, fouling with algae and even black coatings are formed, which practically makes it impossible to detect anything other than very rough cracks or newly formed cracks. The third parameter that can have a major impact on the quality is if there is access to good lighting for the study itself. With increased depth, the need for stronger light increases to compensate for the lack of daylight or sunlight.

2.5.1 Diving inspections

Normally, diving inspections are carried out down to depths corresponding to approx. 18 m, which is the limit for diving with normal air mixtures. The diving times at this depth are about 70 minutes. For deeper dives, other air mixtures are normally required and the diving times are shorter.

During diving inspections, it is recommended that the diver is well informed about what the purpose of the diving inspection is and what is being sought. A joint review between divers and the inspector should be done before the diving commences. At the beginning, the following points should be reviewed:

- The purpose of the diving inspection
- Geometric conditions and study of drawings
- Planning of the diving route
- Work environment and safety

For the high quality of the diving inspection and good documentation for the best condition for follow-up in the future, the diving team must be equipped with a recording camera (on the diver's helmet) and equipment for recording both sound and image. Sometimes even hand held sonar equipment. There must also be equipment for oral communicating directly with the diver and a monitor to observe what is being seen during the underwater inspection. The purpose of the latter is that an expert should be able to monitor the inspection and guide the diver to places of interest for possible supplementary study with e.g. tapping the surface or crack width measurement. The diver should also continuously indicate the approximate position and depth for orientation also on the film during post session review.

2.5.2 ROV inspections

Underwater inspections by ROV are usually performed with small or medium-sized ROVs that are controlled from land by an operator and which can see, inter alia, the current depth and what is being filmed with camera mounted on the ROV. A study of different techniques for ROVs and what possibilities for detection of cracks etc. that have been found have been studied in a thesis [86] which is recommended for an in-depth study on the topic.

Depending on the size of the ROV, different amounts of equipment can be mounted on it. A common limitation on ROVs is the available length of the cable for power and sound & image transmission as well as control of the ROV. Some ROVs may have a few hundred meters of cable, while large ROVs may have several kilometers of cable, which allows for inspections of e.g. long tunnels. Figure 2-31 below shows three examples taken from [86].



Figure 2-31 – Examples of ROVs at different sizes [86].

Depending on the load-bearing capacity of the ROV, different amounts of equipment can be mounted. Usually there is lighting and a camera for video recording. Additional equipment that can be mounted is sonar equipment for detecting deviations e.g. on the upstream side of a dam, or a gripper arm for easier work or examinations. New technology for scanning of e.g. surfaces with green lasers are also available on the market today. However, the visual inspection is still the best method for thinner cracks (<1 mm). Larger cracks may possibly be detected by other techniques.

3 Analysis

3.1 INTRODUCTION

This chapter describes various analyses and analysis methods that focus on determining the origin of cracking or impact from cracks on the safety of the dam or its long-term functionality.

3.2 METHODS OF ANALYSIS

Regardless of what type of analysis is carried out, a model is needed, i.e. an image that describes how to interpret the effect on the structure, thus forming the basis for the simplifications and assumptions being made. By model is meant here everything from a conceptual model, a "mind model", an equation, e.g. a finite element model. There are many different types of analysis methods that can be used depending on application. In this section, the various types of analysis methods have been attempted to be categorized and described based on their application for evaluation of cracking or cause of damage as well as impact from cracking in concrete structures.

3.2.1 Conceptual model

In the conceptual model, an understanding of the effect on the structure is required, i.e. an understanding of how the structure carries the loads, as this affects how much of the dam that needs to be considered, how boundary conditions and loads are applied etc.

Expansion joints are normally suitable zones where it is possible to divide the structure into substructures. This is further described in Chapter 3 in [40], including how much of the surrounding rock that needs to be considered depending on the type of analysis being carried out.

The conceptual model also includes analysing possible and probable causes of any observed damage, i.e. which loads or mechanisms may be behind the damage that has been observed. This becomes input to subsequent calculations where the structure is analysed based on assumptions made with the conceptual model.

The conceptual model forms the basis for which analysis method is applied later. This means that there is already a large risk of sources of error when interpreting a real structure into a conceptual model. In other words, even if the analysis methods (e.g. the calculations) are internally valid (correct), these interpretations/assumptions have a large impact which can lead to the wrong conclusions. It is therefore important that the reviewer is active early on in the project and can be involved in discussions about the basic assumptions in the conceptual model, see [41].

3.2.2 Analytical calculations

Analytical calculation models for evaluation of cracked structures can be applied to simple cases, where e.g. the structure is regarded as a stand-alone element with

well-defined boundary and initial conditions, which are subjected to mechanical (e.g. bent beam) or environmental (e.g., one-dimensional transport through material) stress.

In simpler cases, these methods are often preferred as they are cost-effective, and are therefore suited for parametrical studies. These models should be conservative based either on conscious choices of the operator or due to built-in conservatism in the calculation method.

Examples - (abbreviations are explained in the text below);

- Stability calculations (global/local, probabilistic analyses, etc.)
- Load-bearing capacity (stage I - III, MCFT, strip method (slabs), etc.)
- Behaviour models for prediction of measured data (MLR etc.)
- Decomposition models (1D model for e.g. leaching)
- Dynamic mass-spring systems (1D model)

Most analyses are carried out based on a deterministic model, i.e. where loads and material properties are chosen to correspond to e.g. real response or limit states associated with design, such as; serviceability limit state, ultimate limit state, stability analyses.

In stability analyses, traditional stability calculations are fairly accepted. These are applied by analysing the dam as a rigid body where the dam body must be safe against sliding and overturning. E.g. the RIDAS [3], [4], application guide (RIDAS TV) section 7.3 [42] provides guidance on acceptance conditions, e.g. 1.5 for the ratio between stabilizing and overturning moment for common load cases regarding overturning stability. However, it should be noted that in cases where cracks are present in the dam body, these can lead to internal failure modes which are largely determined by the material strengths of the concrete and the reinforcement. In these cases, design methods according to cross-sectional analyses should therefore be considered according to RIDAS [3], [4], where the analyses are instead carried out according to the partial coefficient method. This will be further discussed in Chapter 3.9.

In analytical methods for load-bearing capacity, the concrete is assumed to be cracked and inactive in parts of the cross sections under tension for stage II (serviceability limit states) and III (ultimate limit state). The same assumptions also apply to the strip method. In these methods, it is only the reinforcement that carries load in the parts of the cross sections exposed to tension. An important difference to advanced non-linear calculations based on the finite element method is thus that these advanced methods also take into account the load-bearing capacity of non-cracked concrete between the cracks.

Analytical calculations are often combined with more advanced calculations, e.g. for more complex cases where calculations are carried out with the finite element method and cross-sectional forces are extracted. These forces are then used in analytical calculations to determine e.g. the amount of reinforcement, etc. In addition, analytical calculations can and should be used for verification in cases where more advanced calculations are carried out, in order to check if the results are reasonable. For this purpose, several different methods have been developed

for calculating the load-bearing capacity such as Modified Compression Field Theory (MCFT) from [43], [44].

In probabilistic analyses, e.g. Monte Carlo simulations, where thousands of analyses are required due to varying input data it is often unmanageable to combine the probabilistic analysis with more advanced numerical methods. This is because the calculation time for all these analyses becomes very long. In these cases, simpler analytical calculations are usually applied, see e.g. [45].

In the prediction of measurement data, it is possible to apply Multiple Linear Regression Analysis (MLR) to define a relationship between two or more variables (e.g., water level, temperature, time, etc.) used to adapt linear equations that can estimate expected behavior based on these variables; [46]. This is particularly useful for defining e.g. threshold levels on measured data if it is outside the expected value. However, it should be remembered that these predictions cannot be used for the assessment of dam safety i.e. determination of how/if any risk of failure etc. exists or if significant change occurs due to non-linear behavior etc.

When considering degradation phenomena and their long-term effect on structures, stationary and transient mass transport models are used to describe heat, moisture or chemical transport. In this context, it is important to consider that there is a large difference between transport in a continuum (e.g. non-cracked concrete) and a case in which cracks are present. These transport processes are often considered in 1D for simple standard cases that can be solved analytically. However, if non-linear properties are considered, a numerical calculation method is needed, e.g. finite element method (see section 3.2.4) or finite difference method (see section 3.2.5)

Dynamic mass-spring systems are mainly used where the response of the structure to a rapid dynamic load is to be determined. The properties of the spring and the oscillating mass are adapted to correspond to the properties of the structure that weigh the stiffness of the cracked and non-cracked parts respectively, see e.g. [47].

3.2.3 Finite element calculations

In many cases, real structures are so complicated that it can be difficult to apply the simpler analytical methods without making very rough assumptions. In case of e.g. a complicated geometry or complicated load conditions, finite element calculations are suitable for use. This is because an arbitrary geometry or arbitrary load conditions can be considered by dividing the structure into a large number of elements which together form an approximation to the structure.

The majority of all numerical simulations carried out are based on the finite element method with the assumption of linear response of structure and material. Linear response is a basic requirement in order for e.g. superposition of loads, e.g. at load combination etc., to be able to be implemented. The finite element method is a general method that can be applied to create arbitrary geometries, load cases etc., which are discretized in a number of elements.

Examples;

- Stability calculations (globally/locally) (see e.g. sections 5.4, 5.5 and 5.8)
- Deformations and load-bearing capacity, such as frame analysis
- Reinforcement measures (pre-stressed cables, overlay, etc.) (see e.g. section 3.4.6)
- Simpler simulations of construction sequence (casting stages or demolition/rebuilding) (see e.g. Figure 3-1)
- Evaluation, often linked to dam measurements

An example of this is illustrated in Figure 3-1, which presents the result of stresses from simulation of stage expansion of an arch dam. In Figure 3-1a a simplified model is illustrated which includes that the dam is described with orthotropic stiffness properties to take into account the effect of joints and in Figure 3-1b is the corresponding, more detailed analysis of each individual dam pier where the interaction between them is described by non-linear contact conditions. In this case, the calculation shows that the simplified way is relatively in line with a more advanced method.

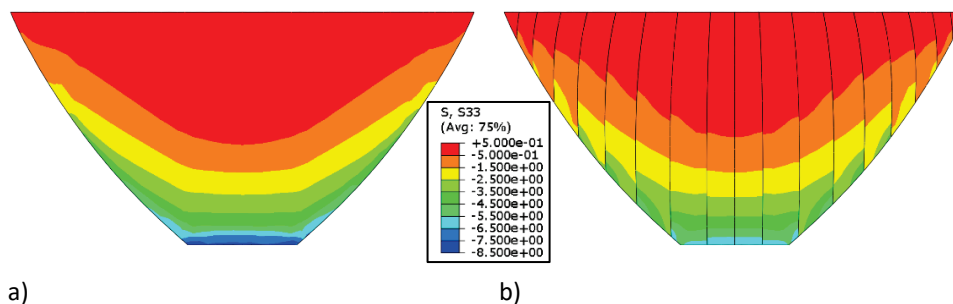


Figure 3-1 Illustration of stresses during simulation of stage expansion of an arch dam, a) simplified method with orthotropic stiffness properties, b) advanced method with contact conditions between each dam pier [48].

3.2.4 Non-linear finite element calculations

By non-linear analysis it is referred to a complex structural behaviour where synergy can exist between different effects so that superposition is no longer possible. There may be several reasons why a structure has a non-linear behaviour;

- Non-linear contact conditions/boundary conditions - the boundary or contact conditions of the structure react differently depending on load or load level (e.g. friction, non-linear springs etc.)
- Non-linear material behaviour - the properties of the material change with respect to time, load etc. (e.g. cracking, plastic deformation, creep etc.)
- Geometric non-linearity - the structure is subjected to large deformations (or has initial imperfections) which can lead to altered stiffness of the structure or instability (large settlement, 2nd order effect, buckling, etc.)

This means that in these cases the load history is important, because if two loads act on one structure, the structure will react differently depending on the order in which they are applied. An example is a gravity dam with non-linear contact conditions (friction) which is subjected to its own weight and water pressure. In this case, the self-weight must first be applied because otherwise there is no normal

force across the friction plane which can withstand the horizontal load from the water pressure.

The most common form of non-linear material behaviour that is considered is reasonably plastic deformation of steel structures or cracking in concrete structures. In these cases, the stiffness of the structure is reduced at increased load, which leads to redistribution of stresses in structures.

Geometric non-linearity can usually be neglected in hydropower structures, as it mainly occurs in slender structures. However, there may be applications where this is important. It can be for analysis of floating debris, slender piers/beams exposed to pressure e.g. between monoliths in a buttress dam or at a spillway.

Below are examples of applications where non-linear analyses are often used.

Examples;

- Stability calculations (globally/locally) incl. risk of material failure and the impact of combined modes of failure
- Deformations and load-bearing capacity
- Reinforcement measures (pre-stressed cables, concrete overlays, etc.) including the influence of initial defects
- Construction sequence (casting stages or demolition/rebuilding) and new concrete
- Evaluation of damaged structures, often related to dam measurements

Two examples of simulation of cracks are illustrated in Figure 3-2 and Figure 3-3. In Figure 3-2, cracking and crack propagation caused by seasonal variations in temperature have been simulated with a smeared crack model. Figure 3-3 illustrates how discrete cracks (physical crack planes) open up due to ASR expansion in combination with drying shrinkage and loading.

Depending on the purpose of the non-linear analyses for cracking, one or the other technique may be more suitable. If the purpose is to find the cause of an observed crack formation or to predict the crack formation in a structure, a methodology is needed that can describe crack initiation and crack propagation, as illustrated in Figure 3-2. If the purpose instead is to assess the impact of already known/observed cracks, it is not necessarily needed to simulate this crack initiation and propagation. In these cases it may be more suitable to include mapped cracks as discrete crack planes directly in the model, where these cracks can open and create a physical crack width directly in the model. This is further described in Chapter 3.5.4.

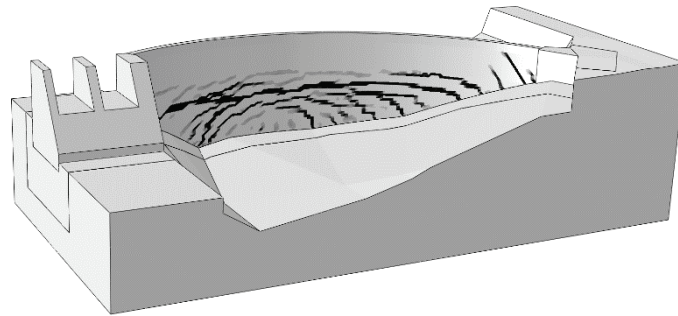


Figure 3-2 Example of a simulation of crack formation in an arch dam [49].

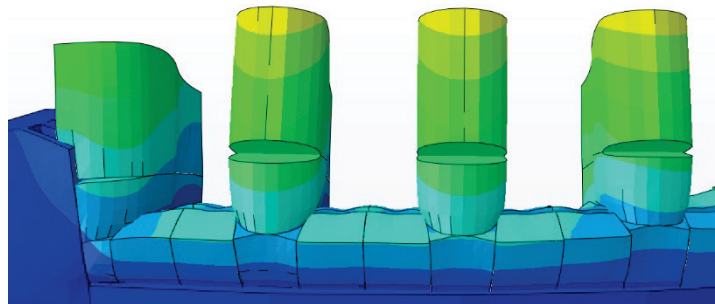


Figure 3-3 Example of discrete cracks in spillway piers.

3.2.5 Other types of calculation methods

In addition to the analysis methods described above, there are also a number of different calculation methods. However, these are applied to a much smaller extent within the construction area. An example of this is the finite difference method. The finite difference method is based on Taylor expansion in order to solve differential equations. Generally, this method is powerful for solving transport equations in mass transfer calculations and is often applied for rock mechanical calculations where things like the impact of cracks in the rock etc. are taken into account. The downside of this method, however, is that it cannot be developed in a simple manner to solve complicated geometries and boundary conditions in the same way as the finite element method. This is the reason why the finite difference method is not applied as frequently as the finite element method in commercial numerical software today.

Thus, one example of an alternative to the finite element method as a tool for numerical analysis is:

- Finite difference (mechanical analysis – primarily rock as well as for flow and transfer calculations).

An example of finite difference calculation is illustrated in Figure 3-4. In this case, it is a model of a Swedish arch dam which was intended to analyse its stability. In this case, the calculation is done in a software based on finite difference, but this type of calculation corresponds to what was described in the finite element calculations in section 3.2.3.

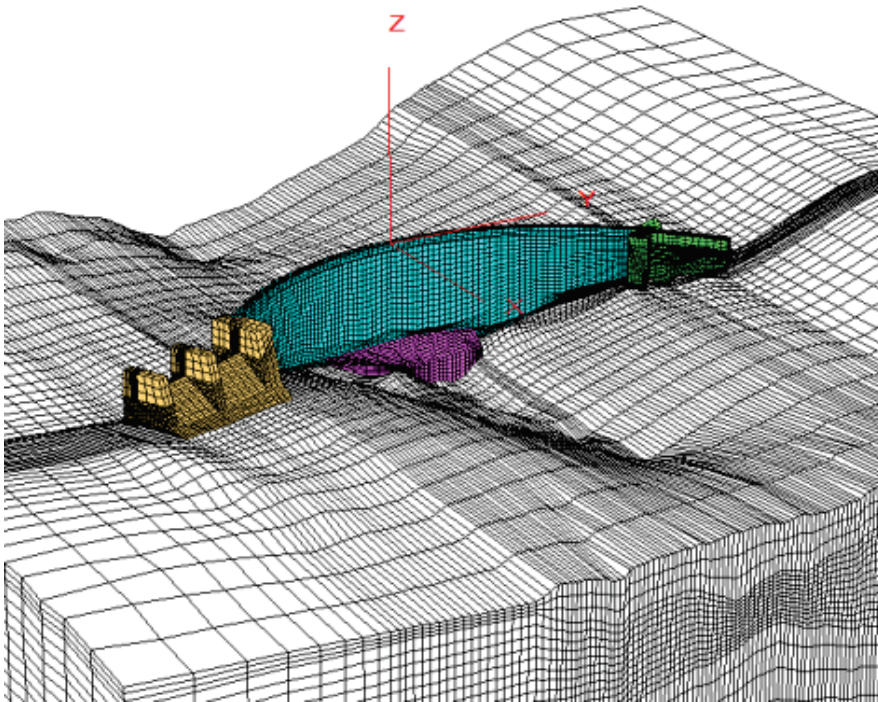


Figure 3-4 Example of finite difference analysis of an arch dam [50].

3.3 CHOICE OF METHOD OF ANALYSIS

As described in section 3.2, the different types of analysis methods can be applied depending on the purpose of the calculation. It is often the requirement of the level of detail that determines whether the more advanced methods are required. In Table 3-1 several different applications of analysis methods are compiled (grouped according to varying requirements of the level of detail), and it is indicated which methods can be used for the analysis.

Table 3-1 Compilation of different methods of analysis in order to map which methods are suitable depending on the purpose of the calculation. Grey=suitable.

Type of analysis (purpose)	Analytical calculations	Finite element calculations	Non-linear finite element calculations	Other types of numerical calculations
- Stability analysis (sliding/overturning) - Simpler geometries and load cases. E.g. gravity dam, buttress dam				
Stability analysis (sliding/overturning) -general E.g. spillways				
Stability analysis – sliding, overturning, material failure and combined failure modes. E.g. arch dams, cracked dams, high material strain, rock bolts.				
Effect from construction sequence (casting stages or demolition/reconstruction) – simpler				
Effect from construction sequence (casting stages or demolition/reconstruction) and new concrete (strength increase etc.)				
Prediction of measured data (expected measured value and definition of threshold limit value)				
Prediction of measured data (expected value and critical limit related to dam safety)				
Determination of strains in a structure (moment, shear force, normal force alternatively stress)				
Determination of the load-bearing capacity of a structure (moment, shear force, normal force alternatively stress)				
Prediction of degradation (e.g. expansion of ASR)				
Simulation of degradation process (e.g. expansion of ASR and strength reduction)				

It is important to point out that increased complexity with a more advanced model does not necessarily lead to better results. As an example, it can be mentioned that for simple cases of stability calculations, exactly the same result is obtained from a classic stability calculation based on rigid bodies compared to a finite element calculation.

Another example is e.g. methods used to predict expected response from dam measurements. Classical dam behaviour models based on regression analysis (e.g. HTT or HST¹) normally work very well to predict expected values, see Chapter 3.7.5. This, however, requires that there is a certain length of a series of measurements that the dam trend model can be calibrated to. In addition, this model can only be used to predict expected values based on the type of events and the extent to which it has been calibrated. This means that this data cannot be extrapolated. This means e.g. that it can be possible to set threshold levels on measuring systems (i.e. when it is outside the expected value), but it is not possible to define critical values (i.e. when there is a risk of dam failure etc.), [45]. Finite element calculations can be used for both prediction of expected values, threshold and critical values. On the other hand, it is complicated to get a finite element model that has just as good a prediction (i.e. less spread) as a dam behaviour model based on regression analysis, see 3.7.5. Even when calibrating a finite element model to measurement data, it can be difficult to get perfect alignment, mainly because there are many different parameters to adjust.

In conventional design, where e.g. reinforcement content is to be determined, simpler analytical calculations are preferable compared to non-linear finite element calculations since the latter take much longer to complete. On the other hand, if the purpose is to determine the load-bearing capacity of an existing structure, non-linear finite element calculations may be more suitable than the simpler analytical ones, especially in cases where safety is not considered sufficient due to conservatism in simpler analytical methods.

An advantage of starting from a possibly more complicated model than what the need requires could be that it could also be applied for any further work, such as evaluation of rehabilitation alternatives, measuring systems etc.

3.4 SIMULATION OF DIFFERENT PHENOMENA

In order to be able to make an assessment of the current state of a structure, its safety against failure, reinforcement measures, etc., it is required that initial conditions, weakening (e.g. cracks), etc. are taken into account. The following sections give a brief description of typical phenomena that are important to consider for hydropower structures with reference to how this is carried out in a numerical calculation.

¹ HST (Hydrostatic, Seasonal, Time) is a basic dam behavior model that is based on regression where water pressure, season and irreversible time-dependent changes are assumed to be the three controlling variables from which the dam response can be determined.

3.4.1 New concrete

The purpose of analysing new concrete is usually to design e.g. cooling of the concrete during hydration. New concrete is designed to prevent or limit the cracking so that a crack distribution with a small crack width must be obtained so that no cracks must occur that can affect the structure at future loads or its durability. In new concrete, initial stresses are built into the structure, but these are usually relatively low and are usually rarely considered in analyses of e.g. the load-bearing capacity of a structure etc.

To analyse new concrete, several different aspects must be considered. On the one hand, the heat development that takes place during the hydration and in the event of cooling, needs to be simulated. In addition, the stiffness and strength growth must be considered in order to be able to couple the heating and cooling effects to the stresses and the capacity of the structure. Both of these aspects are necessary e.g. to be able to design the cooling of the concrete.

For larger structures, where the casting takes place in casting stages, simulation of casting stages also has to be considered. This is normally considered by introducing new elements in the model so that the model gradually becomes larger.

Normally, when analyses are performed in order to determine the load-bearing capacity, no consideration is given to the impact of casting. Instead, it is simulated e.g. only that the initial stresses (often without associated deformation) from their self-weight are taken into account. In e.g. arch dams where the structure is cast as piers, these are usually first simulated as stand-alone piers that are linked to contact conditions.

In [40], the phenomena that must be taken into account and how they are included in numerical models are described.

3.4.2 Long term effects

Long-term effects such as creep and relaxation can have a significant impact on hydropower structures. Generally, the earlier (the newer the structure) the structure is subjected to a constant load and the higher (in relation to the capacity of the material) this load is, the greater the impact is.

Therefore, these effects are particularly important to consider in new concrete, since creep and stress relaxation have a large positive effect which leads to increased deformations and reduced stresses.

When it comes to other long-lasting, permanent, loads such as water pressure, these effects have a relatively limited impact. Firstly, the compressive stress in hydropower concrete structures is usually relatively low (typically $<1/3$ of the strength) so that only linear creep occurs.

There are many short-term loads that act on structures, such as seasonal variations in temperature, ice loads, etc. For these loads, reduction with respect to creep should not be made. This is because the duration of these loads is relatively short and the creep thus has a marginal impact.

In the construction industry, a practice² has been developed, where shrinkage is simulated as a constant temperature load throughout the cross section, which in turn is reduced with respect to creep. Reducing the shrinkage with respect to a creep number determined from the day shrinkage starts is unsuitable and an uncertain assumption. This method is therefore an ad-hoc adaptation which should not be applied, especially in the case of thick structures.

Instead, in the large hydropower structures, the focus should be on better estimation of the drying shrinkage (often there is also one side in contact with water), where cross-sectional differential shrinkage is taken into account. At the thick cross section of hydropower, the concrete often has a very high moisture content in the central parts after a large amount of years.

3.4.3 Cracking, crushing

Cracking is the leading cause of non-linear behaviour in concrete structures. Concrete structures are usually expected to crack and it is only after cracking that the reinforcement is activated in the concrete. The utilization of the reinforcement in non-cracked concrete is normally only a small percentage (typically <5%) due to the high stiffness ratio between steel area and non-cracked concrete area. When the concrete is cracked, the reinforcement carries the tensile forces in the cross-section, although the stiffness contribution of the reinforcement becomes lower than the cracked concrete as a whole, which leads to reduced stiffness of the structure.

When analysing concrete structures in hydropower, it is often necessary to consider existing cracks as these are a deficiencies and can lead to potential internal failure modes, but even then these cracks can propagate or new cracks may arise due to redistribution of stresses.

In [40] the non-linear behaviour of material in concrete and how they are included in numerical models is described. A brief description of this can also be found in Section 3.5.1.

3.4.4 Degradation

Describing degradation processes correctly in numerical analyses is complicated. In addition, several degradation processes exhibit clear synergy effects where a degradation process can lead to initiation or acceleration of other degradation phenomena.

In most cases, these applications are analysed in 1D with analytical calculations since it is possible to get an estimate of e.g. chloride penetration, moisture calculation, leaching front etc. in order to be able to make an assessment of the service life of the structure. In cases where non-linear transfer processes are considered, numerical tools such as the finite difference method or finite element method are applied.

² This comes originally from several cases with slab bridges where the total shrinkage gives rise to very large stress in the cross-section of the bridge.

Implementation of more advanced analyses where transfer processes are linked with mechanical analyses is primarily for research purposes and generally more research work is required in this area before these types of analysis can be applied in conventional condition assessments. In addition, this type of damage is usually very local and takes place e.g. close to the surface layer of the concrete and therefore often has limited impact on the global behaviour. It is very difficult to be able to include these local effects in global models of hydropower structures because the size of the model becomes unmanageable. The element size often needs to be at centimetre-level (or less) which is not compatible with actual structures with contemporary computing power. To simulate the degradation phenomena in a finite element calculation, multi-physics is required so that water or chemical transfer is considered and combined with a mechanical model. E.g. when simulating decomposition caused by frost, this corresponds to the transport of water and then freezing of the water in the pore system. Only then, the effects of the degradation can be considered. This can either be carried out in a linear elastic model, but then only indications are obtained on which area there is a risk of being exposed to frost spalling. Otherwise, the alternative is to connect the simulation of transport and freezing of water with a non-linear material model that describes cracking and crushing (in the same way as described in the previous section, see Section 3.4.3). In a similar way one would simulate e.g. ASR, where the moisture transport is required and coupled with a part that describes the expansion of the cement gel. Finally, in the same way, a non-linear material model is required to simulate cracking and crushing.

It is mainly the transport calculations that require very fine element size, because the gradients in e.g. moisture or concentration of a dissolved material, can be very high closest to the concrete surface layer.

Instead, in finite element calculations, simplified methodologies are generally implemented where the purpose is to capture basic phenomena such as expansion. This means that the transport calculations themselves are simplified and instead a much simpler variant is applied where these are translated into equivalent temperatures and expansion or contraction is handled by the coefficient of thermal expansion.

ASR

An example of this is ASR where the actual expansion is usually simulated in linear finite element calculations, solely for the purpose of describing the deformations that occur. In these cases, the expansion from ASR is considered e.g. through a temperature expansion. Here, the stresses in the material are not studied since these become completely unrealistic because the change in material properties cannot be taken into account. Instead e.g. relative dimensions of stress or deformation as the influence of insertion of slits, sawn expansion joints, which are intended to allow the expansion with low restraint.

Frost action

When simulating the degradation caused by frost action, this too can be simulated in a simpler way where the expansion coefficient is adjusted so that it takes into

account the expansion that takes place during freezing. A method for this is presented e.g. in [51], relating to completely water-saturated material, where the expansion can be described by means of equivalent temperatures. The expansion coefficient that includes the effect of freezing can according to [51] be described as

$$\alpha_{frost} = \frac{b \cdot X}{K_0 \cdot \Delta T}$$

where,

b is Biot's coefficient of expansion, which describes the relationship between the drained and the solid material, $b = 1 - \frac{K_0}{K_m}$

X is a term that takes into account potential occurrence of ice in the pores, which i.a. takes into account the distribution of pores in the concrete.

ΔT is the temperature difference compared to the reference temperature (i.e. at zero stress)

K_0 is the drained compression modulus $K_0 = \frac{E}{3(1-2\nu)}$

To illustrate how a combined expansion number can be defined, the method described in [51] has been applied based on the pore distribution and the input data specified in [51]. The pore distribution used is illustrated in Figure 3-5.

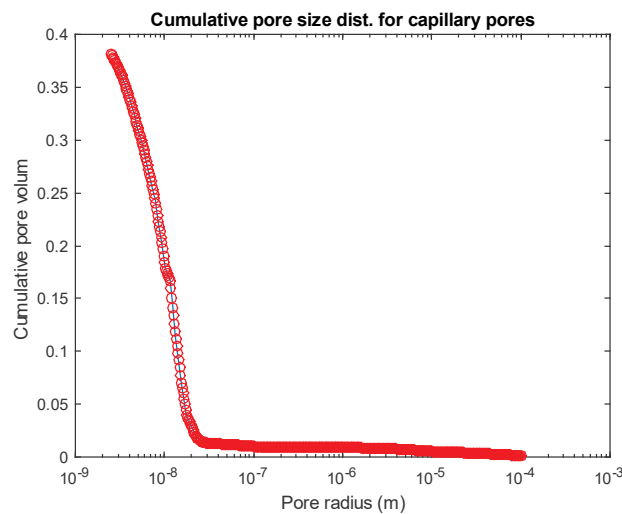


Figure 3-5 Exemplified pore distribution used when calculating the expansion number.

The resulting expansion number that takes into account both temperature change and freezing is illustrated in Figure 3-6. The expansion coefficient for temperature variations for concrete has been assumed to be 10^{-5} and, as can be seen from the figure, the resulting expansion number becomes negative at about -7°C in this case. This means that for temperatures lower than this, the concrete will expand

more because of the freezing of water than the contraction from the temperature reduction.

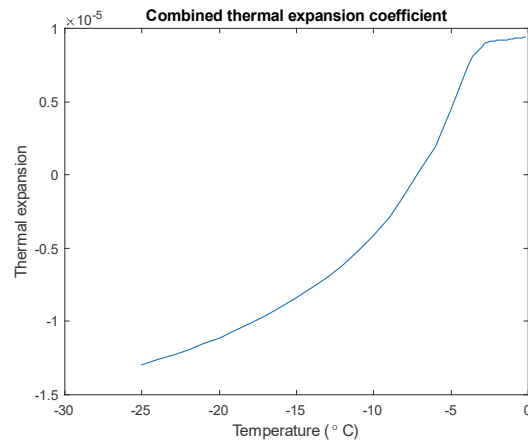


Figure 3-6 Illustration of a combined expansion coefficient that describes both the temperature expansion and the impact from frozen water in the concrete.

Corresponding strain in the concrete is illustrated in Figure 3-7, where it is clear that temperature reductions below the freezing temperature lead to negative (pressure) strain for low freezing temperatures, but at even lower temperatures, positive (tensile) strain is induced in the concrete which can lead to cracking. If the crack strain is assumed to be $1 \mu\text{S}$, the cracking at full water saturation is expected to occur at $-14 \text{ }^\circ\text{C}$.

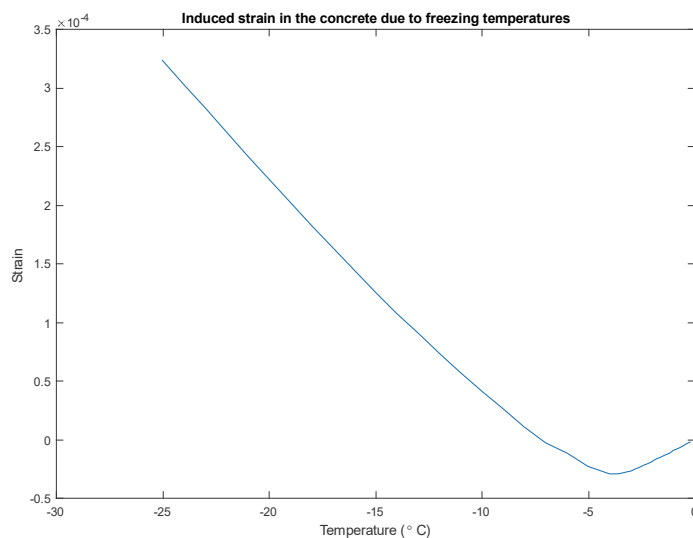


Figure 3-7 Illustration of induced strain at freezing temperatures.

Corrosion

Corrosion of reinforcement and rock bolts is usually taken into account by reducing the cross-sectional area of the steel according to an assumed corrosion rate. This is described e.g. in [52], where a method is presented that calculates the

corrosion rate based on chemical compounds in the water. In total, data from 30,000 water samples taken from 2003 measuring stations in Swedish rivers has been compiled where the result showed that at a log-normal distribution of the corrosion rate, an average value of 20 $\mu\text{m}/\text{year}$ with the associated standard deviation of 5 $\mu\text{m}/\text{year}$ is obtained.

Based on an assumed corrosion rate, it is thus possible to calculate the load-bearing capacity or safety against failure as a function of the degradation, see Figure 3-8. The result illustrated in the figure represents the safety against failure of a buttress dam with respect to degradation of the rock bolts (black dashed curve) where the grey area corresponds to the limits of the 10 and 90 % percentiles. For this case, rock bolts must be considered according to RIDAS [42] with a load-bearing capacity of a maximum of 140 MPa (blue curve), and the case without regard to rock bolts is illustrated with a red curve.

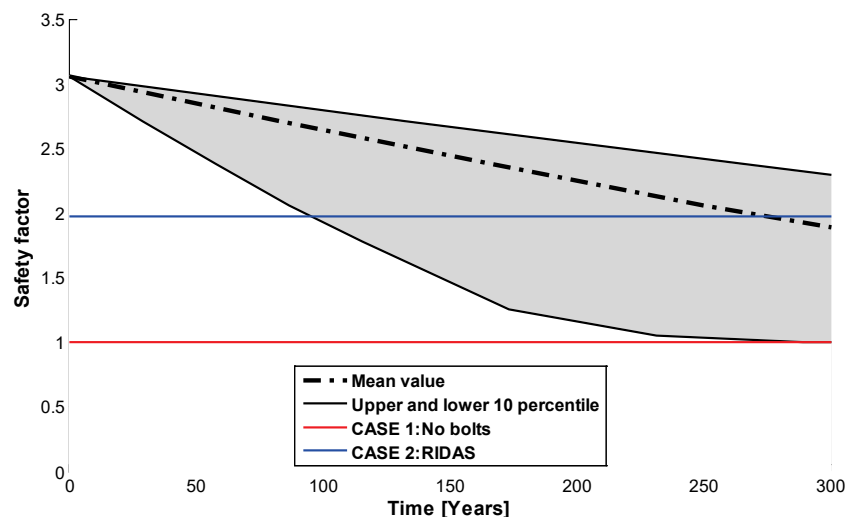


Figure 3-8 Example of calculated safety against failure with respect to corrosion of rock bolts.

3.4.5 Seasonal variation in temperature

Many Swedish concrete dams are subjected to large stresses caused by the seasonal variations in temperature. In many cases, the dams can be exposed to a temperature difference of about 70 °C between summer and winter. Particularly under winter conditions, high tensile stresses occur in the concrete due to thermal strains which in many cases result in cracking.

This problem was analysed for the Storfinnforsen buttress dam where an additional insulated wall resulted in additional stresses in the buttress, see [53]. It has been shown in several subsequent studies that similar problems with cracking related to the seasonal variation in temperature also occurred on many other buttress dams and also on arch dams, see e.g. [54]. It is also apparent from the case studies presented in Chapter 5 that seasonal variations in temperature in particular is a common cause of cracking.

However, there are two specific aspects that are not described in RIDAS [3], [4], but are needed in order to be able to carry out an analysis of the effect of temperature variations. The first parameter is which reference temperature is expected to apply to the object, i.e. the temperature at which the concrete is considered to be stress-free. This temperature corresponds to the temperature that prevailed when the structure was cast together and thereby restrained. If information about this is missing, it can be assumed to be + 10 °C [40].

The second aspect is what ambient temperatures are to be assumed. In Eurocode 1-5 [55], maximum/minimum temperatures are defined based on a return period corresponding to 50 years. These correspond to the maximum and minimum temperatures, respectively, which are expected to occur over a 50-year period with a one hour duration. However, it is important to remember that hydropower structures normally have considerably larger cross-sectional dimensions than conventional structures (and thus greater thermal inertia), which means that short-term temperature cycles (faster than daily average temperatures) cannot propagate into the structure to any great extent. This is illustrated in Figure 3-9 with an example of the temperature distribution in a massive concrete structure varying as a function of how long the temperature difference may act. From this figure, it is clear that the temperature needs to have a considerable duration (days or more) before the temperature can propagate into the structure to any great extent. As a comparison, it should also be mentioned that if a steady-state temperature analysis is carried out, the temperature would vary linearly between the boundaries. For this reason, it is essential that the temperature analysis is carried out as time-dependent (transient) so that the duration of the temperature is taken into account in massive concrete structures.

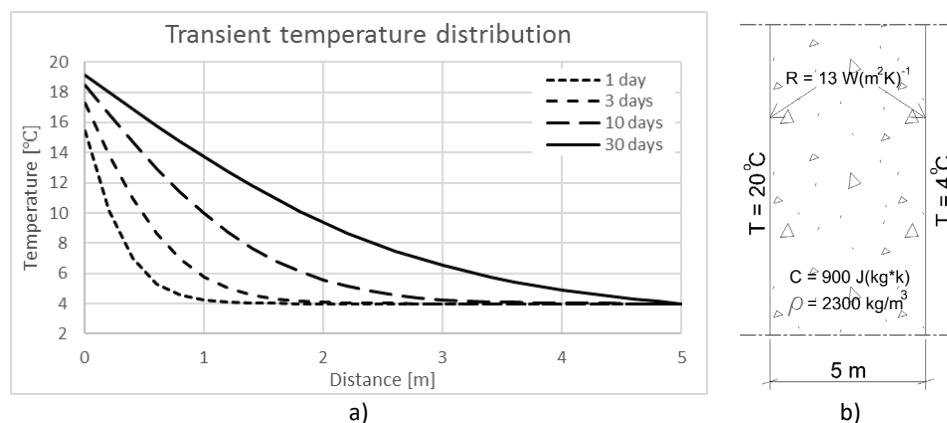


Figure 3-9 Example of temperature distribution in a massive concrete structure depending on the duration of the temperature, from [48].

Usually, it is not reasonable to be able to carry out time-dependent temperature analyses on an hourly basis, at least not if seasonal effects are to be considered. In these cases, it is more suitable to calculate the average temperature on a daily or

weekly basis from measured temperatures³, so that the simulation is performed with a time step corresponding to one day or one week. This therefore suggests using less extreme temperatures than those reproduced in Eurocode. In addition regarding ambient temperatures is the estimate of water temperature. The measurements that have been carried out by the water temperature, see e.g. [56], show that the water temperature is relatively constant through the entire depth regardless of season, where the temperature is approximately zero throughout the winter. Of course, this may depend on how the plant is operated, winter discharge, etc.

3.4.6 Reinforcement measures

When analysing reinforcement measures, it is important to consider current conditions in the dam first, i.e. how existing cracks affect any concrete cover and pre-stressing.

Just as with other types of analyses, the requirement for details is determined by which type of model is required. For studies of global effects, FE analyses can be applied with good results, however when it comes to detailed study of local effects such as reinforcement design etc. it is often more suitable to apply analytical design methods. This is because the design methods are quick and easy to use, while detailed numerical models of attachments, design of anchor blocks for tendons etc. are often more extensive than is normally required.

Concrete overlay

Possible concrete overlay can be included in a model in a similar manner as described in the section on new concrete, i.e. by introducing new elements to simulate casting stages. Important in this case is that effects such as differential shrinkage is considered between old and new concrete and the risk of cracks from restraint forces caused by heat and strength growth from freshly cast concrete. How this can be considered in finite element models is described in chapter 7.2 in [40].

Pre-stress

Pre-stressing with rock-anchored cables is a common reinforcement method for prevention of stability failure. Reinforcement with post-tensioned pre-stressed cables is also applied in cases where larger cracks occur in a structure and any crack propagation is desired to be limited. How this can be considered in finite element models is described in chapter 12.6 of [40].

3.4.7 Stability failure

In many cases, it is sufficient to apply classical stability calculations for the evaluation or design of dams etc. These are applied by analysis of the dams as a rigid body where the dam body is checked to be safe against sliding and overturning.

³ In cases where measured temperatures are missing, open climate data can be used, see e.g. <http://www.smhi.se/klimatdata> (Sweden only).

For dams that are close to the acceptance criteria for the stability checks (whether or not they are met), it is recommended that more detailed investigations is carried out. The reason for this is that it can often be combined failure modes that lead to a theoretical failure which is missed in a conventional stability analysis. This can be captured with non-linear finite element analysis, along with e.g. the risk of material failure. Examples of this were presented in [58], where the effect of the failure mode was analysed as a function of the coefficient of friction, see Figure 3-10. In the analysis, failure analyses were performed on a buttress dam where the coefficient of friction was gradually increased for each case. As can be seen from the figure, pure sliding failures occurred for cases where $\mu < 0.7$ and pure overturning failures for the cases when $\mu > 1.3$. For the cases in between, a combined mode of failure is obtained which is initiated as overturning giving a reduced contact surface so that the dam reaches sliding failure.

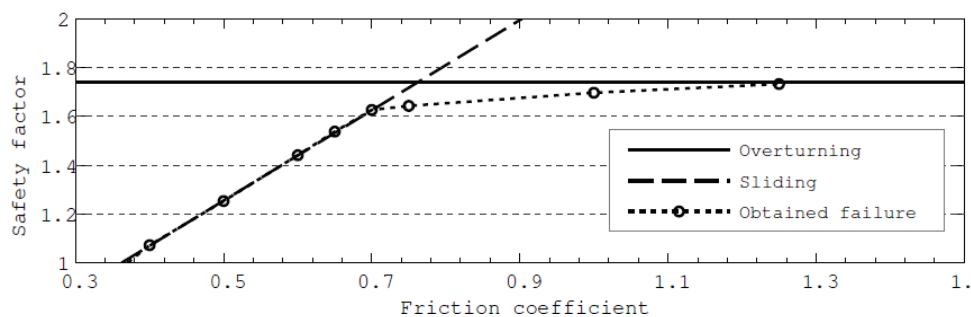


Figure 3-10 Illustration of obtained mode of failure (sliding, overturning or combined) for a buttress dam as a function of the coefficient of friction [58].

In addition, with e.g. probabilistic analyses it is possible to get a clearer picture of which parameters that mainly have a large impact on the assessment of the safety level of the dam. However, the safety concept using a safety factor is not analogous to the assessed safety against failure. This means that two dams with the same safety factor can have different failure probabilities.

In many cases, it can be reasonably faster to perform a stability calculation with an FE analysis than with a traditional analytical stability analysis, especially in the case of more complex geometries. In the case of complicated geometries, the structure may need to be put up in a CAD program to determine the centre of gravity, levers, etc. When analysing dams with extensive rock bolts, it is difficult to assess how these contribute to prevention of a potential dam failure, i.e. if they carry loads via tension, shear (dowel effect) or as a combination. Even in these cases, it is usually advantageous to analyse using FE. Another important reason why FE analyses are beneficial to apply is to get a more accurate distribution of the uplift pressure under the dam, see Chapter 5 of this report or Chapter 7.1.3 of [39]. Examples of applications where this may be relevant to consider are cases where the effect of the properties of the drainage curtain is to be analysed, or if the dam has a complicated geometry or boundary conditions.

3.4.8 Potential failure modes (PFMA)

Potential failure mode analysis (PFMA) is an important part of the safety work of the dam. This is needed in order to be able to judge which modes of failure are theoretically possible, the safety against failures for these modes and in order to be able to assess how the failure process itself looks for these failure modes.

In order to analyse potential failure modes, a conceptual model is often used in which different scenarios are analysed. This step should always be carried out regardless of whether more advanced methods are being used for further investigations of the different modes of failure. The drawbacks of using a conceptual model are partly that it is difficult to estimate which of the failure modes that is estimated to have the lowest safety and above all because this approach does not lead to any information about how the failure process actually takes place.

Therefore, it is usually advisable to perform analytical calculations or FE analyses to analyse potential failure modes. In this type of analysis, existing cracks in the concrete dam and crack planes in the bedrock should be considered. In these analyses; real, observed, crack planes should be analysed, but also with sensitivity analyses so that e.g. existing crack slopes are varied and the extent of the cracks is extended so that they take into account any potential future crack propagation. The advantage of FE calculations compared to analytical calculations is that they also consider combined modes. This can e.g. be that the deformation starts according to one failure mode but turns into another failure mode. E.g. in the event of initial overturning, the crack plane opens up on the upstream side, which leads to less contact surface and thus considerably lower safety against sliding.

Potential cracks in the bedrock can often have a large impact on the dam safety. This can e.g. be a crack plane close to the arch support on an arch dam or shallow crack planes under e.g. a buttress dam. In the case of shallow crack planes in the bedrock under a buttress dam, these cracks have a great influence, primarily because the uplift pressure thus acts on the entire surface instead of under the front slab only (which is often an assumption used for cases where the thickness of the buttress is <2 m). Figure 3-11 illustrates the typical case of two potential crack planes in the bedrock that can lead to stability failure in the bedrock. When analysing these types of crack planes, simplifications are usually introduced so that any counter support along the dam line is neglected, since the extension of the crack plane under adjacent monoliths is often unknown.

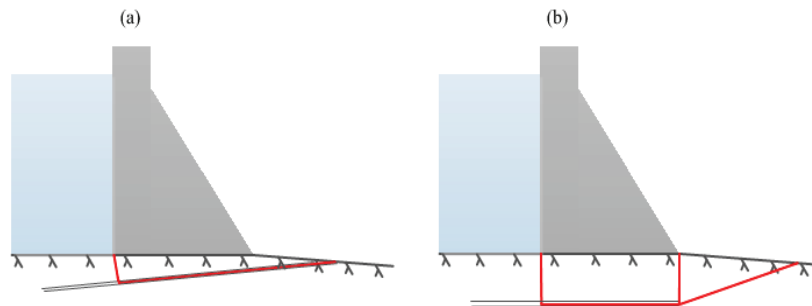


Figure 3-11 Illustration of potential crack planes in the bedrock
 a) inclined crack plane combined with a tensile crack upstream
 b) horizontal crack plane under the dam with a passive rock wedge counteracting

3.5 MODELLING ASPECTS

The purpose of the following section is to describe how different aspects affect the results given by the models and their reliability.

3.5.1 Material models

For simulation of cracking and crushing in concrete and other cement-based materials, there are a number of different constitutive material models. What all these material models have in common, however, is that they are based on fracture mechanics, plasticity theory and/or damage mechanics to describe the reduction of the stiffness of the material due to cracking or crushing.

There are two overarching methods for describing the cracking in a material, either as smeared across the elements or as discrete cracks e.g. in-between the elements, see Figure 3-12. The main difference between these two methods is that in the smeared crack method, the cracks are distributed across the element, i.e. there are no physical cracks in the calculation model. In the discrete crack model, cracks arise, e.g. between the elements and create physical cracks in the calculation model. This can be accomplished by joints between each element described with particular features (interface elements) which correspond to the fracture mechanical behaviour of the cracks. Other elements in the model can then e.g. be described solely with elastic properties.

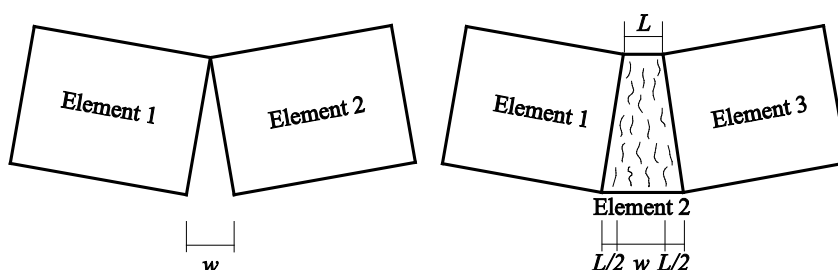


Figure 3-12 Illustration of a discrete (left) and smeared (right) crack model.

One example of a simple fracture mechanical definition of concrete material is presented below, where relation between strain and elongation is defined according to

$$\boldsymbol{\sigma}_{ns} = \mathbf{D}^s \boldsymbol{\varepsilon}_{ns}$$

where

$\boldsymbol{\sigma}_{ns}$ is the stress vector

$\boldsymbol{\varepsilon}_{ns}$ is the strain vector

\mathbf{D}^s is the secant modulus

This equation corresponds to Hooke's Law, in a one-dimensional case for non-cracked concrete (the secant modulus in this case corresponds to the elasticity modulus E), i.e.

$$\sigma = E \cdot \varepsilon$$

In a 2D case with a flat stress state where the transverse contraction is assumed to be zero, the stress and strain terms can be defined according to,

$\boldsymbol{\sigma}_{ns} = (\sigma_{nn}, \sigma_{ss}, \sigma_{ns})^T$ (where $\sigma_{ns} = \tau$) and $\boldsymbol{\varepsilon}_{ns} = (\varepsilon_{nn}, \varepsilon_{ss}, \varepsilon_{ns})^T$ and the secant modulus \mathbf{D}^s is described according to

$$\mathbf{D}^s = \begin{bmatrix} \mu E & 0 & 0 \\ 0 & E & 0 \\ 0 & 0 & \beta G \end{bmatrix}$$

The term μE describes the strain softening in the normal direction during gradual cracking, see Figure 3-13 a), and the term βG describes how the shear resistance is reduced in the case of gradually increased cracking, where β is the shear retention factor which is reduced e.g. according to Figure 3-13 b). An important aspect of this model and damage models is that no plastic strain/deformation occurs after unloading, i.e. cracks are assumed to close completely.

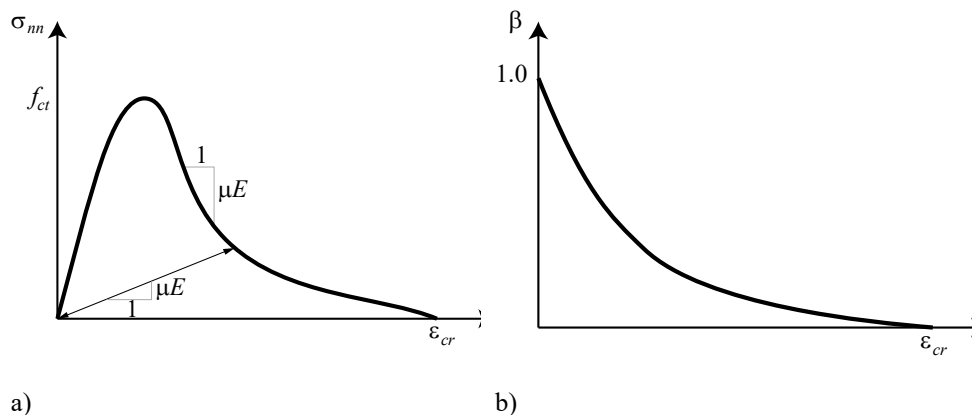


Figure 3-13 a) Working curve at a single-axis tension expressed in stress-strain b) Shear retention factor

Fracture mechanical material models can either be based on fixed or rotating crack direction. In the case of a fixed crack direction, the crack slope is always maintained in each element⁴ regardless of whether the stress field is changed⁵ and in the rotating model, the crack slope in each element is adjusted as the stress field changes⁶. Both when using fixed and rotating crack methods, there is a risk that stress-locking occurs, where the rigidity of the structure is overestimated after crack initiation. This phenomenon is illustrated e.g. in [59] and [53] where the deformation of the structure due to this is significantly underestimated.

In the rotating crack method, there is also a risk of uncontrolled rotation of the crack direction, which leads to problems with convergence or that the crack finds a rotated equilibrium position as the load continues to increase and thus misses the real failure mode, and thus the load-bearing capacity is overestimated, see [44].

A major advantage of fracture mechanical models is generally that few material properties are required to define the model, tensile strength and fracture energy, where these material properties can usually be determined according to conventional standards/codes. For a fixed crack model, it is also required that a function for the shear retention factor be defined, which describes how the shear resistance in a crack is reduced as a function of the crack opening.

At the benchmark workshop organized by KTH (Royal Institute of Technology in Stockholm) in 2017, the participants was given the task to predict the cracking in a typical Swedish arch dam. A total of 16 groups participated and sent in their predictions on cracking and deformation. There was a relatively large spread among the participants regarding the type of material model chosen for this. Most participants applied a material model based on damage mechanics, but generally one of the following types of material models was applied

⁴ Formally, cracks occur in the integration points of the elements where several cracks can occur in each element, see [39] for further information.

⁵ Since the main stress direction deviates from the direction of the crack, shear stresses occur in the crack plane

⁶ Since the crack rotates and follows the main stress direction, no shear stresses occur in the crack plane.

- Fracture mechanical models (fixed or rotating crack models and a further development called micro-plane model)
- Damage-based models (only isotropic damage models)
- Combination of plasticity theory and damage mechanics (only isotropic damage models)
- Combination of plasticity theory and fracture mechanics

The results from participants showed that all types of material models could predict the cracking in the dam with good accuracy. In some cases, simpler material models were applied which only considered single-axis behaviour and where the concrete was assumed to be elastoplastic, although these models did not succeed in predicting the cracking or deformation in a satisfactory manner.

Figure 3-14 illustrates the observed crack formation on the dam and results from some different calculation models. In Figure 3-14 b), the application of a combined plasticity model and damage mechanics is illustrated, and in Figure 3-14 c) a combined model consisting of plasticity and fracture mechanics is illustrated. Figure 3-14 d) illustrates a pure damage model, and in Figure 3-14 e) a fracture mechanical model with a fixed crack slope is illustrated. Any deviation of cracking is believed to be mainly due to differences in input data such as selection of material data and the influence of boundary conditions.

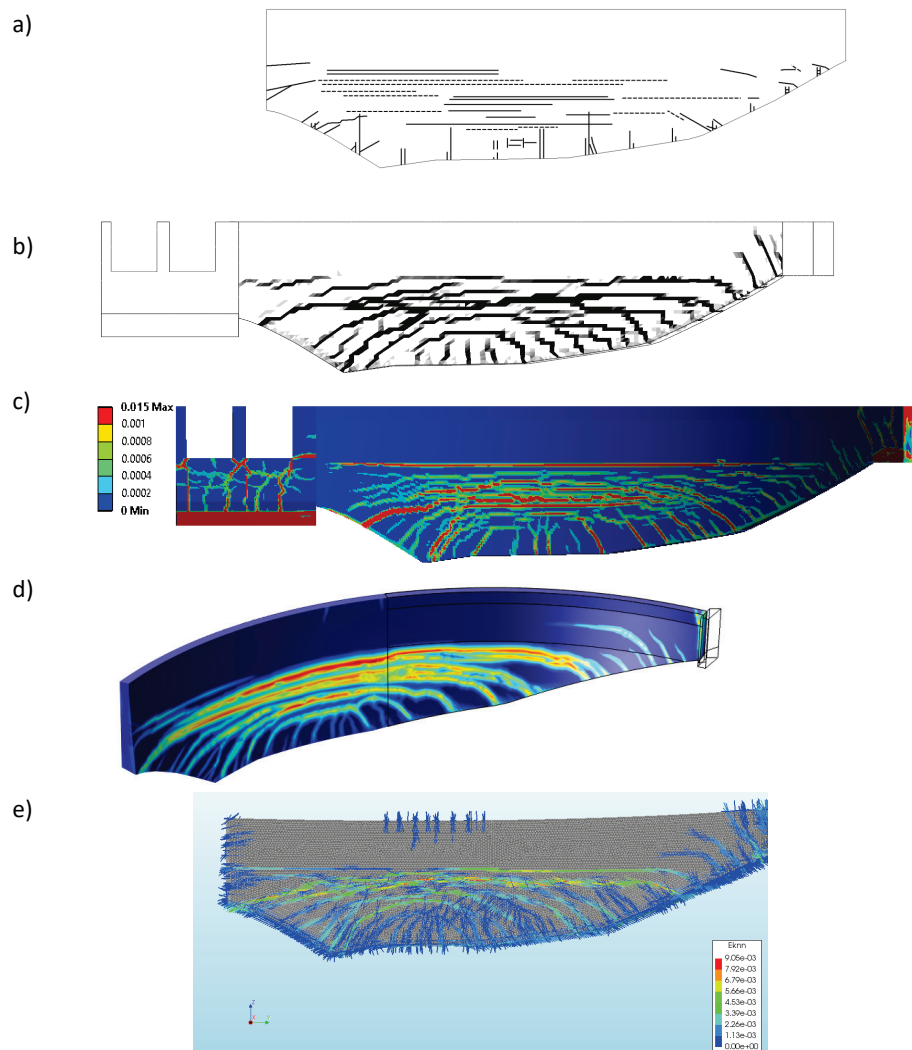


Figure 3-14 Illustration of cracking patterns, a) observed pattern, b) pattern from combined plasticity and damage mechanics, c) combined plasticity and fracture mechanics, d) damage mechanics and e) fracture mechanics

3.5.2 Delimitations

In order to be able to define a model, one needs to introduce delimitations, simplifications, so that only those parts of the structure, load effects or behaviours that are considered most relevant are taken into account. In the conceptual model, an understanding of the mode of action of the structure is required, i.e. an understanding of how the structure carries the loads, since this affects how much of the dam needs to be considered, how boundary conditions and loads are applied etc.

One common simplification in stability analyses is that the dam can be assumed to be a rigid body. When prediction of the behaviour of a dam based on measurement data, it is common to apply behaviour models such as based on the fact that the movement of the dam can be determined based on the water level, seasonal temperature and time (HTT models).

For the delimitation of a finite element model, it is necessary to make a decision as to whether the model should assume linear-elastic conditions or whether non-linear effects should be included. In addition, the size of the model needs to be delimited, since it is often very difficult to do calculations if a whole dam is taken into account. Buttress dams are typically constructed as monoliths with expansion joints between the front slabs, which means that as long as the deformations are not large, it can be assumed that the monoliths act independently from one another. Other typical examples are whether it is possible to introduce symmetry conditions and how much of the bedrock that needs to be considered. Examples of how to delimit a studied facility are described in Chapter 3 of [40].

However, it is important to remember that the conceptual model forms the basis for how the dam is analysed. Therefore, it is important to consider how any simplifications or delimitations in the model may have affected the evaluation of the result.

3.5.3 Boundary conditions, interactions and contact conditions

Boundary conditions are defined in a model by prescribing an expected behaviour on the boundaries of the model. These boundary conditions can of course have a very large impact on the model response, and it is therefore important that the model is defined so that the boundary conditions correspond to actual behaviour.

This applies partly to analytical models where the applied model (equation) is based on a prescribed behaviour, e.g. in the case of overturning calculations where the point of rotation is assumed at the downstream level. In some cases this can be misleading and instead it should be taken into account that the point of rotation moves upstream due to crushing (rock or concrete) according to e.g. [60], see Figure 3-15.

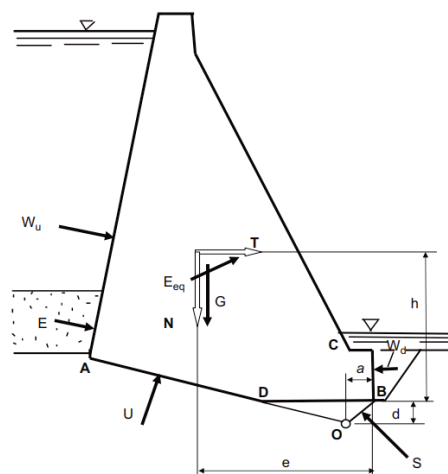


Figure 3-15 Illustration of moved point of rotation due to crushing of the bedrock [60].

In order to understand how the structure acts with respect to the boundary conditions, it is necessary to understand how the selected types of elements work. E.g. if all nodes within a surface of the solid model are defined with prevented

deflections, it means that this surface will act as a moment-rigid connection. Solid elements have no degrees of freedom of rotation but by tying all the nodes in a larger area to a prescribed boundary condition, the same effect is achieved. This of course also applies for contact conditions if the nodes on two surfaces are prescribed to follow each other.

Other important issues that are important to consider are e.g. how much of the bedrock should be included in the model and how should boundary conditions be applied to it. At the benchmark workshop [54], two different models were handed out with different sizes of the bedrock for the same application. The result of this comparison is e.g. the size of the bedrock has no major influence on the behaviour of the structure, as long as it is large enough to describe the temperature distribution closest to the dam. The size of the bedrock can give rise to the rigid body movement of the dam, but these do not cause any stress in the dam, see [54]. When analysing dams and other hydraulic structures, solid elements are mainly applied because of the geometry of these structures. When using solid elements, it is also important to limit the use of boundary conditions or loads that are applied in a single node, instead they should be spread across surfaces, see [40].

The large solid concrete dams have very high thermal inertia, and in addition the Swedish dams are usually enclosed with an insulating wall (and in some cases also heated) which leads to increased thermal inertia. This means that it is important that temperature simulations are carried out so that this is taken into account. This means that temperature analyses may need to be defined as transient (i.e. time dependent) and that the boundary conditions are prescribed with thermal resistance (Robin boundary conditions) instead of prescribing a node temperature (Dirichlet boundary conditions). [40]

3.5.4 Loads

There are many different types of loads that need to be considered in a dam safety evaluation, see Figure 3-16. Firstly, there are loads caused by reactions in the concrete material, such as hydration, shrinkage, degradation processes, etc.

In addition, there are of course also loads related to the water pressure, such as

- Upstream (US) water pressure; Horizontal (P1) - unfavourable, vertical (P2) - favourable
- Downstream (DS) water pressure; horizontal (P3) - favourable, vertically (P4) - favourable (however, leads to an increased uplift pressure but this is another issue)
- Uplift pressure (P5) - unfavourable

In addition to these, there are also typical loads such as;

- The self-weight of the dam (P6) - favourable
- Ice load (P7) - unfavourable
- Load from sediments (P8) - unfavourable
- Loads associated with seismic activity; hydrodynamic pressure (P9) and mass inertial restraint (P10 - P11) - unfavourable

In the above summary, the loads are mentioned as favourable or unfavourable. The reason for this is that loads are considered different when analysing whether they are unfavourable or favourable, e.g. with different partial coefficients for favourable and unfavourable loads.

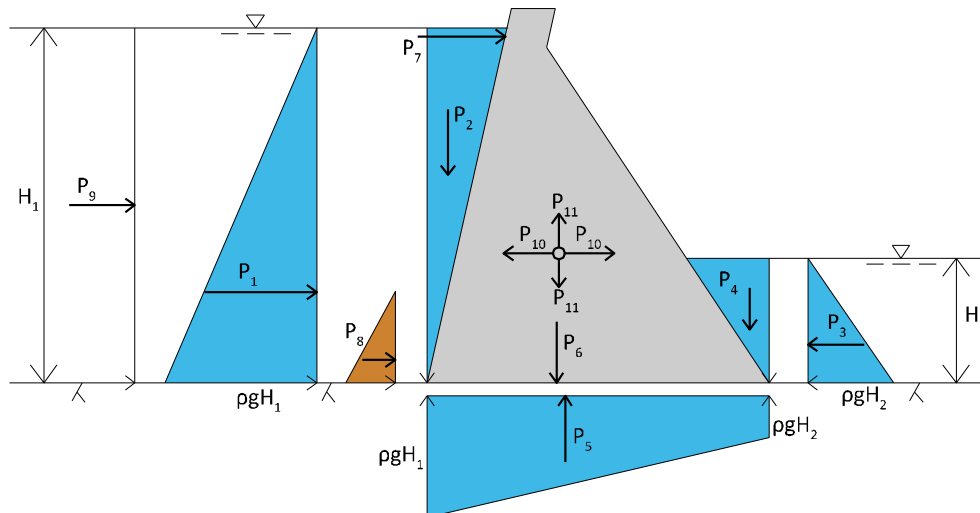


Figure 3-16 Illustration of typical loads applied on a concrete dam [61].

Finally, accidental loads or extreme loads caused by e.g. sabotage may need to be taken into account.

3.5.5 Crack propagation vs. existing cracks/damages

Many of the concrete structures in hydropower are cracked. In some cases, these cracks have no direct impact on the global behaviours of the plant, while in other cases these cracks govern the potential failure modes of the structure.

Significant, and particularly through-going, cracks should be considered when analysing cracked dams. This applies regardless of which type of analysis is being carried out. E.g. in the case of classical stability calculations, existing cracks should be taken into account since they e.g. can lead to an internal overturning modes. Although if the crack for the moment does not completely separate the dam into two bodies, this case should be analysed if there is a risk that the crack can propagate further. An example of this is illustrated in Figure 3-17, where an inclined crack through the buttress of a buttress dam monolith can lead to an internal overturning mode. This type of crack is common on buttress dams and their origin is mainly due to seasonal variations in temperature, see [53].

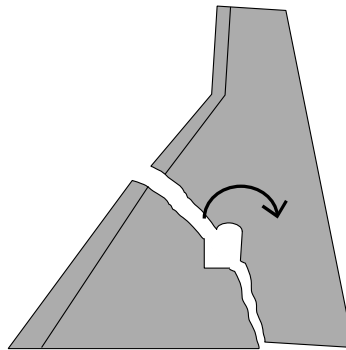


Figure 3-17 Example of an internal overturning mode.

Lift joints can also give weak planes and should be taken into account if relevant since these e.g. can cause sliding planes or open up at loading, see Figure 3-18.

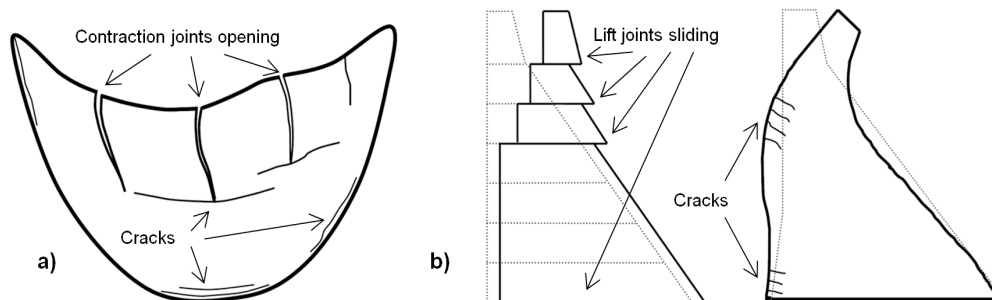


Figure 3-18 Illustration of failure modes related to casting joints.

In finite element calculations, it is relatively easy to add existing cracks to a structure. If these cracks constitute a large number that also cross each other, however, simulations can be very time-consuming by all contact iterations, which makes it difficult to carry out the analysis. Otherwise, in cases where only a few cracks are included as discrete crack planes where contact conditions are defined to describe the shear capability and reinforcing bars crossing the crack are included as beam elements (so that they can take into account the dowel effect), this is quickly fixed by an experienced calculation engineer, see Figure 3-19. In many cases it can be faster to perform a finite element calculation of the corresponding case than to carry out the corresponding traditional calculations which take into account the influence of reinforcement etc. In the FE-analysis, it is also clear which of the cracks will be guiding the crack propagation, i.e. identifies the potential mode of failure that has the greatest failure probability. In this type of model, the intact concrete is defined as linearly elastic, which leads to a simple simulation, however, the user themselves has to carry out checks that the stresses in the uncracked concrete do not exceed permitted values.

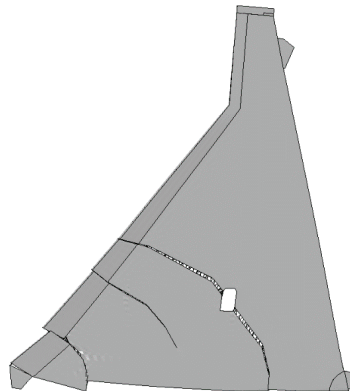


Figure 3-19: Example of calculated deformation at finite element analysis of a cracked buttress dam monolith.

Another option is to simulate the actual crack propagation. This type of analysis is primarily valuable for investigating the underlying causes of an observed crack formation. Thus, this may be necessary if it is not possible to assess the cause of the cracking by means of simpler analyses, such as linear elastic FE simulations. Examples of this are illustrated in Figure 3-20 for a buttress dam and a generator foundation in a power house, from [53] and [62] respectively.

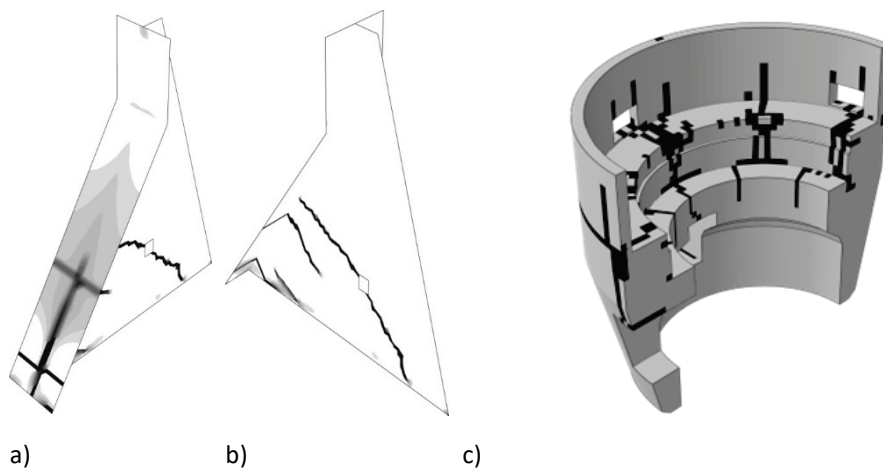


Figure 3-20: Example of simulated crack propagation, a) & b) in a buttress dam monolith, c) in a generator foundation.

3.5.6 Safety format and non-linear analyses

All material parameters are expected to have a certain variation, which means that this should be taken into account, and any uncertainties in loads are taken into account with the help of safety factors/partial coefficients in conventional design. However, in non-linear analyses, it is not suitable to use the concept of partial coefficients, as this can lead to incorrect failure modes and failure processes. This is because non-linear analyses are based on the fact that material properties are reduced as a result of cracking etc. Thus, difficulties arise if both the constitutive material model reduces e.g. the material strength at the same time as this is done with respect to partial coefficients.

In this type of analysis, instead, a security format should be better suited for non-linear analyses. In the report by Malm [40] various alternatives are presented on methods to consider this. The following section describes the model that is considered most suitable for these types of analyses, called ECOV according to the Model Code 2010 [63].

ECOV (Estimation of a coefficient of variation of resistance)

As mentioned earlier, the section about cross-sectional analysis in RIDAS TV [42] is based on the partial coefficient. It is however possible to apply a method for global load-bearing capacity based on this method. The global safety factor can be defined according to

$$\frac{R_m}{\gamma_{Rg}} \geq \gamma_{S1} \cdot S_{k1} + \gamma_{S2} \cdot S_{k2} + \dots + \gamma_{Sn} \cdot S_{kn}$$

where,

R_m is the load-bearing capacity based on analysis with average values of the material strength

γ_{Rg} is the global safety factor for the load-bearing capacity of the dam

In the ECOV method, two failure mode analyses are carried out, where one analysis is based on mean values for strength and where the second analysis is based on characteristic values for material strength.

The load-bearing capacity of the dam is assumed to be log-normal, which leads to the coefficient of variation (V_{Rf}) being defined according to

$$V_{Rf} = \frac{1}{1.65} \ln \left(\frac{R_m}{R_k} \right)$$

where,

R_m is the load-bearing capacity based on analysis with average values of the material strength

R_k is the load-bearing capacity based on analysis with characteristic values of the material strength.

Based on the coefficient of variation for the load-bearing capacity, a global safety level (γ_{Rg}) can be defined according to

$$\gamma_{Rg} = \exp(\alpha_R \cdot \beta_T \cdot V_{Rf})$$

where,

α_R is a sensitivity factor for the load-bearing capacity and can conservatively be assumed to be 0.8

β_T corresponds to the safety index that is relevant for respective dam safety class.

Finally the designed load-bearing capacity can be calculated as follows;

$$R_d = \frac{R_m}{\gamma_{Rg} \cdot \gamma_{Rd}}$$

where γ_{Rd} is a factor that describes the influence of model uncertainty.

The model uncertainty can according to Model Code 2010 [63] be assumed to be 1.06 in cases where the model is validated with high reliability, and in cases with higher uncertainty, $\gamma_{Rd} = 1.10$ is assumed.

According to [57] the safety index $\beta_T = 5.2$ can be assumed for dams in, the highest Swedish, dam safety class A.

3.6 MATERIAL DATA

Material data should, if possible, primarily be based on measured properties in order to obtain representative properties for the studied plant. If material samples are missing, then the material properties need to be estimated. This is most suitably done using Eurocode 2 [32].

Depending on the type of analysis performed, inputs of different degrees are required. Generally, increased complexity means an increase in the number of material data parameters. E.g. for an analytical stability calculation, only the weight of the concrete is needed as a material parameter given by RIDAS TV [42]. In addition, the determination of friction between rock and concrete is also required by RIDAS [42].

For more advanced analyses, e.g. simulation of material failure in concrete caused by cracking and crushing requires the following material data

- E-modulus (also required for linear elastic FE calculation)
- Poisson's ratio (also required for linear elastic FE calculation)
- Tensile strength
- Fracture energy and shape of a single-axis traction curve
- Compressive strength
- Form of a uniaxial pressure curve
- Load-bearing capacity at shearing of cracked concrete
- Relationship between uniaxial and biaxial load-bearing capacity (shape of crack curve at biaxial load)
- Relationship between single and triaxial load-bearing capacity (shape of crack curve in triaxial load)

Similarly, material data is needed for e.g. heat generation, strength increase, creep, etc. when e.g. new concrete is to be simulated.

In these more complicated cases, it is obvious that all of these material parameters are not expected to be available at each individual project. Therefore, it is more of a rule than an exception that material data has to be estimated based on reference literature such as Eurocode 2 [32] and Model Code 2010 [63]. Recommendations and guidelines for selecting material data are given in [40].

3.6.1 Uncertainty in material data

Material properties for linear elastic behaviour

For linear elastic analyses, there is relatively little influence regarding the spread in material properties. The reason for this is that only the elastic modulus, Poisson's

ratio and density are required. All of these parameters have a relatively small spread for conventional concrete and for steel materials.

For concrete, the modulus of elasticity is generally about 30 GPa (E_{cm} varies between 30 – 36 GPa for C20/25 through C45/55 according to Eurocode 2). However, studies have shown that concrete used in previous international hydropower plants often has a slightly lower modulus of elasticity than conventional concrete, see for example Table 3-2 below.

The Poisson's ratio for hardened concrete is normally assumed to be about 0.2 (typically varies between 0.1 and 0.2).

The density of concrete normally varies between about 2000 - 2600 kg/m³ according to the Model Code [63]. According to RIDAS TV [42], a specific weight of 23 kN/m³ is assumed in stability analyses and according to Eurocode of 24 kN/m³ for non-reinforced concrete and 25 kN/m³ for ordinary reinforced concrete.

Material properties for non-linear behaviour

The material parameters related to the description of the non-linear behaviour of the concrete vary considerably more. However, the compressive strength is relatively well-defined when a concrete quality has been defined. Other parameters can usually be derived from the compressive strength, but the values obtained can have a relatively high spread depending on which reference is used, since some sources are more conservative in order to define e.g. tensile strength. However, most of these material parameters can be estimated based on the Eurocodes. The process of cracking caused by tensile load is illustrated in Figure 3-21 and the corresponding case of crushing due to compressive loading is illustrated in Figure 3-22. In e.g. the Eurocodes it is defined how the stress-strain-curve of the concrete (corresponding to Figure 3-22) can be defined. However, the corresponding stress-strain-curve for tensile load (similar to Figure 3-21) is missing.

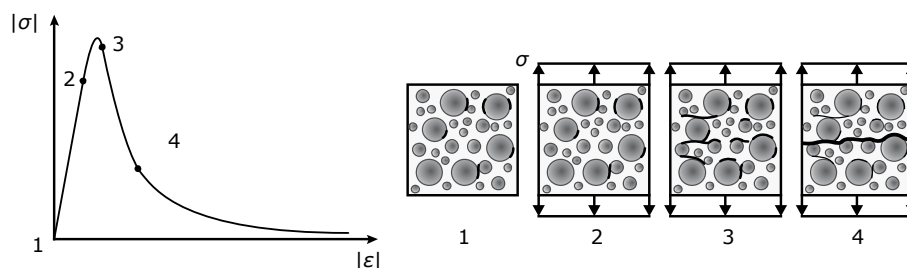


Figure 3-21 Illustration of the course at cracking of concrete, [89].

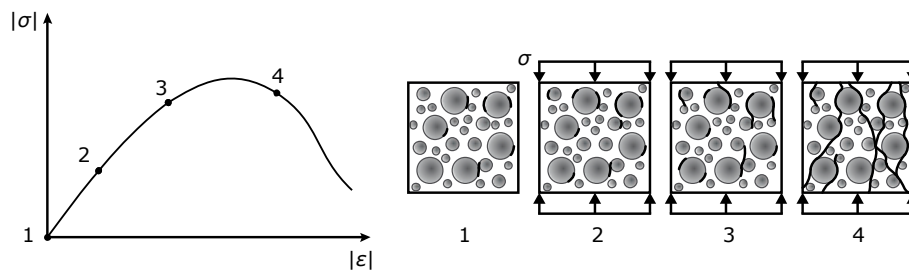


Figure 3-22 Illustration of the course at crushing of concrete [89].

There are some different examples of stress-strain-curves that are usually assumed to describe the unloading of the concrete when cracking, see [40]. In general, it should be mentioned that linear unloading should be avoided as it leads to overestimation of the stiffness of the structure and thereby also the load-bearing capacity. Instead, a curve should be chosen which is better matched to the behaviour obtained in testing, such as bi-linear curve or an exponential one.

However, a parameter that cannot be estimated using the Eurocodes is the fracture energy that defines the ductility of the concrete during the crack propagation. For conventional concrete, the fracture energy can be determined according to the Model Code [63] where it is derived from the compressive strength. However, concrete used for dams and other hydropower structures deviates from conventional concrete, especially in view of the fact that a larger maximum aggregate is used. Using the fracture energy according to Model Code means that you will underestimate the ductility and thereby get a more brittle breakage. The difference in properties between conventional concrete and for concrete used for dam construction is compiled in [64].

Table 3-2 Examples of differences in the properties of the concrete (average) between concrete used in hydropower and conventional concrete [64].

Type of concrete	d (mm)	f_t (MPa)	E (GPa)	G_f (Nm/m ²)	l_{ch} (mm)	w_{cr} (mm)
Arch dam A	80	2.4	36	230	1440	0.25
Arch dam B	120	2.3	27	310	1580	0.30
Arch dam C	120	2.0	29	270	1960	0.37
Conventional concrete	32	3.4	36	140	440	0.16

where,

d is the largest aggregate size (mm)

f_t is the tensile strength (MPa)

E is the elasticity modulus (GPa)

G_f is the fracture energy (Nm/m²)

l_{ch} is the characteristic length (describes the brittleness of the material) (mm)

w_{cr} is the crack width for a stress-free crack (mm)

Several other studies show the same case, e.g. [65] mentions that while the characteristic length of ordinary concrete is typically 0.5 m, it can be up to 3 m for concrete used in hydropower. Although the tensile strength and the modulus of elasticity are somewhat lower for hydropower concrete compared to conventional concrete, the primary reason for this difference is the increased fracture energy from the use of larger aggregate. The fracture energy increased significantly, from 72 Nm/m² to 178 Nm/m² (i.e. 2.5 times higher), if the aggregate was increased from 20 mm to 56 mm according to [66].

It is important to point out, however, that today's concrete structures are rarely cast with such large stones as stated in the examples above. The reason is that the concrete manufacturers rarely have this demand and that concrete pumps etc. are rarely designed for this. This means that for new structures, the recommendations of the Model Code are usually suitable for use.

The difference in choice of fracture energy, however, for reinforced structures usually has a relatively limited effect on the result, because when the crack has arisen, the reinforcement carries load and thus acts in a similar manner as the influence of high fracture energy as long as the stress in the reinforcement does not reach the yield stress. The choice of fracture energy can thus result in the yield stress in the reinforcement being reached or not and may thus have great influence on the deformation behaviour. On the other hand, in non-linear calculations, a fracture energy that is assumed too high makes it impossible to capture individual cracks, but instead a smeared cracking is obtained across large regions in the model. This is illustrated in Figure 3-23 below.

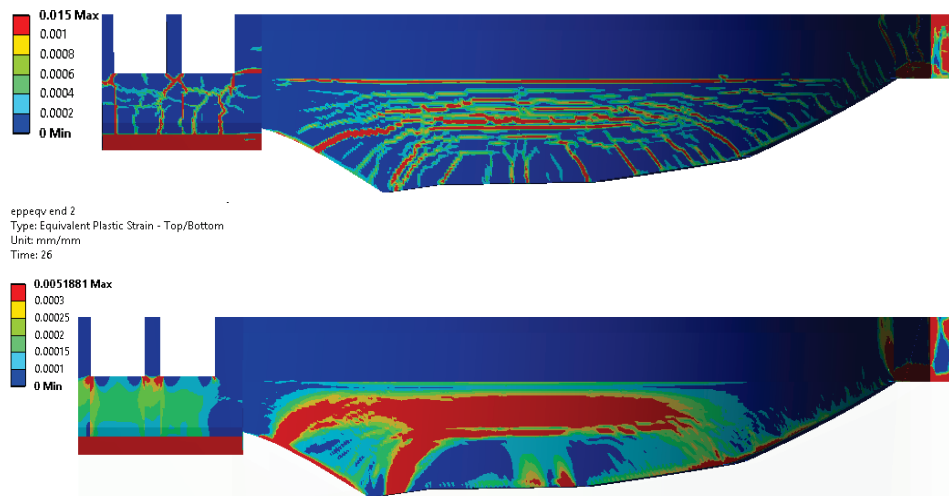


Figure 3-23: Illustration of the impact of choice of fracture energy. In the upper figure a fracture energy of 200 Nm/m² is assumed and in the lower it is assumed to be 500 Nm/m², [54].

For non-reinforced structures, these material parameters have a greater impact. Increased fracture energy leads, as previously stated, to a more ductile material behaviour, but on a structural scale, this also means that the load-bearing capacity increases as the cracks unload at a slower rate and thus the structure can carry higher loads. Increased tensile strength (with retained fracture energy) in turn leads to higher load-bearing capacity but a more brittle crack process. The influence of the non-linear material parameters to describe cracking is illustrated in Figure 3-24.

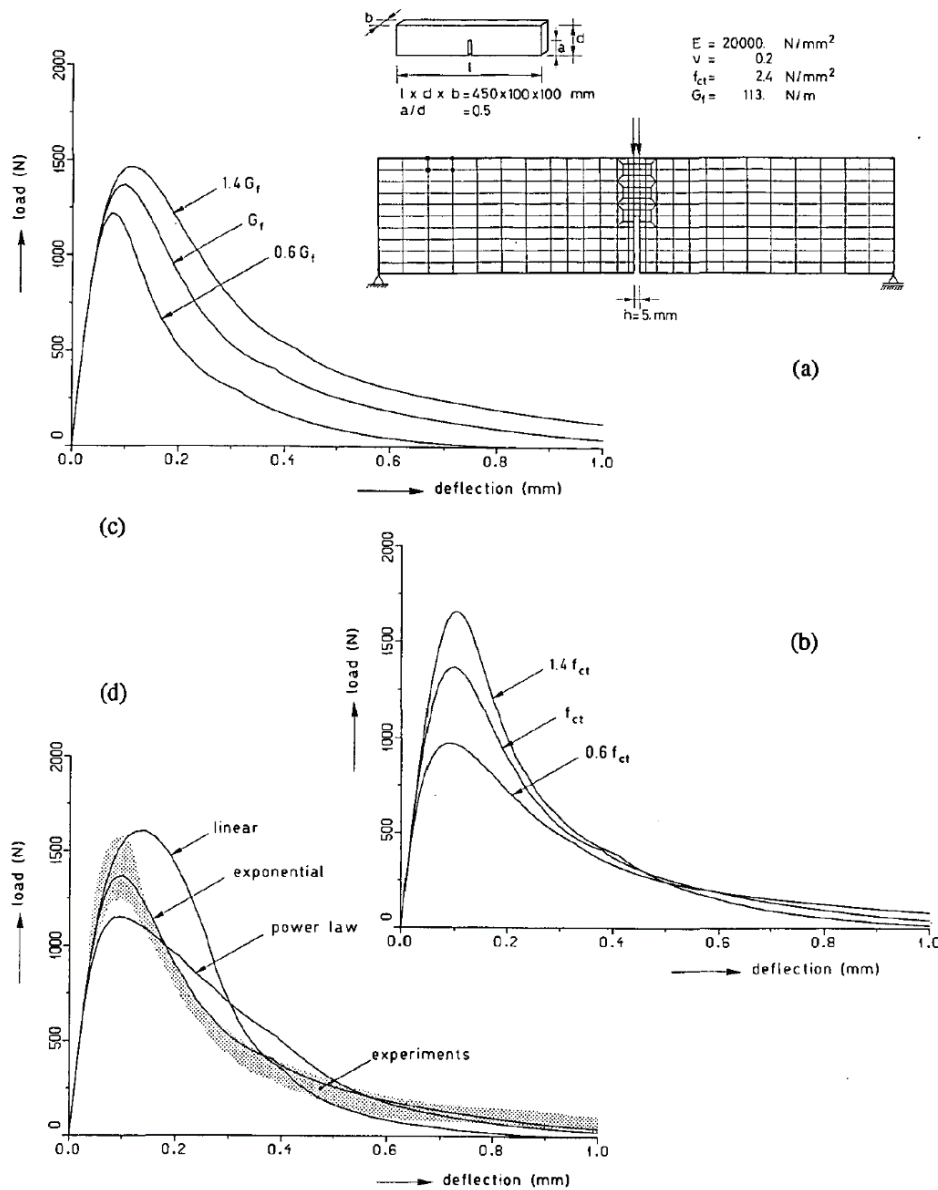


Figure 3-24: Impact of non-linear material parameters on the structural behaviour, a) Impact of fracture energy, b) impact of tensile strength, c) impact of the shape of the unloading curve

3.7 VALIDATION OF CALCULATION MODEL

All numerical models should be validated. The complexity of the model, or whether new applications (for the user) determine how detailed a validation needs to be. To validate a calculation model, several steps are required. This is also described in [41] which relates to the examination of hydropower concrete structures. The present section is formulated to be in line with what is prescribed in [41] but somewhat more extensive.

- Simple models based on conventional, well-proven procedures also need validation. In these cases, it is primarily choice of input (parameters, loads, etc.) and choice of method/model for specific application that may need validation. This can e.g. be performed using sensitivity analyses, where results from different choices of input data are compared in order to study the impact of these choices.
- In more advanced cases, e.g. when self-made material models or new material models (for the user) are applied, or when complicated structures alternatively advanced phenomena are taken into account, a considerably more extensive evaluation is required. This can be done by means of e.g. comparative measurements and/or analysis of typical cases from e.g. the literature in addition to the tests described in the above paragraph.

According to the Model Code (2010) [63], the following can be validated:

- material model (See section 3.7.1)
- structural model (See section 3.7.2)
- convergence (See section 3.7.3)

In addition to these, there are also two further cases presented in this report, which relate to

- Validation by comparison with simpler calculations (See section 3.7.4)
- Validation of calculation model with measurements (See section 3.7.5.)

3.7.1 Validation of material model

In cases when a new (for the user) material model or a material model for a new type of application are applied, validation of the material model is required. This also applies to cases where the material properties differ considerably from previous applications, e.g. use of high strength concrete as opposed to conventional concrete.

The simplest form of validation is to study an element and check that the stress-strain-curves defined in the program for describing behaviour during cracking or crushing of concrete or plastic deformation of steel are recovered by simulation with uni-axial load.

For the validation of a material model, there are also many straight-forward laboratory experiments presented in the literature that have been carried out with three or four-point bending on e.g. non-reinforced concrete beams. An example often referred to is the experiments conducted by Petersson [67]. Figure 3-25

illustrates the concrete beam studied in [67] as well as the measured load and the deformation curves obtained for two different fracture energies.

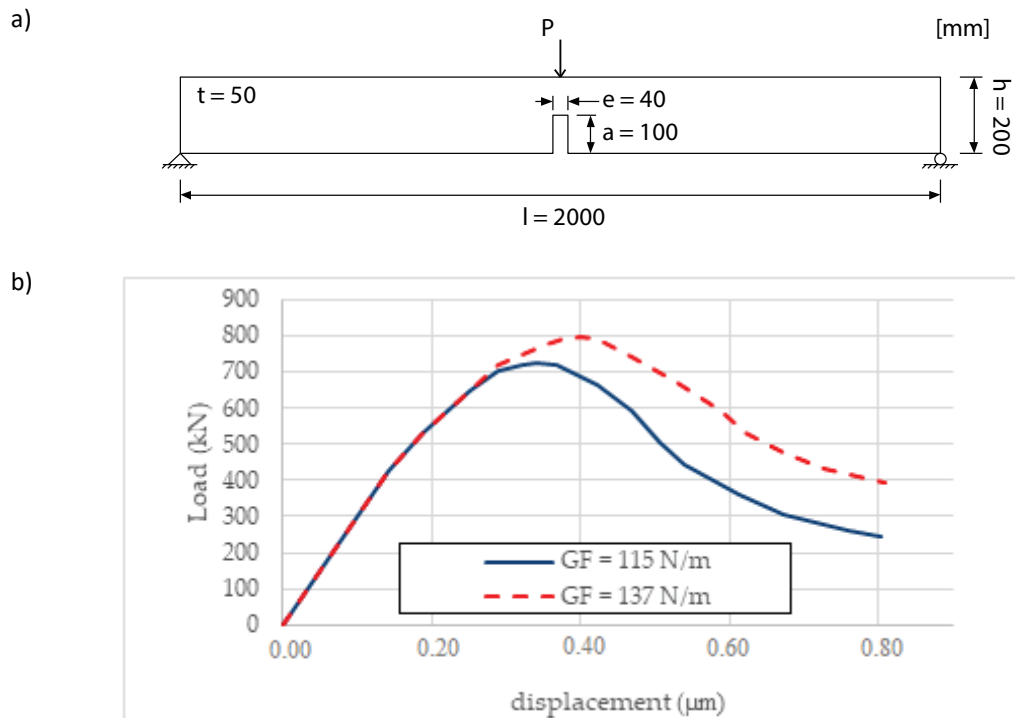


Figure 3-25 Example of beam testing which is normally used for verification of material model, a) geometry, b) result.

Additional examples for the validation of a material model that relate to validation at a bi-axial load on an element are found in [68]. The purpose of this is to study whether the material model can describe reduced compressive strength at cracked cross sections.

3.7.2 Validation of structural model

The purpose of this test is to validate that a specific structural behaviour can be captured by an algorithm or software. This is often carried out with "benchmark examples" in order to be able to investigate the need for e.g. the amount of detail of a material model or investigating a new (for the user) software. It is important that this test is carried out on a type of structure that is similar to and thus represents the structure that will later be analysed (Model Code, 2010) [63].

The ICOLD Committee A (Computational Aspects of Analysis & Design of Dams) has since 1991 arranged 14 Benchmark Workshops for this purpose. These benchmark workshops consist of several generalized cases aimed at developing and presenting best practice in dam construction. The documentation from these is available through the ICOLD website. Work is currently underway within ICOLD

to condense the results and lessons learned from all previous Benchmark Workshops.

3.7.3 Validation of convergence of results and equilibrium

All numerical analyses are approximations. The accuracy of the approximation depends, of course, partly on the input data and how the problem has been interpreted and thus calculated.

In addition, the approximation depends on the accuracy of the model. In a finite element model, the structure is divided into several elements that have certain prescribed movement possibilities. If insufficient numbers of elements or elements of too low order are used, there is a risk that the result will not give the correct solution to the problem being solved. In order to verify that element division (discretization) is sufficient for the problem that is intended to be solved with the FE calculation, convergence tests need to be performed.

A convergence test is carried out so that the same problem is analysed with different elemental divisions. This can e.g. be carried out so that the subsequent calculation is carried out with halved element length, and when the result from two simulations with different degrees of detail give the same (or very similar result), the calculation model is considered convergent with respect to elemental division.

It is also important to remember that precise equilibrium is seldom achieved in finite element calculations. Instead, an iteration is accepted if it is sufficiently close to equilibrium. The concept sufficiently close is governed by how the tolerances in the calculation model are selected. In most conventional calculations with implicit solvers, this occurs automatically in the software. On the other hand, some software programs can pass through iterations even though they do not meet the conditions of tolerance if, for example, a certain number of iterations have been carried out.

Finally, it is important to point out that in non-linear analyses, situations with “cliff-edge” effects can occur. This means that a small change in input data can have a significant impact on the result. For this reason, sensitivity analysis with regard to the choice of input data should always be performed in non-linear analyses.

Users should therefore always make a habit out of making relatively simple checks for this, more information on this is found in e.g. in [40].

3.7.4 Validation with simpler analyses

To verify that the calculation provides reliable results, comparative analyses should be carried out. This should then be done with a simple verification, e.g. analytical calculation methods. There is also a great number of simple calculation software for analysing e.g. load-bearing capacity of concrete cross-sections, stability for concrete dams, etc., see e.g. [40]. These kinds of software are very suitable for the rapid verification of the plausibility of more advanced analyses.

The purpose of these comparative calculations is to assess plausibility of the outcome of a more advanced calculation.

3.7.5 Validation against measurements

In many cases, there are measurements available on dams where mainly crest movement is measured, see for example. Chapter 5.12.

Local effects such as single point strain or crack width variations at a specific crack are generally more difficult to obtain good conformity and largely depend on whether relevant local phenomena can be captured in the model. E.g. if the real crack has a slope deviating from the one in the model, a difference in results will automatically be obtained.

The crest movement is normally a very good measurement of determining the global behaviour of a dam. The crest movement is the summed up effect of various defects and loads and thus does not become as sensitive to local errors. In addition, cracks in dams lead to lower restraints and can thus lead to less forced global deformations caused by constrained loads such as temperature, shrinkage, etc. model that does not consider these cracks. However, this depends on how extensive the crack formation is. Cracks lead to a new deflected equilibrium position, but not necessarily to the fact that the variation in crest movement between e.g. summer and winter change. An example of results from simulated crest movement as compared to measured crest movement for an arch dam is illustrated in Figure 3-26 from [56]. Another case of simulation of crest movement of an arch dam is presented in [49] and shows that in cases of more extensive cracking, these weakenings lead to a changed shape of the deformation curve, see Figure 3-27. The corresponding change in the deformation figure could also be observed on the real dam, see [54].

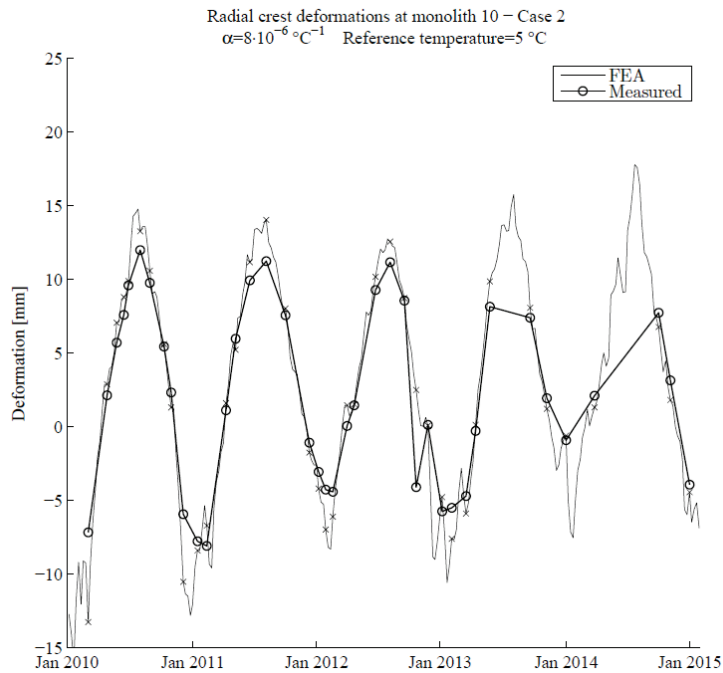
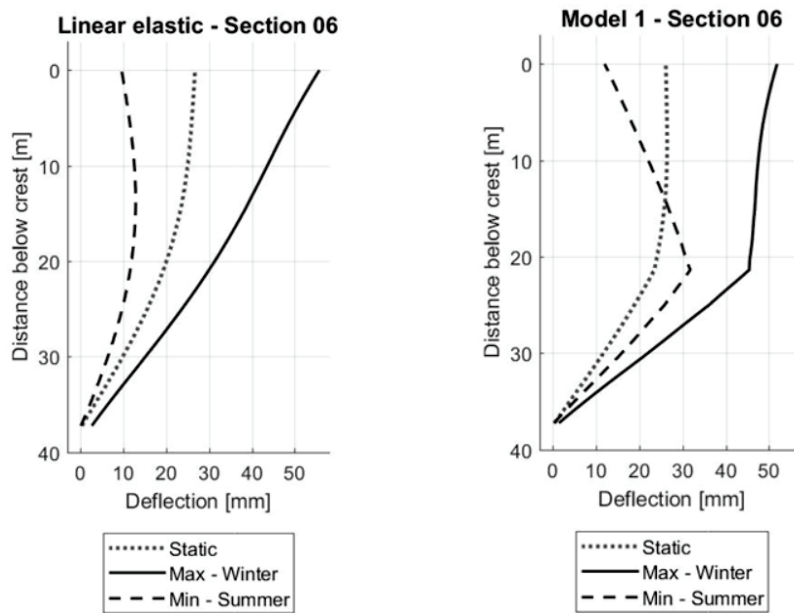


Figure 3-26: Comparison between simulated (linear elastic) crest movement and corresponding measurement [56].



a)

b)

Figure 3-27 Illustration of difference between elastic deformation and deformation when cracking is taken into account [49].

As previously pointed out in Chapter 3.3, the more advanced models may not always be more accurate. One such example is the determination of the expected response of a dam that forms the basis of the choice of critical limits. In [46] a case study that clearly illustrates this is presented, see Figure 3-28. The figure presents the measurements from a four-year period together with three evaluation methods

- FEM - linear elastic finite element model
- HTT - a multilinear regression model that is based on the effect of water level, seasonal temperature variations and time.
- ANN - a machine learning methodology based on artificial neural networks.

The results in this figure show the expected pendulum movement and the spread that is obtained with the different methods. In this case, it is clear that ANN is far superior to the prediction of upcoming measurement values. Then comes HTT and finally FEM. It is important to note that HTT and ANN require a certain amount of measurement data which can be calibrated with, only then can they be used to make forecasts. In addition, ANN is basically a black box where it is not possible to get a great understanding of what is happening in the dam. However, FEM has the advantage of giving great interpretation ability and also that the method can be applied to simulate cracks in the dam so that it is also used to define suitable critical values.

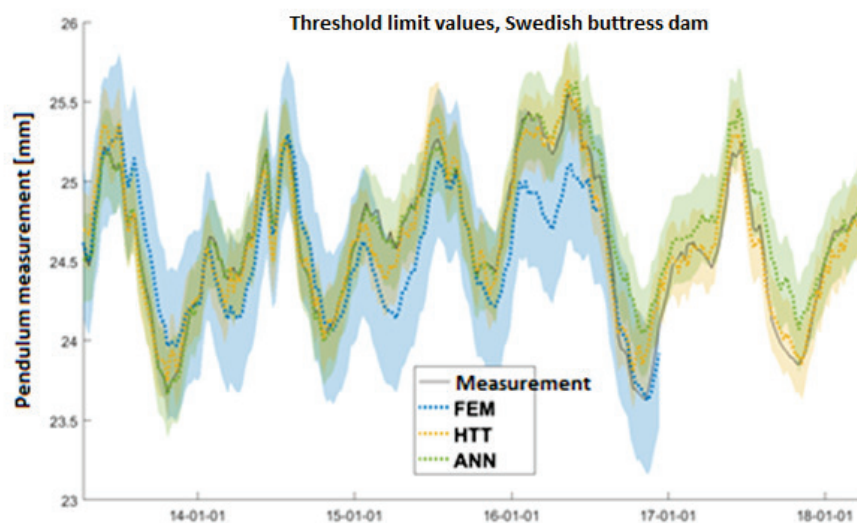


Figure 3-28 Difference in spread between results from different methods of analysis in comparison to measured crest deflection, from Hellgren et al. (2018).

3.8 METHODOLOGY FOR EVALUATION OF THE IMPACT OF CRACKING

First and foremost, it is important to remember that reinforced concrete structures are designed to crack. It is only after cracking that the reinforcement is activated. In addition, the amount of reinforcement in the structure is calculated from the fact that all concrete under the neutral axis is assumed to be cracked (according to stage II and III).

Cracks, however, are weak planes and when formed, the stiffness of the structure drops significantly, which leads to larger deformations at imposed loads. These can thus lead to new potential modes of failure. The cracks can also lead to problems with regard to the long-term load-bearing capacity of the structure due to the degradation that is included, such as e.g. corrosion of reinforcement. If the current state of the dam, despite the crack formation, meets set requirements for water tightness, load-bearing capacity and stability, no measures need to be taken.

According to [12], the following flow chart can be applied to cracked concrete dams, see Figure 3-29. This constitutes a good basis for the procedure for analysing the effect of cracks in dam structures and describes how one can gradually increase the accuracy while evaluating.

The various analysis sequences are described according to [12];

Stable when calculating as uncracked: Global stability for the structure in uncracked condition is checked as this is a prerequisite for the structure to be considered sufficiently safe.

The cracked parts are stable separately: the structure is assumed to be completely cracked in the pattern that the cracks constitute/which the intended extension of the cracks indicates. Then, the cracked parts are analysed separately (reinforcement between the parts is not assumed to be effective) with regard to stability to see if the stability conditions are fulfilled.

The cracked parts are stable if the reinforcement is included: As before, but the reinforcement in the cracks is assumed to be effective.

Cracked parts are stable if they are analysed as joints according to SS-EN 1992 [32]: The transverse force transfer is estimated according to SS-EN 1992 section 6.2.5 depending on the amount of reinforcement, roughness, etc. and it is checked whether the capacity is then sufficient.

Fracture mechanical analysis is the next level of detail that can be used. Such analyses are especially valuable in order to find the cause of the cracks. However, they are advanced to implement and require a lot of experience and knowledge from the operator. A much better alternative is instead to include existing crack planes in a linear elastic model so that no further crack initiation is simulated, only the impact of existing cracks, see section 3.5.5.

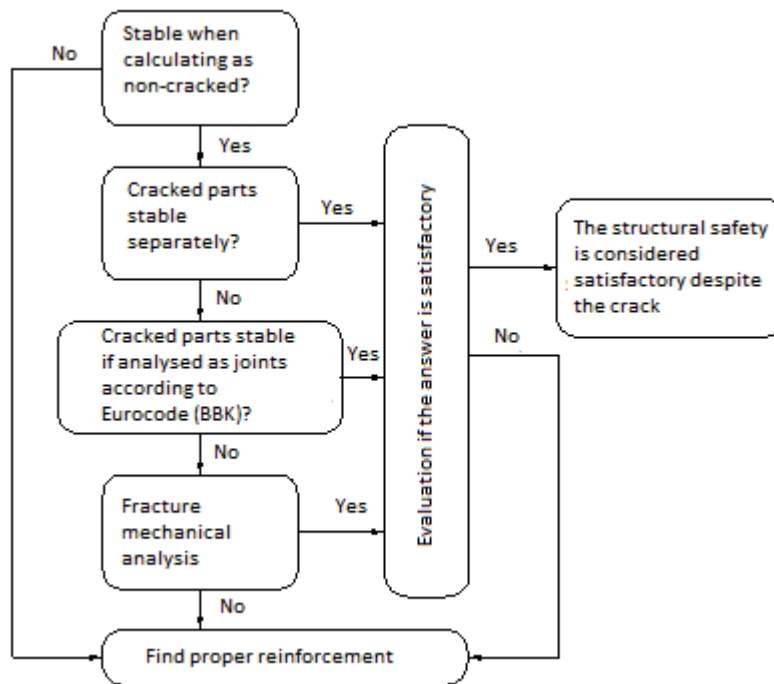


Figure 3-29 Illustration of methodology for evaluation of the impact of cracks in dams [12].

It is important to point out that all of these analyses can be carried out with one of the various analysis methods described in Section 3.2, i.e. they can be carried out with analytical calculations or with e.g. finite element analysis.

The advantage of analytical calculations is that they are usually relatively fast. The disadvantage can be that for complicated geometries and/or load cases it may be time consuming to calculate self-weights, levers and load values. In addition, it is often necessary to carry out a number of simplifications that can lead to great conservatism. Even in the case of a correspondingly simple finite element calculations, it is possible to include the influence of cracks in a more correct manner, both in terms of their shape but also in the case of the shear resistance in the crack.

Another thing that can have a major impact on analytical calculations is how the contribution of the reinforcement is taken into account. In a stability analysis, the reinforcement can either be seen as tensile or compression-loaded (load perpendicular to the crack) or alternatively subjected to the dowel effect (load parallel to the crack). Depending on which of the above is used, different results are obtained. The reality is more complicated than that, and the load in the reinforcement bars can vary depending on where in the crack these are, where some are exposed to shear, other tensile or compressive load or a combination of these. This is very difficult to estimate because it depends on the global behaviour of the structure, and in these cases a finite element calculation is clearly advantageous as this is taken into account automatically.

3.9 ACCEPTANCE CRITERIA

One of the most difficult aspects of an analysis is to make the assessment whether the facility is safe or not. The reason for this is partly that there can be large uncertainties in the input data and the conditions, but also because the crack behaviours are highly non-linear and thus more difficult to predict based on the assumption that the structure acts linearly elastic.

It is also important to consider that different clients may have different requirements. In addition, in some cases it can be taken into account that the safety classification of the dam can change in the future, e.g. if any houses/facilities are built downstream of the plant, a dam can be upgraded to a higher safety class.

It is reasonable and also possible that special acceptance criteria should prevail for the assessment of existing, cracked, structures. This can e.g. due to the fact that the remaining expected service life of the structure is shorter than what was assumed when design the new structure. However, in this section it is assumed that the same safety requirements as defined in RIDAS [3], [4], are also applied when assessing existing, cracked, structures. If the evaluation do not meet the requirements in RIDAS [3], [4],, either a more detailed investigation can be performed or one may judge whether this needs to lead to reinforcement measures or if these shortcomings be accepted. However, in order to develop specific acceptance criteria for existing structures, continued research and development work is required.

Safety concepts – Consistent methodology for evaluation of dam safety

Out of this reason, it is very important that the analyses and the approach as far as possible is based on the design provisions given in guidelines (such as RIDAS [3], [4],) and standards (such as the Eurocodes). This also means that applied methods in more advanced models need to be based on the same definition of safety concept.

For example, in the case of stability calculations (regardless of method of analysis), the safety levels defined in RIDAS [3], [4], should be fulfilled in order for the dam to be considered safe. For dams founded on bedrock, this means $sf = 1.35$ for sliding and $sf = 1.50$ for overturning. If the dam is subjected to a combined failure mode, there is nothing defined in RIDAS [3], [4],, the recommendation from this work is then that the safety factor should be at least higher than the value for sliding.

This means that even if more advanced analysis models such as non-linear finite element models are applied, these should be implemented so that the definition of the safety concept becomes uniform. A clear example of this is if, for example, stability calculations are carried out using the finite element method and the approach defined in Chapter 12.2 of [39] is not applied. This means that for the same definition of safety factor to be obtained, all overturning loads must be increased simultaneously.

Difference between taking into account the stability failure and the cross-sectional failure according to RIDAS [3], [4],

One difficulty in evaluating according to RIDAS [3], [4], is partly that two different formats are used for evaluation of dam safety regarding stability and cross-sectional analysis, but above all because the load combinations stated are not entirely relevant for cross-sectional design.

In cross-sectional design (especially in serviceability limit states), loads such as temperature variations, shrinkage, etc. are highly relevant to consider. However, these are not mentioned in the load cases specified in the current (or previous) version of RIDAS [3], [4].

In addition, the load cases for the serviceability limit state (LC1) and the ultimate limit state (LC2) are defined equally in RIDAS [3], [4], which is strange as they relate to user requirements (good function) and safety requirements. In addition, the same load case is also specified for the stability analysis (LC1). However, it should be pointed out here that other relevant load effects should also be considered in the cross-sectional analyses, e.g. load effects caused by shrinkage should be taken into account in serviceability limit states, temperature effects in both crack and serviceability limit states (but not in stability analyses), etc.

When is stability failure or cross-sectional failure the determining factor for design respectively?

An important aspect in the difference between the different design situations according to RIDAS [3], [4], is that the required safety factor becomes different. As previously mentioned, the safety factor for stability failure is typically 1.35 for sliding and 1.5 for overturning.

When partial coefficients are applied for cross-sectional analysis, the acquired load coefficients are as shown in Table 3-3 for a case with dam safety class A. As shown in the table below, the partial coefficient always becomes higher than the global safety factor for stability analysis, which means that cross-sectional analysis always becomes determinative if the dam risks being exposed to a material failure, or internal failure modes due to cracks.

Table 3-3 Example of partial coefficients of loads at ultimate limit state according to RIDAS [3], [4], at dam safety class A

	Ultimate limit state	
	6.10a	6.10b
Permanent load (G)		
<i>favourable</i>	1.76	1.56
<i>unfavourable</i>	1.00	1.00
Water load (favourable)	1.00	1.00
Water load (unfavourable)	1.76	1.56
Self-weight	1.00	1.00
Uplift pressure	1.76	1.56
Variable load (Q)		
<i>Main Load</i>		1.95
<i>Additional loads (* ψ_0)</i>	1.95	1.95
Ice load ($\psi_0 = 0.8$)	1.56	1.56
Temperature change ($\psi_0 = 0.6$)	1.17	1.95

What is the definition of a failure?

The simpler the model applied, the greater the degree of conservatism should be. This is because there is a risk that the model neglects important aspects and thus, for example, underestimates the risk of a basic failure mode.

For example, in linear-elastic finite element analyses, the maximum stresses acquired in the calculation model should be limited so that they do not exceed the allowed strength values for the current limit state. This means, for example, that the stresses in the concrete should not exceed the tensile strength. In these cases, however, it is very important that the model is not exposed to local hot-spot stresses, since these are not physical stresses, but rather an effect of simplifications in the model. More information on hot-spot stresses is described in Chapter 4.2 of [40].

Serviceability limit state - When analysing cross-sectional failure according to RIDAS [3], [4], yield stresses (with regard to actual partial coefficients) should not be reached in the reinforcement when analysing serviceability limit states. This is in accordance with common conditions in design standards such as the Eurocodes. In addition, at serviceability limit states, there are normally limitations on maximal permissible deformations, maximal crack widths, etc. In dam structures, the characteristic crack width should not exceed 0.2 mm according to RIDAS [3], [4]. The requirement for permissible deformations can e.g. depend on the risk of gates being squeezed.

Ultimate limit state - In the case of a cross-sectional ultimate limit state according to RIDAS [3], [4], the analysis can be carried out until structural collapse is achieved. As previously pointed out, the degree of conservatism in the model affects the assessment of when collapse is initiated. An example of this is e.g. that it is difficult to estimate the load in reinforcement and rock bolts (tension, compressed or sheared) during simpler calculations. In these cases, a conservative

assumption needs to be made about the load of the bolts. In advanced models, the stresses of the reinforcement or bolts are calculated based on the deformation of the dam and in addition, for example, the failure strain of the reinforcement is considered so that the reinforcement is ruptured and thereby redistributes the loads.

When it comes to definition of failure, it is also important to point out that in non-linear analyses that take into account material strengths and crack propagation or plastic deformation, it is important that a methodology is applied which is suitable for this type of analysis. If non-linear analyses are carried out based on design conditions, with reduced strength values, then there is a great risk that faulty failure modes will be captured and thus that incorrect conclusions are drawn. Out of this reason, it is important that, for example, the methodology reproduced in Chapter 3.5.6 is used.

Measured data – Critical and threshold levels respectively

When defining critical and threshold levels on measurement data, it is important that these are defined on sensors that are expected to indicate possible dam failure scenarios. In addition, these critical and threshold levels should be defined on the basis of expected normal measured values and expected measured values in the event of a dam failure. Of course, however, these values should be adjusted with the suitable safety factor so that there is enough space to carry out suitable measures, see Chapter 4.

In order to define threshold levels, methods such as HTT or ANN can suitably be applied, but this requires that a sufficiently long series of measurements is available so that the methods can be calibrated. For defining critical levels, only non-linear FE analyses are suitable.

4 Measures

4.1 INTRODUCTION

In the previous sections, a description has been given of how the condition assessment of a cracked concrete structure can be made in different steps from visual inspection of the cracks to analysis of their origin and significance for the structural integrity. If the current situation, despite the cracking, meets set requirements for water tightness, load-bearing capacity and stability, no measure needs to be taken. The assessment should of course be made from the perspective of the present situation and the desired remaining service-life of the structure. On the other hand, if the assessments give that the requirements are not met, then a measure must be taken to achieve the desired level of requirement or possibly to reduce the risk that the safety margins to the desired level of requirements are not lowered.

In the present section, a suitable workflow is presented to identify possible alternatives for measures and examples of alternatives for managing arising crack formation in the form of monitoring in a systematic manner.

4.2 EMERGENCY MEASURES

It is very rare in the hydropower area that extensive cracking, or, above all, increasing crack development occurs abruptly. Failure loads with crack formation on concrete structures in hydropower plants could arise due to e.g. short-circuit loads from generator or closing the guide vanes too fast with subsequent water hammer, which can give overload to a structure. For older structures in power plants or dams that have been subjected to long-term degradation, there is a progressively increasing risk of cracking. The crack formation then occurs when the load-bearing capacity of the degraded structure finally becomes so low that the structure cannot carry the loads it is subjected to.

The most common process is that propagated cracking occurs through a long-term process. In some cases, however, it may take some time before the propagated cracking is detected e.g. if the structure usually is under water. During diving inspections, cracking that has been present in the structure both for a longer and shorter time can then be detected.

An example of serious cracking below the waterline is the Wanapum Dam in the US [69], where extensive horizontal cracking in a spillway dam was revealed by operating personnel visually seeing changes in the bridge roadway and that the road fence had been deformed (Figure 4-1). Through diving, it was found that a horizontal crack of approx. 50 mm had opened up in a spillway pier on the upstream side.



Figure 4-1 Deformed railing on the dam crest, Wanapum Dam.

In order to immediately reduce the risk of progressive failure in the pier, the water in the reservoir was lowered by around 9 m after an estimate of load-bearing capacity and stability in the current condition. **The drawdown** of the reservoir also gave time to investigate the causes of cracking.

In addition to the reduction of the load made in the Wanapum Dam, an **increase in the stabilizing weight** can also be achieved by placing e.g. trucks fully loaded with gravel on the crest. It is an emergency measure if a stability failure due to overturning or sliding of a concrete dam is within the risk of occurring. Obviously, the load-bearing capacity of the dam bridge must be sufficient before loading can take place.

Emergency measures can also be measures to **reduce or stop heavy and/or troublesome leakages** through cracks, e.g. into a power house where the risk of flooding or contact with electrical equipment and of production loss otherwise can be the consequence. Leakage can be stopped quickly by e.g. plugging with coal dust, wood chips, horse manure or sand. The risk of plugging, however, is that it can be more difficult to make a permanent seal with e.g. grouting when the crack is partially filled with fine material. However, in an emergency situation, it may be an alternative. Another way is to place a cloth-like material such as tarpaulin in front of the cracked area where the tarpaulin is "sucked" against the crack area and thereby seals it. If divers are to be used to detect the area or place the sealant, great care must be taken in those cases where the leak is large/the crack is wide. In the event of larger leakage, there is always a risk that the diver themselves can be sucked in with e.g. one hand at the leaking point.

Suitably, all of the **potential emergency measures** of the facility are mapped in advance and preferably prepared with instructions that can easily be activated in the event of an emergency measure. This is preferably done in an emergency preparedness plan. E.g. it should be clear with contact information on where you can get hold of trucks, gravel and what load-bearing capacity the dam bridge has.

4.3 MONITORING DEVELOPMENT

An initial analysis of the impact of crack formation may in some cases conclude that cracking in the present, or in the near future, is not considered to be a direct threat to the safety and load-bearing capacity of the structure. Instead, a better basis may be needed to assess the actual status, e.g. by detecting whether the crack formation is dynamic (active/still under development) or static (constant). In that case, one measure can be to instrument the structure to obtain more information and monitor any possible development. Monitoring a crack can also provide a basis for understanding why the crack has occurred and what drives a possible crack development. If the crack is dynamic, the purpose is also to clarify what affects the crack propagation (e.g. ongoing concrete expansion, substandard load-bearing capacity, reservoir level, temperature changes due to season, ice load etc.).

4.3.1 Prerequisites

The knowledge of current static mode of action is crucial for the design of a monitoring system on a concrete structure. Without this, effective monitoring cannot be designed in the best way possible. Understanding how the structure is intended to carry loads and what impact current cracking has on the mode of action must be clarified in order for measurements to take place in the right positions and with the correct measuring methods. If the cracking is extensive, a numerical model can also be a good tool for identifying which cracks and in which position along the crack where a possible crack propagation or movement is first revealed (see also section 3.2.3).

4.3.2 Strategy for systematic design of a monitoring system

A well-designed monitoring system on a dam provides good conditions for being able to evaluate whether dam parts meet set safety levels/performance and get early warnings if performance deteriorates. In order to make sure that the dam is safe, the following must be considered in the assessment, according to ICOLD [70], [71]:

- **Threats**
 - × External (floods, earthquake, landslides in reservoir, human error)
 - × Internal (design/construction errors, maintenance measures, operation)
- **Failure modes, and how the dam failure can develop**
 - × Stability (overturning, sliding)
 - × Cross-sectional failure
- **The consequence of a dam failure**

In RIDAS TV [42], some common risk factors/zones of weakness for concrete dams are exemplified, their connection to threats, failure modes and consequences as well as examples of how to monitor the weakness/risk.

In summary, cracking usually has a connection to the risk that a cross-sectional failure occurs due to the load exceeding the load-bearing capacity of the structure, either because of the crack itself or because the performance of the concrete has been reduced by some degradation process in connection with the crack. Less likely, but still conceivable, is that a stability problem would arise in the form of

partial overturning or sliding due to cracking in a monolith that is stable in uncracked state.

Table 4-1 Example of monitoring adapted to failure modes for concrete dams

Weakness/risk	Threat	Failure mode	Consequence	Example of monitoring
Overtopping	External	Overtopping Cross-sectional failure	Leakage Dam failure	-Automatic water level monitoring - Dam overtopping protection system
Increased uplift pressure	Internal	Overtopping Sliding	Leakage Dam failure	Pore pressure measurement
Erosion in downstream toe	External/Internal	Overtopping	Dam failure	Visual Pendulum
Crack/movements in bedrock	Internal	Overtopping Sliding	Leakage Dam failure	Pendulum Crest measurement
Anchoring	Internal	Overtopping	Leakage Dam failure	Load cells Crest measurement
Joints	Internal	Cross-sectional failure	Leakage Dam failure	Visual Movement sensor Crack width measurement
Leaching/degradation	Internal	Cross-sectional failure	Leakage Dam failure	Visual Leakage measurement Strain gauge Crack width measurement
Crack formation	External/internal	Cross-sectional failure	Leakage Dam failure	Visual Strain gauge Crack width measurement

4.3.3 Selection of equipment

Usually, the process of cracking is slow, but also temperature dependent, which can complicate the interpretation of measured crack widths unless simultaneous temperature measurement in concrete, air and reservoir is made. The recommendation is therefore to always make both crack width and temperature measurements, regardless of what caused the crack. If the crack formation affects the global behaviour of the dam, it may be especially effective for high buttress

dams to measure the crest movements of the dam with pendulum sensors at the same time as crack width and temperature are recorded. Since a direct pendulum is mounted at the top of the dam bridge roadway and the change is measured at the bottom at the foundation level, a good result is obtained on the crest movement and thus a measurement of the effect of possible cracking in the dam pier.

Crack width and temperature measurements can be done in different ways and with different precision. In order for the measurements to provide the desired quality and reliability to be used to trigger a warning or an alarm about an unwanted event or to follow a behaviour, the recommendations below must be followed when selecting equipment. Superior quality drives costs, but sufficient quality provides good dam safety. The equipment should:

- be adapted for the current exposure environment
- be calibrated and easy to calibrate after time
- have an accuracy and resolution that fits the expected change (at least 5/100 mm or 0.1 ° C)
- have a measuring range that covers the expected variation with regard to any other parameters that can cause variations in crack width (e.g. temperature).

Some examples of suitable equipment are given below for each measurement type:

Movement Sensors

In order to follow movements in concrete dams, pendulum measurements are an effective way. The pendulum measurement can be used where it is suspected that cracking gives rise to large-scale movement in the structure. One case may be e.g. if there are horizontal cracks in the front slab of a buttress dam and a suspicion that these may be a result of a large-scale movements from e.g. temperature changes. The direct pendulum measurement of the crest movements combined with the crack width measurement then gives a good image of changes over time, and an early indication of possible propagation of crack width.

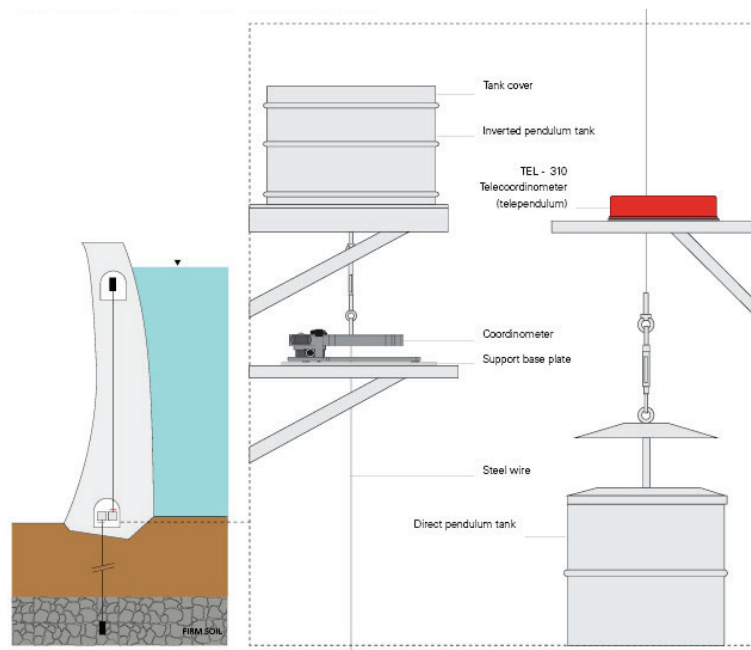


Figure 4-2 (Left) Dam with inverted and direct pendulum. (Right) Direct and inverted pendulum. (www.sisgeo.com)

Crack width sensor

In order to measure the crack width and any changes in the crack width over time, there is a whole variety of different types of sensors. Everything from manual measurements with crack width gauge (see Figure 4-3) which are relatively rough, but easy to perform where you can easily access, to more advanced, permanently installed, accurate, 3D measurements that are logged and stored continuously (see Figure 4-4). The choice of transducer type is partly a matter of taste, but should be based on how much knowledge there is about the origin of the crack and its behaviour. Sometimes combinations of equipment can be good where a few cracks with greater priority are continuously logged with high precision and several others with cheaper fixed crack width measurements

Initially, simpler manual measurements can be made to create a perception of whether the movements are dynamic or static, or to map any pattern in the distribution and occurrence of the crack widths. Any changes are detected by repeating the measurements with time.

If calculations show that any crack width changes are small or if the cracks are located in a place that is difficult to access, a connected sensor with good accuracy may be preferred. A connected sensor also becomes necessary in a system where a crack has dam safety significance and where a critical limit is defined so that measures can be taken to prevent e.g. a dam failure.



Figure 4-3 (Left) Manual fixed crack width measurement. (Right) Crack width ruler/gauge.

Figure 4-4 shows 2D and 3D sensors that can be used where you suspect movements in 2 or 3 dimensions. The reported 3D sensor can be used for both manual and automatic crack width measurements. At the latter, e.g. LVDT sensors are permanently mounted in the holes.

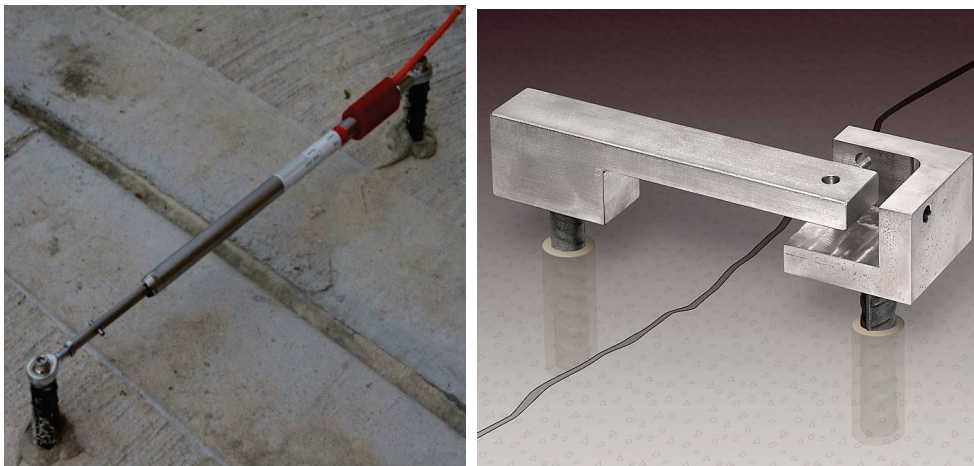


Figure 4-4 (Left) 2D-crack width sensor of the type Geosense VWCM-4000. (Right) 3D-crack width sensor of the type Geocon 4415.

Temperature sensors:

In order to be able to interpret measurements of concrete and crack movements and be able to derive the state of the crack (static/dynamic) and the reason for its occurrence, it is crucial to keep track of the prevailing temperatures. The interpretation is facilitated if temperature measurements are made by:

- The *internal temperature* of the concrete structure. Thus not only the surface temperature but also the internal temperature of the concrete. Suitable depth for the measurement is determined by the thickness of the concrete structure and an estimate of how its average temperature changes over the year.

- Ambient *air temperature*. If the main part of the structure is "indoor" then measurement of the indoor temperature can be sufficient, otherwise the outdoor temperature should also be measured.
- In dam structures where the *water temperature* of the reservoir, or exposure to air at low levels, is deemed to have an effect on any crack movements, the temperature of the upstream side of the dam should also be measured at different depths. The water temperature is also important for structures that adjoin inner waterways in the power house.

Waterproof resistance thermometers of the type Pt100 are common and robust for measuring temperatures where the processes are relatively slow. In air, one could use a so-called thermocouple, consisting of bimetallic sensors that react faster than the Pt100 sensors.

Loggers

There are many different types of data collection systems. A data logger is often an important component and it can collect measurement data from different types of sensors and perform operations such as programmed calculations, convert to other units or store data. Data loggers are sometimes used to forward data for analysis, sharing and reporting in other systems (e.g. SCADA systems). If a system for transmitting measurement data is not present on the facility, it can be stored locally in the logger to be emptied manually. If a mobile connection is available, transmission with GSM modems can also be arranged to avoid site visits for emptying measurement data. If there is a system for collecting measurement data in place, new sensors are also preferably connected to that system.

4.3.4 Optimisation and installation

In the current edition of RIDAS [3], [4], little or no guidance is given about how a concrete dam should be instrumented and, if possible, even less when it comes to how a measuring system on a concrete dam should be optimised if the plant is large.

In RIDAS [3], [4], for concrete dams, it is stated that:

"The need for instrumentation should be analysed for each facility. For existing dams, installation of measuring instruments is sometimes necessary to verify the assumptions made at the design or to monitor any changing processes in the dam or bedrock, especially for foundations on soil or foundations on rocks where especially adverse conditions prevail. For concrete dams, it should therefore be considered whether these should be provided with devices for measuring uplift pressure, leakage and movement."

At a large facility with many cracks that give cause for concern, it can be difficult to decide which cracks should be monitored and which type of sensor is best suited. It is not always easy to determine where along the crack the best conditions for catching any movements.

As stated in section 4.3.2, the choice of instrumentation should be based on which threats and failure modes may be the cause of actual or potential development of cracking. In order to create further guidance on where the focus on an

instrumentation should be placed, the noted deficiencies or current status of different structural parts can also be compiled. Parts of the dam with a large number of deficiencies or generally low status are more likely to fail than other parts.

If the threat and failure mode assessment and the current status is supplemented with an assessment of which levels of consequence that failure in individual monoliths give rise to, further guidance is provided. If the consequence is a dam failure, then of course on all levels it is a serious consequence. However, there will still be differences if one or a few monoliths that are tens of meters high face failure compared to failures in a part of the dam that are only a few meters high. In any case, in terms of dam failure flow and the risk of human lives being lost. Likewise, it is reasonable to assume that a crack in a monolith that adjoins an embankment dam is likely to give a total dam failure even in the embankment dam. A failure in a single concrete monolith can very well confine itself to a failure in adjacent or a few monoliths and not the entire concrete dam.

Figure 4-5 shows an example where a weighting of identified deficiencies and consequences of different monoliths in a long dam was the basis for an evaluation of risk. The risk level of the different monoliths has then been used for a division into three different classes for instrumentation degree (Extensive, Medium, Basic). The principle provides that the monoliths that have known deficiencies, and also the largest consequences in the event of a dam failure, also have the most comprehensive monitoring.

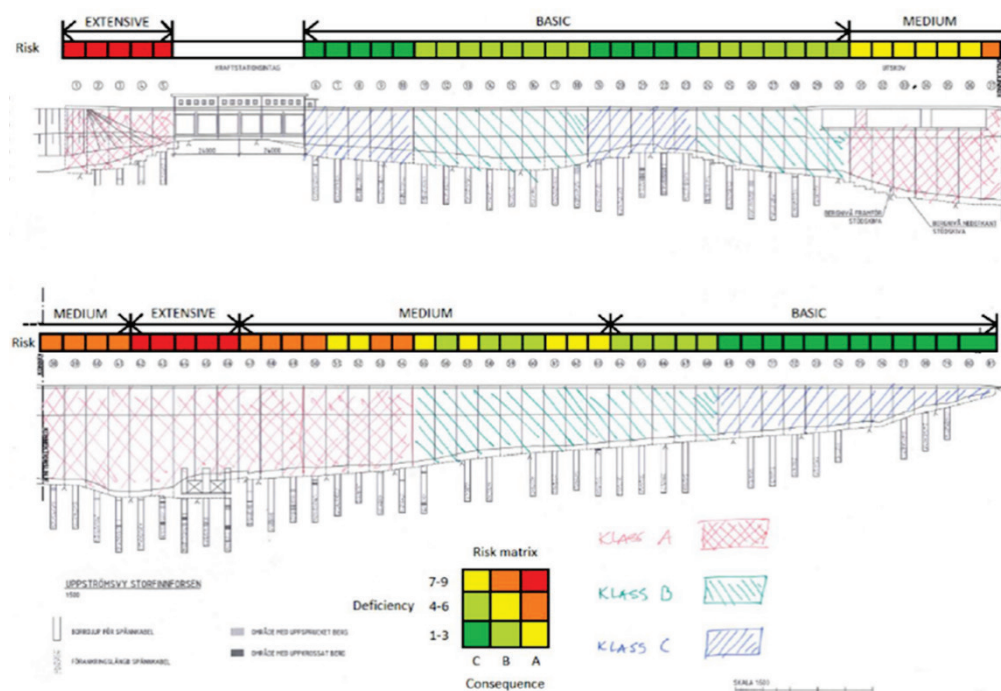


Figure 4-5 Example of a risk based optimisation of instrumentation up to three levels (Extensive, Medium, Basic)

The reason for the choice of placement of each individual sensor should always be based on an investigation or assessment of how the structure is expected to move. Estimations or numerical models are helpful (see also section 3). Sometimes the location of the sensor becomes a compromise due to difficulties in providing good access to the measuring point for function control and calibration of sensors. However, the compromise must not be so large that the value of the measurement data becomes poor. Then it can instead justify creating access with e.g. a gangway or ladder to get high quality in the measurement.

4.4 MITIGATING MEASURES

Mitigating measures refers to various types of methods that give a delay or decrease of crack propagation and/or a reduction of the impact of crack formation if it causes durability problems. The primary purpose of mitigating measures is usually one of the choices:

- Surface protection - reduce the penetration of the substances that drive a degradation process (H_2O , CO_2 , Cl^-)
- Climate protection - reduce the impact of the surrounding climate through protective building (precipitation, temperature variations)

4.4.1 Surface protection measures

In order to reduce the penetration of moisture or chlorides that are driving several types of degradation processes, impregnation can be a way to slow down e.g. cracking or reinforcement corrosion. According to SS-EN 1504 [72], surface protection methods are usually divided into water-repellent impregnation, impregnation and surface coating. The two former methods are based on the fact that the impregnation penetrates the concrete surface/crack area and creates a protection against the penetration of e.g. moisture. The difficulty with impregnation is that the existing moisture state in an old structure can make it very difficult to reach a penetration depth that is large enough to achieve the desired effect. The application time for the active substances (type 1, often silanes) also becomes an important factor in achieving penetration into existing structures. Often the surface is coated with a carrier, e.g. a gel containing the impregnating agents so that the active substance has time to penetrate into the pores.

Surface protection of type 3 can be of either polymer type or of cement-based products, which primarily creates a mechanical surface protection against entry of substances.



Figure 4-6 (1) Water repellent impregnation. (2) Impregnation. (3) Surface coating

4.4.2 Climate protection

Making a cladding of a dam is an effective way to get a more even climate on the dam both with regard to humidity and temperature. Especially for buttress dams with relatively slender dimensions, it has proved effective since the seasonal temperature variations otherwise can give rise to large movements. Cracking movements and crack propagation can be greatly reduced in buttresses and front slab after construction of a climate wall. Figure 4-7 shows the construction of an insulating climate wall on a buttress dam.



Figure 4-7 Assembly of an insulation wall to decrease thermal movements on a buttress dam

In the same way as for a buttress dam, an insulation wall is an effective measure on arch dams, which in addition usually has relatively large restraint forces from its arch support and thereby great risk of cracking at large thermal movements.

Although a dam structure usually always has access to water from the upstream side, a downstream side and crest insulation can be effective in slowing down degradation of e.g. frost. In Norway, there are cases where climate protection of concrete has been done to slow down the expansion of dams with ongoing alkali silica reactions through the limitation of humidification from precipitation.

One aspect that should be considered is the moisture state in the space behind the climate wall and any risk of condensation or ice formation at cold surfaces. Often, it is perhaps difficult to avoid condensation towards the underside of the bridge roadway or the front slab above the maximum retention level. Fans that keep the warm air evenly distributed in the inspection gallery or other arrangements that prevent dripping or ice falling down against e.g. inspection gangways below.

4.5 REPAIR

There are several methods for repairing a cracked concrete structure, and it should be clarified what purpose the repair has and what the desired service life of the repair and structure is. Purposes refer to e.g. if the repair measure should only remedy any leakage or if it is a structural reinforcement. Service-life should be

reasoned, e.g. whether the measure should provide a temporary solution that gives lower risk/mitigated damage development up until an upcoming major refurbishment or if the purpose is to make a measure that has very long service life without additional needs in the foreseeable future. Some guidance can be obtained from the European repair standard SS-EN 1504 [72] in the selection and specification of repair measures.

When choosing a repair measure it should also be reasoned what kind of risk the dam is exposed to with present crack formation and what risk reduction is sought with the repair measure. E.g. if the formation of cracks risks a non-monolithic stability failure, the level that one wants to achieve with the stabilizing measure must be defined in terms of how much the risk is reduced, or what security level is desired compared to the current situation.

Below a few examples of repair methods used at crack formation are shown.

Sealing:

If it has been found that the cracking does not have an immediate or serious impact on the load-bearing capacity of the structure, but that there is leakage and potential or ongoing leaching of the structure, a seal of the crack mouth may be an alternative. The seal can be made by e.g. application of geomembranes that are glued in strips for discrete or single cracks or as whole layers for extensive cracking. See Figure 4-8 for fully sealed layers/sheets on the upstream side which was mounted at the low reservoir surface and Figure 4-9 for an example where application of strips over individual cracks has been carried out. The decisive factor for good function when applying sealing layers with strips is that the connection to fresh concrete is carefully done so that the sealing function is fully achieved. Geomembranes in full-cover layers can also be mechanically fastened and joints are welded for continuous sealing. Creating water-tight connections of the geomembrane to the abutments and the bottom can be problematic and give high costs.

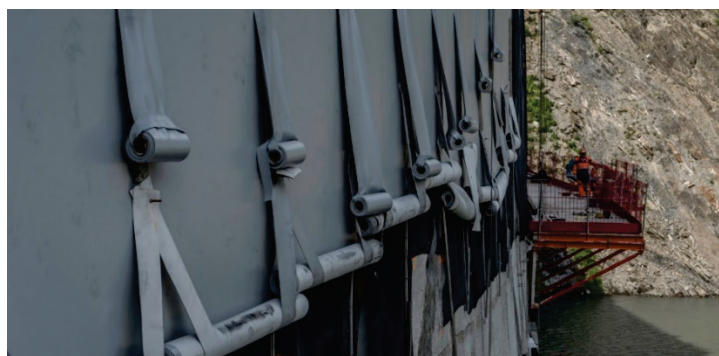


Figure 4-8 Sealing of upstream side of concrete dam



Figure 4-9 Sealing of cracks with strips of sealing material on concrete dam of the massive type

For all types of crack repairs, some basic questions need to be answered before selecting the suitable repair method and in order to be able to determine what type of material should be used. The main issues are:

- Is the crack static or dynamic, i.e. will the crack width change or is it relatively constant?
- Which is the smallest crack width in the area to be repaired?
- Does water flow through the crack, and to what extent?

Grouting – general

In cases where it is deemed difficult to apply sealing layers over the cracked concrete, or if for some other reason filling is needed in the cracks, grouting may be a suitable measure. At relatively constant (static) crack widths, cement-based grout is a good alternative. Epoxy or polyurethane grouting where one can choose elasticity is better suited where variations or increasing crack width can be expected (dynamic).

The significance of the crack width for which type of grout is best suited for good penetration into the crack is great. Generally, the most common cement-based grout is suitable for crack widths larger than 0.5-1 mm, while both epoxy and polyurethane also work for smaller crack widths.

When it comes to cracks with water flow, polyurethane generally suits best because the material itself reacts with water and solidifies. Even cementing agents can work unless the flow is very large. The possibility of lower w/c ratio or possible addition of accelerator to get faster curing can, however, be used to also use cement-based grout.

Regardless of which grout is used, a high competence level should be required from the designer and the person who performs the grouting work itself. More guidance on grouting can be found in [73].

Grouting – cement based

Drilling before grouting is usually done with core drilling or hammer drilling (diameter 40–70 mm). Hammer drilling is done much faster and is more gentle to

the reinforcement. On the other hand, there is a risk that drill cuttings will clog the crack planes that are to be grouted. Usually, the bore hole walls also become rougher which is favourable for the bond to the grout in the hole, which in some cases may be important. Core drilling takes time, but gives smooth walls inside the holes and does not risk in the same way as hammer drilling to re-open the crack. Near the edges of the structure, the risk of cracking is reduced when using core drilling. There are also those who claim that hammer drilling is better due to "cracking up" crack orifices and the surroundings around the hole so that it is easier to grout, but it is judged to have a less positive effect compared to the risk for clogging the cracks with drill cuttings. At times, core drilling is not an option due to time constraints and it is therefore often the case that hammer drilling is used despite the risks mentioned above.

The initial hole spacing shall be based on investigations on the condition of the structure (crack frequency and crack width inside the hole) and the selected grouting concept (cement type, w/c ratio, pressure, pressure time, etc.). Before the grouting is started, the holes should be examined with Lugeon tests to investigate if and where along the hole there are prerequisites for getting grout spread in the structure.

The most commonly used Swedish grout cement, "Grout 30" (Cementa), has a d₉₅ value (the grain size that > 95% of the grains pass during sieving) of 30 µm. There are also finely ground and ultra-finely ground cement (e.g. UF 12) with even finer grain size distribution. Awareness that the challenge of dispersing and keeping the cement grains dispersed during mixing/grinding increases with increased fine grinding of the cement. A successful dispersion of cement in the mixing water is a prerequisite for being able to penetrate cracks without the cement grains flocking at the crack mouth. Good dispersion is commonly achieved when using colloid mills with relatively high rotational speeds (1450–1750 rpm).

The choice of w/c ratio is a trade-off between getting the performance in hardened conditions as desired and actually getting good penetration. High w/c ratios are easier to grout, but they get lower strength and resistance to leaching, while low w/c ratios are difficult to grout in long distances, but they get a better performance in hardened condition.

In order to be able to follow the grouting result through renewed core drilling, pigmentation of the grout is suitable. However, the grain size of the pigments must also be taken into account because it in itself should not impair the penetration properties.

Pressure must be set based on the prerequisites of the structure to withstand hydraulic pressure without the risk of cracking (hydraulic jacking).

Accuracy in the choice of product and mix design, as well as testing of the chosen concept of both material and the equipment that the contractor is to use are important success factors. At all grouting efforts, one should be highly aware that the concept probably needs to be changed during the process. Changed hole spacing, pressure times, pressure, mix design etc. etc. are common, and necessary depending on the running result of the grouting.

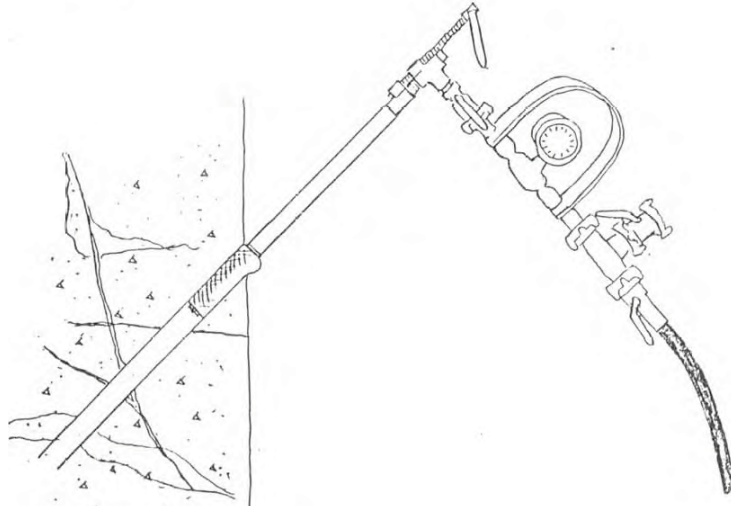


Figure 4-10 Conceptual drawing of cement grouting of crack

Grouting – chemically based

The basics for grouting cracked concrete with chemical grouts are largely similar to the principles of cement based grouting. In the category of chemical grouts, the present report includes, for example, silicates, acrylate and methacrylate polymers, mono- and two-component polyurethane, epoxy, and also polymer-modified grout based on cement. The different types of grout have different properties and a good review is given by [73].

In the case of the pure chemical grout without cement, they are usually used for relatively small crack widths ($<0.5-1$ mm) due to better opportunities for good penetration compared to cement-based products. There are also greater possibilities than with mortar to adapt the chemical grout according to prevailing conditions with respect to water flow, temperature, elasticity etc. High water flows, for example, result in impaired bond between epoxy and concrete, while a two-component polyurethane with a lot of hardener can also stop strong leakage. The choice of glass transition temperature when grouting with epoxy is important when grouting into concrete near warm parts. This is due to the epoxy material being able to soften again and lose its ability to transmit load or stop penetration of e.g. water.

Another difference to cement-based grouting is that sometimes the grouting nipples are placed in the middle of the crack instead being drilled into the side of the crack but angled towards the crack plane to cross this. Figure 4-11 below shows both ways of placing nipples. Generally, much smaller hole sizes are used when drilling to place nipples or even flat nipples that are mounted directly into the crack. The hole sizes are in the range 5-10 mm and can be drilled with hand-held rotary percussion drill.

Accuracy in cleaning with water or compressed air in the crack area or careful control of the grout spread are success factors for chemical grouting.

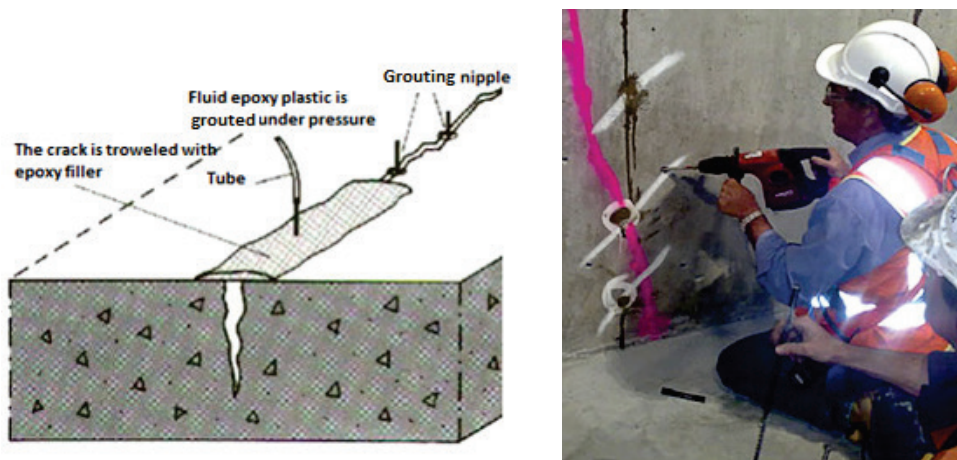


Figure 4-11 Preparations of epoxy grouting of crack

Crystallisation technique

Sealing cracks with crystallisation technique can according to [74] used in several ways. It can either be done by spraying on surfaces with thin cracks, or as in the widen-seal technique which is described later in the section. The material applied consists of organic additives, Portland cement and silica. The technique is based on the material migrating into cracks and the pores of the concrete through osmosis. This creates crystals that seal concrete and cracks, but which are still the diffusion-open for water vapour and air. According to the suppliers, the penetration depth can be a few decimetres and last as long as there is access to moisture.

If the cracks to be repaired have a water flow to such degree that makes it difficult to apply the products, a bottoming can be done with quick-hardening mortar or mechanical support/stop at the concrete surface.

The crystallisation technique cannot be used if the cracks are dynamic since the repair material has similar properties to concrete and is thus brittle.

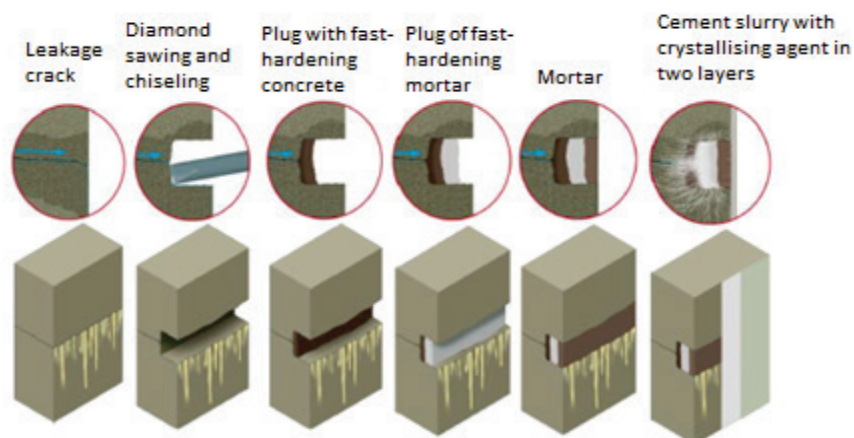


Figure 4-12 Sealing of crack with crystallising technique [75]

Drill-plug technique

The drill-plug technique is best suited when there is a crack that is relatively straight without major bends. Then, a hole can be core drilled parallel to the crack plane so that the crack ends up centrally or as close to centrally as possible in the hole. With the drill-plug technique it is possible to create a barrier so that a crack grouting material does not spread through e.g. a thinner structure (guide wall, soil-retaining wing wall, etc.) with leakage at the back where it can be difficult to control. Plugging and grouting material are chosen depending on whether the crack is assessed to be static or dynamic. In the example shown in Figure 4-13, a concrete plug is shown which has a bitumen layer around the surface area in order to prevent bonding to the wall of the hole and to create tightness. The advantage of a rigid plug is that a force transfer is also restored across the wall. If the wall thickness allows, two holes can also be drilled and provided with optional material for filling and plugging. Suitable hole diameter is approx. 50–75 mm.

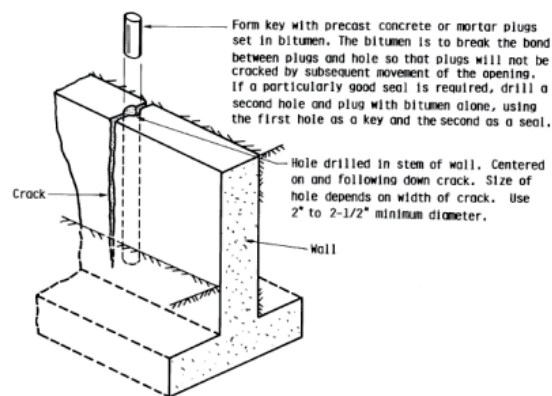


Figure 4-13 Conceptual sketch for the repairing of cracks using the drill-plug technique

Widen-seal technique

If a crack mainly needs to be sealed at the surface to improve the appearance or to reduce the risk of penetration of moisture, chlorides or other substances, the so-called widen-seal technique may be used. The principle is based on creating a slightly larger space at the mouth of the crack in order to more easily seal the crack.

The choice of material must be based on whether the crack is expected to move due to expansion in the concrete, thermal movements (dynamic crack) or if the crack can be expected to be static without movement. For dynamic cracks, an elastic material must be selected at the surface, while for static cracks one could use e.g. dry pack technique with cement-based material, which is presented in the next section. Elastic materials can e.g. be bitumen, polyurethane or polyurea.

If the crack width is large, a so-called bottom strip may need to be installed in order not to require such large amounts of sealing material. It also prevents the material from flowing into the crack after completion of the filling. To maintain the ability of the sealing material to absorb deformations (elasticity), a layer for breaking the bond to the sawn-up bottom can be installed, as shown in Figure 4-14.

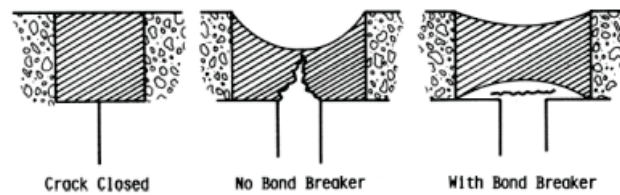


Figure 4-14 Conceptual sketch for repairing cracks using the widen-seal technique.

Dry pack technique

The dry pack method may be useful for static cracks with a slightly larger width (> 5 mm) and cracks on vertical surfaces where it may be difficult to make the repair material stay in the crack opening if cement-based materials are to be used. The basic principle is to cut or mill the crack opening to approx. 25-40 mm wide and deep along the crack. The purpose of the increase in crack opening is to create opportunities for manual processing of the cement mill on site. See Figure 4-15.

The dry pack itself is made with a mixture of cement, sand and water. The mixture should have such a low water content that it is possible to form a ball with the hand, but not so little that it falls apart when laying the ball on a flat surface. The ratio of cement to sand should be between approx. 1: 1 and 1: 2. The mortar is then placed in the perforated crack and is packed by tapping with a hammer on a wooden stick to fill the space and increase the density of the material.

Since the material has a low w/c ratio, the drying shrinkage becomes very small and therefore effectively seals the crack even after the material has fully hardened.

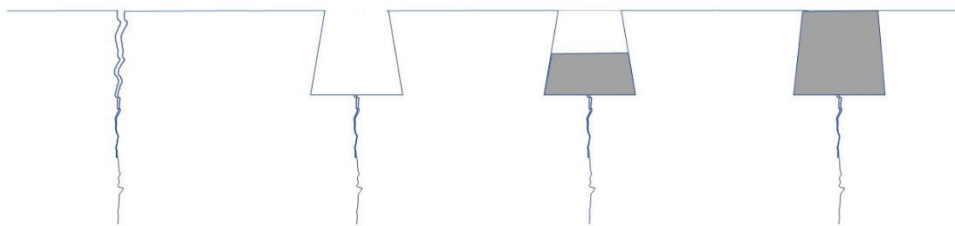


Figure 4-15 Conceptual sketch for the widen-seal technique using dry packed mortar.

Structural upgrade:

In situations where the crack formation caused one, not acceptable, reduction of the structural load-bearing capacity, the structure needs to be strengthened. The cause may be a single crack in a sensitive position giving a risk for non-monolithic behaviour in e.g. a dam pier or extensive cracking that gives rise to doubts about e.g. interaction between concrete and reinforcement.

Reinforced overlays is the most common method of repairing damaged concrete. It is done by chiselling or hydro-jetting the cracked, damaged concrete and replacing it with new concrete. Just as in general when choosing a repair method, it is

important to have identified which mechanism has caused the cracking. If the cause of the crack originates from e.g. poor curing or temperature-related cracking after casting, then it is uncomplicated to replace the outer parts with new concrete. If it was instead found to be an ongoing expansion of e.g. alkali silicate reaction, it must be taken into account in the design of the casting that a continued expansion may occur beneath the overlay.

Generally, as with all concrete repairs, damaged and loose concrete must be removed to such an extent that good bond for the new concrete is ensured. For all structures, an assessment must be made of how the actual stage of construction affects the load-bearing capacity of the structure. For slender, heavily utilised structures, it is not obvious that you can remove a lot of concrete around the reinforcement without deformations and problems when you recommission the structure with a new overlay. Temporary support or sequential repair of parts of the structure may be a solution. A good review of the design and implementation of concrete overlays is given in the REHABCON manual [77].

In the case of extensive and deep damages, an enclosing reinforced overlay which is anchored well into the existing structure can also replace any expected inadequate bond. A reinforced overlay can also be a structurally detached structure designed to "take over" the load-bearing function from the old damaged structure. E.g. when repairing the Öland Bridge, Sweden, a sliding layer against the existing pier was created instead, and the overlay acted independently around it. The design must simply be adapted to the conditions and purpose.

For ASR-damaged structures, a reinforced overlay can also be created to give a counter-measure to future expansion in the old concrete. The expansion force that can arise due to ASR has been found to have limitations. Large variations occur depending on the type of aggregate and the exposure environment, but a description of the phenomenon can be found in [78].

In addition to the above guidance, all common recommendations regarding the scope of the removal of old concrete and boundary conditions apply to the pouring of new concrete. A good guide in the area can be found e.g. in the portal www.betongreparation.se (in Swedish) [79]. Some important things to consider are:

- Thorough cleaning of the substrate and possibly existing reinforcement before casting.
- Sufficient reinforcement overlap when connected to existing reinforcement.
- Distance between reinforcement and substrate at least two times the maximum aggregate size in the pouring concrete, however never less than 16 mm.
- Sharp-edged ends against any existing concrete
- Careful curing

Anchoring of structures with post-tensioned anchors or pre-stressed cables is a way of ensuring e.g. monolithic effect in a pier with horizontal crack formations. By installing anchors or cables across a crack plane and applied thereto a force holding the structure together. The measure reduces the risk of e.g. a spillway pier partially failing because of the loads it is subjected to. Figure 4-17 shows a typical installation of pre-stressed cables where a concrete structure is tightened to the

underlying rock. A good overview of pre-stressed anchorage at Swedish hydropower plants is given in [88].

Things that should be taken into account when designing and implementing post-tensioned anchors are:

- If there are conditions for good anchorage to the support or are measures such as grouting required to reach it?
- Can the existing concrete structure withstand the loads that are applied during tensioning or are structural reinforcements required?
- How should the anchors be placed to give the best desired reinforcement, and is there anything in the structure that must not be drilled off (reinforcement, castings, pipes, cables etc.)?
- Does the tension need to be controlled during its service life?
- How to create the best corrosion protection? (grease-filled hoods, grease or plastic-cladded anchors or wires).

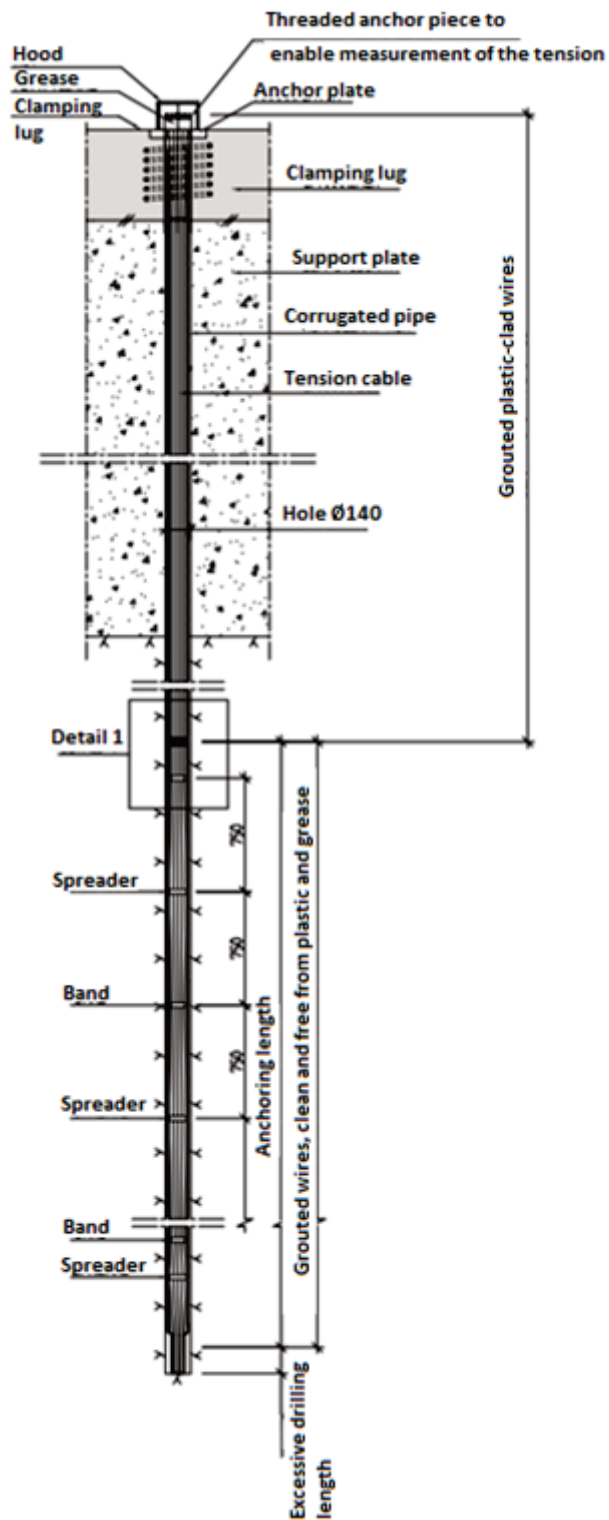


Figure 4-16 Pre-stressed cable anchoring, type VSL 6-12, conceptual sketch

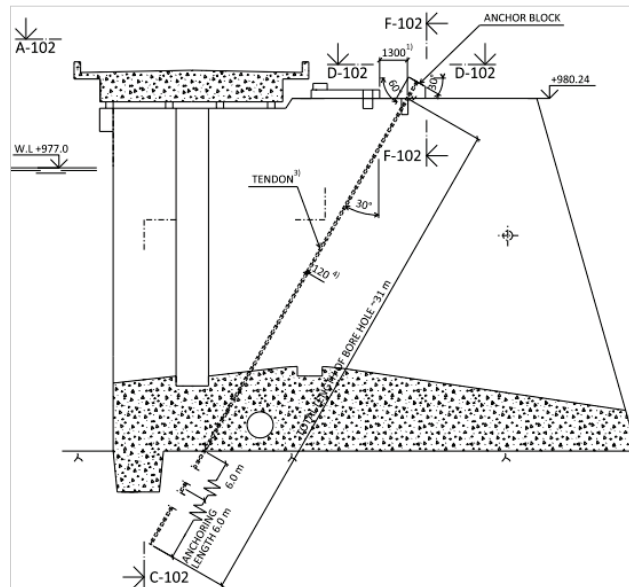


Figure 4-17 Pre-stressed cable anchoring in dam pier, conceptual sketch



Figure 4-18 Ongoing installation of pre-stressed cable in buttress dam.

Composite reinforcement of structures can be used in cases where new or additional tensile strength is needed and for some reason it may not be suitable to cut out and replace concrete and reinforcement. Good guidance can be found in [80]. There the systems are described as:

"A polymer composite can be defined as a material with continuous or short fibres which are in place and joined together by a polymer matrix. The fibre material often consists of glass, aramid or carbon fibre, but there are also other fibre materials available, e.g. basalt fibre. The matrix material is usually some type of thermosetting polymer, e.g. epoxy or vinyl ester, in some cases also thermoplastics are used as matrix materials, however, these are not commonly found in the use of composites for the purpose of reinforcement. The material properties of the materials are determined by the properties of the fibres, the properties of the matrix and contact layers, and by the fibre orientation. The above mentioned fibres have a ultimate tensile strength than e.g. reinforcement and are linear elastic up to the breaking point. The volume fraction of fibres in an FRP is 35 -75% depending on material selection, manufacturing process and desired material properties. The rest of the FRP is made of the matrix material.

When reinforcing concrete structures, carbon fibre together with an epoxy matrix is the most common FRP combination. Normally, the composite is glued to the concrete surface or in the concrete cover, but there are also reinforcement systems where you rely solely on mechanical anchoring without gluing. "

Three common ways to create reinforcement with the most common type, carbon fibre, in concrete contexts are:

- Laminate (surface applied)
- Weave/mesh (surface applied)
- Rods (mounted on cover layer)

The difference between the three is that the laminate is glued in strips with epoxy on a well-cleaned and prepared surface and the laminate has the fibres oriented in one direction. Weave is applied in the same way as laminate but may have fibres in one or more directions. The rods can be glued in slits that have been milled in the concrete cover outside the existing reinforcement. In addition to epoxy adhesives, the rods can also be moulded with a polymer-modified use. Figure 4-19 shows the application of laminates and rods to the underside of bridge roadways to provide reinforcement in the bending.



Figure 4-19 Reinforcement in bending with carbon fibre composite. Laminate (left) and anchors (right). [80].

5 Reference projects

5.1 INTRODUCTION

The purpose of this section is to show a number of real cases where the cause and effect of cracks in concrete dams have been studied. The methodology of the studies has more or less followed the proposed methodology shown earlier in this report, i.e. from observation of cracks, analysis of cause and effect, possibly comparison to dam measurements and finally possible measures carried out on the dam.

The purpose of the cases has almost always been two, partly to find or to estimate the cause of the cracks, and partly to estimate the effect on the structure, usually in terms of how safe it is now and in the future. Generally, it turned out that it was most often, on-site, or through tests, or through calculations, easier to determine the cause than to estimate the effect. The cause of the crack formation could often be attributed to thermal movements but also due to frost or ASR damage. That it often involved cracks due to thermal movements could usually be verified with an FE simulation. The cracks occurred in the simulations almost always in the same place and with a similar appearance as in the actual structure. However, it was often more difficult to estimate what the effect on the structure was, e.g. a quantitatively stated, remaining load-bearing capacity. The load-bearing capacity of the overall global structure was often complex to estimate. First, there was an uncertainty about whether the calculation model reflected the behaviour of the real, perhaps damaged, structure, as well as how far the damage had occurred and how it will develop in the future. The full extent of the damage is often hidden from the viewer, e.g. how continuous a crack is, how much force is transmitted, damage to the reinforcement, etc.

In general, it can be said that the more measurements one makes of relevant variables and the more observations one can make, which are then compared with the calculation result of the calculation model, the more valid the model should be. With a valid model one can better estimate how the structure will behave at other load cases or events, or after possible reconstruction/ refurbishments.

Below are a number of examples of investigations for different concrete structures in hydropower plants. The chapter includes both investigations and measures with a relatively limited scope, as well as more detailed investigations and analyses and more far-reaching measures. A summary is given in Table 5-1.

Text inside the parentheses in the main headings indicates what the problem has been at resp. facility.

Common cracks given in Figure 5-1 are referred to.

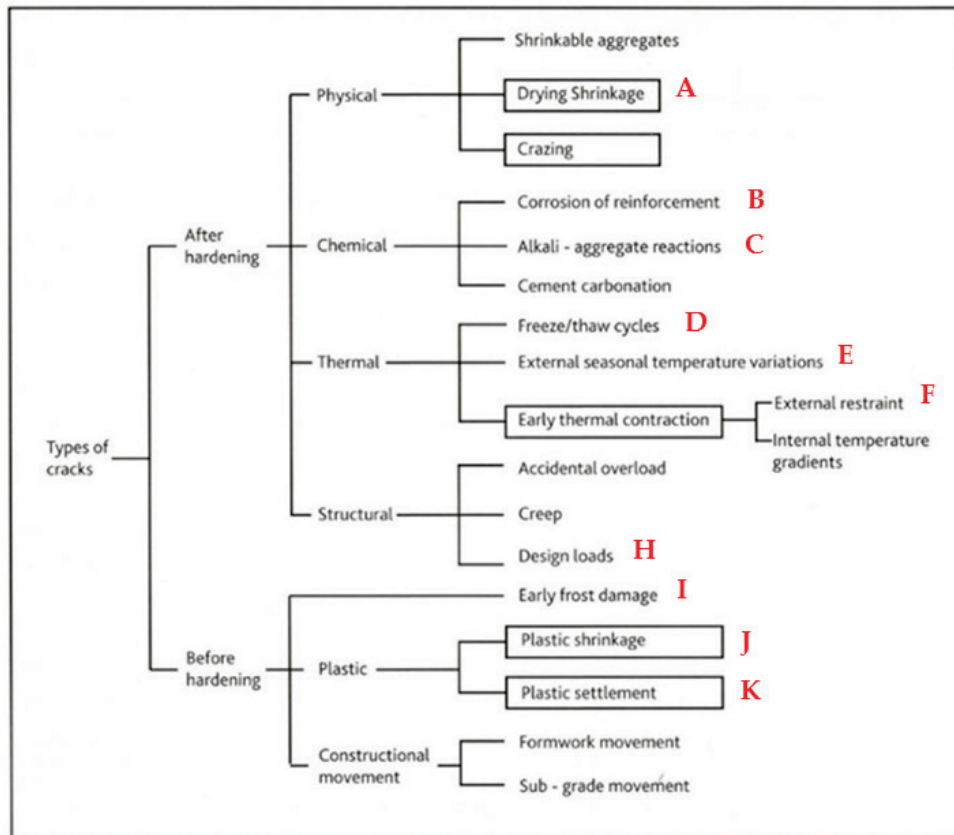


Figure 5-1 Common types of cracks and their causes [9].

The reference objects that are presented are a selection of projects that have covered to different extent, i.e. how many of the points below that have been dealt with and how deeply the cases have been studied.

- a) Investigation:
 - i. Overview visual
 - ii. In-depth inspection
 - iii. Sampling/measurement
- b) Analysis:
 - i. Simpler mind models
 - ii. Analytical calculations
 - iii. Linear FEM calculations
 - iv. Non-linear FEM calculations
- c) Measures:
 - i. No measure
 - ii. Emergency measures

- iii. Monitoring
 - iv. Reduce load effects (lowering reservoir level, insulating wall to reduce thermal stress, ice protection)
 - v. Repair (restoring load-bearing capacity)
 - vi. Reinforcement (increase load-bearing capacity)
 - vii. Replacement
- d) Follow-up
- i. Scheduled inspections
 - ii. Measurement data evaluation, trends
 - iii. Measurement data evaluation compared with calculation model
 - iv. New surveys after time

Figure 5-2 shows a conceptual flow chart on how a study of a cracked concrete dam can be carried out. The reported cases have usually also followed this schedule.

The problem with the cracked dams has usually been discovered during a planned inspection, or in the case of more rapidly occurring cracks, by the operating personnel having stated that cracks have been formed or widened, at level 1 in the figure.

According to the schedule level 3, one can then leave the problem without any measure if the cause is obviously not critical, one can keep it under supervision during a somewhat more serious damage, or one can take some sort of measure, e.g. to directly repair or reinforce the structure if the damage is more critical. In the case of an obviously serious and perhaps critical damage, measure is taken urgently.

Level 4 shows various steps of measure. If there is no great risk of immediate and unacceptable damage, the measure should be started by gradually analysing the cause and effect. In the reported cases, the studies have usually started with a "preliminary analysis of AC", where AC stands for Assessment Class, followed by a more "Detailed analysis of AC", where the detailed analysis has most often involved an FE analysis. In none of the cases shown has repair or reinforcement been done directly without making a relatively detailed theoretical analysis beforehand, i.e. via the red box in Figure 5-2.

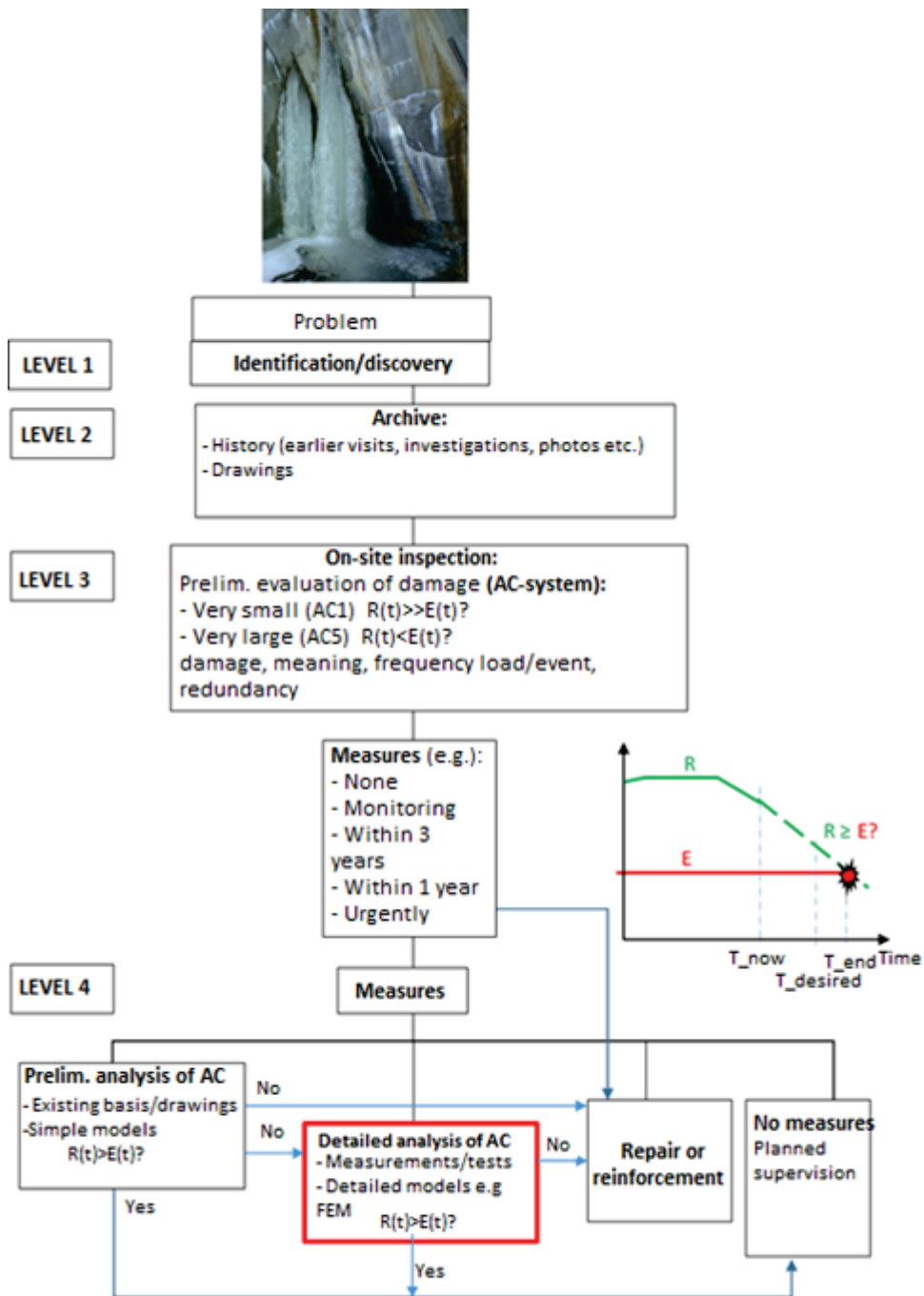
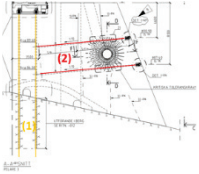


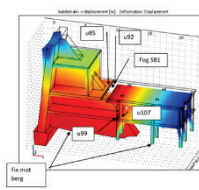








Figure 5-2 Flow chart on how the investigations in this section have been carried out, R=bearing capacity, E=Load

5.2 SUMMARY

Table 5-1 shows a summary of the presented reference projects in section 5.3 – 5.14.

Table 5-1 Summary of reference projects. (i),(ii), etc. refers to the points described in the above text. PFM="Probable failure mode". Notations with 1) through 8), see below the table. E.g. (i):5):05 in the column "Investigations" in Spillway dam 1 that the investigation was "Overview visual" and where a simpler crack mapping was done.

Plant	Problem ¹⁾ /risk (PFM)	Investigations	Analyses	Measures	Follow-up
Spillway dam 1	Vertical cracks (F,E ¹⁾ / lower overall stability. Cracks at gate shaft(F,E,H ¹⁾ /gate is pushed out	 (i):5):05	(i) on-site (ii): 2):02	Performed (vi):3):04	(i)
Spillway dam 2	Horizontal cracks due to concrete lifts (J) & temperature (F,E)/Pier top sheared.	 (i):5):05	(i) on-site (iii):4):01, 02,03, 2):03	Not needed	(i)
Spillway dam 3	ASR(C), Frost(D), Cracking(J), horizontal and vertical cracks (F,E)/mtrl failure, overall stability, gate pushed out	 (i):5):05	(i) on-site (iii): 4):01, 02,03, 2):03	Suggested 3):01,02,03 ,04	(i)
Power house 1	Cracks, wide joints(A,E)/no direct risks	 (i):5):05	(i) on-site (iii): 4):02,03	Suggested 8):02	
Arch dam 1	Frost damage (D), crack in arch support (spillway pier)(E,H)/Cantilever on top of pier sheared at the upper arch ring	 (i) (ii):5):05 (iii):5):0 3,04	(iii): 4):01,02,03, 2):03	Suggested 3):04	
Spillway dam 4	ASR(C), frost(D), crack(H)/overall stability, cross-sectional force failure in piers	 (i):5):05 (iii):5):0 1,02,03, 04	(iii):4):01,02,0 3	(iv):7), (v):8) and (vi):3):04	
Buttress dam 1	Cracks in front slabs and buttresses(F,E)/overall stability.	 (i):5):05	(i) on-site (iv):4):02,04	Not needed	
Spillway dam 5	Vertical (F,E) and horizontal(E,K) cracks, crazing (D,J)/Overall stability, gate shaft pushed out.	 (i):5):05 (iii):5):0 1	(i) on-site (iv):4):02,04	Performed (vi):3):04,0 5	(i)

Spillway dam 6	Vertical and horizontal cracks (F,E) in spillway piers and buttress dam monoliths/Overall stability		(i) (ii):5):05	(i) on-site (iv):4):02,04	Performed (iii):9):01,0 2,03 (iv):7)	(i)
Buttress dam 2	Vertical and horizontal cracks (F,E) in buttress dam monoliths/Overall stability		(i):5):05	(i) on-site (ii):2):01,03 (iv):4):02,04	Performed (iii):9):01,0 2,03,04 (iv):7)	(i)
Arch dam 2	Cracks in the arch(F,E,H), in the crest of the arch support(E,H), in the sides of the arch support(F,E), at gate shaft and spillway pier(F,E,H).		(i) (ii):6):05 (iii):6):0 2,03,04	(i) on-site (ii):2):01,03 (iv):4):01,02,0 3,04	Performed (iii):8):01,0 2,04,05 (iv):7) (v):3):04,0 5	(i)

- 1) Cause of damage A-I, see Figure 5-1. Bold font = main cause, if possible to distinguish.
- 2) Analytical calculations: 01 = Stability, 02 = Comparison of shear force and capacity of the reinforcement going through the crack, 03 = Analytically determined shear capacity (BBK04 [6], 3.11.3) in cracks with stresses from FEM (4): 03).
- 3) Measures: 01) Sampling, 02) Sealing u.s Sides, 03) Ice protection, 04) Tension anchors, 05) crack grouting
- 4) FEM calculations: 01) pore water pressure, 02) temperature and 03) linear elastic stresses/strains, 04) stresses/strains with plastic damage model.
- 5) Tests/measurements: 01 = Coating/carbonation, 02 = ASR, 03 = Risk of frost, 04 = Strength, 05 = crack mapping.
- 6) Thermally insulating climate wall.
- 7) Clear bad concrete and re-cast.
- 8) Instrumentation: 01 = temperature, 02 = crack width, 03 = pendulum, 04 = pore pressure, 05 = extensometer

5.3 SPILLWAY DAM 1 (TEMP/GATE LOADING)

5.3.1 Brief description of plant

The concrete spillway dam, see Figure 5-3, located in Ångermanland, Sweden. It was commissioned in 1947.



Figure 5-3 Downstream side of the spillway dam.

5.3.2 Assessment of stability and the load capacity of the gate shafts

- a) Investigation: During a visual inspection (i) in connection with IDSE (2012) and II (2013), a relatively extensive crack formation was noted in all the spillway piers, see 1) and 2) in figure 5-4 for e.g pier 3. In the archive search, there was a crack mapping of the piers from 1974 where cracks were found in the positions indicated by 3). A comparison showed that the cracks from 1974 had multiplied and grown. The cracks can be found on both sides of the respective piers and inside the inspection shaft and can thus be continuous but it has not been investigated. No material investigations were made. Material properties were estimated from the literature.
- b) Analyses: A simple conceptual model, a mind model, (i) indicated that seasonal thermal stresses may have probably caused the cracks. Possibly, the cracks adjacent to the weirs and around the door shafts have been initiated in the casting stage. In a simpler analytical calculation (ii), where existing reinforcement may take full force from the door at the attachment of the gate shaft, it was found that the current amount of reinforcement was insufficient, whereby the gate shafts and the gate in their respective spillways could be pushed out and an uncontrollable flow through the spillway arises. In addition, the cracks degrade the monolithic action of the spillway piers, thereby reducing stability.

- c) Measures: New, near-horizontal, pre-stressed anchors have recently been mounted in the spillway piers (vi), see red lines in Figure 5-5, to secure the cracks and continued monolithic action of the piers. Anchors have also been placed in the upstream end, yellow lines, vertically down into the rock to increase stability. On some of the anchors, surveillance is set in the form of load cells which register changes in tension.
- d) Follow-up: Possible force changes in some of the anchors are recorded with load cells. All other anchors should be test tensioned at certain intervals. The cracks must be visually monitored and preferably mapped in overview, preferably at each IDSE, or more preferably at each II (i).

Conclusions: In an IDSE, heavy cracking was observed in the spillway piers, which degrades the stability and reduce the loadabsorption from the gates. In a simple analytical force comparison, where the cracks are assumed wide enough that the reinforcement carry the entire gate load, the capacity of the reinforcement was found to be too small. Therefore, the piers were reinforced with pre-stressed anchors above and below each gate hatch. These anchors also ensure the monolithic effect of the piers, which improves stability.

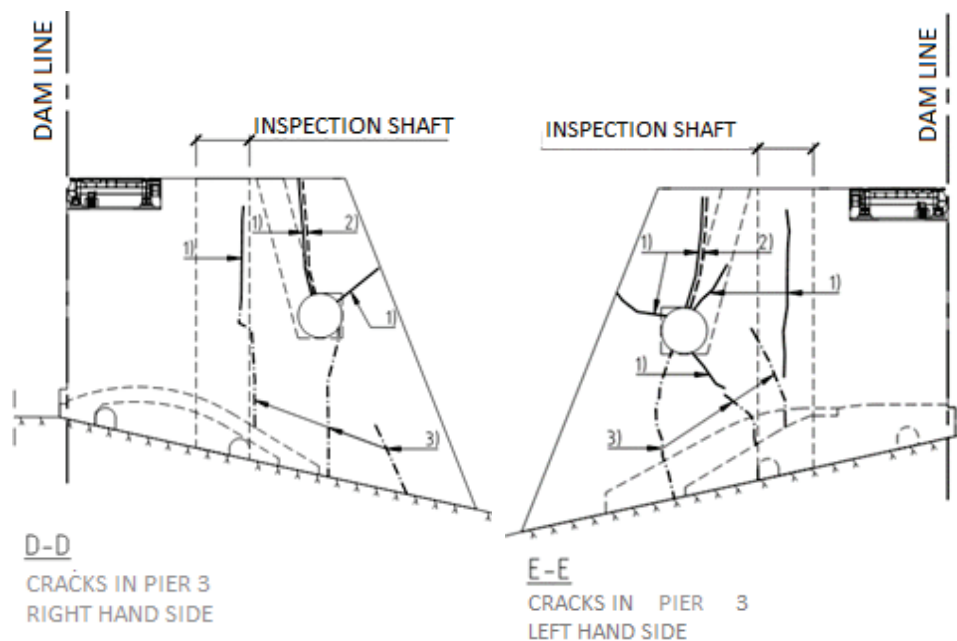


Figure 5-4 Cracks in spillway pier 3. 1)=Cracks on the outside observed in 2012, 2)=Cracks on the inside of the shaft observed in 2012 and 3) on the outside observed in 1974.

5.4.2 Assessment of the stability of the spillway

In an attempt to assess the safety against material and stability failures in the spillway piers, an analysis was carried out with a relatively simple FE model in 2016. Calculated shear stresses in an assumed crack plane (red surface in Figure 5-7) were compared to the shear capacity in the same crack plane calculated by "force transfer through joints" according to BBK 04, equation (3.11.3c), see below. See also Appendix D for a more detailed description.

- a) Investigation: In an overview visual (i) inspection in connection with II (2016), it was observed that there are cracks in the spillway piers, which can impair the monolithic effect of the spillway piers, whereby the stability deteriorates. No material investigations were made. Material properties were estimated from the literature.
- b) Analyses: A simple mind model (i) indicated that the cracks may be initiated by weakness zones/lift joints during casting and exacerbated by subsequent seasonal thermal stresses. In a separate assignment in 2017, a simpler FE analysis (iii) with a linear elastic material model was performed. Estimated shear and normal stresses in conceived crack planes where the cracks can actually be observed were extracted from the FE model and analysed analytically against a calculated shear capacity according to BBK 04. The capacity of the cracks was found to be greater than their calculated shear stresses. It was therefore assessed that the cracks can transmit shear and normal forces and that the structure acts as a monolith. On the other hand, seasonal temperature variations may possibly cause the cracks to grow and become slightly longer and wider. With the same FE model, stability was also checked. The monolith was then located along two lines in the downstream end. As a monolith, the calculated stability met the RIDAS [3], [4], conditions. A more advanced FE model, e.g. with non-linear material was not considered necessary, because the extent of the damage and the assessed safety together with relatively low consequence in the event of dam failure were not critical.
- c) Measures: No measures (i) required for safety margins in the short and medium (10 year) term.
- d) Follow-up: Supervised during upcoming inspections (i).

Conclusions: In an FE model, the temperature variations were calculated during a fictitious computational year, which in the model caused varying stresses in the concrete. The calculated shear stresses in conceived crack planes, where cracks can actually be observed, were compared to the calculated shear capacity based on the calculated normal stress and reinforcement content. In the present case, the capacity exceeded the calculated shear stress and no measure was needed.

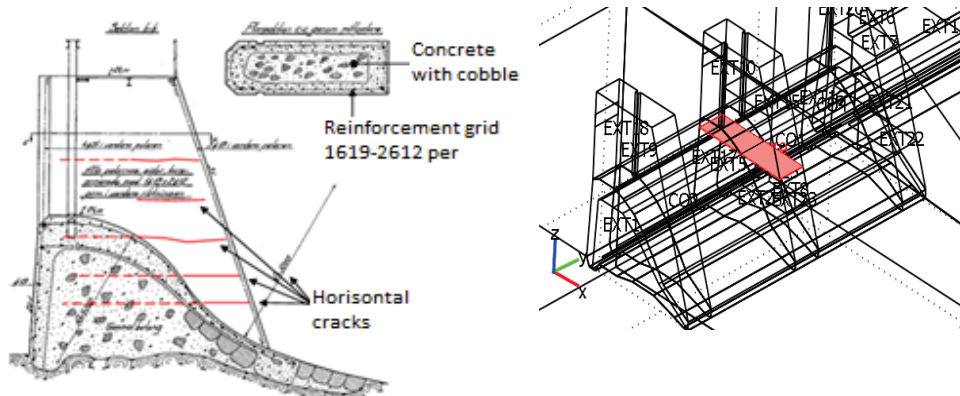


Figure 5-8 Cracks in spillway piers (red lines in left-hand figure), analysed in a crack plane (red surface in right-hand figure)

5.5 SPILLWAY DAM 3 (ASR/FROST/TEMP)

5.5.1 Brief description of plant

The dam is located in Dalarna, Sweden. The plant was commissioned in 1956. The regulating dam constitutes dam unit 1 and consists, from left to right, of a short diversion embankment dam, the power house intake and the spillway dam made of concrete and finally the right-hand embankment dam. Figure 5-8 shows the spillway dam. Virtually all concrete in the spillway dam has extensive ASR and frost damage and cracking.



Figure 5-8 Downstream side of the spillway dam. P1=studied middle pier.

5.5.2 Assessment of stability of the middle pier of the spillway

- a) Investigation: In an overview visual inspection (i) in connection with IDSE (2014), it was observed that there are cracks in the spillway piers among other things, which can impair the load-bearing capacity and stability. No material investigations were made. Material properties were estimated from the literature.
- b) Analyses: A simple mind model (i) in place gave the cracks caused by ASR in synergy with frost, and may be exacerbated by seasonal thermal stresses. Standard cement was used for the concrete, which may have aggravated the ASR damage. It was thought that crack 1) in Figure 5-9 and Figure 5-10 reduces the overturning stability, or if the gate force gives a risk for shearing the pier horizontally along the crack 2). In the assignment, a simpler FE analysis (iii) was performed by the centre pier P1 with a linear elastic material model. Calculated shear stresses in an assumed crack plane (red and blue surface in Figure 5-10) were extracted from the FE model and analysed analytically and compared to a calculated capacity with "force transfer through joints" according to BBK 04, equation (3.11.3c). The analysis indicated that the calculated shear capacity in the cracks is greater than the calculated shear stresses in the same cracks. It was therefore assessed that the cracks can transmit shear and normal force and that the structure acts as a monolith. Thus, the pier was considered to behave as a monolith with sufficient overturning stability and no sliding along crack 2) can occur. With the same FE model, stability was also checked. The monolith was then founded along two lines in the downstream end. As a monolith, the calculated stability met the RIDAS [3], [4], conditions.
- c) Measures: Proposals for further measures are:
 - Sampling for examining potential ASR and/or frost damage and expected strength, particularly tensile strength, of the concrete in critical parts.
 - Seal upstream and upper sides with e.g. new concrete (v).
 - Ice protection at the dam (iv).
 - Possible pre-stressed anchors to secure cracks and stability (vi).
 - Or
 - Replace ASR-damaged structures with new ones (vii).
- d) Follow-up: When ASR and frost damages further can degrade the concrete in the long term, pier 1, as well as other damaged concrete at the dam, should be kept under supervision during upcoming inspections (i).

Conclusions: In an FE model, the temperature variations were calculated during a fictitious computational year, which in the model caused varied stresses in the concrete. The calculated shear stresses in assumed crack planes, where cracks can actually be observed, were compared to the calculated shear capacity based on calculated normal stress and reinforcement contents. In the present case, the capacity exceeded the calculated shear stress and no measure was needed. However, the dam should be refurbished/replaced with regard to the long-standing ASR and frost damages.

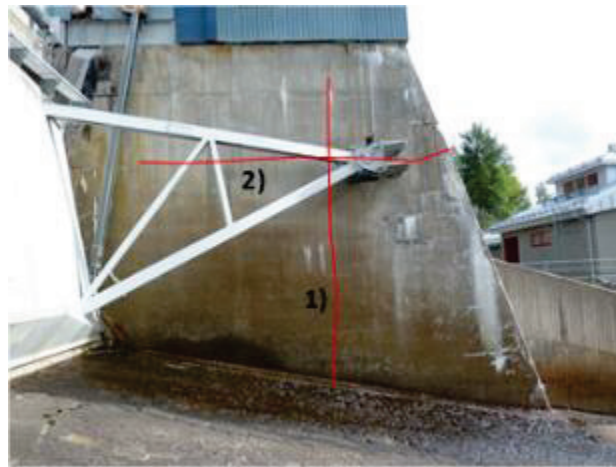


Figure 5-10 Side view of spillway 1. 1) och 2) are two of the larger cracks found in the structure

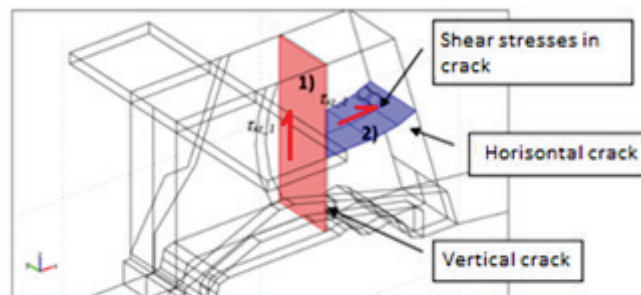


Figure 5-10 Crack plane in the model in the same places as in the real case of pier 1. $\tau_{xz,1}$ and $\tau_{xz,2}$ show conceptually where the shear stresses were analysed in the cracks.

5.6 POWER HOUSE 1 (DRYING/TEMPERATURE)

5.6.1 Brief description of plant

The power plant is located in Lapland, Sweden, and was commissioned in 1955. The power plant has three units that together provide the expansion water supply 450 m³/s. The gross head is 15.5 m. The dam facility consists of the following parts from the left in the flow direction of the river; left-hand earthfill dam, left-hand non-overflow concrete dam, power house intake, spillway dam, right-hand non-overflow concrete dam and right-hand earthfill dam. The total crest length of the dam is about 333 m and the largest dam height is about 23 m.



Figure 5-11 Upstream side of the power house

5.6.2 Assessment of widened joints and cracks in the station

It has recently been observed that expansion joints have widened and cracks have occurred in the power house building. The question arose about the reason for this and whether it is a serious problem for the structural ability of the building.

- a) Investigation: At an overview visual (i) inspection in February 2016, it was observed that most of the "cracks" had to do with expansion joints that widened, but there were also cracks that opened up and later widened. An expansion joint between monoliths included in the buttress dam and the workshop on floor 2 (Figure 5-12) and another on floor 1, see at the designation u85/u92 and u99/u107 respectively in Figure 5-13, were analysed particularly. The joints have expanded about 2-3 mm. No material investigations were made. Material properties were estimated from the literature.



Figure 5-12 Crack (joint) Sb1 under bjl +83,70.

- b) Analyses: A simple mind model (i) on site provided the possible causes
- i. Drying Shrinkage
 - ii. Temperature variations
 - iii. Settlement in the foundation
 - iv. Horizontal components of vertical loads have pulled apart the parts.
- In a simpler FE analysis (iii), the shrinkage was calculated assuming a cold winter and a drying shrinkage since the time of construction.

The shrinkage in the concrete on either side of the joints in question due to a temperature drop during the winter gave an estimated widening of the joints of about 0.97 mm and 0.60 mm between the node points 85 and 92 and between the points 99 and 107, i.e. u_{85}/u_{92} and u_{99}/u_{107} respectively, where u_{85} stands for calculated motion u in node 85 in the x direction etc. for u_{92} , u_{99} and u_{107} , see Figure 5-13. In the calculation, the starting temperature of the concrete was assumed to be $+20^{\circ}\text{C}$ (casting in warm summer) and a cold winter period of -5°C in the water of the upstream side of the buttress dam $+15^{\circ}\text{C}$ in the workshop part. The temperature difference of 20°C is probably a little too much and the movements are thus slightly exaggerated in the example.

Although the calculated thermal movements were large, 0.97 mm and 0.6 mm respectively, it is not enough to explain the real gap in the joints of about 2-3 mm. Therefore, the movements were also calculated during an intended drying shrinkage. The front slab of the buttress dam was assumed not to dry out since it is in contact with the water, but the other parts, towards the power house, were assumed to have a fully developed drying for 60 years and RH 60%. See [82].

Assume $C = 350 \text{ kg} / \text{m}^3$, $w/c \text{ ratio} = 0.5 \Rightarrow \epsilon_{c0} = (\text{fig. 15.2:5}) = 0.5$

Assume full drying (60 years) $\gamma_t = 1$

Assume RH in the room to 60% $\Rightarrow \gamma_{RH} = (\text{fig. 15.2:9}) = 0.09\%$

With these assumptions, the shrinkage in the present case will be:

$$\varepsilon_{cs} = 1 \cdot 0.09 \cdot 0,5 = 0.045\%$$

This shrinkage is applied in all parts of the model except in the front slab.

The estimated widening of the expansion joints during its 60 years was 3.7 mm and 3.8 mm respectively, see Figure 5-14, which is more than measured movements. Probably the final shrinkage has not yet been obtained, so the joints may widen slightly more.

The fact that it can mainly be due to drying shrinkage indicates the fact that the cracks/movements have grown with time. The longer time passes and if the RH is relatively low, the concrete dries out and shrinks. RH can become very low indoors during cold winter seasons. The season when the indoor temperature is higher and thus the indoor is drier than outdoors is many months at the facility.

It is conceivable that the RH inside the parts with the workshop and the power house, is considerably lower than what is assumed above. The average humidity over the year is perhaps about 5-6 g/m³ with a maximum of about 9 g/m³ in the summer and minimum of about 3 g/m³ in the winter. Inside the workshop/power house there is no direct moisture production and the temperature addition indoors is relatively large, perhaps +23 ° C. It gives over the year an RH of $6/20.55 = 30\%$ that the concrete stabilize around. Drying shrinkage as the main cause therefore seems likely.

In the above calculations, there are probably a few more "counterbalancing" parts than what was included in the calculation models above, which lowers the movements somewhat compared to the calculated ones. So, the calculated 3.7-3.8 mm as well as a certain amount of temperature movement are in fact slightly smaller, perhaps about 2-3 mm which was observed in place.

The drying in solid concrete structures is relatively slow, which means that seasonal moisture movements are small.

Some of the concrete, such as in the outer walls and the outer roof, does not dry out as much as the parts that are indoors, as these are colder which gives a higher RH.

Other parts, such as those close to the exterior walls and ceilings, in which widenings of joints and cracks have been observed, may have been more exposed to temperature variations/thermal movements. Of course, at the following summer, the concrete expands again, but the cracks are never completely closed due to the crushed material in the crack.

If cracking sensors are mounted, it can be further studied whether the movements vary over the year (thermal movements) and partly whether they continue to grow (dehydration shrinkage).

The consequence of the movements in cracks and expansion joints and the influence on structural safety and other functions, e.g. sealing, depends partly on where they are located and what safety margins there are and what function the part has, e.g. sealing against rain.

- c) Measures: The preliminary assessment was that the load-bearing capacity or personal safety were not under any risk, but a closer study of the load-carrying capacity was recommended. It was suggested to set up some cracking sensors (iii) to study variations with time.
- d) Follow-up: There is no currently decided measure taken to the knowledge of the author.

Conclusions: The FEM calculations showed that the observed movements in the expansion joints and in cracks most probably were caused by drying shrinkage. Relative humidity during the winter months can be very low in Northern Sweden and the drying out of the concrete can then be relatively far-reaching. In building parts in contact with the outside air, e.g. ceilings and walls, the movements can also depend on seasonal temperature variations.

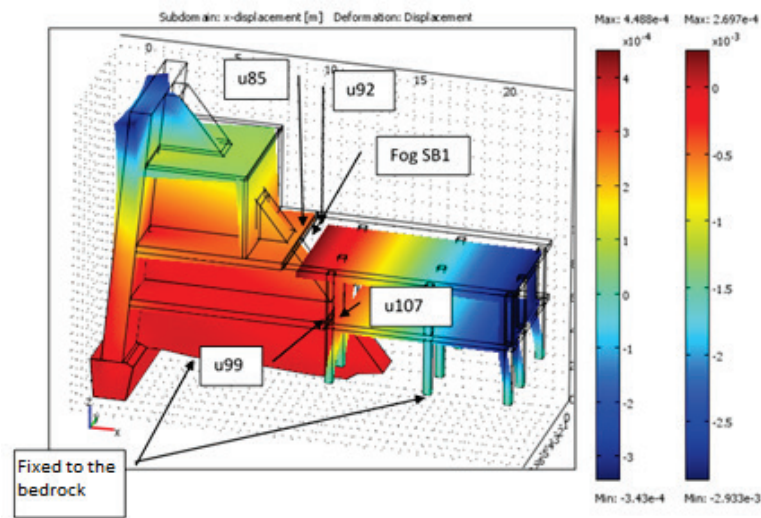


Figure 5-13 Calculated movements due to temperature variations.

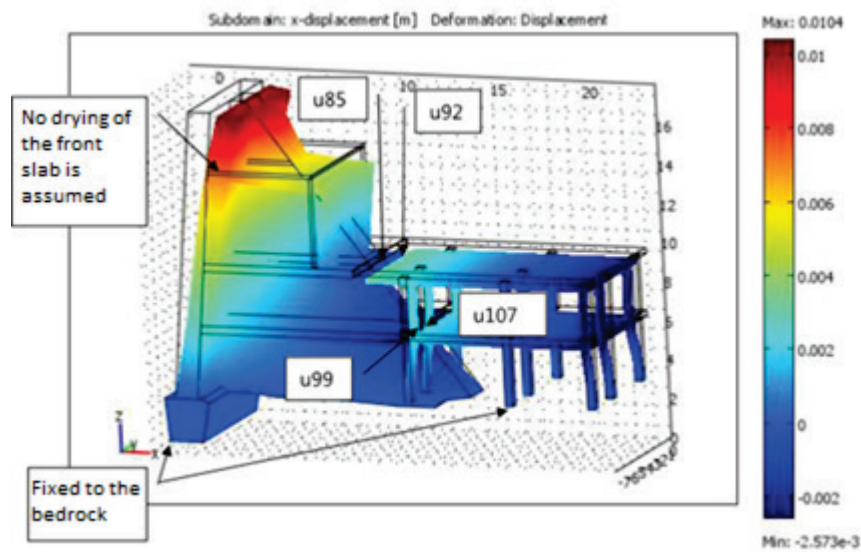


Figure 5-14 Calculated movements due to drying shrinkage.

5.7 ARCH DAM 1 (FROST/TEMP/ICE LOAD)

5.7.1 Brief description of plant

The power plant is located in Västerbotten, Sweden. It was built in 1968-70. The concrete dam consists of the left-hand crest, power house intake, arch dam and the spillway dam (the regulating dam) and the right-hand crest. The arch dam was built for a possible future new unit. The arch dam is 15 m high to the maximum retention level.

On the downstream side of the lower part of five in the arch (part 1 of 5), early leaching and frost damage were observed, especially in the lower lifts of the arch. Therefore, a thermally insulating space was constructed facing the downstream side of the lower lifts. During a diving inspection in 1994, the concrete on the upstream side was assessed to be in good condition, but during a diving inspection in 2012, frost damage was found on the bottom part of the arch. In 2014, a new thermally insulating wall was built against the downstream side, this time all the way from the foundation to the crest of the dam, see Figure 5-15.



Figure 5-15 The arch (Westberg-Wilde, 2014).

5.7.2 Assessment of arch

At an in-depth inspection in 2015, the cracks/damages in the arch and the crack in the right-hand arch support were considered a potential dam safety risk.

Possible modes of failure are:

- PMF 1: Failure in one of the arch lifts.
- PMF 2: Failure in right-hand arch support, at crack S1.

- a) Investigation: In an assignment in 2016, a material investigation (iii) and a theoretical analysis of the load-bearing capacity were carried out. Cores were drilled from the upstream and downstream sides of the arch and tested on CBI (The Swedish Cement and Concrete Research Institute). The material test showed a water-tight and strong concrete without ASR and notable frost damage. The current concrete quality is higher than the K300 that the original drawings prescribed. The damages that can nevertheless be observed are caused by the fact that the air pore system has been filled, partly with secondary substances and that the air pores have also been filled with water after the 46 years that the water pressure has been acting against the wall. Where the cold then could penetrate the arch, frost damage occurred.
- b) Analysis: In the assignment, calculations of temperature and mechanical stresses using a 3D FE model (iii) were performed. The calculations showed that the arch in its original state had a satisfactory safety against failure from water pressure and ice pressure. However, the calculations show that large temperature-related stresses have probably arisen when it was uninsulated, which may have caused cracks in the arch. It was also damaged by frost. These damages theoretically lowered the load-bearing capacity of the arch. If the arch had not received a new insulating wall, the load-bearing capacity would have been dubious in the long run. But due to the fact that the arch is

now insulated, the concrete stresses have dropped drastically and the risk of continued frost damage has decreased completely. Only in the still uninsulated crest there are large stress variations over the year and some risk of frost damage, but it is secondary from a dam safety perspective. However, there were some risks in the calculations with the crack found in the right-hand arch support, as well as the spillway piers. That part is uninsulated and the observed crack there can grow with time. If a large ice load occurs, there is a risk of shear failure in the crack, red surface in Figure 5-22, when the upper arch portion presses against the pier, blue surface.

- c) Measure: In the assignment it was proposed that a pre-stressed anchor (KB1 in Figure 5-22) should be placed vertically from the crest and down through the crack and anchored under the crack (green solid line) to reinforce the crack (vi), possibly down into the bedrock to also improve the stability (vi) of the spillway pier simultaneously (dashed line). Possibly a short anchor (KB2) can also be placed horizontally to hold the bearing console together where the arch presses with the rest of the pier.
- d) Follow-up: If anchors are used as stated above, no follow-up is needed apart from planned check-up (i) of anchors. Analysis continued: The temperature of surfaces against outdoor air (T_{out}) and against water (T_{water}) was assumed according to Figure 5-16. T_{out} , max/min = +33/-43°C. Temperatures as low as -43°C may well have occurred. In Jokkmokk and Glommersträsk, for example, -44°C and -35°C respectively were measured in 1999-01-27 (<https://opendata-download-metobs.smhi.se/explore/#>). Later measurement of water temperature indicates that it was higher during the summer months for larger water depths than the figure shows, which, however, is on the safe side because then possible tensile stress on the upstream side will decrease due to less temperature difference between the downstream and upstream side.

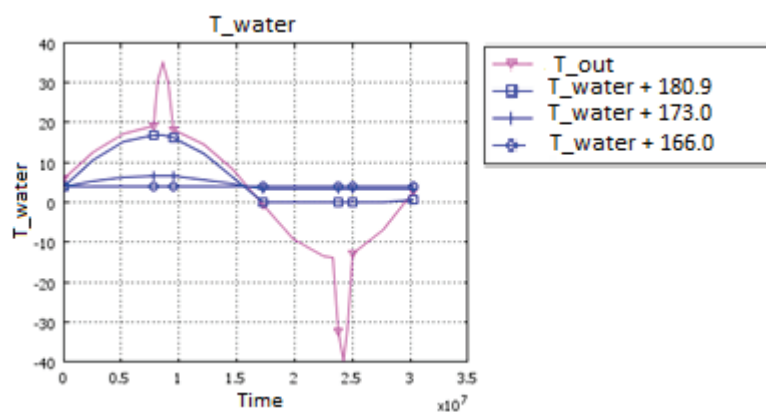


Figure 5-16 Assumed temperatures in air and water. $T_{max} = +33$ °C, $T_{min} = -42$ °C.

- e) Assumed boundary temperatures are also shown in Figure 5-17 for the original non-insulated arch, in the cases of warm summer day (+33°C) and cold (-43°C) winter day. During a cold winter, the upstream side of the arch is reached by freezing temperatures and if the concrete there is water-saturated, it can get frost damage, which has also happened in reality.

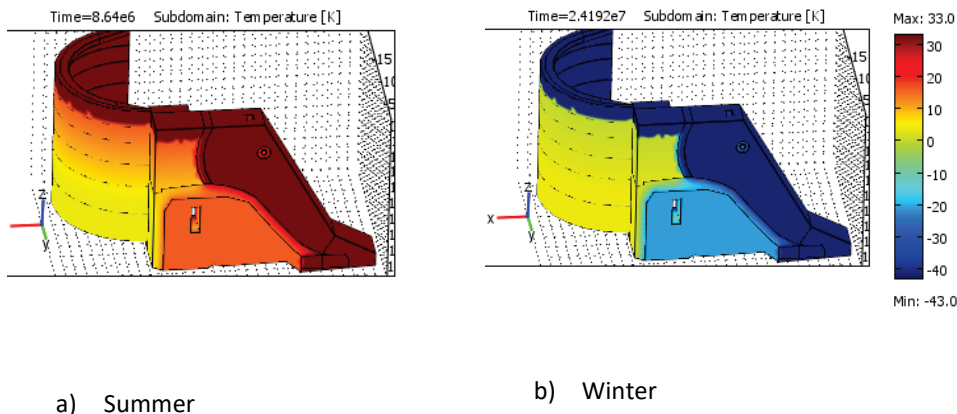


Figure 5-17 Assumed temperatures (a) summer and (b) winter.

Figure 5-18 shows the calculated main tensile stresses. Maximum main tensile stress in the arch is about 15 MPa. In the pier P1, the main tensile stress is about 20 MPa. An initially stress-free concrete temperature was assumed to be +4°C, which may be slightly low. If it is set higher, the calculated stresses increase during the winter but decrease during the summer, because then ΔT increases or decreases respectively. As seen, there are very high tensile stresses, red color, in the downstream side of the arch when this is uninsulated during a cold winter.

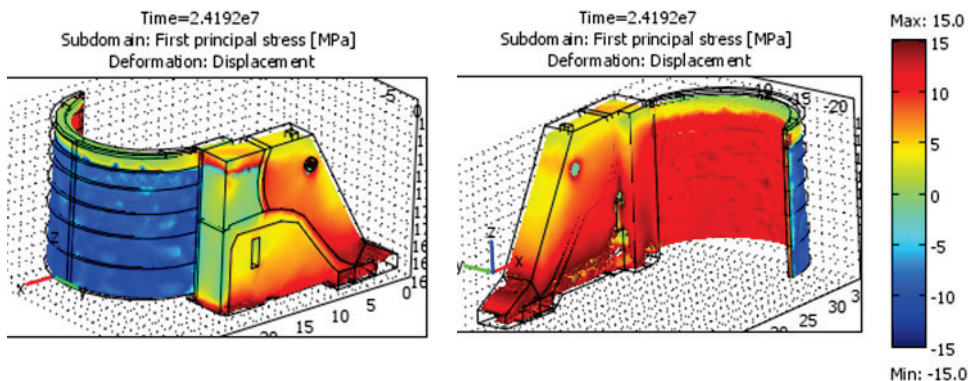


Figure 5-18 Calculated main tensile stresses at $T_{out} = -43\text{ }^{\circ}\text{C}$.

Figure 5-19 shows the calculated main compressive stresses. Maximum stress in the arch is 15 MPa

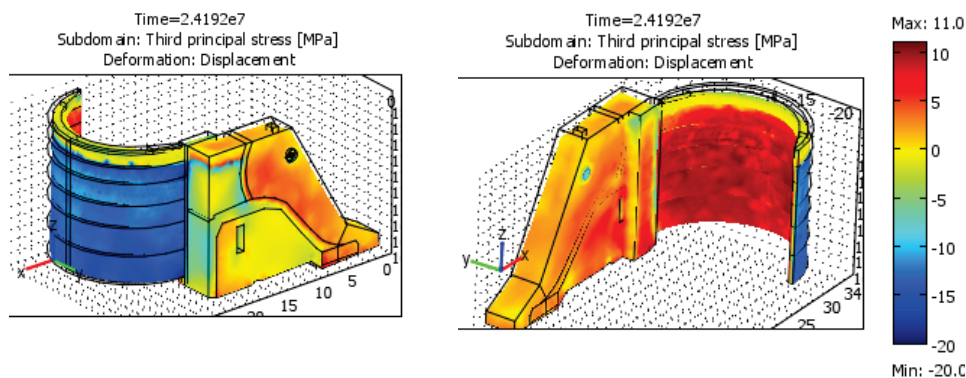


Figure 5-19 Calculated main compressive stresses at $T_{out} = -43\text{ }^{\circ}\text{C}$.

The arch dam is now, after 2014, thermally insulated with a climate wall on the downstream side. The arch then falls into a much more favourable climate, see Figure 5-20, where the temperature inside the climate wall ends up at or just below $0\text{ }^{\circ}\text{C}$. Further frost damage in the arch is therefore avoided. Only the crest that is uninsulated will have large temperature fluctuations, but on the other hand, it is not as moist and exposed to water and ice loads as further down the arch.

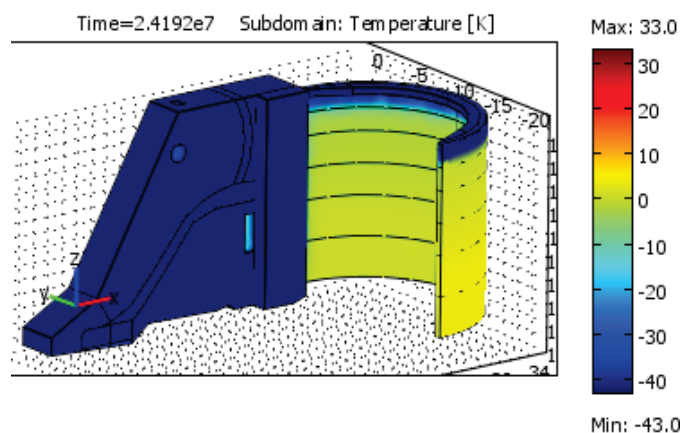


Figure 5-20 Calculated temperatures in the inspection gallery T_{in} during the winter.

Figure 5-21 shows calculated main tensile stresses during an extremely cold winter but with a now insulated dam. The main tensile stresses in the arch within the insulating wall have now decreased considerably compared to before the insulation wall was there, see above. The maximum main tensile stress is about 3 MPa. However, the stresses in the upper part, the crest, which are uninsulated, are approximately the same as before, about 5-8 MPa.

In the P1 pier, the main tensile stress is the same as before, because it is still uninsulated.

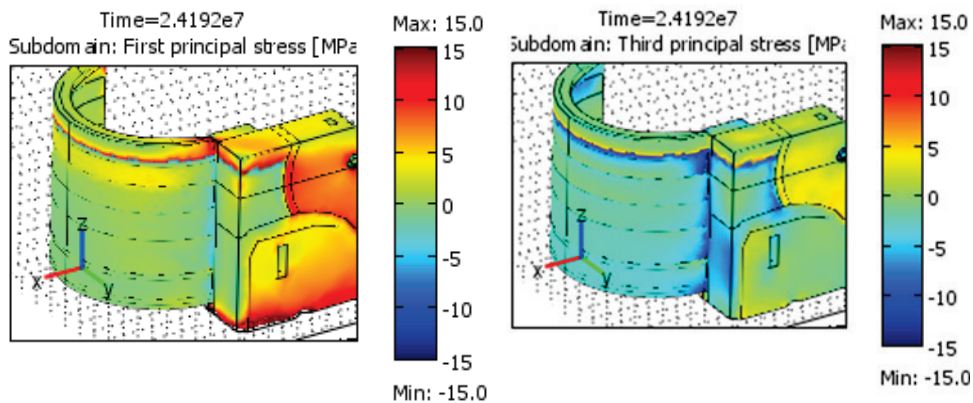


Figure 5-21 Calculated main tensile (left) and compressive (right) stresses against the arch support (right) at $T_{out} = -43$ °C.

The arch was also checked analytically with the assumption of a perfect 2-member arch. Only 2D effects in x and y planes are assumed. No 3D effects, in this case vertical, are assumed. This should be a realistic assumption when the arch parts are not interconnected to each other, just a sliding joint.

If the normal stress in the cross section is assumed as $\sigma = P/t$, a critical compressive stress can be calculated for a meter-long strip of an arch

$$\sigma_{cr} = EI(\pi^2/\alpha^2 - 1)/R^2/t \quad (\text{Pa})$$

Where P_{cr} = failure load = $EI(\pi^2/\alpha^2 - 1)/R^3$ according to BYGG T table A25:44e-1 (N); E = Elastic modulus (Pa); I = second moment of inertia (m^4); α = half the opening angle for the arch (rad); R = radius of the arch; and t = the thickness of the cross section (m).

The calculated compressive stresses did at no point surpass the critical compressive stress. OK!

Conclusions: Relatively thin and uninsulated arch dams are very sensitive to frost damage. The subzero temperatures goes through the dam from the downstream side and meets a moist concrete, whereby frost damage can occur. The current arch dam is now insulated and should be secured against material failure. The only weakness can be a crack in the right-hand arch support (pier), which should be reinforced with pre-stressed anchors.

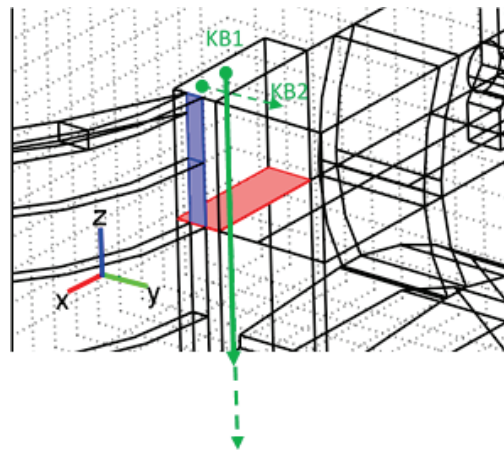


Figure 5-22 Principle sketch of right abutment. The force from the top lift of the arch is acting at the blue surface. A crack is found as the red surface. Green lines KB1 och KB2 indicate the suggested position for anchors.

5.8 SPILLWAY DAM 4 (ASR/FROST/TEMPERATURE)

5.8.1 Brief description of plant

The dam is located in Jämtland, Sweden. The regulating dam was originally built in 1940 – 1941 as a low wooden "buck dam". In 1970-71, the dam was rebuilt and the only the floodgate was retained from the previous plant, see Figure 5-23. A power house adjacent to the dam was commissioned in 1978.



Figure 5-23 The regulating dam

5.8.2 Assessment of floodgate

Possible modes of failure with regard to the spillway are:

- PMF 1: Failure in rocks in canal sides 3) and thus the overturning of spillway.
 - PMF 2: Cracks in horizontal cracks 2) in the spillway piers.
- a) Investigations: During an overview visual inspection (i) in connection with the IDSE (2011), it was observed that there are cracks and crazing in the spillway piers and guide walls in the floodgate, see 1) -3) in Figure 5-24 and that the bedrock directly downstream of the spillway is cracked. Earlier (2001) material studies (iii) showed that there was a cracking in the piers caused by ASR and that there was a risk of interaction with frost attacks in the future. Lime precipitates can increase the frost risk since moisture is bound in the surface. New material studies (iii) (2013) again showed ASR and frost damage. The air content and frost resistance were low. ASR was judged to be able to continue with a continued moist environment.
 - b) Analyses: The horizontal cracks in the piers, see 2) in Figure 5-24 may possibly have occurred during overload from water and ice pressure. At this level, or just below, the piers are "wedged" into the rock so there may have been such bending and shear stresses that cracks have arisen (i). A linear-elastic FE model (iii) was used to estimate stresses and to estimate the stability before and after the reinforcement (see below).
 - c) Measures: New pre-stressed anchors were set in 2015 in the spillway piers, see 4) in Figure 5-24, which partly raised the stability (vi) and partly secured the cracks 2) (vi). A new heat-insulating wall was built in 2015 around the entire floodgate to protect the concrete against precipitation and cooling (iv), see Figure 5-25. With added heat and dehumidification, the RH should drop below around 70-80%, which would hopefully prevent any further ASR and frost damage.
 - d) Follow-up: RH and temperature meters have been set to different positions in order to follow up (iii) the more favourable RH and temperature levels that should currently prevail. The pre-stressed anchors must be checked (iii) at regular intervals with regard to the locking force.

Conclusions: The floodgate is damaged by ASR and frost. Many and relatively large cracks are found. The spillway is dependent on the rock abutment for its stability. New pre-stressed anchors were set to secure horizontal cracks in the piers and improve stability and make it independent of the rock abutment. The entire spillway was covered with a heat-insulating wall to avoid precipitation against the concrete and to raise the temperature and lower the moisture level, in order to reduce further ASR damage. Moisture sensors have been mounted to check that RH does not exceed 80%. Otherwise, dehumidifiers will be added.

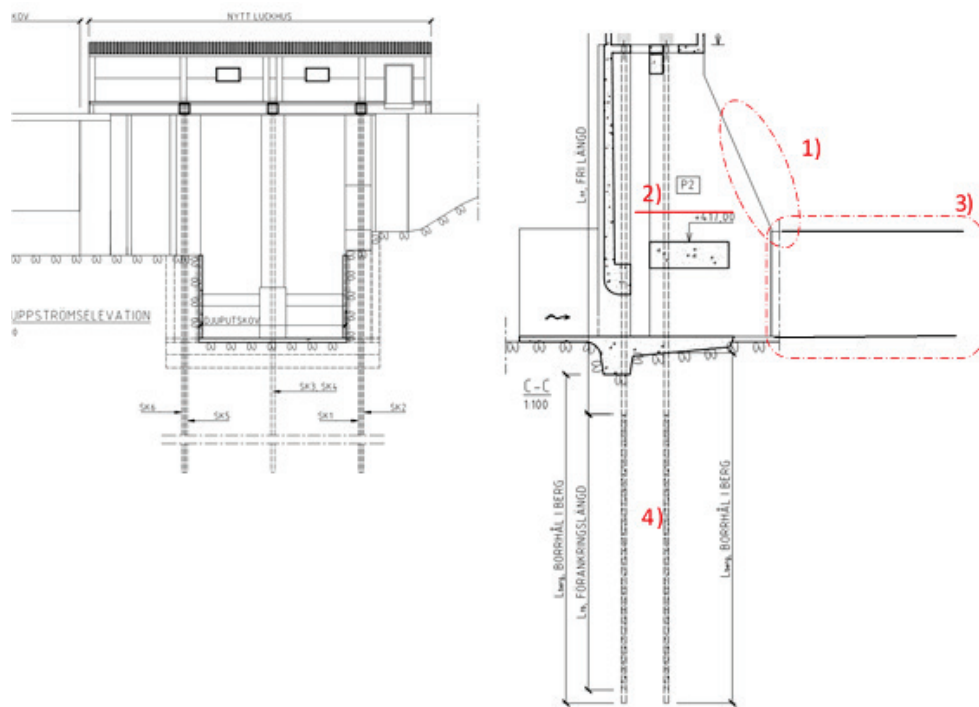


Figure 5-24 Upstream view and cross section (2015). 1) = crazing/cracks in the downstream side of the spillway piers, 2) = horizontal through-going cracks in the piers, 3) = cracks/crazing in guide walls.



Figure 5-25 Floodgate rebuilt with a climate wall.

5.9 BUTTRESS DAM 1 (TEMP)

5.9.1 Brief description of plant

The plant is located in Medelpad, Sweden, and was commissioned in 1962. The head is 21 m and the maximum retention level is +288.75 m. The plant consists of two dams. Dam unit 1 consists of an embankment dam and a regulating dam made of concrete. Figure 5-26 shows an upstream elevation of the concrete dam.



Figure 5-26 Upstream elevation of the dam. The red box marks the studied monolith 34.



Figure 5-27 The concrete dam in dam unit 1.

5.9.2 Assessment of stability

Possible modes of failure are:

- PMF 1: Crack going through the buttress and from the front slab down to the rock, i.e. so that the slab is divided into smaller parts, whereby overturning can occur.
- a) Examination: During an overview visual inspection (i) in connection with the IDSE (2010), cracks were observed in the front slab and buttresses. No material surveys were done. Material properties were estimated from the literature.
 - b) Analyses: A simpler mind model (i) pointed out that seasonal thermal stresses may have caused the cracks, possibly they may have been initiated in the casting stage. A more advanced FE analysis (iv) with a non-linear material model, see Appendix F, was performed in Comsol Multiphysics.

There, in addition to self-weight and water pressure against the front slab, temperature differences calculated in a separate temperature model were taken into account.

Temperature in the pier was calculated with a 3D model for 10 computational years with fictitious assumed temperatures, see Figure 5-28. 10 computational years proved to be unnecessarily many. For upstream water surfaces, T_{water} was assumed, against rock surfaces T_{rock} and against the climate wall and the part of the pier that is located outside the climate wall, T_{out} was assumed. Figure 5-28 and Figure 5-29 show assumed temperatures surrounding the dam, for the 10 computational years.

Figure 5-30 shows calculated temperatures for the warm and cold period of the 1st year.

The mechanical model consisted of a 2D plane stress model with a plastic damage model, see Appendix F.

Figure 5-31 shows calculated plastic strains ϵ_{pl} during the warm summer season and the cold winter season respectively of the 1st computational year. It can be seen that the cracks primarily could have formed during cold winters, when the downstream side and the lower part shrink and are restrained by the rock. Figure 5-32a shows strains that exceed $5 \cdot 10^{-5}$ (m/m), where cracks can be assumed to occur during the cold 1st winter. Since the model is a so-called "smeared crack model", only strains (m/m) are acquired, not discrete cracks (m).

Figure 5-32b shows that the strains did not increase after 10 computational years, even despite a high upper water surface=crest as well as an ice load of 200 kN/m were assumed for the autumn and winter respectively for the last year. But the temperatures surrounding the dam were more normal according to Figure 5-28. It shows that it is primarily temperature variations and the stresses that then occur that created the cracks.

On-site with the naked eye observed cracks were of less extent than those calculated according to Figure 5-32.

The calculated extent of cracking and, above all, the relatively small extent of cracking observed on-site were not considered any risk to the monolithic effect of the pier and thus not causing any lowered stability.

- c) Measures: None (i). Relatively small extent of the cracks, assessed little impact on stability and that an existing climate wall after all protects against further cracking.
- d) Follow-up: Normal supervision in connection with II and IDSE (i).

Conclusions: The FE analysis with a plastic damage model gave a crack appearance that was partly in line with reality. But apparently the environment is in fact somewhat more favourable than in the model assumption, because the real cracks are of a lesser extent. No further measure was considered necessary.

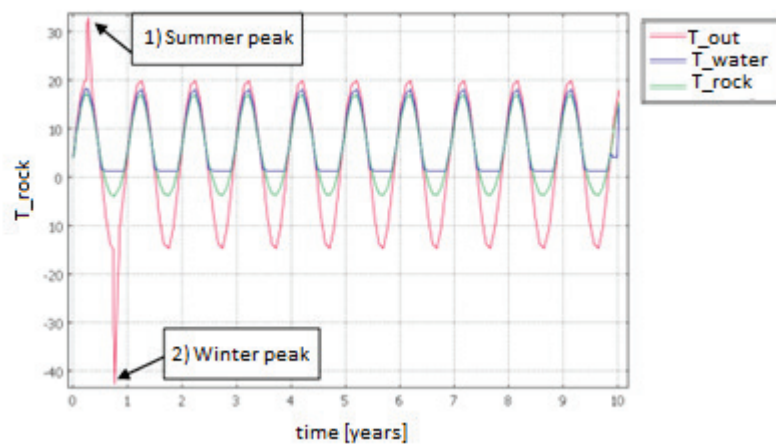


Figure 5-28 Assumed temperatures against the outside of concrete and climate wall (T_{out}), on the water sides (T_{water}) and on rock surfaces outside (T_{rock}).

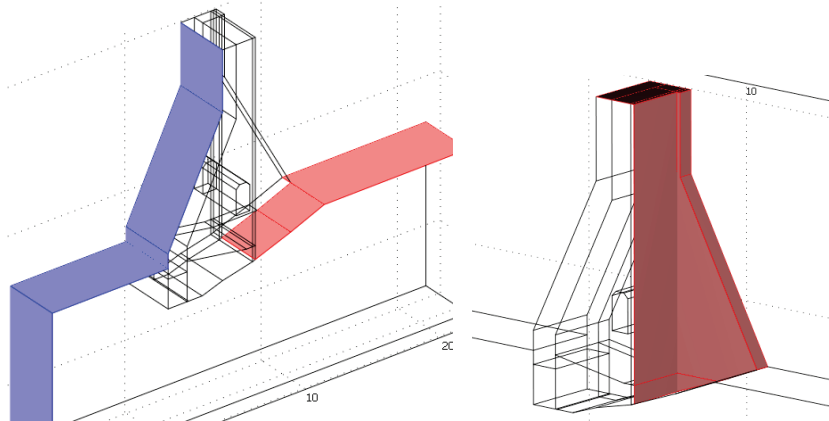


Figure 5-29 Assumed temperatures in water (T_{water} , blue surfaces), against rock (T_{rock} , bright red) and against concrete surfaces against outdoor air (T_{out} , dark red surfaces).

Figure 5-30 shows calculated temperatures in the dam and in the rock, exactly at the summer peak and the winter peak. The calculated temperatures are then automatically entered in the mechanical calculation, after which the mechanical additional stresses due to temperature variations are calculated with

$$\Delta\sigma = \alpha \cdot (T - T_{c0}) \cdot E$$

Where $\Delta\sigma$ = additional stress due to temperature expansion (Pa); α = thermal expansion coefficient ($1/^\circ\text{C}$); T = current, calculated temperature ($^\circ\text{C}$); T_{c0} = the reference temperature when the concrete is assumed to be completely free of stress ($^\circ\text{C}$); and E = modulus of elasticity (Pa).

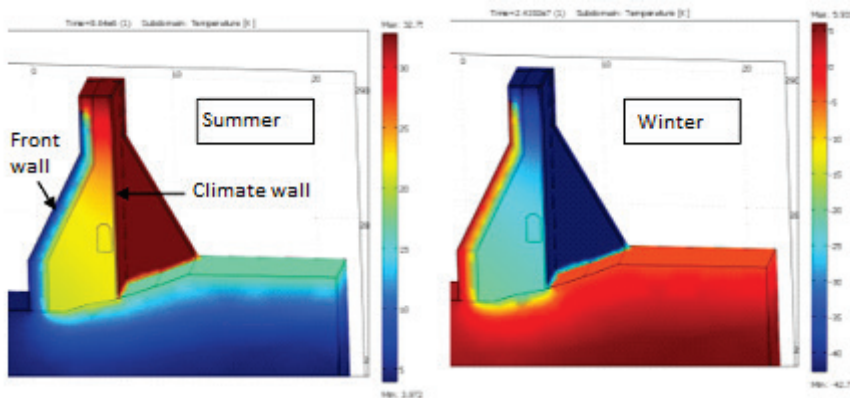


Figure 5-30 Monolith number 34: Calculated temperatures for summer and winter respectively with extreme outdoor temperatures.

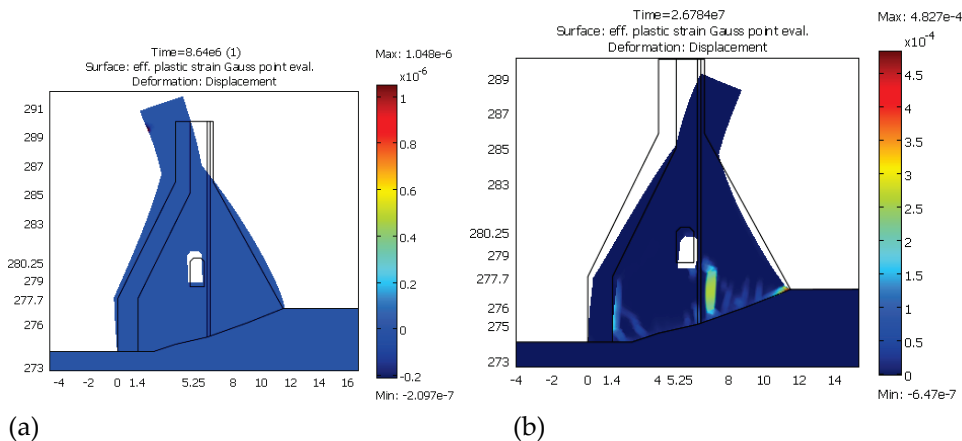


Figure 5-31 Calculated strains and cracking at (a) a warm summer according to 1) in Figure 5-28, and at (b) a cold winter period according to 2) in figure 5-28.

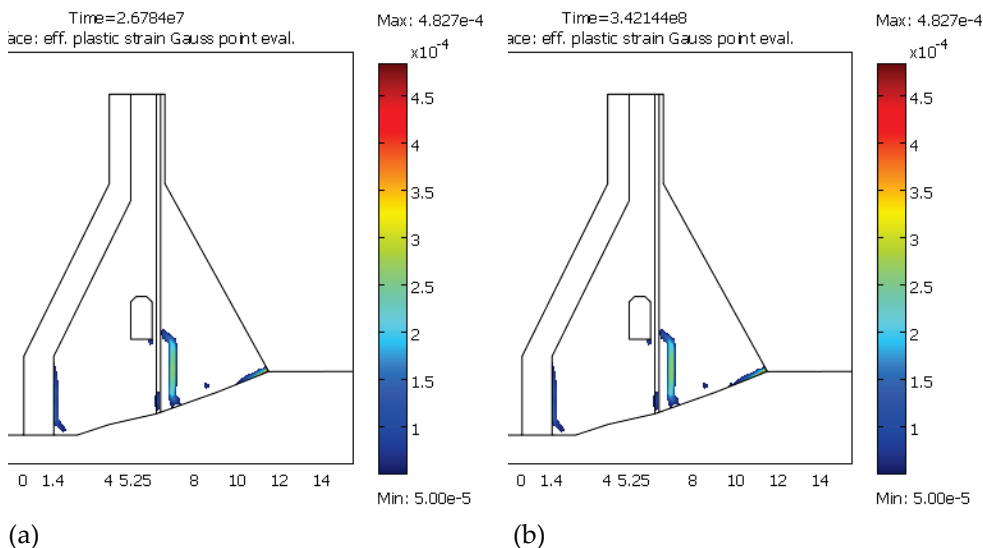


Figure 5-32 Strains exceeding $5 \cdot 10^{-5}$, i.e. approximately when cracks are thought to occur, at the winter peak 1) 1:st year, at $T_{out} = \text{approx. } -43$, and the winter of the last year respectively.

5.10 SPILLWAY DAM 5 (TEMP)

5.10.1 Brief description of facility

The dam is located in Jämtland, Sweden. It has a total length of about 330 m, maximum height 13.5 m and was constructed in 1974-75. The plant consists of an earthfill dam across the left-hand riverbed connecting to the left-hand shore, a spillway dam across the right-hand riverbed, power house and a short earthfill dam that connects to the right-hand shore. In the plant, a head of about 16 m is utilized at an expansion water flow of 90 m³/s.

The spillway dam from left to right consists of a short non-overflow concrete dam, a spillway (two gates) with concrete piers on both sides, an arch for a future new unit and a power house intake, see Figure 5-33.

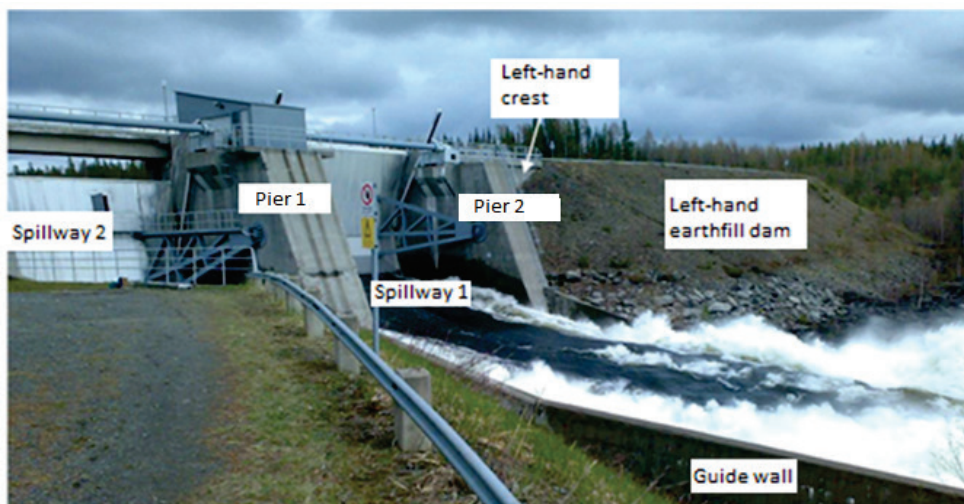


Figure 5-33 Downstream side of the spillway dam (IDS, 2009)

5.10.2 Assessment of stability

Possible modes of failure are:

- PMF 1: Crack going through the cross-section of the spillway pier and the rock all the way to the top, i.e. so that the pier is divided into smaller parts, whereby overturning can occur.
- a) Investigation: In an overview visual inspection (i) in connection with the IDSE (2008), a relatively extensive cracking was noted in all the spillway piers 1, 2 and 3, see e.g. for pier 2 at 1) in Figure 5-34 and Figure 5-41. Measurements (phenolphthalein in drilled holes) inside the inspection shaft gave a depth of about 30 mm on the carbonation front. The depths of the reinforcing bars were measured with a cover thickness gauge to vary between 35-45 mm. The concrete was 37 years old at the time of measurement, which meant that the front will reach the bars at the depth of 35 mm around 2080, where carbonation is assumed to be diffusion-controlled as $\text{Front Depth} = k \cdot \text{time}^{0.5}$. No other material investigations were made. Material properties were estimated from the literature.

- b) Analyses: A simpler mind model (i) pointed out that seasonal thermal stresses may have caused the cracks, possibly they may have been initiated in the casting stage, especially for pier 2 that was cast under slightly more difficult and colder conditions. A more advanced FE analysis (iv) with a non-linear material model, see Appendix F, was performed with the FEM program Comsol Multiphysics. There, in addition to self-weight and water pressure against the pier and from the gate via the gate shaft, temperature differences in the weir were taken into account in a separate temperature model. There is considered to be no risk for carbonation-initiated reinforcement corrosion.

The weir was also taken into account in the calculation because it also shrinks and expands during the winter and summer respectively, and thus the inter-locking forces between the pier and the weir are somewhat lower. Temperature in the weir was calculated with a 2D plane stress model for 8 computational years with fictitious assumed outdoor air and water temperatures, see Figure 5-35. Towards upstream water surfaces, T_{water} was adopted, and the part of the weir which is located downstream of the gate was assumed as T_{out} . Figure 5-36 shows the calculated temperatures for the warm and cold period of the 1st year. Against the pier sides, T_{water} and T_{out} were employed directly in the mechanical model for the upstream and downstream parts of the gate.

Figure 5-37 shows calculated plastic strains (m/m) ε_{pl} during the cold winter period of the first computational year. However, the calculation was cancelled at $-38\text{ }^{\circ}\text{C}$ due to numerical convergence problems. The figure shows strains that exceed $5 \cdot 10^{-5}$ (m/m), where cracks can be assumed to occur during the cold 1st winter. Since the model is a so-called “smeared crack model”, only strains (m/m) are acquired, not discrete cracks (m). The plastic strains did not increase in the model after the more extreme outdoor temperatures of the 1st year, because for the following year, according to Figure 5-35, more normal temperatures were adopted. Not even when the upper water surface was raised to the dam crest or when an ice load of 200 kN/m was applied in year 8 did more plastic strain occur. It shows that it is primarily temperature variations and the stresses that then arise that caused the cracks.

The calculated cracks occurred and had about the same position and extent as in reality. The model was therefore considered relatively valid.

The cracks were considered to give a risk of degrading the monolithic effect of the spillway piers, thereby reducing stability.

- c) Measures: The middle pier, P2, which has the greatest load on it, has both gates dependent on it and which has the most cracks, was strengthened in 2016 with 2 new pre-stressed cables (vi), see Figure 5-41. Through the placement of the cables, the vertical crack up to the gate bearings and the horizontal level just below (vi) were also secured.

- d) Follow-up: The anchors should be tested at certain intervals. The cracks must be visually monitored and suitably mapped, preferably at each IDSE, or more preferably at each II (i).

Conclusions: The FE analysis with a plastic 2D damage model gave a crack appearance that is in line with reality. The cracks were considered critical to the stability of the pier and the ability to carry the gate loads. New pre-stressed cables have been placed obliquely downwards, above and below the gate shaft, down into the rock where they are anchored, in order to secure cracks and increase the stability.

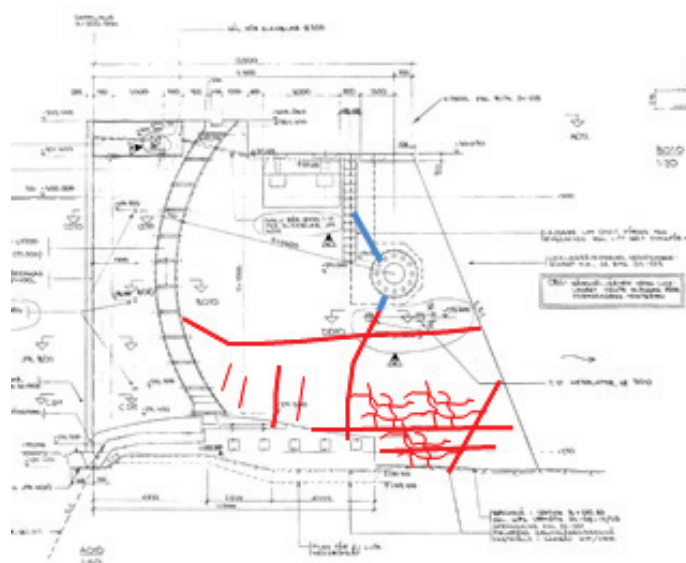


Figure 5-34 Pier 2, right-hand side: Observed cracks 2011-10-31. Blue lines show cracks observed both on the outside and the inside of the shaft down to the gate shaft.

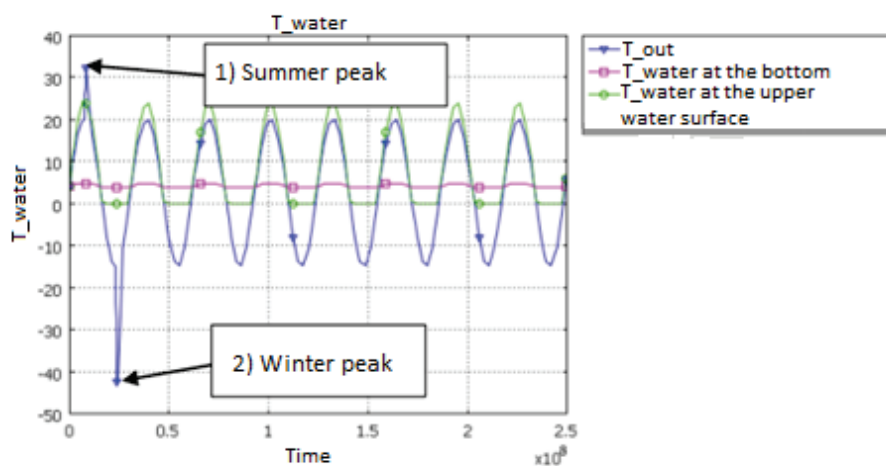


Figure 5-35 Assumed temperatures of the air side of the concrete (T_{out}), against water sides (T_{water}) at two different levels, at the bottom and the upper surface. Between the upper surface and the bottom the water temperature varies linearly.

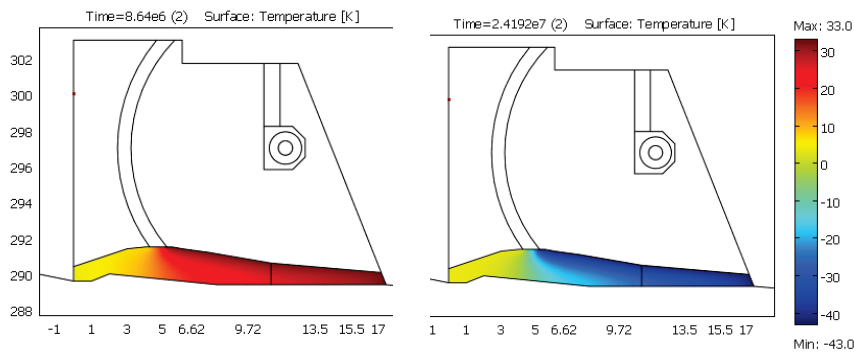


Figure 5-36 Calculated temperatures in the lower part of the pier for summer (1) and winter respectively with extreme outdoor temperatures (2).

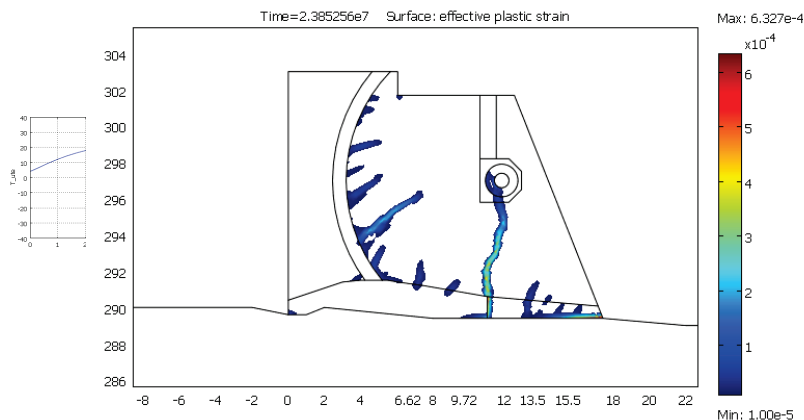


Figure 5-37 Calculated plastic strains ϵ_{pe} for the concrete exceeding $5 \cdot 10^{-5}$, i.e. around the point where cracks are expected to occur, in the beginning of the winter peak of the 1st year, around -38°C , where the calculation was stopped due to convergence issues.

Figure 5-38a and b show calculated stresses in the x and y direction respectively. With an assumed yield limit f_y of 290 MPa, yield stress is achieved in the certain parts of the reinforcement, which is also shown against the gate shaft in Figure 5-40.

Maximum calculated plastic strain is 0.007, i.e. approximately 0.7%, which is not much compared to the failure strain of about 16% in hot-rolled reinforcement steel. Note that the calculation was interrupted at -38°C due to numerical convergence problems, which means that the plastic steel strain would have become greater at maximum assumed winter temperature -43°C . Note that the calculated strains are based on a spring model which is assumed to reflect the bond between concrete and reinforcement. This bond and how it probably diminishes at high reinforcement elongations when the bars begin to slip against the concrete is important. If the iron bars are assumed to be completely fixed to the concrete, it is obtained that the bars takes a larger proportion of the cross-sectional forces. If the stresses in the reinforcement are relatively high and at the same time the cross-sectional forces alternate, e.g. when temperature changes, a fatigue failure in the bars is theoretically obtained rapidly. More likely, the bond is rapidly decreasing

and the bars become unloaded along a certain distance. The concrete must then take a little more of the cross-sectional forces and may crack a little more and longer, but the bars do not reach fatigue failure.

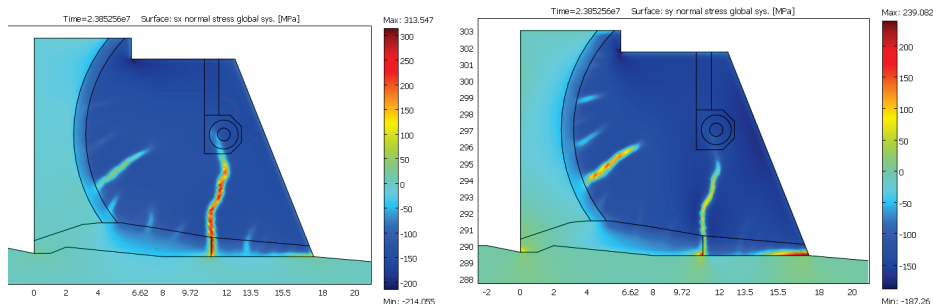


Figure 5-39 Calculated reinforcement stresses in the x and y direction respectively (vertical and horizontal respectively) and plastic strain ϵ_{pe} .

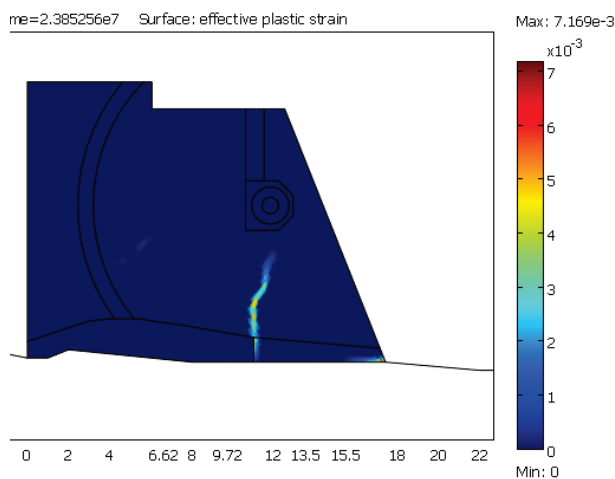


Figure 5-40 Calculated plastic strain ϵ_{pe} in the reinforcement.

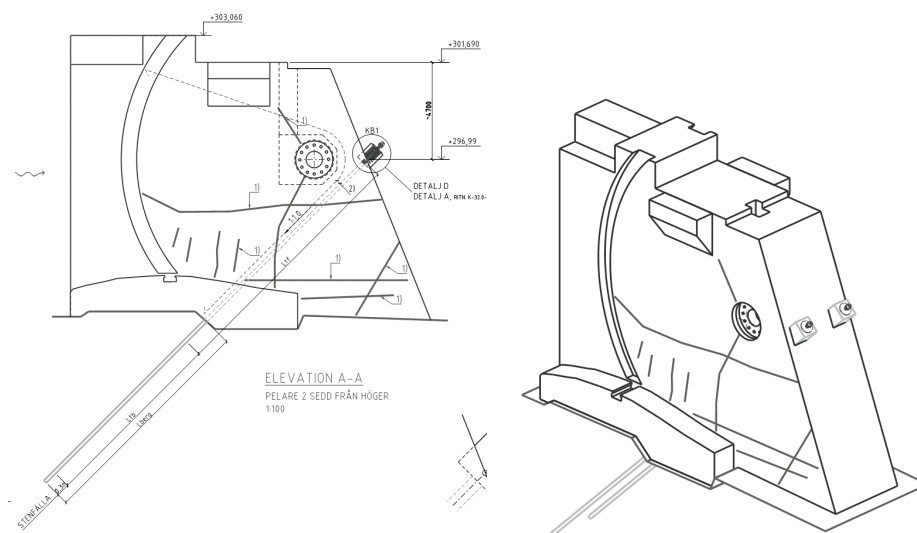


Figure 5-41 New pre-stressed anchors that increase the stability and secures cracks 1) in the pier.

5.11 SPILLWAY DAM 6 (TEMP)

5.11.1 Brief description of plant

The spillway dam is located in Jämtland, Sweden. It was built during the period of 1971-74. It consists of a 110 m long concrete dam with a spillway in the middle. Maximum height 18 m. Each side connects to an embankment dam, see Figure 5-42.



Figure 5-42 The spillway dam before a new climate wall was built.

5.11.2 Assessment

Possible modes of failure are:

- PMF 1: Crack going through the buttress and from the front slab down to the bedrock, i.e. so that the slab is divided into smaller parts, whereby overturning can occur.
- a) Investigation: In an overview visual inspection (i) in connection with a pre-study (2010), a relatively extensive cracking was noted in the left-hand spillway pier, monolith 4, Figure 5-44a, and most buttress dam monoliths, see e.g. Figure 5-46a for monolith 12. The cracks are found on both sides of the respective piers and can thus be continuous. No material studies were made. Material properties were estimated from the literature.
 - b) Analyses: A simple mind model (ii) pointed out that seasonal thermal stresses may have probably caused the cracks. Possibly, some cracks have been initiated in the casting stage. A more advanced FE analysis (iv) with non-linear material model according to Appendix F was performed with Comsol Multiphysics. There, in addition to self-weight and water pressure against the monoliths, temperature variations in the monoliths were taken into account. For the existing stage, before the new climate wall, a fictitious seasonally varying outdoor air temperature T_{out} directly against the concrete, see Figure 5-43, was assumed. Against upstream water surfaces, a water temperature was assumed which follows T_{out} in the upper part and is more uniform, around $+4^{\circ}\text{C}$, towards the bottom of the river

The mechanical model consisted of a 2D plane stress model with a plastic damage model, see Appendix F.

Figure 5-44b shows calculated plastic strains ε_{pl} during the cold winter period of the 1st computational year for the left-hand spillway pier, monolith 4. The figure shows strains exceeding 10^{-4} (m/m), where cracks can be assumed to occur during the cold 1st winter. Since the model is a so-called "smeared crack model", only strains (m/m) are acquired, not discrete cracks (m). The calculated "cracks" agree well in terms of location and distribution with the ones observed on-site according to Figure 5-44a.

Figure 5-45 shows calculated plastic strains during the warm summer of the 1st computational year, when the monolith bends upstream, and cold winter respectively, when the monolith bends downstream, for a typical monolith in the buttress dam. It is mainly during the cold winter period that the cracks are formed. Figure 5-46b shows the cracks in the form of all the main tensile strains over 10^{-4} , which includes both the elastic one, in this case small, and the plastic one, in this case the dominant. The calculated "cracks" agree well in terms of the location and distribution with the ones observed on-site as shown in Figure 5-46a.

The plastic strains did not increase in the models after the more extreme outdoor temperatures of the 1st year, because for the following year more normal temperatures were assumed, according to Figure 5-43. Not even when the upper water surface was raised to the dam crest or when an ice load of 200 kN/m was applied did additional plastic strain arise. This shows that it is primarily temperature variations and the resulting stresses that caused the cracks.

The calculated cracks occurred and had about the same position and distribution as in reality. The model was therefore considered relatively valid.

The cracks were considered to give a certain risk of degrading the monolithic effect of the spillway piers, thereby reducing stability.

- c) Measures: A new heat-insulating wall was constructed in 2014 covering almost the entire buttress dam and its monoliths, see Figure 5-49 and Figure 5-50, only the crest protruding above it. The wall even out the temperature differences over the year and reduces the stresses in the concrete (iv). It is not possible to put insulation on spillway piers due to the water flow there. However, a new weir was built at a higher level for the left-hand spillway, and by doing so the lower part of monolith 4 ended up in a more uniform climate (iv). Instrumentation was also mounted on the dam (iii), one pendulum, crack sensor and temperature sensor, partly to be able to warn of unnatural events/trends and partly to calibrate the calculation model.

Figure 5-47 shows calculated temperatures for summer and winter when the new climate wall is mounted. Since the concrete piers now end up inside the wall, the temperature climate becomes much smoother and thus the stresses in the concrete become lower and no new cracks should form. Figure 5-48

shows that the calculated and expected crest movements decrease considerably after the new climate wall is mounted. Its movements should then be compared with the measured ones from the pendulum that was mounted.

Figure 5-49 and Figure 5-50 show the dam with the new heat-insulating climate wall.

Despite some doubts about fulfilling the RIDAS [3], [4], stability conditions, it was for the moment chosen not to strengthen the dam. The above-mentioned load reduction of thermal stresses, new monitoring and ice protection (iv) was considered sufficient at the time.

- d) Follow-up: The cracks must be visually monitored and suitably mapped, preferably at each IDSE, or more preferably at each II. Measurement values from the instrumentation shall be evaluated against trends and the calculation model. Possible reinforcement with stability-increasing pre-stressed anchors will be considered after evaluation.

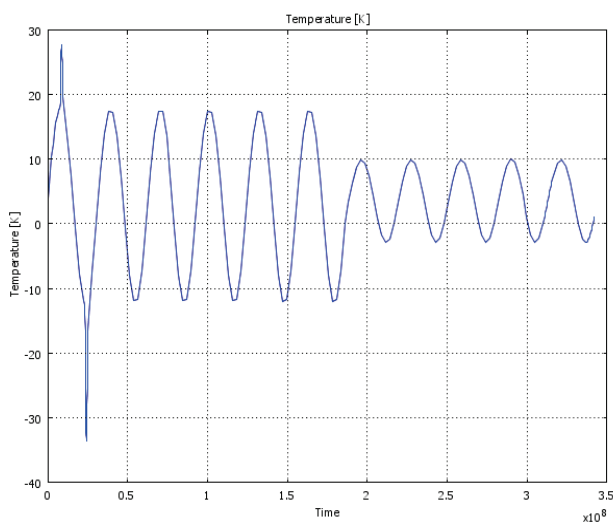


Figure 5-43 Calculated temperature against the downstream sides of the monolith. For year 7 a heat-insulating climate wall has been built against the downstream side of the dam, resulting in the smaller temperature fluctuations.

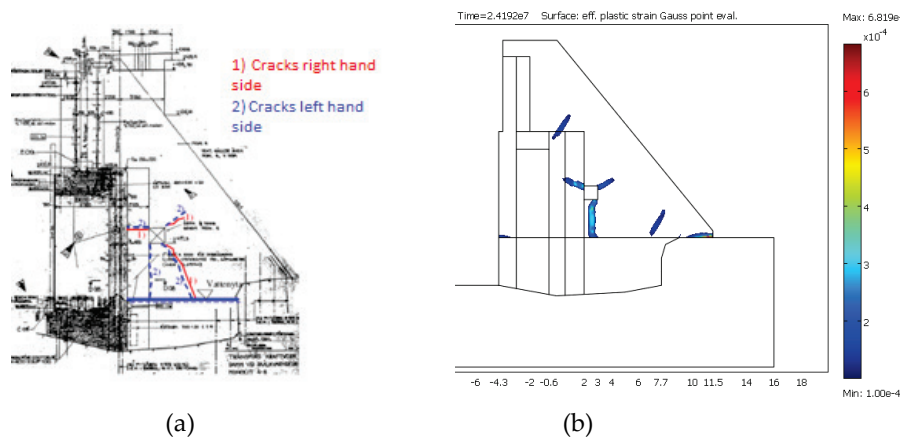


Figure 5-44 Spillway pier M4: (a) observed cracks and (b) calculated plastic strain exceeding the assumed crack strain 10^{-4} in the concrete, i.e. cracks have arisen, at the winter peak, approx. -43°C , in the middle of January in the 1st computational year.

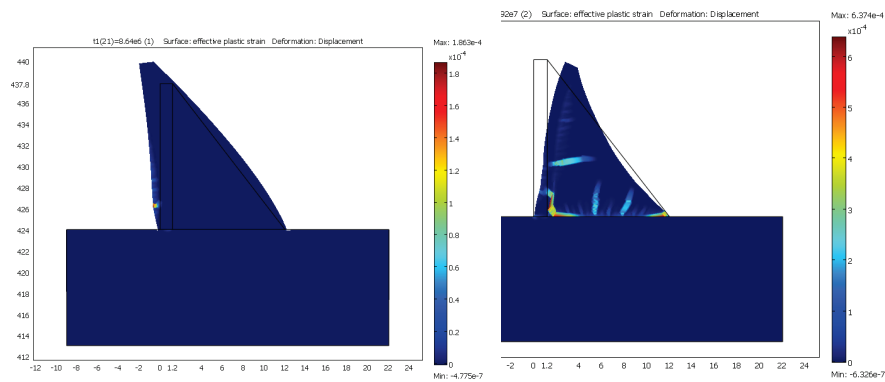


Figure 5-45 Buttress monolith: Calculated plastic strains during a warm ($+33^{\circ}\text{C}$) summer and cold (-43°C) winter.

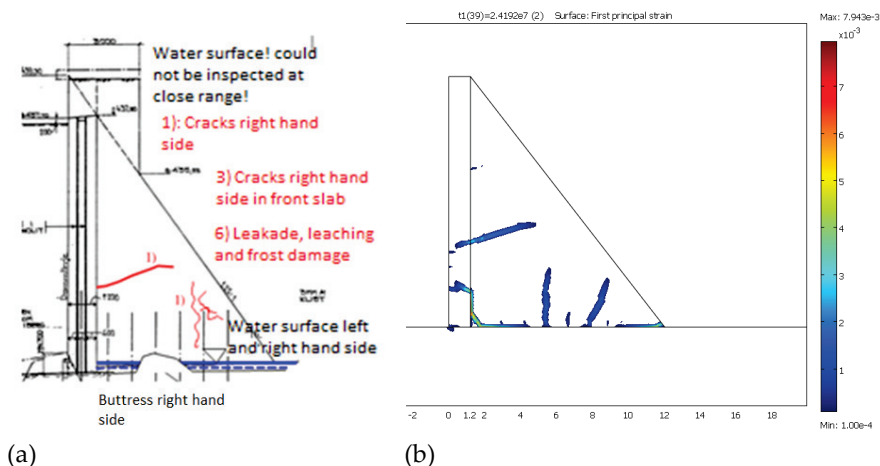


Figure 5-46 Buttress monolith M12: (a) Observed cracks and (b) calculated main tensile strains exceeding the strain 1×10^{-4} for concrete, i.e. cracks have arisen at the winter peak, approx. -43°C , in the middle of January in the 1st computational year.

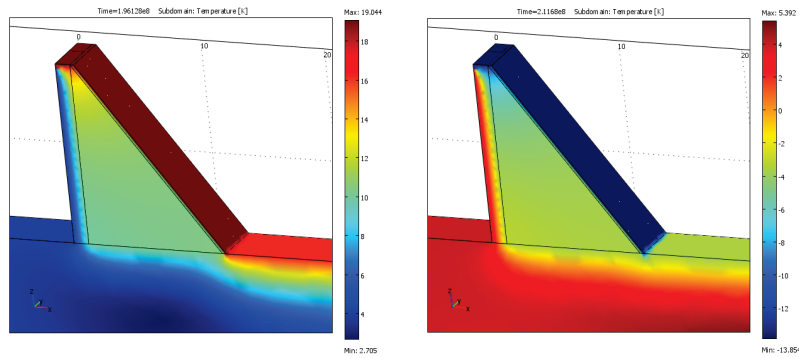


Figure 5-47 Buttress monolith: calculated temperature during the summer and winter respectively after a new climate wall has been built.

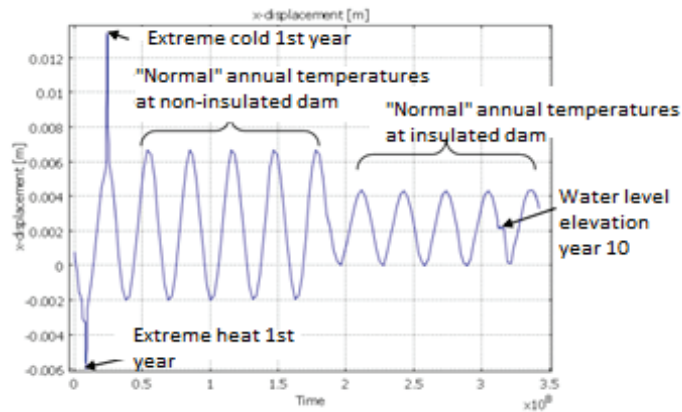


Figure 5-48 Calculated horizontal strain of the dam crest for the whole calculation period.

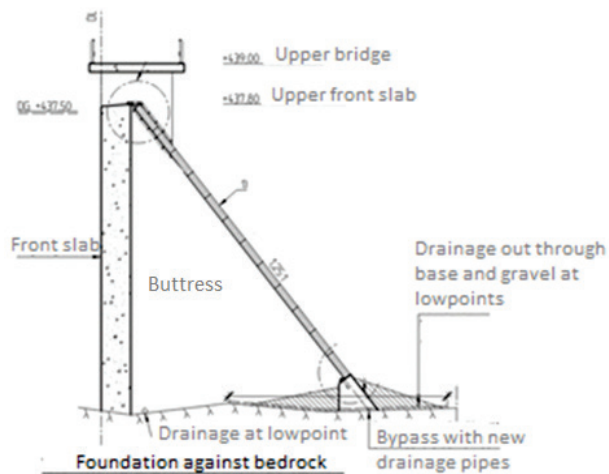


Figure 5-49 Measure: New heat-insulating climate wall 3) which protects the entire monoliths, except for the crest.



Figure 5-50 The dam in 2017 with a new heat-insulating climate wall

5.12 BUTTRESS DAM 2 (TEMP)

5.12.1 Brief description of plant

The power plant is located in Lapland, Sweden, and was commissioned in 1958. The concrete dam has a crest length of 530 m and consists from left to right of a 43 m long connecting dam, a 137 m long weir dam, a 90 m long spillway section with 1 segment, 1 sector and 1 segment gate, an approx. 80 m long non-overflow concrete dam with a bottom spillway, an 8 m long section with alog-driving spillway closed with stop-logs, a 40 m long buttress dam, a 57 m long intake part and finally a 78 m long connecting dam. See Figure 5-51. The highest height is 34 m. Before 2012, a climate wall of thin concrete elements was placed just downstream of the front slab and formed a narrow inspection space of about 2-3 m, see Figure 5-53.

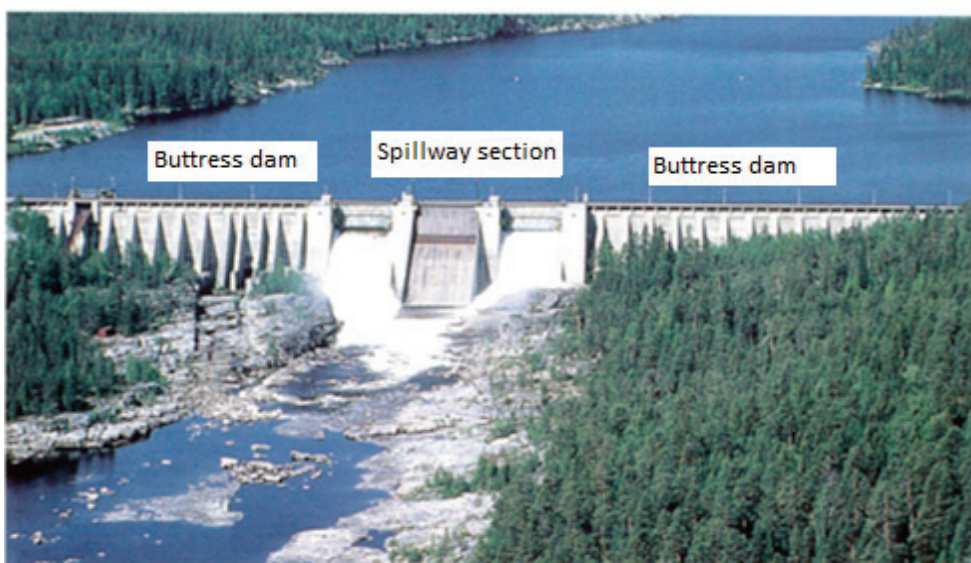


Figure 5-51 The spillway dam before a new climate wall was built in 2012

5.12.2 Assessment

See also Appendix E for a more detailed description of the assessment.

Possible modes of failure are:

- PMF 1: Crack going through the buttress and from the front slab down to the bedrock, i.e. so that the slab is divided into smaller parts, whereby overturning can occur
- a) Investigation: In connection with overview visual inspections (i) attention has been paid to cracks in the front slab and buttress. Typically, for the buttress dam, cracks are present in the front slabs, see Figure 5-52a and 1) in Figure 5-53, from the front slab to the upper corner of the inspection gallery, see 2), a vertical crack 3) from the inspection gallery down to the rock and some vertical cracks 4) from the rock and a bit up the buttresses outside the old climate wall. See also a basic view in Figure 5-54. The cracks can be found on both sides of the respective piers and can thus be continuous. An uncertainty existed if the cause of the cracks was due to, for example, occurring during the construction phase, during the impounding, normal load impact in the operating phase, seasonal temperature variations, or a combination of these. There was an uncertainty about how much the stability is affected by the cracking. An uncertainty also existed as to how the concrete dam and the crack formation would be affected by a planned new heating system for the dam. No material studies other than carbonation and surface layer measurements were made. Material properties were estimated from the literature.
 - b) Analyses: Some simpler calculations (ii) regarding stability, overturning and sliding are performed in conjunction with previous IDSEs. The calculations for an assumed non-cracked structure showed that the stability requirements according to RIDAS [3], [4], were partially not met.

In a later feasibility study (2009), with a simpler calculation (ii), the conclusion was again drawn that the stability of the monoliths was doubtful, depending on whether any rock abutment could be assumed to be mobilized or not and whether the cracks can be considered to be force-transmitting or not. The stability may possibly have been reduced as cracks have arisen, see principle in Figure 5-55.

In a further feasibility study (2010), a simpler calculation (ii) showed that the RIDAS [3], [4], stability requirements are fulfilled if the monoliths are assumed to be uncracked and if either the existing slack rock anchors are included or if the ice load does not exceed 150 kN/m. In this case, the term "uncracked" means that the cracks are sufficiently force-transmitting and do not significantly lower the stiffness and do not divide the monolith into smaller parts. A more advanced (iii) FE analysis in the same study (2010):

- In addition to water pressure, the temperature was calculated in the concrete in a separate 3D model. The assumed outdoor temperature (T_{out}) is shown in Figure 5-59 with a 1st computational year with only the old climate wall and extremely warm and cold summer and winter respectively. Then followed a 2nd year with "normal" T_{out} . Beginning

in the third computational year, the new climate wall was assumed to be built in 2012 as well as normal T_{out} . During the last computational year, the upper surface was also raised and in the last late winter an ice load was applied.

- A linear elastic material model and with the old climate wall, before 2012, (Figure 5-56) showed high tensile stresses in the cracked areas.
- Using a non-linear material model according to Appendix F, it was shown that the main cause of the cracks has been seasonal variations in temperature. Most of the buttresses were outside the old climate wall (see Figure 5-54) and were subjected to varied outdoor temperatures. They expanded and contracted during the summer and winter respectively. During the assumed very warm summer during the 1st computational year, the front slab cracked on the upstream side, see Figure 5-57a, when the monolith expanded in the downstream edge and exerted tension on the upstream side facing the relatively cold water. During the subsequent assumed very cold winter, the monolith shrank outside the climate wall while the upstream side towards the now relatively warm water was retained and instead received tensile stresses and cracks, see Figure 5-57b. The cracks may to some extent also have been initiated in the casting stage, especially against the rock, previously cast parts and in courses, e.g. around the inspection gallery, but later been exacerbated by the seasonal temperature changes.
- In the study another year was calculated, but with more normal temperatures, see Figure 5-59, between year 1 and year 2. No significant additional cracks occurred at that time.
- Starting at 2012, computational year 2, the current insulating climate wall was put into the model. The crest deflection only increased slightly, from 3.47 mm in the year 3 to 3.64 mm in the year 11. I.e. as long as the temperature against the concrete does not exceed the extremely warm or cold temperature that was assumed during the first computational year, the cracks in the calculation do not grow significantly.
- Seasonal temperature variations, especially during warm summers and cold winters, give the completely dominant movements, stresses and crack width changes. This also applies with the new climate wall in place in 2012, but at a significantly lower level.
- Ice loads or a high upper water surface have in relation to the temperature variations very low impact, which Figure 5-59 shows as barely discernible additional deflections. On a lower dam, the ice load would have had a somewhat larger impact.
- So, if the dam is completely covered in with a heat-insulating climate wall, the stresses on the dam drop dramatically and safety is increased. It was therefore proposed that a new heat-insulating climate wall should be built on the outside and along the buttress dam, which was carried out in 2012. Furthermore, instrumentation in the form of temperature

sensors, crack sensors, pore pressure sensors and a pendulum suspended from the dam crest according to Figure 5-60 was proposed and also carried out in 2012.

- Shear and normal stresses in intended crack planes in the support plate were calculated. The stresses were extracted from the FEM calculation and compared analytically to the calculated shear capacity "force transfer in joints" according to BBK 04. The result showed that the capacity exceeded the stresses, even before 2012 with a new climate wall, whereby the conclusion was drawn that the buttress behaves monolithically and there is no risk of failure in the cracks.
- c) Measures: A new heat-insulating wall was applied covering the entire buttress dam and its monoliths, see Figure 5-61. Only the crest protrudes above the wall. The wall should be able to discharge water that flows over the weir in the upper part of the dam. The wall should provide a more even temperature climate for the concrete (iv). Instrumentation was also applied to the dam (iii), one pendulum, crack sensor, pore pressure sensor and temperature sensor according to Figure 5-60, partly in order to be able to warn of unnatural events/trends and partly to calibrate the calculation model.

In 2016, a measurement data evaluation was performed by comparing measured values with calculated values and the conclusion that follows.

Since the concrete piers now end up behind the wall, the temperature climates are much more uniform and thus the stresses in the concrete become lower and no new cracks should form. Calculated expected crest movements decrease significantly after the new climate wall is mounted.

- d) Follow-up: The cracks must be visually monitored and suitably mapped to see differences with time, preferably at each IDSE, or more preferably at each II. Measured values from the instrumentation should be evaluated against trends and the calculation model.

Conclusions measurement evaluation 2016:

Temperatures:

- Comparison between measured temperatures in the dam shows good agreement with calculated temperatures, if heat has been added to the dam via the drum located under the inspection gallery. Reportedly this is true in reality.
- The new climate wall meets well its expected insulation capacity, i.e. to bring about a more even temperature variation in the dam.
- Thus smaller stresses and stress fluctuations should occur than was previously the case and no further cracking should occur. However, it should be considered not to add any heat during the summer, as the OCM manual (Operation, Condition check and Maintenance) for the dam also prescribes, in order to further reduce thermal movements during the summer.

Movements:

- A review of measured crest movements (pendulum) and crack movements show relatively small movements. The movements correspond to the expected (calculated) ones according to the model.
- For crack sensors S6 and S7 (Figure 5-60), the measured crack movements were less than expected (calculated), which may indicate that there is no significant crack between concrete and underlying rock or the sensors are not representatively (too shallow) attached to the rock .
- The studied measurement period 3/12-2012 to 8/1-2014 was relatively short. A longer, continuous measurement period should be studied next time. Since then values have been measured through the autumn of 2018 but are not evaluated.
- The mechanical model can be considered relatively valid as conformity is good compared to measured crack and crest movements

Other:

- Thermally insulated concrete dams are generally protected from temperature-related cracks and frost damage.
- It is suggested that the evaluation will be repeated within a certain time with more updated temperature and motion measurements, but then only with a simpler comparison with the calculated values from this study.
- The shear force transmitting capacity in the cracks was sufficient to transmit the shear forces that exist there, even before the new (2012) insulating wall was mounted. The monoliths are therefore deemed to act as monoliths and be able to meet the RIDAS [3], [4], stability requirements.
- The ice load had only a marginal impact in the FE model.
- Threshold limit values of measured values should be set so that they reflect seasonal variations. E.g. a certain movement can be harmless if it occurs (naturally) during the winter, but if it occurs during the summer it can be dangerous.

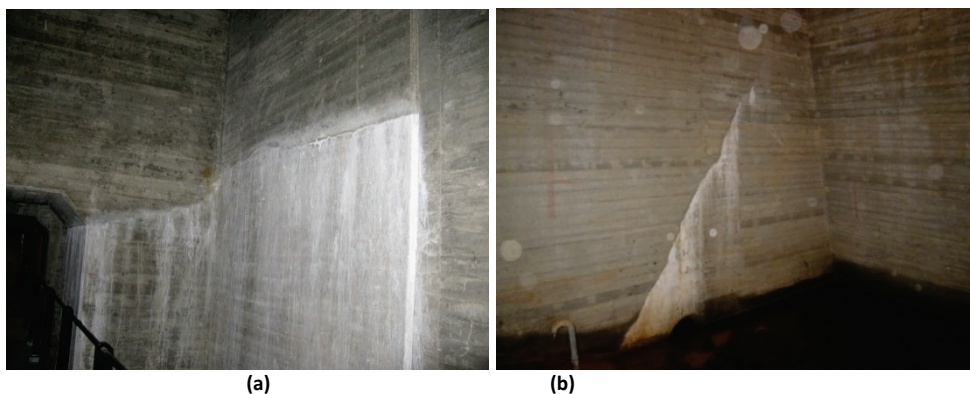


Figure 5-52 (a) Cracks in front slab and buttress and (b) oblique crack in buttress up against the front slab.

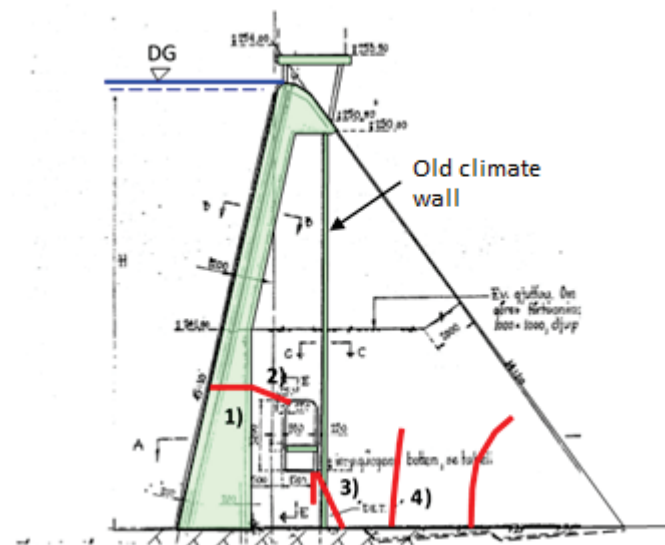


Figure 5-53 Conceptual appearance of cracks (red lines) observed in the buttress dam.

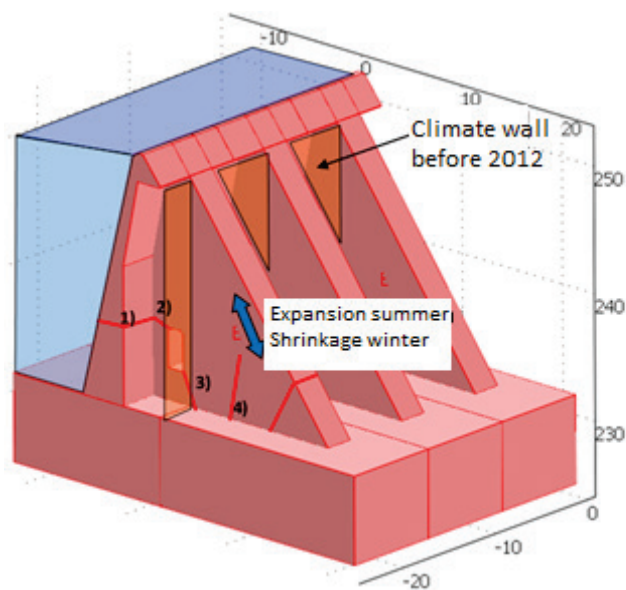


Figure 5-54 The original climate wall (orange) was not well placed as the main parts of the buttresses were located outside and expanded and contracted during warm summers and cold winters respectively, and cracks were therefore formed.

A conceptually assumed decrease in load-bearing capacity of a dam monolith that cracks up is given in Figure 5-55.

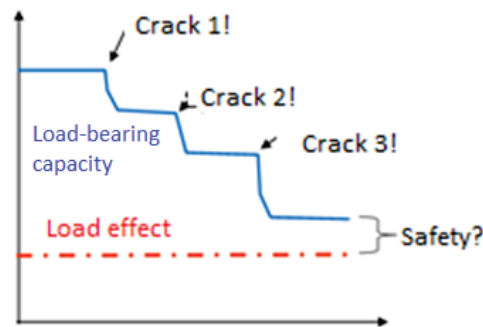


Figure 5-55 Conceptual sketch of how total load-bearing capacity/stability can possibly fall for each new crack that is formed.

Figure 5-56 shows calculated principal tensile stresses with a linear elastic model during the cold period of computational year 1. Calculations with linear elastic models do not give any distinct cracks but give an indication of where high stresses can occur and thus where cracks can occur, at green-yellow-red areas in the figure. In reality, such high stresses cannot be absorbed by the concrete, but instead it cracks in these areas, as the plastic model shows in Figure 5-57.

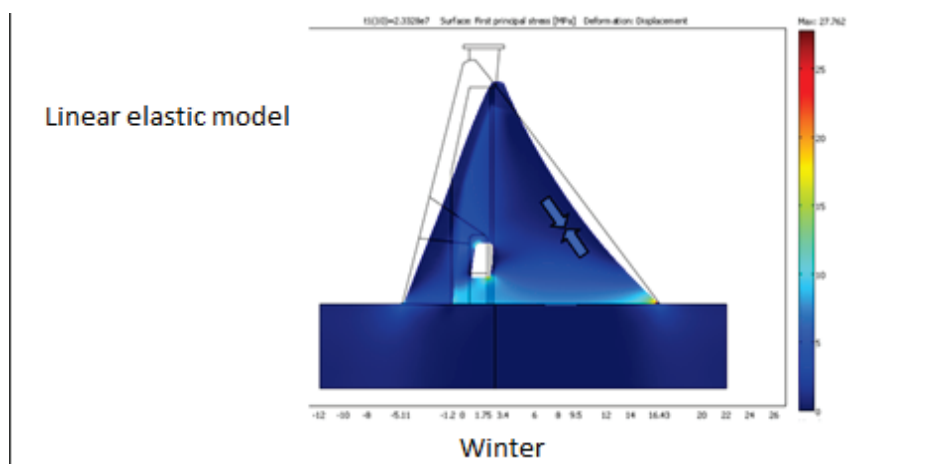


Figure 5-56 Study 2010: Calculation with linear elastic model shows where high stresses occur during a cold winter and an indication of where cracks could possibly occur.

Figure 5-57 (a) shows residual strength f_c when the front slab cracks up during the first summer when the downstream side of the monolith expands and pulls apart the front slab. (b) shows when the pier also cracks up during the winter when it contracts in the cold temperatures and is restrained to the rock and the front slab, with tensile stresses occurring.

Since the model is a so-called “smeared crack model”, it is only available for strains (m/m), not discrete cracks (m). The calculated “cracks” correspond well to the location and distribution of the ones observed on the site as shown in Figure 5-53.

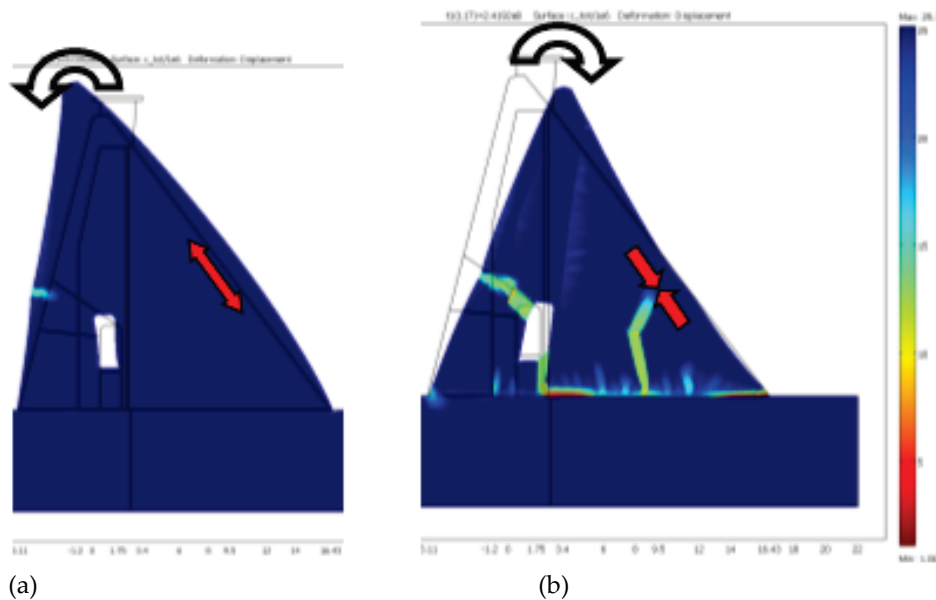


Figure 5-57 Study 2010: Calculated residual strength f_c (c_{tot} MPa) during (a) the first summer and (b) the first winter. In red areas the strength has decreased so much that cracks may have occurred.

Figure 5-58 shows the principal tensile strain exceeding $2 \cdot 10^{-4}$, which here was assumed to be the limit at which concrete cracks. In other words, the figure shows where the cracks computationally occur in the monolith. These correspond very well to the location with the actual observed cracks in the dam.

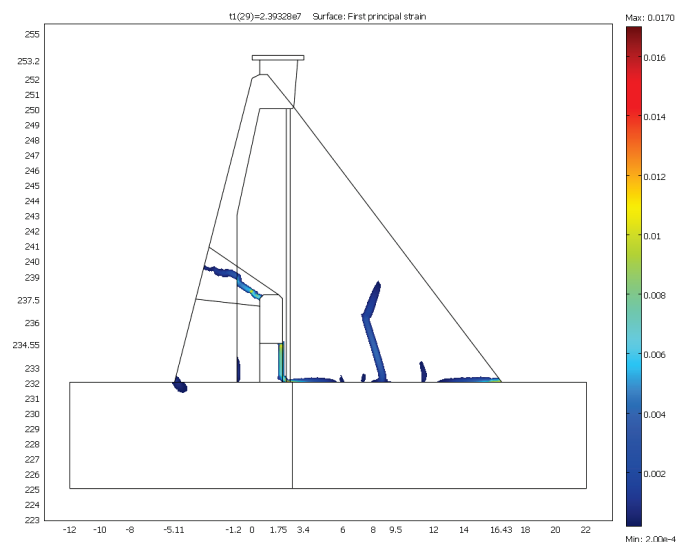


Figure 5-58 Study 2010: Main tensile strain exceeding $2 \cdot 10^{-4}$, which is considered to be the limit at which concrete cracks.

Figure 5-59 shows the calculated curvature of the dam crest in the direction of the current during year 1, with extreme temperatures, during year 2 with normal outdoor temperatures and with the old climate wall, and finally during the years 3-10 with the new climate wall and normal outdoor temperatures. Thanks to the new climate wall, the temperature fluctuations significantly decrease inside the dam and thus the movements and stresses of the monolith are reduced. Although new extreme temperatures would occur, the monolith will not be significantly affected. It should be mentioned that the bridge deck at the top of the dam is still uninsulated, but does not affect the dam monolith below.

For the dam with a new climate wall and between year 3 and year 10 new small plastic deformations occur, which is evidenced by the fact that the crest bends out a little more, $3.64 - 3.47 = 0.17$ mm more, which is negligible in the context.

Early spring 10, the water surface is assumed to be raised for two months, see 1), but this does not cause any major downstream movement in the crest, much less than at the temperature load impact.

During the last winter of year 10, an ice load is assumed to grow from 0 to 300 kN/m, but causes only a negligible deflection 2) in the figure.

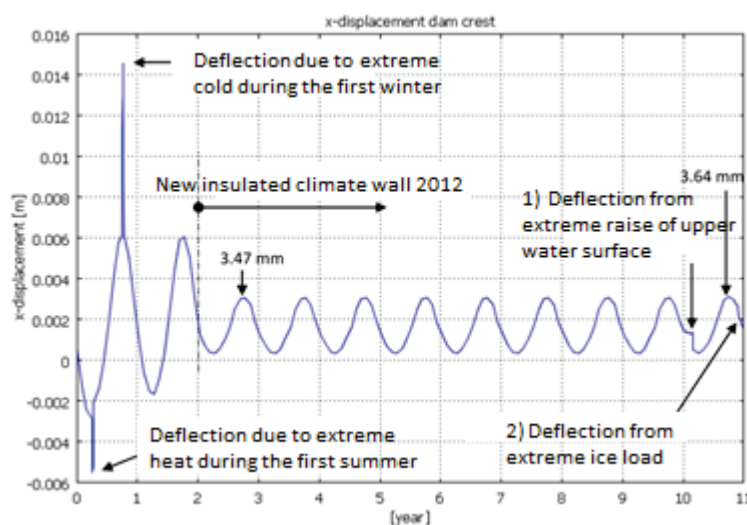


Figure 5-59 Study 2010: Calculated deflection of crest for 11 computational years. (+) values refer to downstream and (-) values refer to upstream direction.

Figure 5-60 shows placement of sensors on monolith 18. Similarly, sensors were also placed on monolith 38, except that no pendulum was placed there.

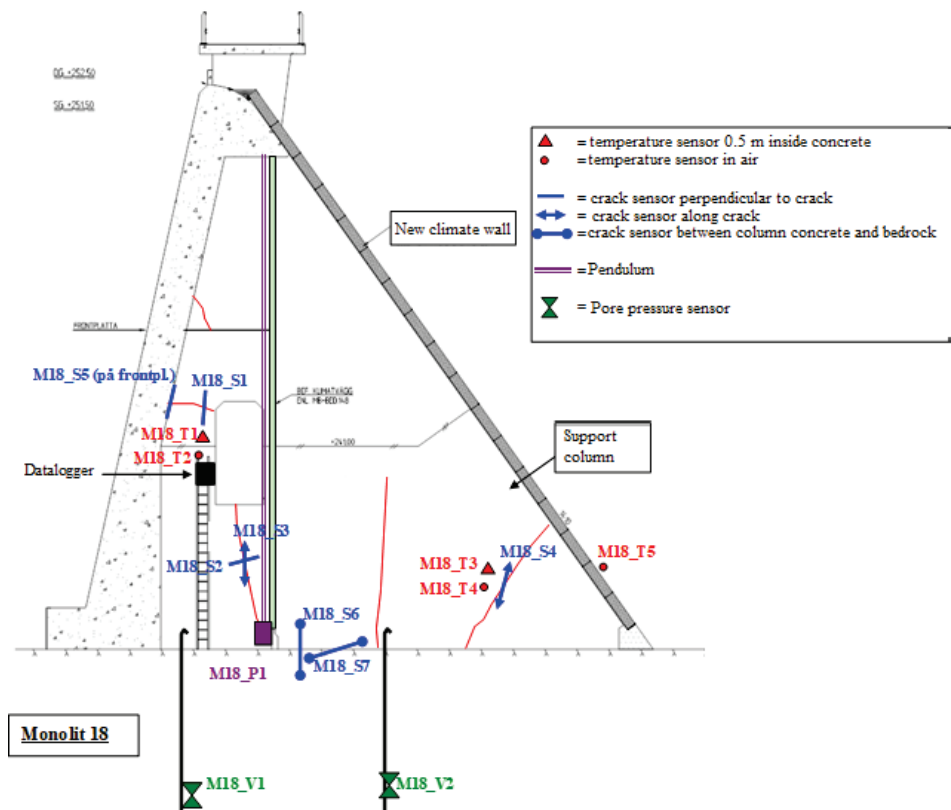


Figure 5-60 Measure: At non-overflow concrete dam monolith 18, new instrumentation with temperature sensors (2 inside the concrete and 2 in the air inside of new climate wall and 1 in the outdoor air), 7 crack sensors, 2 pore pressure sensors in the bedrock beneath the monolith and 1 pendulum at the crest. At non-overflow concrete dam monolith 38, new sensors like the ones at M18, but no pendulum and with 3 temperature sensors in the water at 3 different depths.

5.13 ARCH DAM 2 (TEMP)

5.13.1 Brief description of plant

The plant is located in Västerbotten, Sweden, and was commissioned in 1961. Cracks are found in the arch dam, left-hand arch support and right-hand arch support (spillway pier).

Possible modes of failure are:

- PMF 1: Failure in the arch dam itself
- PMF 2: Failure in the left-hand arch support (transitional monolith or the bedrock)
- PMF 3: Failure in the right-hand arch support (spillway)
- PMF 4: Failure in the bedrock or beneath the arch dam

5.13.2 Assessment

- a) Investigation: Overview mapping of cracks has been done (i) for several rounds over the years. The depth of the cracks in the crest of the arch supports was examined with vertically drilled cores (iii), as also the tensile splitting strength and risk of ASR were measured.
- b) Analyses: A simple mind model (i) indicated that the main cause of the cracks is seasonal thermal stresses but also overload from water pressure. Various, more or less (vi) - (ii) detailed and advanced analyses of the arch dam, the rock below the arch, the rock at the left-hand arch support, the transitional monolith on the left-hand arch support and the right-hand arch support (the spillway) have been carried out over the years, especially between the years 2008 and 2017. Both linear elastic and plastic damage models have shown the great correlation between seasonal temperature variations and the cracking that has been observed.

The crack formation is believed to degrade the arching effect of the arch dam and the ability of the arch support to absorb the loads from the arch dam, whereby the stability of the entire arch dam and the spillway part deteriorates.

- c) Measures: New thermal insulation for the arch dam in a new climate wall and on the dam crest, and a heat-insulating climate wall for the left-hand monolith have been built in 2012 and 2017 respectively (iv). A monitoring system with new dam measuring equipment has been installed in the fall/winter of 2017-18 (iii). New pre-stressed anchors (vi) have been installed in 2017, partly to secure two cleavage cracks in the left-hand arch support monolith and the right-hand arch support (spillway pier) respectively, as well as to secure a vertical crack in the pier and finally to improve the stability of the pier.
- d) Follow-up: Evaluation of measured data should be done, partly in order to obtain general trends, to verify the used calculation model (the FE model), and partly to notify in the case of a serious event.

5.14 BUTTRESS DAM (TEMPERATURE)

5.14.1 Brief description of plant

The dam is located in Sollefteå municipality in Ångermanland, Sweden, and was commissioned in 1954. The dam consists of 81 monoliths of varying sizes, the tallest being 41 m and the lowest being 6 m, see Figure 5-62 and Figure 5-63. All monoliths consist of one front slab with a width of 8 m which has expansion joints in the middle of each compartment between the buttresses. The thickness of the front slab varies from about 1.2 m at the crest and gradually increases towards the bedrock to about 3 m. The buttress has a thickness of 2 m. See Figure 5-64 a).

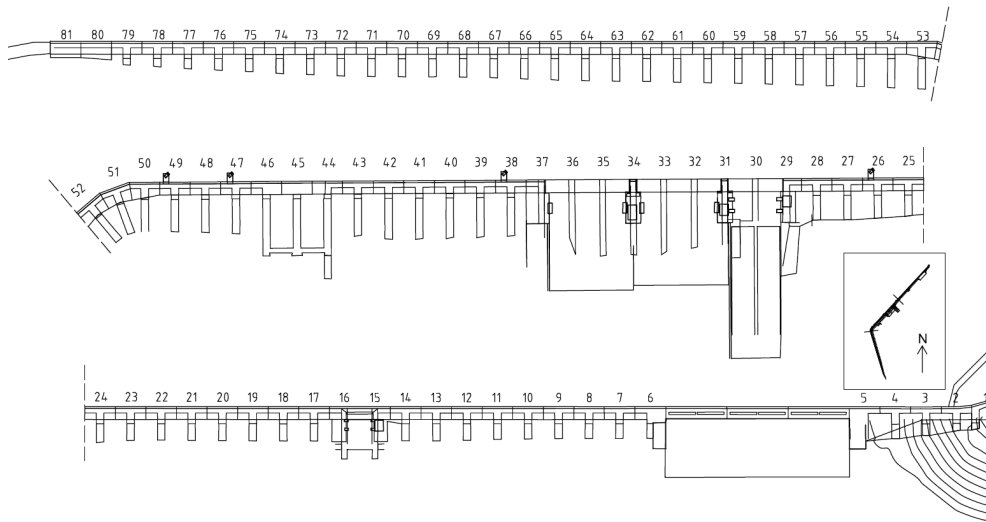


Figure 5-62 Illustration of the studied plant, plan view.

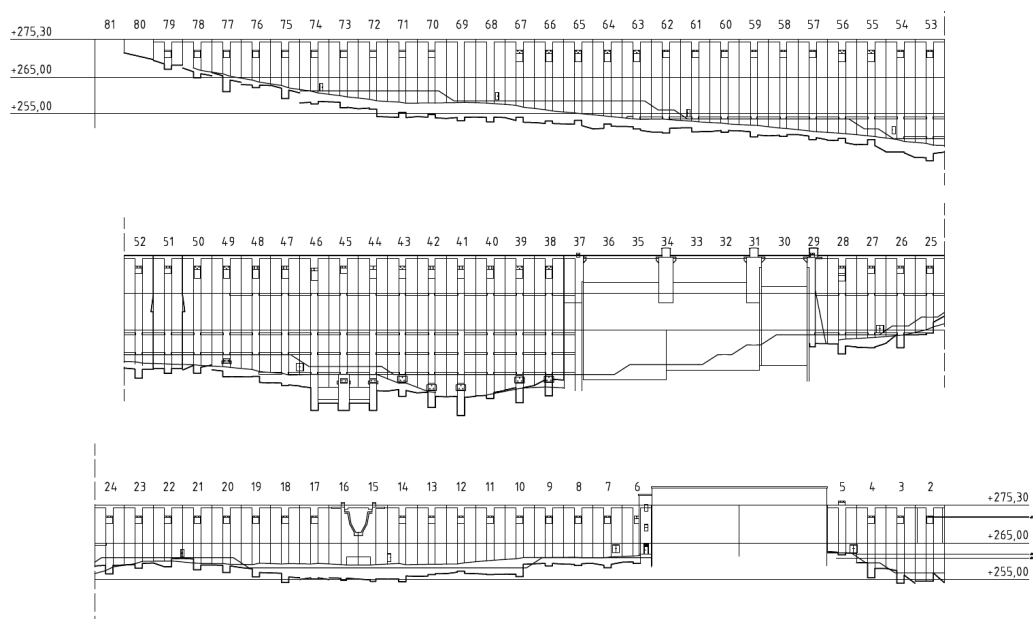
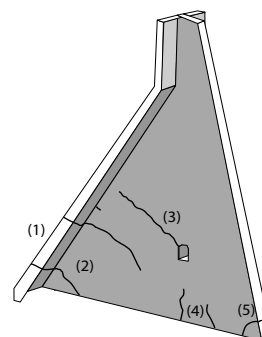


Figure 5-63 Illustration of the studied plant, downstream view.

Soon after the dam was constructed, horizontal cracks were observed in the front slab and oblique cracks propagated down into the buttress, see crack type (1) and (2) in Figure 5-64 b). These cracks increased in width and in number over time and caused some leakage through the front slab and leaching. In addition, frost damage was observed through upstream side of the front slab. In order to prevent further frost damage, an insulating wall was built in the 1990s, see Figure 5-64 a). The insulating wall enclosed an area so that about half the buttress ended up in a controlled climate and other halves were exposed to the surrounding climate. However, this insulating wall exacerbated the crack image in the buttress and cracks of type (3) and (4) were observed a few years later. It is possible that some of these cracks may have existed before the insulating wall was built, but it has inevitably led to increased stresses in the buttress. In addition, cracks near the dam toe have also been discovered after excavation of the lower part of the buttresses.



a)



b)

Figure 5-64 a) Photo of monoliths closest to the spillway, **b)** illustration of typical cracks.

5.14.2 Assessments

The cause of the crack formation in the dam was not clear and a study of this dam was therefore initiated in the middle of the 2000s within the framework of the common R&D program of the power industry within Elforsk. There were also several other facilities that had similar crack formations and this dam was thus used as a case study to understand how the cracks had occurred. However, it was found via this project that the cracks were caused by seasonal variations, where the cracks (1), (2) and (5) had occurred after the dam was constructed and the cracks (3) and (4) occurred after the insulation wall had been built. This was illustrated in [52], see Figure 5-65.

In some cases, the cracks of type (3) and (4) were also interconnected and could potentially lead to an internal overturning mode where the monolith is divided into two parts, see Figure 5-66.

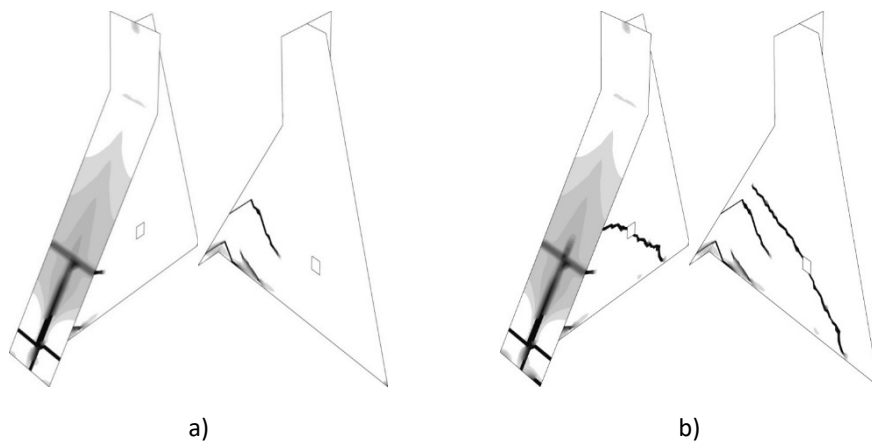


Figure 5-65 Illustration of simulation of cracks in the monolith due to seasonal variations in temperature, a) before the insulation wall, b) after the insulation wall.

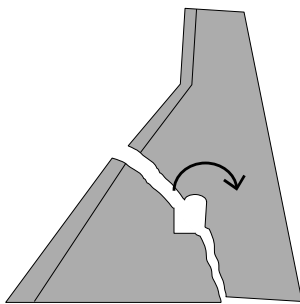


Figure 5-66 Illustration of potential internal overturning mode caused by cracks.

In the subsequent section, the focus is on the reinforcement measures that relate to the reinforcement work to prevent possible internal failure modes and measures to create a better climate for the monoliths.

- a) Investigation: As previously described, cracks were discovered in the front slabs during visual inspection whereupon extensive crack mappings were carried out in 1961, 1989 and 2007. The first two mappings focused on the front slabs, type (1), since the intention was to prevent leakage, leaching and frost damage. Cracks of type (2) are also mapped for the buttresses

and these cracks are also evident from photo documentation. The latest mapping, 2007, also mapped cracks in the buttresses.

- b) Analyses: Many different types of analyses have been carried out to investigate this dam. The conceptual models are based (usually) on the fact that each monolith can be seen as completely independent, where the deformation largely depends on seasonal variations in temperature. Conventional methods of analysis have been applied for e.g. design of reinforcement measures with pre-stressed cables, where classical stability analysis based on internal overturning modes has been applied. Several different advanced numerical models have been applied in order to, inter alia
- Find underlying cause of cracking
 - Sensitivity analyses with impact of the spread in loads and material properties
 - Potential failure modes (PFMA),
 - Impact of reinforcement measures
 - Impact of new insulation wall
 - Instrumentation of monoliths and expected response

In the earlier analyses, simpler scale element models were used to describe the cracks, while as the computer capacity has been evolving, this has to a greater extent been applied 3D solid models. This section presents some of the various models that have been used.

Another big difference between the different models is also whether the purpose is to simulate crack growth or if the purpose is only to analyse how existing cracks affect the behaviour of the dam. If the purpose is to find underlying causes for cracking, smeared constitutive material models based on e.g. fracture mechanics are well suited to describe the crack. However, if cracks have been observed and the purpose is to analyse how these affect dam safety, the methodology with discrete cracks is instead preferred, see Chapter 3.4.7.

One reason why discrete cracks are preferable is that they can describe in a more realistic way how the cracks are opened, but the main reason is that this methodology is considerably much less demanding for computer capacity. This is because analyses can be performed with linear elastic material models for the concrete (if no further cracking occurs) and only a non-linear contact formulation for the cracks.

Since the modelling refers to existing cracks, no resistance to opening of the cracks (tension) is defined, but instead it is defined that the crack can be closed and transmit compressive stresses and has a resistance to shear, with the friction number $\mu = 0.5$ based on Malm (2016). In the Abaqus software, this is defined as

- Normal direction - *Hard contact (allow separation)*
- Tangential direction – *Penalty (friction = 0.5) with elastic slip 0.5 %*

This is also illustrated in Figure 5-67 where the contact condition in normal and tangential direction is illustrated. Figure 5-67 a) illustrates the relationship between compressive forces (p) and crack opening (c), where crack opening can take place without resistance. In Figure 5-67 b), the relation between shear stress in the crack (τ) against compressive force (p) and the fact that elastic slip occurs at sufficiently large strain (γ_{elastic}) are illustrated.

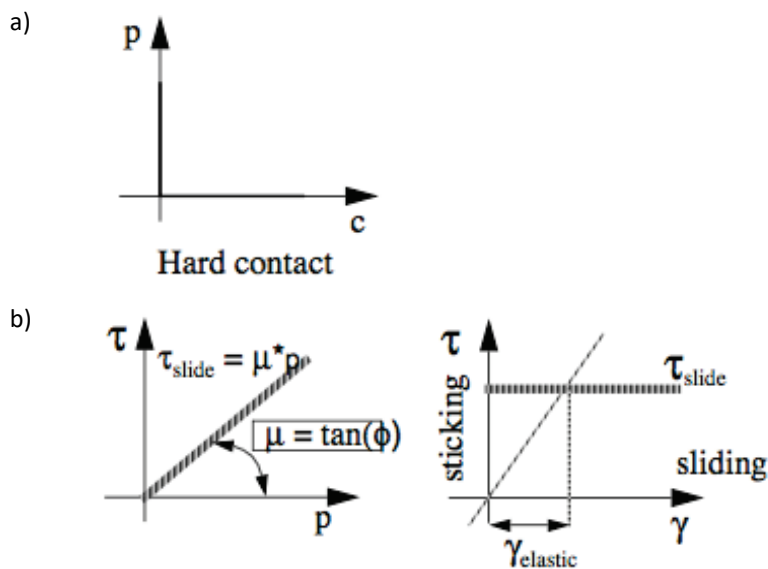


Figure 5-67 Illustration of contact conditions for existing cracks, a) normal direction, b) tangential direction.

A resistance to crack opening and shearing of the crack arises from the reinforcing bars that cross the cracks. In these models, each reinforcing bar is modelled as separate bar elements. The reinforcement is defined as non-linear where the stress-strain curve includes both plastic deformation and failure, see Figure 5-68. Full bond is defined between the concrete and the reinforcement. In reality, some slip of the reinforcement will occur, but this is very difficult to implement on large models with many reinforcing bars. A methodology with complete bond will lead to a more conservative result where the reinforcement stress at the crack becomes slightly higher compared to a case where slip is allowed to occur.

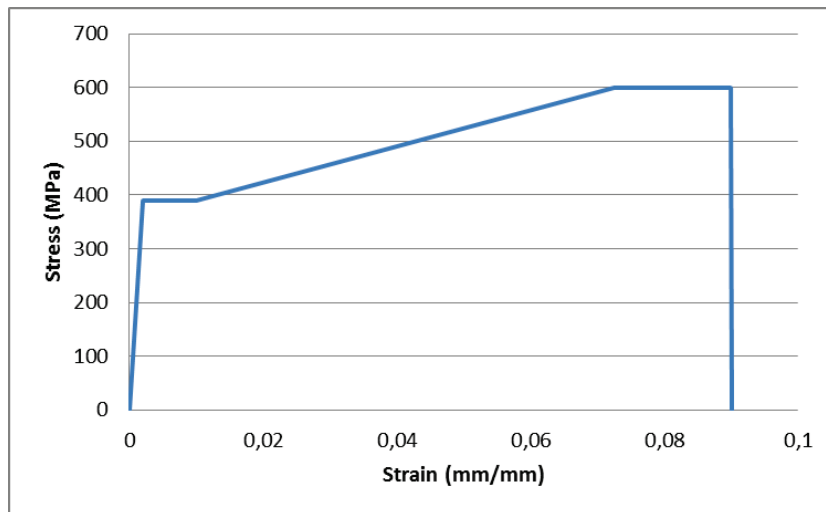


Figure 5-68 Working curve for reinforcement.

Figure 5-69 illustrates the result of one of the models that is showing results at the calculated potential failure mode, where Figure 5-69 a) shows crack opening at failure and Figure 5-69 b) shows reinforcement stresses in all reinforcement bars.

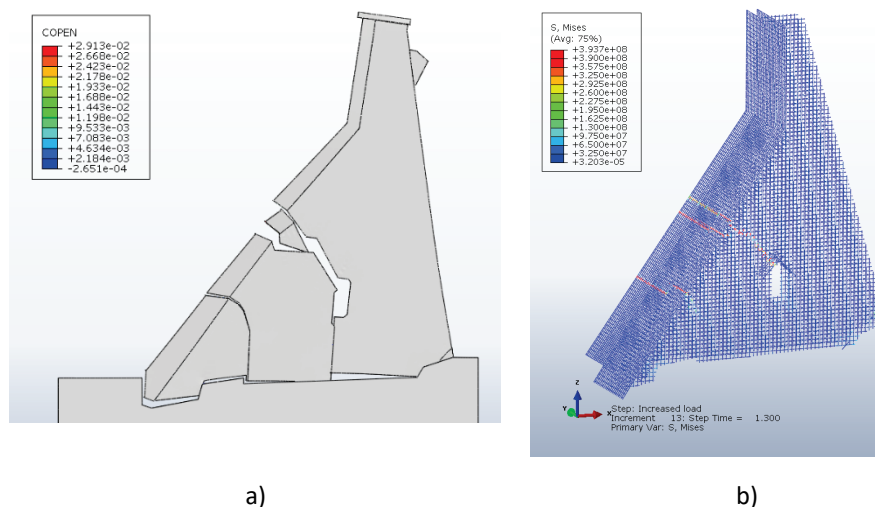


Figure 5-69 Example of result with discrete pre-defined cracks, a) crack opening right before failure (scaling factor 50), b) induced stresses in reinforcement bars (red colour means the yield limit has been reached).

Figure 5-70 illustrates an example from a simulation regarding safety against failure. In the simulation, the driving forces gradually increase, which ultimately leads to dam failure, in accordance with the methodology described in Chapter 3.4.7. The maximum load factor achieved before excessive deformation occurs is the equivalent of the dam safety factor. In the figure, results are presented partly for the case without cracks (solid line), with observed cracks (dashed line) and observed cracks and continued crack propagation (dotted line). The figure clearly shows how cracks affect the dam safety in this case. For this monolith, a lower safety factor was obtained due to cracks and also increased deformations in relation to the case of non-cracked monolith.

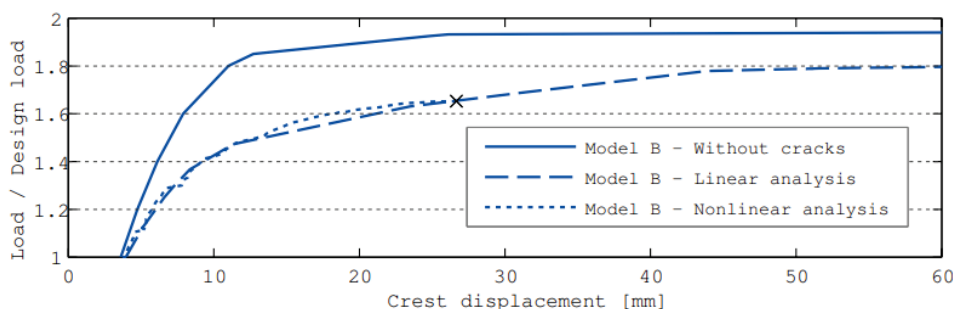


Figure 5-70 Example of simulation of a dam failure scenario. The three cases correspond to; without cracks (solid line), observed cracks (dashed line) and with observed cracks and continued crack propagation (dotted line).

Table 5-2 shows the difference in crest displacement between summer and winter for one of the tallest monoliths based on measurements and various finite elemental analyses. The table also shows how large the insulation wall location is for the size of the crest displacement. As can be seen in the table, the size of the crest displacement increased by more than 140% when the insulating wall was placed so that only half of the buttress is enclosed (i.e. the design introduced in the 1990s). With the new insulation wall, the crest displacement is greatly reduced, and even more so if the enclosed area is heated so that the temperature never falls below + 2 °C during the winter. With the new location of the insulation wall, the displacement is only about 10% of the displacement with the old insulation wall (alternatively about 25% of the case without the insulating wall). Figure 5-71 illustrates the location of the old and the new insulating wall, respectively.

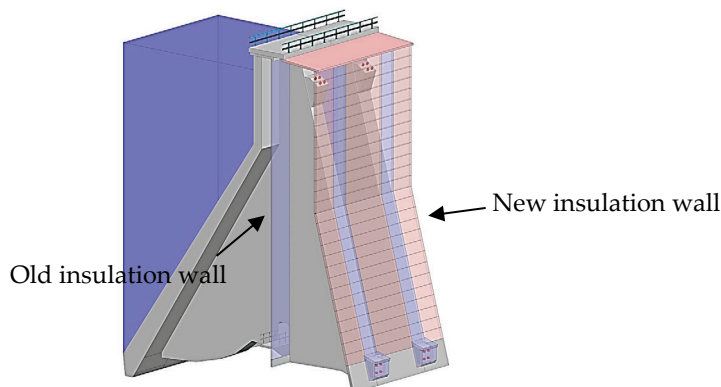


Figure 5-71 Illustration of old (blue) and new (red) insulation wall respectively.

Table 5-2: Measured and calculated difference in crest displacement due to seasonal variations.

	Maximum change in crest displacement ($\Delta_{\max - \min}$) at seasonal variation of temperature		
	Measurements (2007 – 2012)	Previous project at Elforsk	Updated model 2013
Original design (no insulation wall)	-	7.7	9.2
Old insulation wall	20.0	20.8	22.3

New insulation wall (without heating)	-	-	3.6
New insulation wall (heating up to +2 °C)	-	-	2.2

The reason why the earlier models (the project at Energiforsk) gives slightly lower variation in crest displacement compared to the new, more advanced models, is that new models also take into account greater differences in the surrounding climate.

- c) Measures: The monoliths have been partly strengthened with rock-anchored pre-stressed cables. For this, holes were drilled through the buttress and down into the bedrock, where pre-stressed cables of type VSL6-19 were mounted and pre-stressed to 3 MN each. For the tallest monoliths, four pre-stressed cables were installed and for the lower, two were installed. In order to achieve the transport on the dam, a new bridge deck was also built on the dam. In addition to the rock-anchored pre-stressed cables, horizontal pre-stressed cables were also installed at the dam toe, which is intended to prevent movement in the crack called type (5). In Figure 5-72, the pre-stressed cables installed on the monoliths are illustrated.

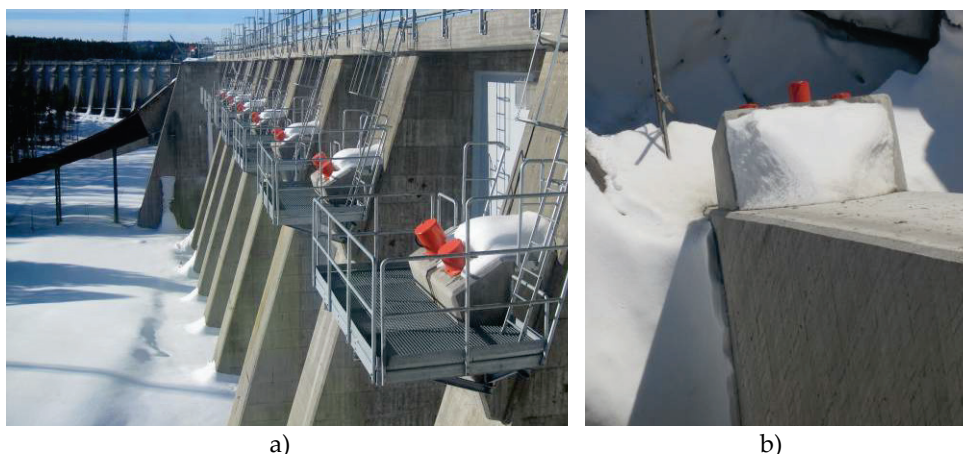


Figure 5-72 Photo of anchor blocks and arrangement of pre-stressed cables, a) rock anchored cables, b) horizontal cables at the dam toe

In addition to this, the old insulation wall was torn down, see Figure 5-73 a), and a new insulation wall was built that encloses the entire monoliths on the downstream side, see Figure 5-73 b).



Figure 5-73 a) Photo with the old insulation wall (Foto: Christer Vredin/Sweco), b) photo with the new insulation wall (Photo: Maria Marklund/Sweco)

Finally, work is underway to expand instrumentation for monitoring on the dam. Within this framework, the various monoliths were classified based on known deficiencies and potential consequences in a failure, which was the basis for the selection of six monoliths that were initially installed with dam monitoring systems [87]. In the dam monitoring system, the various parts are monitored using pendula for crest movement, 1D crack sensors, load cells on pre-stressed cables, 3D sensors that measure relative movement between monoliths, etc.

- d) Follow-up: Special platforms have been installed on the dam to facilitate access and visual inspections. A special program for visual inspection/round-up has been developed in order to detect possible damages and threats to the dam. This program defines both weekly and monthly roundings. In addition, there are also routines for inspections (twice a year), in-depth inspection (at least every three years) and in-depth dam safety evaluation (IDSE) at least every 12 years.

In addition, the resulting measurements from the instrumented dam monoliths will be continuously monitored. For this, simulations have been carried out to define threshold levels on the sensors that are considered detectors of potential failure modes. The threshold levels are initially defined based on simulations of different failure processes, but may be

defined using multilinear regression models for forecasting, such as e.g. HTT (Hydrostatic, Thermal, Time).

5.15 DISCUSSION

Generally, based on the presented reference objects, it can be said that:

- Seasonal temperature variations and thus varying and high concrete stresses are a common cause of cracks in concrete dams, especially in thin and non-heat-insulated parts. Any cracks may have been initiated when cooling during the casting stage, but have subsequently been extended and multiplied over the years. Seasonal temperature variations often provide the most dominant and largest movements and stresses.
- The water pressure against a dam is usually roughly the same over time and therefore does not cause any varying movements and stresses. A properly designed dam should therefore not get any severe cracks from water pressure.
- Ice loads vary over the year but usually constitute a scarcely significant cause of large movements and stresses, partly because they often occur in the late winter when the ambient temperature causes the dam to have small movements and partly because the ice load gives stresses very locally in the front slab only. For small dams, however, the ice load can cause a larger and significant part of the stresses and movements.
- The thinner a concrete structure is in relation to length and height, the greater the risk of cracking. The cracks can then be continuous. This is especially true if any side, e.g. the base of a dam pier, is locked against rock or previous castings. If the structure is thicker, surface cracks are more common.
- Thus, the buttresses (piers) in so-called buttress dams and spillway piers are especially exposed.
- If the buttress dam is heat insulated, the risk for cracking radically decreases. For natural reasons, spillway piers unfortunately cannot be thermally insulated.
- If the cracks are through the cross-section, and divide the structure into smaller parts, e.g. from the rock up to a gate shaft or crest, there is a risk that the stability decreases radically. Remaining force transfer capacity in the cracks is crucial for continued monolithic action.
- Relatively often, there are cracks around the gate shafts of the spillway piers in segmented spillways. Here it can be a combination of cracks caused by cooling during the casting stage, seasonal temperature variations and gate loads.
- There is a risk of frost damage in case of non-heat-insulated front slabs or arch dams. If the slab is relatively water-tight, ice lenses can be formed on the upstream side that can give "pop outs". If the slab is relatively permeable, frost damage can occur further downstream in the cross section. "Curtains" of lime on a downstream side raise the moisture content of the concrete and increase the risk of frost damages.
- Arch dams with a flat arch in relation to their length are more sensitive to cracks in their downstream side, especially if they are small or not at all heat insulated. They can then create bending tensile stresses in the downstream surface that exceed the tensile strength.

- In concrete located in heated parts, e.g. in power houses, cracks can arise from drying shrinkage, especially in cold parts of the country as RH indoors can be very low during the winter season. Such shrinkage is usually a slow process. The lower the RH and the thinner the structures, the quicker the process.

With reference to section 2, the following can be said about the reference objects:

- It is very valuable if there are crack mappings that are updated during the service life of the dam. It can then be seen when cracks occurred and how their development has been. It is however the case that a mapping made from distance and by various surveyors is highly dependent on the accuracy of the implementation. If both sides of a wall are mapped, it can often be concluded that the crack is continuous.
- The crack mapping at the various objects was usually carried out in a simple manner, by making a drawing of the crack propagation. By this, an initial mind model, hypothesis, of the cause and to some extent the effect could often be suggested.. It was often immediately assumed that the cracks had been caused by temperature changes. Later, FEM calculations could usually also be verified against the mapping in the form of high stresses, in linear elastic calculations, or cracks, in non-linear calculations, being found in the same places and with the same appearance as in reality.
- Where there was a more "fine" mesh of cracks, e.g. crazing, the first hypothesis was often that it was caused by frost and/or ASR. In such cases, it was valuable to take samples to be tested in the laboratory for verification of these damages.
- Since cracks are almost always due to a tensile stress having exceeded, or will exceed, the tensile strength, the tensile splitting strength of drilled cores is often an important test feature.
- Frost resistance and ASR risk can preferably be tested from the same cores at the same time. Sometimes also the degree of leaching can be tested if the concrete is obviously permeated by water, or, as with the front slabs of the buttress dams, the degree of leaching in the upstream side of the slabs.

With reference to section 3 the following can be said:

Methods of analysis:

- For the initial visual inspection, it was often assumed that the cracks were caused by restraint forces, e.g. seasonal temperature variations causing relatively large expansion and contraction of the concrete, but restraint from bedrock or other concrete parts, or from different layers in thick cross-sections, had caused large tensile stresses, exceeding the tensile strength.
- In order to assess the remaining safety of the objects, an analytical calculation of the shear stress capacity according to BBK04 [6], section 3.11, was often carried out, compared to FEM calculated shear stresses in the same section as where the cracks were present. If the capacity exceeded the shear stresses, it was considered that the structure behaved monolithically and thus it could be verified with regard to stability with the assumption of rigid body.
- In the reference objects, the FEM calculations included self-weight, water pressure, ice load and seasonal temperature variations. The material models were linear-elastic or non-linear.

- Linear elastic calculations are much easier and faster to perform, but as a result sometimes give a misleading stress image. If the stresses exceed the strength, usually the tensile strength, the model does not take the equalization and redistribution of cross-sectional forces that take place in reality, due to micro or macro cracking. The stresses are therefore often unreasonably high along boundaries, corners, load attacks or where the stresses are high for other reasons.
- Non-linear material models in the projects just mentioned and with the used FE models were often relatively difficult to get to converge in a computational manner. This especially for 3D models or large differences that there was for width/height compared to the thickness of the calculated structure. Nowadays, there are more effective models, see section 3. It should be added that the fracture energy G_f was set relatively low, about 120 Nm/m^2 , instead of up to 200-300 as stated in Table 3-2, which made it a little harder to get the calculations to converge. However, the non-linear calculations for the reported objects often provided such a good match with the actual crack appearance that the model could all be assumed to be valid and reflect the mode of action and the cause of the crack.
- Almost always the FEM calculations showed that it was temperature variations that caused the cracks, which, incidentally, was already adopted in the mind model in place as mentioned above. The cracks may have been initiated to some extent already in the cooling stage of the casting stage, but in the just-mentioned objects no calculations were made for the casting stage.
- Any other direct quantitative estimate, in addition to the above-mentioned comparison between calculated stresses and shear capacity according to BBK, of residual safety of the cracked dams could usually not be done, just a qualitative one, e.g. that calculations and visual inspection showed a crack going through the cross-section and from the rock to the crest/side, whereby the safety was then more subjectively assessed.
- If the purpose is mainly to determine the cause of cracking, linear elastic, or more preferably non-linear, FEM calculations are quite excellent. Complex geometries, load cases and phenomena can be studied in a nuanced way.
- If the purpose (in addition) is to determine a structural safety, there is currently no accepted method specified in the current RIDAS [3], [4], to do this with FE models that are suitable for concrete dams. However, a method that is relatively well suited is presented in chapter 3.5.5.
- In some simple FE models, e.g. for distinct slabs, beams and piers, linear elastic stresses and moments can be calculated and compared analytically to acceptance criteria according to norms and standards. Partial coefficients are then applied to the loads or the load effects and the cross-sectional forces are compared to the design load-bearing capacity according to standards, including partial coefficients.
- FEM fits perfectly with stability checks. Then the monolith is placed on two lines where the resulting horizontal and vertical forces are evaluated. The fact that the monolith is deformed is ignored due to the fact that the supports on the lines make the monolith statically determined. For complex geometries and loads, it can be easier and safer to count on FE models than by hand.

- But for most types of dams, such as buttress dams, arch dams, spillway piers, gravity dams, etc., which have cracks and which crack in the calculations, there is no pronounced method or criterion in RIDAS [3], [4], to quantitatively determine the safety with respect to the impact of the cracks.

Simulation of different phenomena:

- The calculation models in the reported cases did not include the casting stage, creep effects or degradation from e.g. corrosion, leaching, ASR or frost. However, in a few cases it was obvious that cracks/crazing were largely caused by ASR and frost. But the damage process itself was not modelled, only the effect of the cracks with some assumptions about the state of the cracks.
- If the crack formation was from frost damage or ASR, no calculation was made for this, but cause and effect was analysed by tests, see above.
- Fatigue effects may well have partly led to cracks occurring more easily in the examples shown. In concrete, it is considered (BBK 04) that there is a risk of fatigue at a number of stress cycles exceeding 500. Many dams are 60-70 years old and have thus been exposed to 60-70 summers and winters. But, in addition to that, the temperature often varies a lot monthly, weekly and perhaps even daily, depending on various factors. E.g. during sunny spring-winter days, temperatures can vary a lot, especially for structures facing the sun. Thus, the number of stress cycles may well have exceeded 500 during the heretofore service life of the structure. In cracks, depending on how the bond is assumed between the concrete and the reinforcement, a large stress width may arise for the reinforcement. With high bond between reinforcement and concrete, larger stresses will be obtained in the reinforcement. At the number of stress cycles exceeding about 10,000 (BBK 04), the strength is considered to decrease for the reinforcement. If the bond drops from the concrete closest to the reinforcement bars starting to crumble then the force-absorbing length L increases and the strain in the reinforcement drops because then the force is smeared out on a longer distance ($\varepsilon = \Delta L / L$). Fatigue can therefore be a possible partial explanation for the occurrence or aggravation of cracking in concrete. However, the fact that the reinforcement would eventually break in the crack is more uncertain, it is very much dependent on how fixed the reinforcement is to the concrete.

Modelling aspects:

- In the non-linear material models, a decrease in the tensile strength and E-modulus of the concrete was used, as well as a slip between concrete and reinforcement according to Appendix F. Since there were no decisive compressive stresses in the structures in question, the material model was simplified to not include any decrease in compressive strength or in the E-modulus for compression.
- In the calculated objects, the rock had no decisive significance for the crack formation calculated with the non-linear material model. If the rock was included in both the temperature model and in the mechanical model, the rock moved to a certain extent along with the concrete, and the rock did not give as large restraint as if the boundary of the concrete had instead been firmly restrained and thereby the stresses and the crack formation dropped slightly

the contact zone between the concrete and the rock, but this did not have a decisive impact on the crack formation further up in the concrete.

- The non-linear material models used in the examples shown were more or less their own assembled models, based on the literature. In later releases of the used FEM program (Comsol), non-linear material models are available. Other FEM programs, e.g. Abaqus, Diana, etc., have non-linear material models included. This should result in a more verified modelling methodology and with a better solver.

Material data:

- In virtually all calculations, the properties of the concrete were assumed based on literature and were therefore not measured through testing. In a few cases the density and tensile splitting strength were measured.

Validation of calculation model:

- Calculation variables were generally based on the literature.
- Some sensitivity analyses were made for some of the calculation variables.
- The plausibility of calculated stresses as well as elastic and plastic strains in concrete and reinforcement were checked at certain critical points.
- In some cases, calculated, expected values have been compared with measured values in the same spots as in the model. This is generally preferred in order to verify the validity of a calculation model.
- Crack appearance was checked against the cracks of reality.

Acceptance criteria:

- With credible calculation variables and a good match between calculated high tensile stresses or calculated cracks and the cracks in reality, the *cause* of the cracks was often accepted.
- If in reality and in the calculations it emerged that the monolith considered, despite the cracks, most likely still acted as a monolith, the stability of the monolith assumed as a uncracked, rigid body was calculated, compare step 1 in Figure 3-29.
- If the cracks more clearly divided the monolith into smaller parts, the criterion was set in two different ways: If the cracks were of a smaller extent and width, calculated shear stresses were compared to a shear capacity calculated according to BBK04 [6] section 3.11. It was often also recommended to construct a heat insulating wall and install instrumentation. If the cracks were of a greater extent and wide, a reinforcement was often also recommended based on a qualitative, more subjective assessment.

With reference to section 4, the following can be said:

- In the studied objects, no emergency measures were deemed necessary.
- It was often recommended that a fixed monitoring in the form of instrumentation of certain important parameters should be set up on the dam, such as temperatures, pore pressure and movements. E.g. measurement of temperatures in water, concrete, in outdoor air and, where suitable, behind climate walls, as well as measurement of crack width changes and crest movements (pendulum).
- It was often recommended to set up a heat-insulating wall that would enclose as much of the concrete as possible, in order to obtain a more even temperature climate and not get freezing temperatures. If it is chosen to set up heat-insulated walls, a careful analysis should precede, so that it does not exacerbate the situation. There are examples of where the wall has only partly covered a buttress in a buttress dam, whereby unfortunate temperature gradients have been created in the buttress.
- In one case, section 5.8, damaged concrete was restored through a repair by removal and re-casting of concrete.
- In several cases, reinforcement was proposed, usually with pre-stressed anchors, to secure the cracks and sometimes at the same time raise the stability.

With reference to RIDAS [3], [4], the following can be said:

- In the RIDAS TV section 7.3.2.1, most of the loads that may act on a concrete dam are mentioned. However, it is only briefly stated that "consideration must be given to the restraint forces that may arise due to temperature variations and shrinkage of the material". There is no more detailed guidance on which variables should be used, e.g. characteristic temperatures or method and variables for calculating drying shrinkage. Considering the great impact on cracks that the restraint forces often have for dams, see for example in the reference projects, such forces should be highlighted and guided for in RIDAS [3], [4].

- Nowadays, in the latest version of section 7.3.2.3 (2017) there is guidance for cross-sectional design with the partial coefficient method according to the Eurocodes and load reduction factor, as well as for temperature changes. However, there is no guidance regarding characteristic values, load cases and methodology regarding temperature calculations. There is some guidance in [57].
- In RIDAS TV 7.3.2.4 there are conditions for simpler stability calculations with rigid bodies specified for load cases according to section 7.3.2.2.1. On the other hand, there is no direct guidance on failure conditions for complex structures such as concrete dams. Dams are often relatively special regarding the structural way of action and therefore it would have been valuable to get guidance on e.g.
 - × Suitable static models, e.g. for a buttress dam monolith, spillway pier, gravity dam or arch dam. However, see section 3 of this document.
 - × Suitable material models, e.g. linear or non-linear material models. However, see section 3 of this document.
 - × Requirements in ultimate and service limit state. For example, when does a "failure" occur in a dam? Is it when linear elastic stresses exceed the strength of the concrete? Is it when "too large" cracks occur with non-linear calculations? Is it when the reinforcement begins to yield to a lesser or greater extent? Is it if a crack divides a monolith in a way that is critical to the stability? See also section 3.9.
- RIDAS TV 7.3.3 deals with "constructive design". Here, there is no general instruction that concrete dams should be constructed with as uniform a temperature and humidity environment as possible. Degrees of frost should be avoided if possible. More specifically, it can be stated that heat-insulating climate walls should be built around concrete structures where possible.

With reference to the CEATI report [1] the following can be said:

Figure 5-74 shows the principle of the temperature history of a concrete structure.

- Most of the examples in this section deal with, i.e. temperatures during the operating time of the structure.
- In [1] no specific guidance is given on how to do a more advanced analysis, e.g. with non-linear FE models according to section 3 and practical cases in this section 5, of how concrete dams crack in the operating stage.

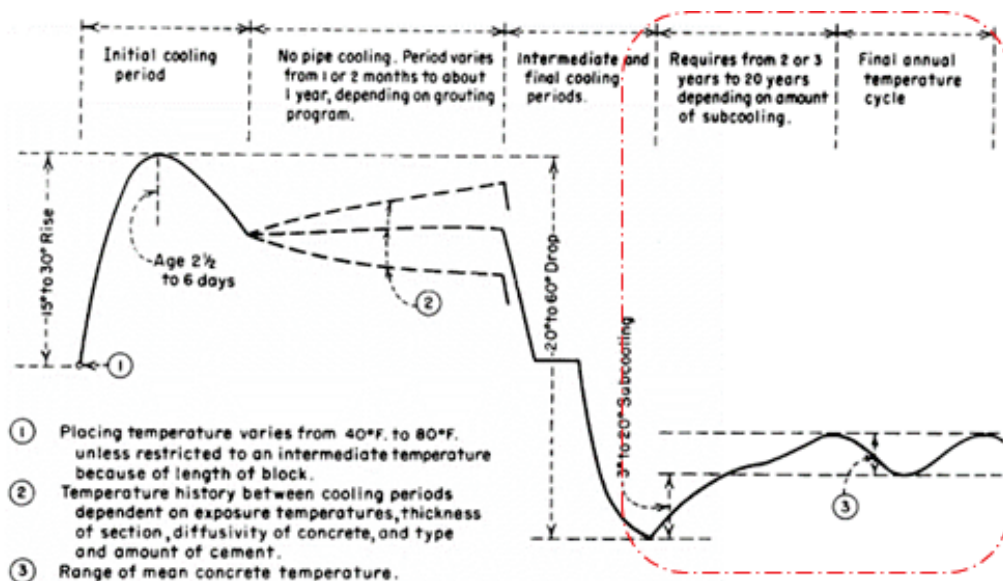


Figure 4-6. An example temperature time history of concrete from USBR Monograph 34 [6].

Figure 5-74 Conceptual image of the temperature history of a concrete structure (Tarbox & Charlwood, 2014). Red dot-dashed line = studied time for the examples in this section.

With reference to failure modes, the following can be said:

- Figure 5-75 shows a possible conceptual event tree for how dams, e.g. some of them in this section, hypothetically may fail. At event A, the dam is flooded due to insufficient capacity or defects in the spillways. Events D and E can then also occur. Even if event A, or B, does not occur, the dam can still fail due to C-E. Failure due to low stability can be an end event in cracked dams. Depending on how "brittle" the dam is, this can occur at different speeds. E.g. at a slender, damaged arch dam with an asymmetrical load, or a slender, poorly reinforced buttress dam that is continuously cracked, the failure may happen relatively quickly. The more reinforced the dam is and the less sensitive it is to non-linear tendencies, the "tougher" the failure becomes and as a result there is more time to discover and fix the damage.
- The examples in this report deal primarily with failure mode E and a little bit with C regarding leaching.

A = **External erosion** due to overflow of dam crest due to insufficient spillway capacity, malfunctioning of the discharge system or clogging of spillway. Can apply to all kinds of dams but is most critical for earthfill dams.

B = **External erosion** due to discharge. Can occur on both the upstream and downstream sides. Can apply to all kinds of dams but is most critical for earthfill dams.

C = **Internal erosion**. Most critical for embankment dams. For concrete dams it can be caused by leaching but is a slow process.

D = Low **stability** and instability in embankment dams and foundations. Can be a case of incorrect design, new requirements, damages, new major loads or a combination.

E = Low **stability** and instability in concrete dam/spillway. May be caused by incorrect design, new requirements, damages, new major loads or a combination.

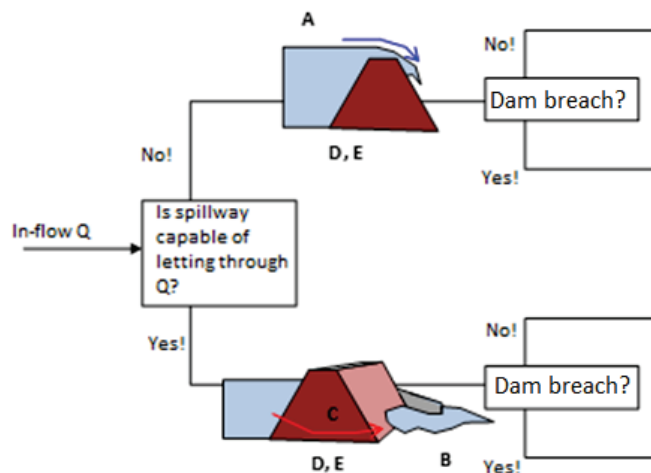


Figure 5-75 Conceptual figure (event tree) of a hypothetical dam failure.

Figure 5-76 shows examples on why failure may occur in concrete dams.

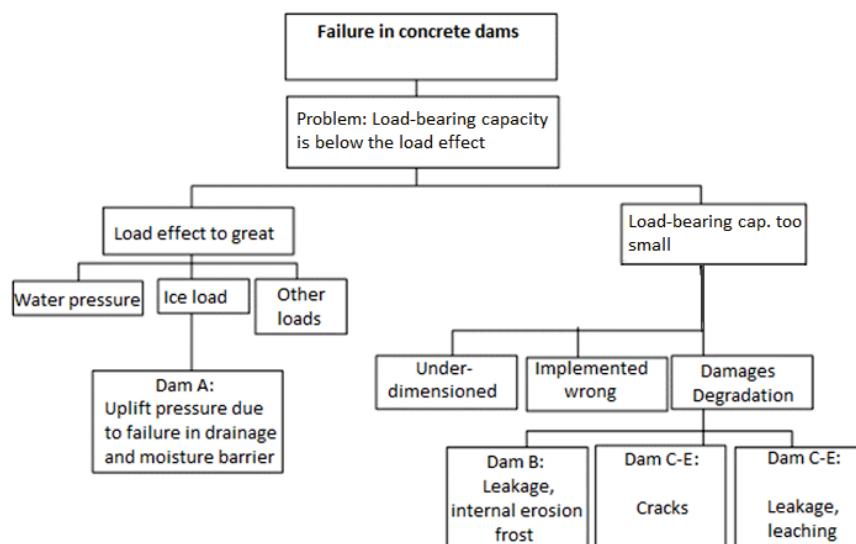


Figure 5-76 Conceptual figure for potential failure modes (PFM). The dams showed in this section have all been affected by "Cracks".

5.15.1 Conclusion of discussion

- Seasonal, or shorter, temperature variations and thus stresses in the concrete were very often assessed to be the main cause of cracks in the objects shown.
- FEM and especially since non-linear FE analyses proved to be an excellent method for finding the cause of the cracks. Linear FE analyses are considerably simpler and faster to execute numerically, but often give unrealistically high stresses at point loads, corners, etc.
- There are no common industry guidelines and established methods/criteria to ensure the structural safety of a cracked dam calculated with non-linear FE models.
- The safety is often estimated with simpler analytical models, or with a mixture where stresses are calculated with FEM which are then compared to analytical acceptance criteria according to BBK or the Eurocodes. A good alternative is also described in chapter 3.5.5.

6 Referenses

- [1] Tarbox G.S., Charlwood R. (2014), "Investigating the structural safety of cracked concrete dams", CEATI report No. T122700-0226, April 2014.
- [2] Bernstone, C. "Utvärdering av befintliga metoder för oförstörande provning av betong i kraftanläggningar". Elforsk, rapport nr. 99:45. (In Swedish)
- [3] RIDAS (2016). "RIDAS 2016 – Kraftföretagens riktlinjer för dammsäkerhet, kapitel 1-3". Energiföretagen Sverige. (In Swedish)
- [4] RIDAS (2012). "RIDAS – Kraftföretagens riktlinjer för dammsäkerhet". Energiföretagen Sverige, kapitel 4-8. (In Swedish)
- [5] Trafikverket (2015). "*BaTMan - Handbok för inspektion av byggnadsverk*". <https://batmanbibliotek.trafikverket.se/sok/>. (In Swedish)
- [6] BBK 04, (1994), "Boverkets handbok om betongkonstruktioner". Boverket. (In Swedish)
- [7] SS-EN 206:2013+A1:2016, (2016): "Betong – Fordringar, egenskaper, tillverkning och överensstämmelse", SIS. (In Swedish)
- [8] Concrete Repair Manual, (2003), Second edition, volume 1, Published jointly by: ACI international, BRE, International concrete repair institute and concrete society.
- [9] Concrete Society, (2010): "Non-structural cracks in concrete, A concrete Society Report", Technical Report No. 22 – Fourth Edition, CCIP-048, December 2010.
- [10] SS-EN 1504-9:2008, (2010): "Betongkonstruktioner – Produkter och system för skydd och reparation – Del 9: Allmänna principer för val av produkter och system.", SIS. (In Swedish)
- [11] Hassanzadeh, M., Westberg Wilde, M. (2016), "Inventering av spricktyper i vattenkraftens betongkonstruktioner", Rapport 2016:257, Energiforsk, www.energiforsk.se. (In Swedish)
- [12] Westberg Wilde, M., Janz, M., Ekström, T. (2016), "Sprickors påverkan på betongdammars säkerhet", Rapport 2016:310, Energiforsk, www.energiforsk.se. (In Swedish)
- [13] Rombén, L. (1994), "Kemiskt angrepp", Kapitel 23 i Betonghandboken – Material, utgåva 2, AB Svensk Byggtjänst och Cementa AB, 1994. (In Swedish)
- [14] ICOLD, (1997), "Concrete Dams – Control and treatment of cracks, Review and case histories", Bulletin 107, <http://www.icold-cigb.org/home.asp>.
- [15] Nordtec Instrument (2018), "Fakta mätteknik", <http://www.nordtec.se/matteknik>. (In Swedish)

- [16] Johansson, P. (2016). Fuktmätning i betong med lågt vct, steg 3. Sweden: SBUF, ID: 12941 & 13085. (In Swedish)
- [17] RBK - Rådet för byggkompetens. (2017). RBK. Hämtat från <http://www.rbk.nu/>. (In Swedish)
- [18] Oxfall, M. (2016). "Climatic conditions inside nuclear reactor containments: Evaluation of moisture condition in the concrete within reactor containments and interaction with the ambient compartments", PhD Thesis, TVBM-1035, Division of Building Materials, Lund University of Technology.
- [19] Fagerlund, G. (1992) "Betongkonstruktioners Beständighet – En översikt". Cementa AB, Danderyd. (In Swedish)
- [20] Rosenqvist, M. (2013) "Moisture conditions and frost resistance of concrete in hydraulic structures". Rep. TVBM-3173, Division of Building Materials, Lund University.
- [21] Rosenqvist, M. (2016) "Frost-induced deterioration of concrete in hydraulic structures Interactions between water absorption, leaching and frost action". Rep. TVBM-1036, Division of Building Materials, Lund University.
- [22] SS 137244:2005 (2005) "Betongprovning – Hårdnad betong – Avflagning vid frysning". Fastställd 2005-02-18, Utgåva 4, SIS. (In Swedish)
- [23] Nordström, E., Rosenqvist, M., Sjödin, G., Hautakoski, M., (2013). "Field investigation on the risk for ASR when using potentially reactive aggregates and low alkali-cements – Results after 50 years in Sweden." ICOLD 2013, International Symposium – Seattle USA.
- [24] Somerville, G. (2001). "CONTECVET – A validated users manual for assessing the residual service life of concrete structures, Manual for assessing concrete structures affected by ASR", EC Innovation Programme IN309021.
- [25] Dyer, T. (2014). "Concrete Durability.", CRC Press, Tylor & Francis Group.
- [26] Werner, D., Gardei, A., Simon, S., Meng, B. (2015). "Microscopic investigation of building materials affected by alkali-silica reaction." In proceedings of 15th Euroseminar on Microscopy Applied to Building Materials, 17-19 June 2015, Delft, The Netherlands.
- [27] RILEM STAR Report (2013) "Guide to Diagnosis and Appraisal of AAR Damage to Concrete in Structures – Part 1 Diagnosis (AAR 6.1)". Springer ISBN 978-94-007-6566-5.
- [28] LCPC Techniques et méthodes, (1997). "Détermination de l'indice de fissuration d'un parement de béton." Methode d'essai LPC No. 47, Ministère de l'Équipement, du Logement, des Transports et du Tourisme.
- [29] Fagerlund, G.(2000). "Leaching of concrete, The leaching process. Extrapolation of deterioration. Effect on the structural stability", Report TVBM-3091, Division of Building Materials, Lund Institute of Technology, Lund, Sweden.

- [30] Petersons, N. (1994), "Sprickor", Kapitel 19 i "Betonghandboken – Material", utgåva 2, AB Svensk Byggtjänst och Cements AB. (In Swedish)
- [31] Rosenqvist, M., (2017). "Bestämning av frisk och urlakad betongs kemiska sammansättning", Energiforsk, Rapport 2017:251, www.energiforsk.se. (In Swedish)
- [32] Eurocode 2 (2008): Design of concrete structures. Part 1-1: General rules and rules for buildings. SS EN 1992-1-1:2005, SIS
- [33] Mattsson, E., Kucera, V.,(2009). "Elektrokemi och korrosionslära.", Upplaga 3, Swerea/KIMAB, ISBN: 978-91-633-4918-8. (In Swedish)
- [34] Betongrapport nr 12 (2007). "Vägledning för livslängdsdimensionering av betongkonstruktioner". Svenska Betongföreningen, ISBN 91-973445-8-3. (In Swedish)
- [35] Camitz, G. (2011). "Korrosionsskydd av stål i betongkonstruktioner – Handbok.", Swerea/KIMAB ISBN: 978-91-633-7956-7. (In Swedish)
- [36] Grönholm, R. (2000). "Utvärdering av borrkärnor från betongkonstruktioner". Rapport 01:01. Elforsk, Stockholm. www.energiforsk.se. (In Swedish)
- [37] SS-EN 12504-1:2009, "Provning av betong i färdiga konstruktioner – Del 1: Borrkärnor – Uttag, undersökning och tryckprovning", SIS, Stockholm, Sweden. (In Swedish)
- [38] Eriksson, M., Stille, H., (2005). "Cementinjektering i hårt berg". SveBeFo, Rapport K22. ISBN 91-631-6632-1. (In Swedish)
- [39] SS-EN 12715:2000, "Utförande av geokonstruktioner – Injektering". SIS, Stockholm, Sweden. (In Swedish)
- [40] Malm, R. (2016). "Guideline for FE analyses of concrete dams.", Energiforsk report 2016-270- Retrieved from <https://energiforskmedia.blob.core.windows.net/media/21281/guideline-for-fe-analyses-of-concrete-dams-energiforskrapport-2016-270.pdf>
- [41] Ekström T., Gustafsson P-J., Hallgren M., Hassanzadeh M., Malm R., Nilsson L-O., Thelandersson S. (2016) "Granskning av beräkningar i betongkonstruktioner – Vägledning för granskning av datorberäkningar av mekanik och transportprocesser". Energiforskrapport 2016:259. <https://energiforskmedia.blob.core.windows.net/media/21310/granskning-av-berakningar-i-betongkonstruktioner-energiforskrapport-2016-259.pdf> (In Swedish)
- [42] RIDAS TV (2017), Avsnitt 7.3, Betongdammar, Tillämpningsvägledning, Energiföretagen Sverige, 2017-03-21. (In Swedish)
- [43] Vecchio, F., Collins, M. (1986). "The Modified Compression Field Theory for Reinforced Concrete Elements Subjected to Shear". Journal of the American Concrete Institute, Vol 83, No 2, 219-231.

- [44] Malm, R. (2006): "Shear cracks in concrete structures subjected to in-plane stresses". Licentiate Thesis, Bulletin 88. Department of Civil and Architectural Engineering, KTH Royal Institute of Technology, Stockholm, Sweden.
- [45] Westberg Wilde, M., Johansson, F. (2016) "Probabilistic model code for concrete dams – Part I, Part II, Part III and example". Energiforskrappport 2016:292.
<https://energiforskmedia.blob.core.windows.net/media/21554/probabilistic-model-code-for-concrete-dams-energiforskrappport-2016-292.pdf>
- [46] Hellgren, R., Malm, R., Nordström, E. (2018) "Modeller för övervakning av betongdammar". Energiforskrappport 2018:xxx (in press) (In Swedish)
- [47] Magnusson J (2007) Structural concrete elements subjected to air blast loading. Lic. thesis, KTH Royal Institute of Technology. <http://kth.diva-portal.org/smash/get/diva2:12322/FULLTEXT01.pdf>
- [48] Goldgruber, M. (2015). "Non-linear Seismic Modelling of Concrete Dams". PhD Thesis, Graz Technical University
- [49] Enzell, J. & Tollsten, M. (2017) "Thermal cracking of a concrete arch dam due to seasonal temperature variations", KTH Royal Institute of Technology, <http://kth.diva-portal.org/smash/get/diva2:1114901/FULLTEXT01.pdf>
- [50] Gustafsson A, Johansson F., Krounis Guerro A. (2010) Stabilitetsanalys av Krok-strömmens valvdamm. In: Bergmekanikdagen, BeFo Stiftelsen Bergteknisk forskning, Mars, 2010, pp 133 – 148. (In Swedish)
- [51] Zuber, B., Marchand, J. (2004) "Predicting the volume instability of hydrated cement systems upon freezing using poro-mechanics and local phase equilibria". Material and structures, concrete science and engineering, vol. 37, May 2004, pp 257 – 270.
- [52] Malm, R., Johansson, F., Hellgren, R., Rios Bayona, F. (2017) "Load capacity of grouted rock bolts due to degradation.", Energiforskrappport 2017:374.
<https://energiforskmedia.blob.core.windows.net/media/22595/load-capacity-of-grouted-rock-bolts-due-to-degradation-energiforskrappport-2017-374.pdf>
- [53] Malm, R. (2009): "Predicting shear type crack initiation and growth in concrete with non-linear finite element method", PhD Thesis, Bulletin 97. Department of Civil and Architectural Engineering, KTH Royal Institute of Technology, Stockholm, Sweden.
- [54] Malm, R., Hassanzadeh, M., & Hellgren, R. (2018). "Proceedings of the 14th ICOLD International Benchmark Workshop on Numerical Analysis of Dams. Stockholm", KTH Kungliga Tekniska Högskolan, Rapport, TRITA-ABE-RPT-1802001. Retrieved from <http://kth.diva-portal.org/smash/get/diva2:1186453/FULLTEXT01.pdf>.
- [55] Eurocode 1-5 (2003): Actions on structures. Part 1-5: General actions – Thermal actions. SS EN 1991-1-1-5, SIS.

- [56] Andersson, O., & Seppälä, M. (2015). "Verification of the response of a concrete arch dam subjected to seasonal temperature variations.", MSc thesis. Retrieved from <http://urn.kb.se/resolve?urn=urn:nbn:se:kth:diva-169917>
- [57] Andersson, P. & al. (2016) "Eurokoder för dimensionering av betongdammar – förslag på tillämpning i Sverige". Energiforsk, rapport nr. 2016:309. (In Swedish)
- [58] Fu, C., & Hafliðason, B. (2015). "Progressive failure analyses of concrete buttress dams: Influence of crack propagation on the structural dam safety", MSc thesis. Retrieved from <http://urn.kb.se/resolve?urn=urn:nbn:se:kth:diva-169707>
- [59] Rots J.G (1988): "Computational Modeling of Concrete Crack". PhD Thesis, TR diss 1663, Civil Engineering and Geosciences, TU Delft, Netherlands
- [60] Fishman Y. A (2007): "Features of shear failure of brittle materials and concrete structures on rock foundations". International Journal of Rock Mechanics and Mining Sciences 45 (6), 976–992.
- [61] Broberg L., Thorwid M. (2015) "Evaluation of failure modes for concrete dams". KTH Royal Institute of Technology. <http://kth.diva-portal.org/smash/get/diva2:824953/FULLTEXT01.pdf>
- [62] Malm, R., Hassanzadeh, M., Gasch, T., Eriksson, D. & Nordström, E. (2013). "Cracking in the concrete foundation for hydropower generators: Analyses of non-linear drying diffusion, thermal effects and mechanical loads." Elforsk, rapport nr. 2013:63.
- [63] Model Code (2010): "fib Model Code 2010" bulletins 55 and 56, International Federation for Structural Concrete, Lausanne, Switzerland, 2012.
- [64] Brühwiler E. (1990) "Crack of mass concrete under simulated seismic action", Dam Engineering Vol 1, issue 3, pp 153 – 176.
- [65] Bažant, Z. P. (2002). "Concrete crack models: Testing and practice." Engineering Fracture mechanics, Vol. 69 (2), pp. 165-205.
- [66] Ghaemmaghami A. & Ghaemian, M. (2006). "Large-scale testing on specific fracture energy determination of dam concrete". International Journal of Crack, Vol. 141 (1), pp. 247-254.
- [67] Petersson, P.E. (1981) "Crack Growth and Development of Crack Zones in Plain Concrete and Similar Materials." Division of Building Materials, University of Lund, Sweden, Report No. TVBM-1006.
- [68] Rijkswaterstaat (2012): "Guidelines non-linear Finite Element Analysis of Concrete Structures, Scope: Girder Members." Document RTD 1016:2012, Ministry of Infrastructure and Environment, the Netherlands.
- [69] Hunter, I. & al. (2016). "Repairing Spillway Damage at Wanapum Dam." <http://www.hydroworld.com/articles/hr/print/volume-35/issue-7/cover-story/repairing-spillway-damage-at-wanapum-dam.html>.

- [70] ICOLD, (2012). "Dam Safety Management: Operational Phase of the Dam Life Cycle Committee on Dam Safety International Commission". Bulletin 154.
- [71] ICOLD, (2013). "Dam Surveillance Guide". Bulletin 158
- [72] SS-EN 1504. "Betongkonstruktioner – Produkter och system för skydd och reparation. SIS. (In Swedish)
- [73] Rosenqvist, M. (2011). "Vägledning för cementinjektering av betongkonstruktioner". Elforsk rapport 11:60. (In Swedish)
- [74] Molin, C & Syvertsen, B. (2007). "Tätning av läckande sprickor i betong med kristalliseringsteknik – En översiktlig studie". Projekt nr. 11672, SBUF (In Swedish)
- [75] Molin, C & Syvertsen, B. (2007). "Kristalliseringsteknik – effektiv tätning av läckande sprickor i betong.", Informationsblad nr. 07:35, SBUF (In Swedish)
- [76] ACI (2007). "Causes, evaluation and repair of cracks in concrete structures". ACI Committee 224. Report ACI 224.1R-07.
- [77] [REHABCON, Annex I]
- [78] Hassanzadeh, M. & Åhs, M. (2017). "Modellering av betongkonstruktioner skadade av alkalisilikareaktioner.", LTH, Teknisk rapport nr. TVBM-7221. (In Swedish)
- [79] www.betongreparation.se (In Swedish)
- [80] Täljsten, B.; Blanksvärd, T. & Sas, G. (2016) "Kompositförstärkning av betong", Svensk Byggtjänst. (In Swedish)
- [81] RIDAS TV 7.3 (2011), "RIDAS, Avsnitt 7.3, Betongdammar, Tillämpningsvägledning", 2011-12-15. (In Swedish)
- [82] Jonasson, J-E. (1994), "Krympning hos hårdnad betong", Kapitel 15 I Betonghandbok – Material, utgåva 2, AB Svensk Byggtjänst och Cementa AB, 1994. (In Swedish)
- [83] Neville, A. M. (2008), "Properties of Concrete". Harlow, Essex, England: Pearson Education Limited.
- [84] SS 137215 (2000), "Betongprovning – Hårdnad betong – Krympning". Byggstandardisering, fastställd 2000-10-27, SIS. (In Swedish)
- [85] SS-EN 14630:2005, "Betongkonstruktioner – Provning av produkter och system för skydd och reparation – Bestämning av karbonatiseringsdjup". SIS (In Swedish)
- [86] Sundberg, S.; Amsköld, T., (2015): "Inspektionsmetoder för inre vattenvägar i vattenkraftverk". Examensarbete nr 447, Betongbyggnad, KTH. (In Swedish)
- [87] Nordström E., Malm, R., Blomdahl, J., Tornberg R., Nilsson, C-O. (2015) "Optimization of Dam Monitoring for long concrete buttress dams." In: ICOLD 25th Congress in Stavanger, Q99, 13-20 June, 2015.

- [88] Lundqvist, P. & Bernstone, C. (2017). "Sammanställning över spännstag inom vattenkraften". Energiforsk, rapport nr. 2017:398. (In Swedish)
- [89] Mang, H., Lackner, R., Meschke, G., Mosler, J., (2003). "Computational modelling of concrete structures. Comprehensive Structural Integrity, Vol. 3.10, 536 -601.

APPENDIX A – TEMPERATURE AND MOISTURE MEASUREMENT

TEMPERATURE MEASUREMENT – CHOICE OF SENSOR

There are various types of thermometers/sensors for measuring temperature. Before choosing the type of sensor, one should consider the following criteria (Nordtec Instrument, 2018):

- Measuring range
- Accuracy
- Design
- Response Time
- Resistance

The temperatures that apply when inspecting hydropower plants can vary between -40°C (extremely cold winter) and about $+50^{\circ}\text{C}$ (sunny day warm summer). The accuracy required for measurements depends on the inspection object, about 0.1°C accuracy is sufficient for most applications within concrete technology.

The choice of thermometer design is controlled by the inspection object and the purpose of the measurement. One can distinguish between the following types of sensors, (Nordtec Instrument, 2018):

- Strap-on temperature sensor
- Air sensor
- Immersion/insertion probe

Response time shows how fast a sensor reaches equilibrium with the temperature of the object. Resistance characterizes the type of sensor and controls its accuracy, speed and measurement range among other things.

Temperature sensors can be divided into the following categories (Nordtec Instrument, 2018):

- Thermocouple
“Temperature measurement with thermocouple is based on the thermoelectric effect. Thermocouples consist of two welded wires. The wires are made of different metals or alloys.”
- Resistance Sensors
“When measuring temperature with resistance sensors, the temperature-dependent change in the resistance of platinum is being utilized. The measurement resistance is applied to a constant current. Measurement is then performed on the voltage drop, which changes with the resistance value via the temperature.”
- Thermistor
“Temperature measurement with thermistors is also based on a temperature-dependent change in the resistance of the sensor element. Unlike resistance

thermometers, thermistors have a negative temperature coefficient (resistance decreases with increasing temperature). Properties and tolerances are not standardized."

Rule of thumb according to (Nordtec Instrument, 2018): "Sensors with thermocouples are fast and have a wide measuring range. Resistance and NTC sensors are slower but more accurate. The wider the measurement range, the more general the applications are. "

Material radiates (emits) infrared radiation (electromagnetic waves). The length and energy of the waves is controlled by the temperature of the material. This effect is used in IR temperature measurement, which is a contact-free measurement. The accuracy of the IR instruments is lower than the sensors described above. The advantage of the IR instruments is that one can determine the temperature of an object from a distance. The method allows rapid scanning of temperature variations across a distance/surface. In the market there are infrared cameras that take an infrared image of the object. The images can be used to determine the temperature distribution over a larger area and detect heat/liquid leakage. By combining IR measurement with regular temperature measurement, one can increase the measurement accuracy of the IR measurements.

MOISTURE MEASUREMENT

Background theory

The relative humidity of air is defined according to the following relationship:

$$\phi = \frac{v}{v_s} = \frac{P}{P_s} \quad (1)$$

v = the current vapour content of air [kg/m³]

v_s = vapour content of air at saturating point [kg/m³] at the current temperature

P = the partial pressure of the vapour [Pa]

P_s = the partial pressure of the vapour at saturation point [Pa], at the current temperature

ϕ is a ratio: $0 < \phi < 1$. At $\phi \geq 1$ the excess vapour condenses in order to satisfy the condition $\phi < 1$.

The relative humidity is also given in %, i.e. $100 \times \phi$. The vapour content of air at saturation point is the maximum vapour content possible at a given temperature. The warmer the air is, the more vapour it can contain. The relation between v_s and the temperature (θ , °C) is as follows:

$$v_s = e^{\left(a - \frac{b}{T}\right)} \quad [\text{g/m}^3] \quad (2)$$

$$T = 273.15 + \theta \quad [\text{K}] \quad (3)$$

$a = 20.111$ and $b = 5060.730$ for $\theta > 0$

$a = 23.077$ and $b = 587.990$ for $\theta < 0$

The relation according to Equation 2 is tabulated in several handbooks.

The relation between v and P is as follows (Burström, 2007):

$$P = 461.4 \cdot T \cdot v \quad [\text{Pa}] \quad (4)$$

RF in air cannot exceed 100%. Completely dry air, i.e. air with 0% RH does not occur in more common civil engineering contexts. Air that has first been dried over ice at a temperature of -40°C and then heated can have RH equal to 0.

Given is air (L_0) with the temperature θ_0 and the vapour content v_0 . If the temperature of the air is gradually lowered while v_0 remains unchanged, condensation eventually occurs. The reason is that lowering the air temperature leads to a reduction of v_s , which in turn leads to an increase of $\phi = v_0/v_s$. When the condition $\phi \geq 1$ is met, the excess of the water vapour ($v - v_s$) in the air condenses. The temperature just before the temperature at which condensation occurs is called the dew point (θ_s) for the air L_0 . The dew point is the lowest temperature at which humid air can occur without the water vapour condensing, (Burström, 2007). The dew point is thus a measurement of the moisture content of the air. The current vapour content of the air is equal to the air vapour content at the point of saturation at the dew point.

Types of sensors and measuring principle

The modern RF meters are built with one of the following types of sensors:

- Capacitive

In a capacitive humidity sensor, a capacitor changes its capacitance depending on the ambient air humidity. The sensor is fast and can measure RH with $\pm 1\%$ (RH device) accuracy. According to (Nordtec Instrument, 2018), the sensor can measure RH in air temperatures from -40°C to $+180^\circ\text{C}$.

- Dew point mirror

A mirror is cooled down until condensation occurs after the dew point temperature is obtained. The condensation on the mirror is monitored and then the dew point is measured (Nordtec Instrument, 2018). The method is accurate provided the temperature measurement is accurate. The method is not adapted to field measurements.

- Psychrometer

A psychrometer consists of two temperature sensors. One temperature sensor is covered with a damp cotton sock. Both temperature sensors are blown with the air whose humidity is to be determined. The temperature sensor covered with the damp cotton sock cools more than the dry temperature sensor. The reason is that the evaporation of water cools the sensor. The temperature difference between the dry sensor and the wet sensor depends on the humidity of the air. The temperature difference increases with reduced humidity. By means of the temperature difference, the humidity of the air can be determined. The method is not fast and is

not as accurate as the others. It is suitable for a point determination. It is not suitable for cases where you want to measure the air humidity at several points.

REFERENCES

Nordtec Instrument (2018), *Fakta mätteknik*, <http://www.nordtec.se/matteknik>. (In Swedish)

Burström, P. G., (2007), *Byggnadsmaterial – Uppbyggnad, tillverkning och egenskaper*. Studentlitteratur AB, Lund. (In Swedish)

APPENDIX B – FROST DEGRADATION

CENTRAL TERMS AND PARAMETERS

Cement paste

Cement adhesive that surrounds the aggregate particles and includes reacted and unreacted cement and pores. Cement paste may contain reacted and unreacted addition, fines and filler aggregate.

Aggregate

Granular material used for construction. Aggregate can be natural, industrially produced or recycled, (SS-EN 12620 + A1: 2008). Here only natural rock material is assumed which has not been subjected to anything more than mechanical processing (SS-EN 12620 + A1: 2008), including both natural gravel and crushed rock.

Fines

Fraction of a aggregate sample, whose grains passed the 0.063 mm sieve (SS-EN 12620 + A1: 2008).

Filler aggregate

Aggregate which mostly passes a 0.063 mm sieve, and which can added to concrete materials to obtain certain properties.

Degree of saturation

Volume of water vaporisable at 105 °C divided by the volume of the open porosity of the cement paste/concrete.

Open porosity

The pore volume in concrete that can be filled with water if vacuum-treated concrete is soaked in water.

Freezable water

The amount of pore water that freezes when cooling concrete. Due to the forces prevailing in the cement paste pore system and the salts dissolved in the pore water, the pore water does not freeze when the temperature drops below 0 ° C. Only at about -2 ° C does the water freeze in the coarse pores. The water in the fine pores freezes considerably later. There is non-frozen water at -20 ° C or -30 ° C. All of the water in the pore system of the cement paste freezes at -40 ° C. Thus, the amount of freezable water is dependent on the pore size distribution and temperature of the cement paste.

Critical degree of saturation

The degree of water saturation at which the concrete is damaged in connection with freezing. The critical degree of water saturation is dependent on the pore size distribution and temperature of the cement paste.

Air pores

Pores that are air-filled when the concrete is in fresh condition. Air pores can be divided into two groups: 1) Natural air pores (about 1 mm in diameter) that occur due to incomplete compaction and may constitute between 1.5 and 2.5% of the

volume of the concrete; 2) Extra air pores (diameter between 0.01 mm and 1 mm) added by mixing in air entraining agents.

Capillary pores

Small continuous channels in concrete with the ability to transport water. Capillary pores occur in the spaces occupied by the mixing water that does not react with cement. The pore size is about 0.1 - 100 μm .

The spacing factor

The average distance between the air pores.

THE MODE OF ACTION OF FROST ATTACKS

The frost attack is discussed below with reference to the properties of the cement paste. The discussions below assume that Swedish aggregate has low porosity, does not absorb moisture and is frost resistant. Consequently, the frost resistance of the concrete paste is determined by the frost resistance of the cement paste.

Frost attacks are caused by the fact that the moisture contained in the pores of the cement paste expands in connection with freezing. The expansion of the ice can lead to high pressure in the pores of the cement paste and in the channels that connect the pores. The pressure in the pores and connecting channels results in tensile stresses in the cement paste skeleton which result in cracking and tensile failure if the local tensile strength of the material is exceeded.

The ice density is 917 kg/m^3 , i.e. the volume increase of the water is about 9 % when it is converted to ice. Theoretically, one could argue that if the degree of saturation of the cement paste is equal to or less than 91%, the cement paste could cope with the frost attack, which in practice has proved to be not sufficiently low. Cement paste with degree of saturations lower than 80% has been damaged due to frost attack. Because the pores of the concrete have varying sizes, the degree of saturation of the individual pores varies, i.e. that the cement paste as a whole can have a degree of saturation of 91% or just under 91%, while the larger and smaller pores in the same cement paste can have degrees of saturation which are lower and higher than 91%, respectively. In connection with freezing, the excess water in the pores filled to more than 91% of their volume must be pressed out to the pores that have space. The excess water is expelled via capillary pores to adjacent coarser pores (air pores). When the water is pressed out into the capillaries, a hydraulic pressure occurs. The size of the pressure depends on the distance between the spaces exchanging the excess water. The resulting hydraulic pressure, including the pressure that the ice, in the more than 91% filled pores, exerts on the cement paste can lead to tensile stresses that cause cracking in the cement paste.

From the above description it can be seen that a cement paste can be frost damaged even though its degree of saturation is lower than the theoretical value of 91%. Although there is enough space for the ice to be able to expand, the distances to the available spaces are so large that hydraulic pressure occurs, which damages the cement paste.

APPENDIX C – ALKALI-SILICA REACTIONS

MECHANISM

Here the ASR (Alkali Silica Reactions) phenomenon is briefly described, including the mechanisms that cause the expansion and the parameters that affect the expansion. Only local effects are taken into account and ignored from the global effects. The local effect is presented by the free expansion of a representative test specimen, the shortest edge of which is at least 3 times larger than the largest enclosed particle.

The ASR area is quite complex and relatively unexplored. There are many unanswered questions that currently employ many researchers. Here, the questions that form the research front are not discussed, but the presentation is held on a general level.

Alkali-Silica Reactions

According to (Dyer, 2014), siloxane bonds on the surface of minerals containing silica are attacked by hydroxide ions at high pH levels. The reaction converts the silica network into an open gel-like network susceptible to water molecules. The gel absorbs and binds water and expands. The expansion, which can be significant, is controlled by the ability of the gel to absorb water and the amount of water available. The attack continues until the outer layer of the gel breaks down and dissolves. The silicate that dissolves reacts with calcium ions and forms CSH gel, calcium silicate hydrate. The reactions are similar to the pozzolanic reactions that occur in the binder containing pozzolans.

The reactions can also occur inside an aggregate grain. Water and alkali and hydroxide ions can diffuse from the cement paste to the inside of an aggregate grain and accumulate where the reactive mineral is. According to this mechanism, the reactions take place as above, but with the difference that the silicate ions do not exit from the reaction site and dissolve. They may be trapped due to the product formed by the reaction of calcium and ASR gel. Consequently, the reaction between the gel and the calcium ions can prevent the ASR gel from dissolving and exit. This causes the gel to expand inside the aggregate and crack the aggregate.

Alkali content

ASR occurs when the alkali present in the concrete reacts with the reactive silica of the aggregate. The reaction is controlled by the prevailing pH in the pores of the concrete. According to results from Min and Mingshu i (Dyer, 2014), the reactions start when the pH exceeds 12. The concrete expansion caused by ASR increases with increased pH and the increase accelerates when the pH approaches 13. The pH of the concrete is controlled by its alkali content and the high pH values are controlled by the sodium and potassium content of the concrete. The alkali content of cement and concrete is normally expressed by equivalent sodium oxide content (% of cement weight kg/m³ of concrete). Equivalent sodium oxide is calculated as follows:

$$(Na_2O)_{eq} = Na_2O + 0,658K_2O$$

where Na_2O is the amount of sodium oxide [kg/kg, or %] in cement or the amount of sodium oxide in concrete [kg/m³], and K_2O is the corresponding value for potassium oxide (Dyer, 2014).

The alkali content can also be given as the equivalent sodium content:

$$Na_{eq} = Na + 0,588K$$

For concrete, the total alkali content should be determined, i.e. the sum of the alkali content derived from the cement and the aggregate.

The expansion of the concrete due to ASR increases with increased alkali content. There is, however, a limit value for alkali content for when the risk of expansion due to ASR is significantly reduced, e.g. 3 kg/m³ $(Na_2O)_{eq}$ is a limit value specified for concrete. The corresponding limit value for alkali content in cement is 0.6%.

It should, however, be noted that the alkali content of the concrete is controlled by the type of binder and amount of binder that is mixed in the concrete. Furthermore, it should be noted that the ratio between reactive silica and alkali content is also a controlling parameter. The expansion of the concrete increases with increased value of the ratio between reactive silica in concrete and alkali content in concrete. The increase continues, however, to a certain value of the ratio and then decreases. According to results from D. W. Hobbs in (Dyer, 2014), the pessimum ratio is somewhere between 4 and 8.

Reactive aggregate

Aggregate containing reactive minerals can react with alkali and expand. In (Rombén, 1994) various types of reactive aggregate and minerals are presented. It should be noted that the type and placement of the reactive mineral in the aggregate particle is important and affects the reactions and the expansion of the concrete. In concrete containing flint - an opal-containing rock that occurs in Scania - the reactions occur in the boundary layer between aggregate and cement paste. In other cases, the reactive mineral is embedded in the aggregate grain and is more or less surrounded by dense minerals. The crystal form of the reactive minerals and placement in the aggregate grain affect their reactivity and reaction rate. (Trägårdh, 2014) divides the aggregates that occur in Sweden into three main groups:

- A) Rapidly reactive rocks: opal flint, low metamorphic sedimentary rocks such as greywacke and opal sandstone. Scania and locally in the mountain area.
- B) Medium-reactive rocks: very fine-grained (flint-like) meta-vulcanites, fine-grained mylonites that have not been re-crystallized, deformed quartzites, sandstones/sparagmites, greywackes, and fine-grained quartz-rich meta-sediments. The mountain range as well as parts of Bergslagen and south of Bergslagen.
- C) Slowly reactive rocks: porphyry and other fine-grained meta-vulcanites, fine-grained granites, fine-grained quartzites, finely-grained meta-

sediments. Cataclastics along east-west fault zones in the middle of Sweden.

According to (Dunant & Scrivener, 2012), slowly reactive aggregate causes micro cracks in both aggregate and cement paste. In concrete structures, all crack growth initiated by ASR is initiated with micro-cracking. Micro-cracking occurs

- i. only in the cement paste for concrete with rapidly reactive aggregate,
- ii. in both aggregate and cement paste for concrete with slowly reactive aggregate.

Medium-reactive aggregate concrete constitutes an intermediate position between the above-mentioned cases.

The size and shape of the aggregate affect the expansion of the concrete. According to (Dyer, 2014) there is a pessimum for the aggregate particle size below and above respectively which decreases the expansion of the concrete. The pessimum aggregate size sometimes varies within wide size ranges and is dependent on the aggregate type.

EXPANSION AND CRACKING

The expansion of the concrete is controlled by the expansion of the ASR gel. The reaction products may appear on the surface of a aggregate grain or inside a aggregate grain. Figure 77 shows a small test specimen subjected to an ASR attack. The specimen is believed to contain reactive aggregate grains that are evenly distributed in the specimen and that the reaction conditions are met in all parts of the test specimen. Furthermore, it is assumed that the specimen is free to expand in all directions.

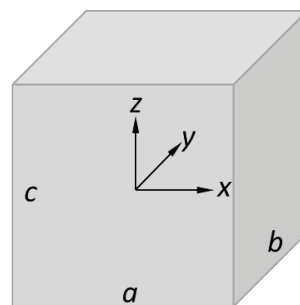


Figure 77 – Small test specimen subjected to ASR attacks.

In the beginning, ASR takes place simultaneously in all reactive aggregate grains. Because the reaction products are evenly distributed and the specimen is sufficiently small so that strain gradients and restraints do not occur - this is a consequence of the above-described assumptions - the specimen expands in multiple directions. The reactions lead to gel formation and expansion of the specimen. Local expansion cells exert multidirectional pressure in the pores of the concrete and cause the concrete to expand. In connection with the expansion, the

concrete matrix is subjected to tensile stresses and strains. The expansion continues until the concrete strain limit is reached and the concrete cracks. The micro-cracking is initiated prior to the strain limit but rapidly increases in number and size when the limit is exceeded. In some cases, the gel fills the micro-cracks completely or partially. However, the process is controlled by the type of aggregate and mineral. In cases where the gel dissolves and forms CSH gel, the micro-crack is slightly reinforced and regains some of the lost strength.

Figure 78 shows the test specimen of Figure 77 but now with growing reaction cells and micro-cracks. The reaction cells and micro-cracks grow until they form a continuous fracture plane that divides the specimen into two parts. In a uniaxial tensile test, a crack width of the order of 0.15 to 0.25 mm is required to separate a test specimen into two parts. If the process takes place slowly, it takes a certain time before the specimen cracks completely and is separated into two parts. Concrete can transmit tensile stresses even if it cracks. If the micro-cracks are filled with reaction products which form a CSH gel, the damaged concrete is slightly reinforced. The formed CSH gel causes some cohesion and contributes to the strength.

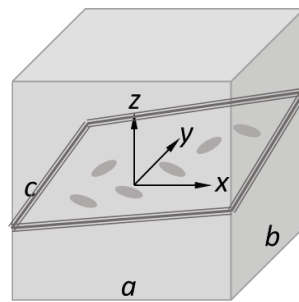


Figure 78 – A small test specimen with cracking caused by ASR.

One should, however, distinguish between expansions caused by different types of rocks. When the reactions occur inside an aggregate grain, it is more difficult for the gel to be converted into a CSH gel and the pressure can become relatively high within the aggregate because the gel cannot reach the cement paste pores and reduce the pressure. On the other hand, when the reactions take place outside the aggregate grain, the ASR gel fills a part of the cement paste pores, which can cause some relief.

Stresses that work in the area where the reactions are going on affect both the expansion and the crack formation. The stresses do not affect the chemical reactions, but they affect the direction of expansion. Studies performed by Dunant and Scrivener with concrete containing slowly reactive aggregate show that the axial expansion is inhibited if the test body is loaded with axial compressive stress corresponding to 5 to 10 MPa. The study shows that the axial expansion at 5 MPa is a fraction of the free expansion. Furthermore, the study shows that the axial expansion stops completely at stresses between 10 and 15 MPa. According to the same examination, the lateral (direction perpendicular to the direction of the stress) expansion increases with increased axial stress. The volume increase is the greatest

in the unloaded (free expansion) specimen, while it is the lowest of the specimen that is loaded with 5 MPa and then it increases with increased stress. According to Dunant and Scrivener (2012), the load affects the expansion kinetics.

Figure 79 shows a test specimen exposed to ASR. If the specimen is loaded with compressive stresses corresponding to $\sigma_x > 5 \text{ MPa}$ and $\sigma_z > 5 \text{ MPa}$, the expansion takes place in the y-direction and the fracture surface is formed perpendicular to the y-axis. If the specimen is loaded only in one direction, z-direction, it is possible that two fracture planes are formed, one plane perpendicular to the x-axis and another which is perpendicular to the y-axis, or a fracture plane angled to both the x-axis and y axis.

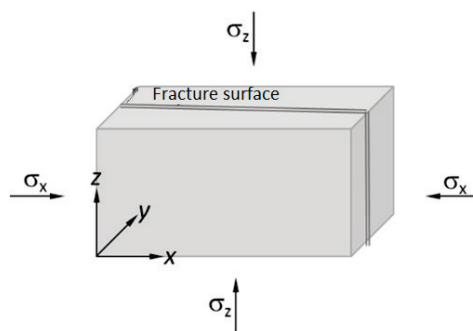


Figure 79– The effect stress has on expansion caused by ASR

In a structure, different kinds inhomogeneity occur, which in combination with the boundary conditions can lead to varying crack patterns.

REFERENCES

Dunant, C. F., & Scrivener, K. L. (2012). "Effects of uniaxial stress on alkali–silica reaction induced expansion of concrete". *Cement and Concrete Research*(42), 567-576.

Dyer, T. (2014). "Concrete Durability"., CRC Press, Tylor & Francis Group.

Rombén, L. (1994), "Kemiskt angrepp". Kapitel 23 i *Betonghandboken – Material*, utgåva 2, AB Svensk Byggtjänst och Cementa AB, 1994. (In Swedish)

APPENDIX D – SPILLWAY DAM 2 (CONCRETE LAYERS/TEMP)

DESCRIPTION OF STRUCTURE

See main document.

ASSESSMENT

In an attempt to assess the safety against material and stability failures in the spillway piers, an analysis was carried out with a relatively simple model. Estimated shear stresses were compared with the calculated ability to "transfer forces through joints" according to BBK 04, equation (3.11.3c), see below.

The piers were calculated with the multi-physics/FEM program Comsol Multiphysics and as a "solid" model.

The calculation model consisted of three physical modes; (i) pore water pressure, (ii) temperature and (iii) mechanical stresses.

Load combinations for stress calculations were added to:

- LC1a (common load case): upper water surface (uws) = Maximum Retention Level (MRL), ice load 50 kN/m
- LC1b similar to LC1a but also $T_{out} = +10\text{ }^{\circ}\text{C}$
- LC14a (excl. Load case): uws = MRL and $T_{out} = +37\text{ }^{\circ}\text{C}$
- LC14b (excl. Load case): uws= MRL and $T_{out} = -31\text{ }^{\circ}\text{C}$

The geometry of the dam was taken from drawings. The geometry of the cracks was estimated, partly from previous site visits and partly from photos.

Pore water pressure in concrete and rock was calculated as shown below. Temperature in concrete and rock was calculated as shown below, based on assumed seasonal temperature variations in air and water.

In the stress calculations, all water pressure was set as pore water pressure in the concrete.

First, the stresses in the intended crack plane were calculated, assuming completely linear elastic conditions, that is, that "there are not really" any cracks and that no degradation of strength or E-module exists in the cracking area. This is a simplification but can be accepted when the cracks are not very wide. The crack surfaces were assumed to be so rough and in contact with each other that the capacity to transmit shear force between the surfaces is still good.

The calculated stresses in the crack plane were compared with the shear capacity in the crack plane, with assumption according to "force transfer in joints" in BBK04 [6], section 3.11, see below. If the calculated shear stresses exceed the capacity, there is a risk of continued cracking and the risk of reduced interaction in the crack

plane. It is then assumed that there is a risk that the monolith no longer acts as an entire monolith, but divided into smaller parts. The method was:

- Calculate shear and normal stresses in the current crack plane with the FE model assuming linear elastic material. i.e. no plastic damage model is used.
- Use equations force transfer through joints, raw surface in BBK04 [6].
- Shear stress > capacity according to. BBK?
 - Yes: Risk of further cracking and not completely monolithic behavior of the pier.
 - No: No greater risk of the above happening.

BBK 04, section 3.11.3:

Rough, cleaned surface:

$$f_t = 1,2(\rho f_{st} + \sigma_k) \quad (3.11.3c)$$

$$f_t = \frac{f_{cc}}{25} + 0,8(\rho f_{st} + \sigma_k) \quad (3.11.3d)$$

$$f_t = 0,4 f_{cc} \quad (3.11.3e)$$

When calculating the stresses, the structure was assumed to be placed and fixed to the underlying bedrock. In this case, the rock volume was locked in its lower edge in the model. This case somewhat underestimates the stresses in the cracks, because in reality the concrete may be separated slightly from the rock when tensile stresses occur in between, and then the stresses in the column may increase slightly.

CALCULATING PORE WATER PRESSURE

Water pressure was calculated using the continuity equation and Darcy's law:

$$\nabla \cdot (k_w \nabla H) = 0$$

$$H = z + p_w / (\rho g)$$

where ∇ = nabla operator ($\nabla^T = [\delta/\delta x \ \delta/\delta y \ \delta/\delta z]$) (1/m); v_w = water velocity (m/s); k_w = hydraulic conductivity (sometimes called permeability) (m/s); H = water pressure head (m.a.s); z = height above reference level ± 0.0 (m.a.s); p_w = pore water pressure (Pa); ρ = density of water (kg/m³); and g = gravitational acceleration (m/s²).

The material (rock and concrete) was assumed isotropic, meaning that k_w (10^{-7} and 10^{-11} m/s respectively) is constant at all points in one and the same material and in all directions. Stationary flows were assumed. The materials were assumed fully saturated.

Figure 80 shows the calculated pore water pressure $p_w = \rho g * (H - z)$ (kPa).

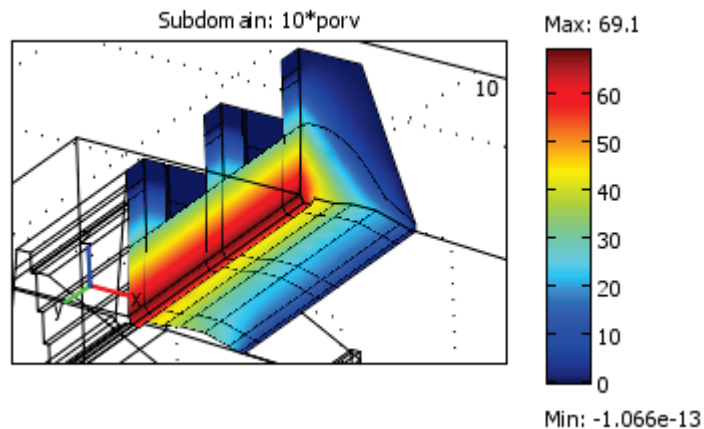


Figure 80 Calculated pore water pressure (kPa) in the spillway section (kPa).

CALCULATION OF TEMPERATURES IN THE DAM:

The temperature in concrete and rock is calculated with an FEM-formulated balance equation on the form:

$$\rho C_p \partial T / \partial t + \rho C_p \mathbf{u} \cdot \nabla T - \nabla \cdot (k \nabla T) = Q$$

where k = thermal conductivity; T = temperature; Q = heat source, assumed zero in this example; C_p = specific heat; \mathbf{u} = flow of substance, e.g. heat transfer with the moisture flow, assumed zero here as this flow is negligible in dense materials such as rock and concrete.

The boundary conditions were assumed according to Figure 81. It is assumed that the summer has a peak temperature of +37 °C and the winter has a coldest peak at -31 °C at one 20 day period each. The assumed temperature curve should reflect "normal" average temperatures over the day, except for the "peaks" that should reflect the highest measured maximum or minimum temperature in the past fifty years. At +10 °C in the spring, the maximum ice load is assumed to occur at warmed up and expanding ice cover.

- For parts against water: $T = T_{\text{water}}$
- For parts against air: $T = T_{\text{out}}$

T_{water} is assumed to depend on T_{out} as: $T_{\text{water}} = 0.8 * T_{\text{out}}$

which, in the case of various measurements of the water temperature, where a large turnover of water can be assumed in front of the spillway and intake, has proved to be a relatively good assumption.

The time scale shown in the calculation result is in calculation seconds.

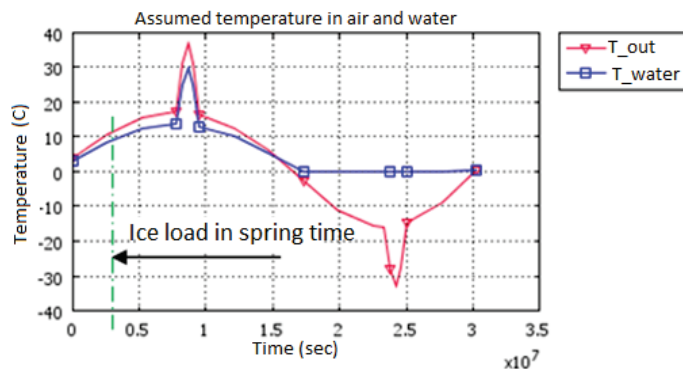


Figure 81 Assumed temperatures in air and water. T_{water} varies with the water depth.

Figure 82 shows the calculated temperatures during the (a) and (b) cold periods in the summer and winter respectively. Of course, calculated temperature is also obtained for all intermediate times, but here the temperature is only shown for summer and winter.

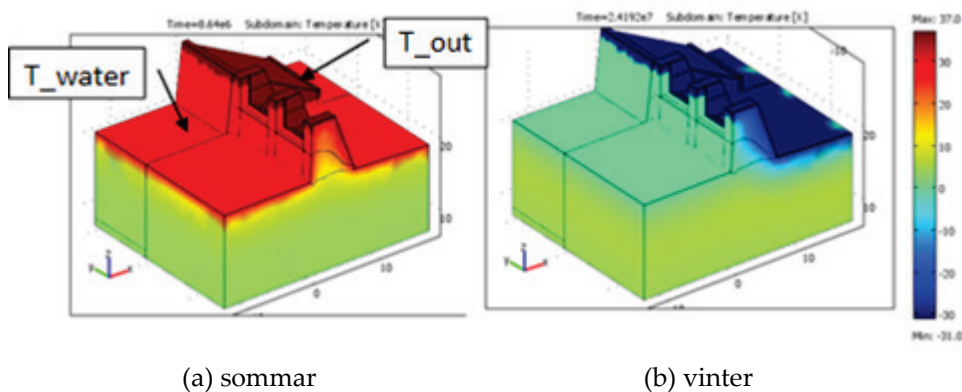


Figure 82 Calculated temperatures in the dam and the rock.

CALCULATION OF MECHANICAL STRESSES:

The stresses were calculated with an FEM-program (Comsol Multiphysics) based on

$$\sigma' = \sigma - p_w$$

Where σ' = effective pressure (pore water pressure) between the solid particles/the phase of the material (Pa); and ∇p_w = pore pressure gradient (Pa/m).

$$\sigma = D \varepsilon_{el} + \sigma_0 = D(\varepsilon - \varepsilon_{th} - \varepsilon_0) + \sigma_0$$

where D = the elasticity matrix (Pa); ε_{el} = total elastic strain (-); ε = strain (-); ε_{th} = thermal elastic strain (-); ε_0 = initial strain (-), in this case zero; and σ_0 = initial strain (Pa), in this case zero.

$$\varepsilon_{th} = \alpha_c \cdot (T - T_{c0})$$

Where α_c = thermal expansion coefficient (1/°C); T = current temperature (°C); and T_{c0} = initial temperature (°C). The temperatures in the structure are assumed calculated in separate temperature mode.

Reinforcement:

Safety class 3 is assumed according to RIDAS TA (2011). Reinforcement Ks40.

$$f_{yd} = 390/1.15/1.2 = 283 \text{ MPa}$$

Drawing shows that reinforcement has probably been installed on both sides and both vertically and horizontally at 1 ϕ 19 and 2 ϕ 12 per metre.

Assume that the surface reinforcement has effect throughout the thickness of the pier, about 1.5 m.

1 ϕ 19+2 ϕ 12 per m are installed in the form of square grids and on both sides.

$$A_s = (\text{horizontal}) = \pi \cdot (0.019^2 + 2 \cdot 0.012^2) / 4 \cdot 2 \text{ sides} = 1019 \cdot 10^{-6} \text{ m}^2/\text{m}$$

The shear capacity according to equation (3.11.3c) in BBK is obtained directly from the Comsol model as:

$$f_t = 1.2 \cdot [1019 \cdot 10^{-6} \cdot 283 \cdot 10^6 / 1.5 \text{ m} + \sigma_y / (1.2 \cdot 1.2)] = 0.231 \text{e}6 - 0.83 \cdot s_z \text{ (MPa)}$$

If the stress normal to the crack is compressive ($s_z < 0$) the normal stress helps increase the shear capacity.

On the other hand, if the stress normal to the crack is tensile ($s_z > 0$), the normal stress does not increase the shear capacity, but it is then only the through-going reinforcement that assists reaching the value 0.231e6 MN/m.

This can be summarised in Comsol with the equation

$$f_{t_s1} = (0.231 \text{e}6 - 0.83 \cdot s_z \cdot (s_z < 0))$$

where s_z = calculated normal stress (vertical) across the crack.

If the shear stress s_{xz} in a certain part of the crack exceeds the shear strength f_{t_s1} in the same part, then additional reinforcement, or pre-stressed anchors, are needed, so that that part of the crack is not to be sheared. E.g. the crack walls in the red dashed areas in Figure 83 will be sheared against each other as the shear force is greater than the counteracting frictional force. If the shear capacity F_t in total across the entire crack is greater than the total shear force V_d , there is a risk that a larger shear failure occurs in the structure. If not, there will probably be less consequences and then only in the operation phase stage when the crack widens in the "red areas".

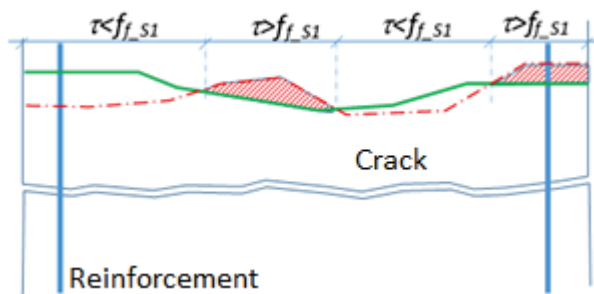


Figure 83 Conceptual figure of calculated shear stress τ and shear capacity $f_{t,s1}$ around a crack.

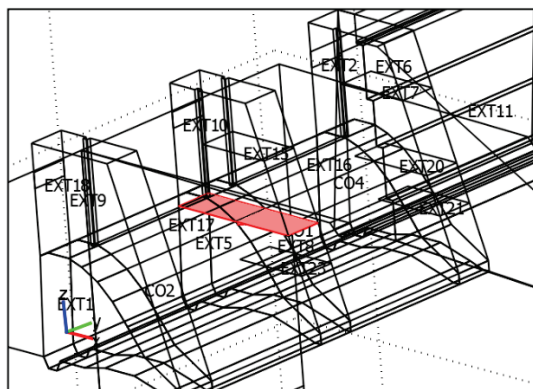


Figure 84 Assumed crack. Visible, above/on downstream side of the weir, in real life.

CALCULATIONS:

LC1b: Self-weight+pore water+ temperature +10°C

Figure 85 and Figure 86 show calculated shear and normal stresses respectively in the crack for a fictitious case in spring-winter, when an ice load of 50 kN/m is also applied.

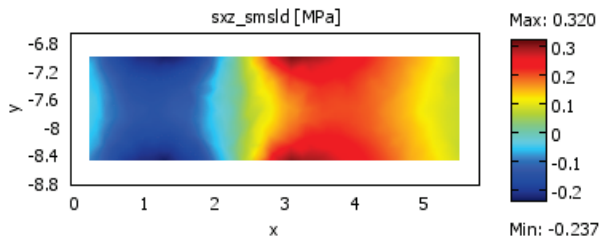


Figure 85 Calculated shear stress in crack 1 in spring +10°C with an ice load of 50 kN/m.

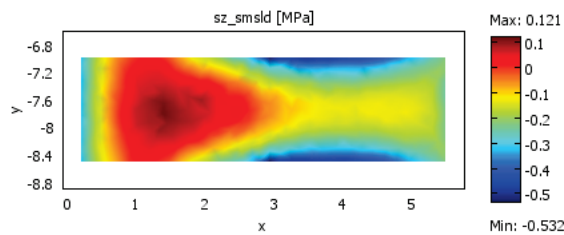


Figure 86 Calculated vertical normal stress in crack 1 in spring

The coloured small areas in Figure 87 show where the shear capacity $f_{f,S1}$ is insufficient against the shear stresses. Thereby there is a risk that the crack in this area widens slightly.

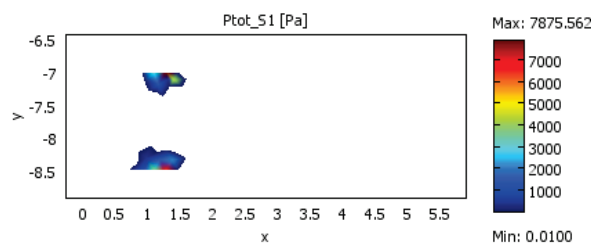


Figure 87 Area where the shear stresses exceed the capacity.

In order to assess the shear capacity of the entire crack compared to the entire shear force, an integration is made over the crack plane, see below. Integration over lines, surfaces or volumes is easily done in Comsol if requested.

Integration over the entire crack surface gives a total shear capacity of $F_f = 3.11$ MN. Integration of the shear force over the entire crack surface gives $V_d = 0.44$ MN. In other words, the calculated shear capacity exceeds the calculated shear force overall, for the entire crack plane.

$F_f > V_d$ OK!

No new extra reinforcement, e.g. in the form of new pre-stressed cables, needed for this load case!

LC14b: Self-weight+pore water+ice+temperature -31°C

The same load combination as LC1b, but for a very cold winter when the outdoor temperature is -31°C.

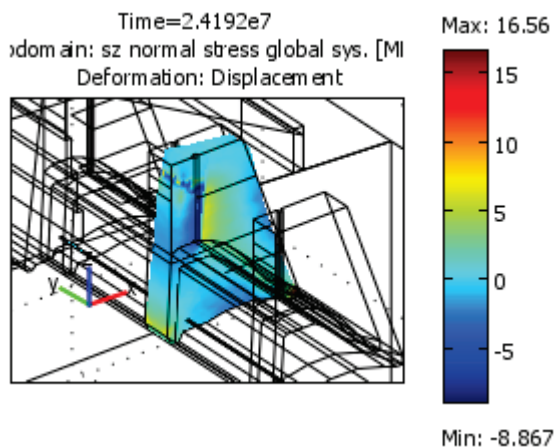


Figure 88 LC14b: Calculated vertical normal stresses in the crack 2-1.

Figure 89 and Figure 90 show the calculated shear stress and vertical normal stress respectively.

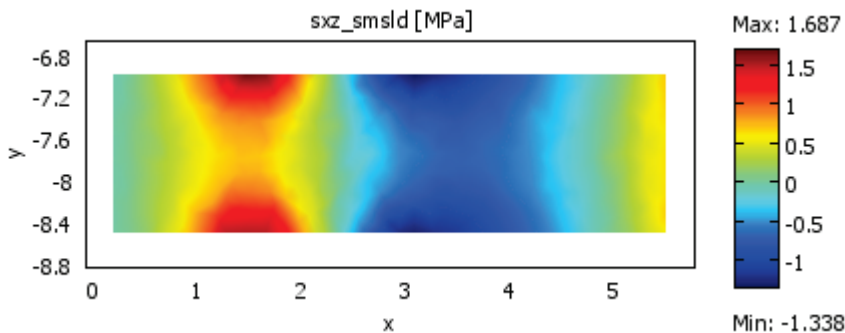


Figure 89 Calculated shear stress in crack 1 during the cold winter -31°C.

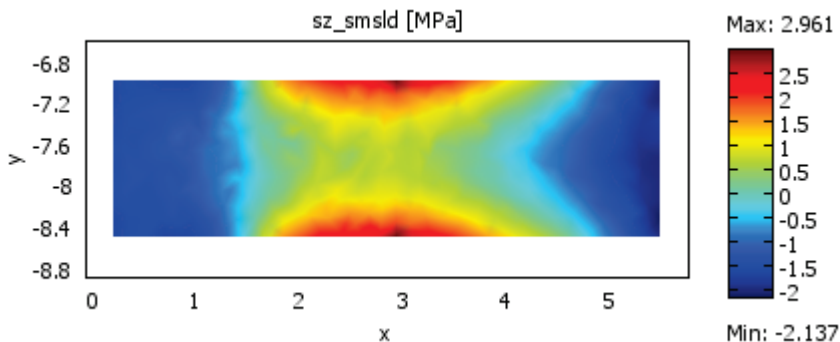


Figure 90 Calculated vertical normal stress in crack 1 during the cold winter -31°C.

Figure 91 shows where the shear capacity $f_{f,S1}$ is not sufficient against the shear stresses, the coloured surfaces. Thereby there is a certain risk that the crack in this area will expand somewhat. Note, however, that the shear stresses in the range $x =$ about 1-2 and $x =$ about 3-4 counteract each other, i.e. different directions, so if a larger part of the crack is considered then the shear stresses generally take each other out, see more about this below.

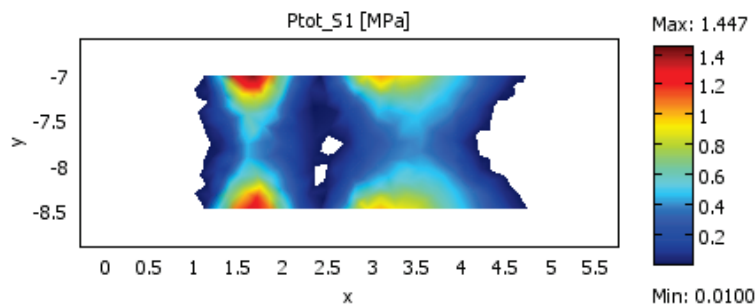


Figure 91 Calculated need of extra cohesive force in crack 1 during the cold winter -31°C. For values <0 , no extra force is needed.

In order to assess the shear capacity of the entire crack compared to the entire shear force, an integration is made over the crack plane, see below.

Integration of $f_{f,S1}$ over the entire crack surface gives a total shear capacity of $F_f = 5.52$ MN

Integration of the shear force over the entire crack surface gives $V_d = 0.09$ MN

The fact that V_d is so small is due to the shear stress acting in different directions and summing up the components means that there will only be a small total shear force in the x direction. In other words, calculated shear capacity exceeds the calculated shear force overall, for the entire crack plane.

$F_f > V_d$ OK!

No new extra reinforcement, e.g. in the form of new pre-stressed cables, is needed for this load case!

CONCLUSIONS:

The calculations showed relatively small shear stresses in the cracks compared to the shear capacity assumed to be there. It was therefore assessed that the safety against local failures in the cracks and thus the risk of instability of the spillway piers and the spillway dam was very small. On the other hand, seasonal temperature variations may be possible causes for the cracks to grow and become slightly longer and wider.

APPENDIX E – BUTTRESS DAM 2 (IN-DEPTH)

DESCRIPTION OF DAM

The concrete dam consists of a spillway section with one segment gate and two segmented spillways, as well as two buttress dam sections on each side of the spillway section.

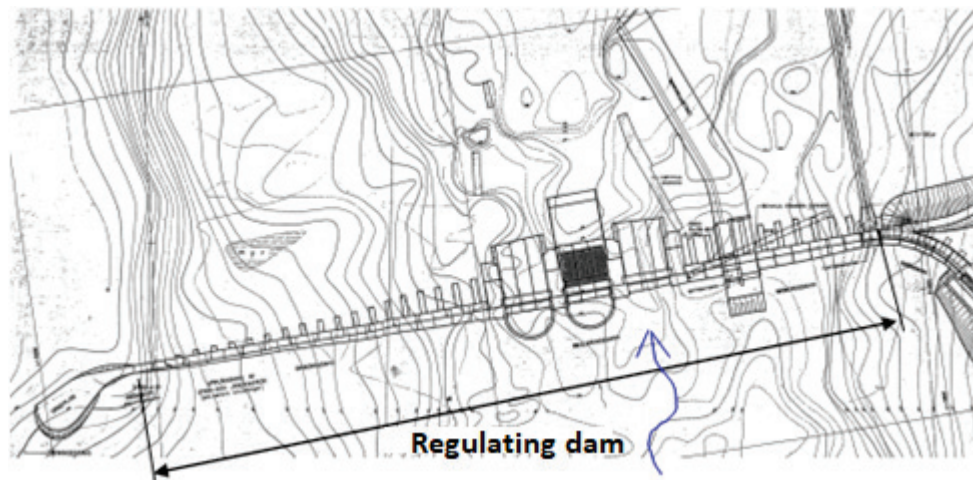


Figure 92 Plan of the regulating dam

Monoliths M18 and M38 were especially studied with calculations.

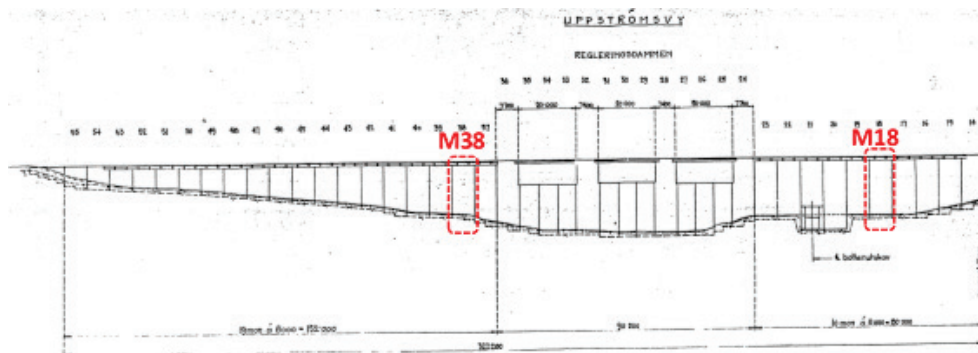


Figure 93 Upstream view of the concrete dam.



Figure 94 The downstream side of the regulating dam, before any measures were taken.

ASSESSMENT

In the calculations, it is important to adopt a realistic model for how the concrete and the reinforcement adhere to each other. The stiffer the interaction between the reinforcing bars and the concrete, the more the bars will strain in the cracked areas. If no slip is assumed, the strain on the bar becomes very large inside the crack, perhaps above the yield limit of the steel as Figure 97 shows. If the stresses and thus the strains change, the bar will very quickly reach fatigue failure, which is also shown in the basic Figure 98. In reality, the concrete is probably crushed around the edges of the bars and the bond decreases, thereby increasing the length on which the tensile force will strain the bar, which in turn should mean that the strain decreases in the bar and does not reach as high levels.

In the model, a linear elastic spring model is used for the bond between the concrete and the reinforcement of the form

$$K_x = k_0 \cdot \exp(\text{slip}_x \cdot c1)$$

$$\text{Slip}_x = \text{abs}(u2 - u)$$

where K_x = bond force between concrete and reinforcement in the x direction (N); k_0 = initial bond strength (N); slip_x = slip between the concrete and the reinforcement in the x-direction (m); u, v = the movement of the concrete in the x and y directions; $u2, v2$ = the movement of the reinforcement in the x and y directions; and $c1$ = assumed degradation coefficient (1/m). Springs in the y-direction are adopted in a corresponding manner.

In the model, the more the concrete and the reinforcement move relative to each other, the more the bond is weakened, in an attempt to mimic the measured bond according to Figure 95. However, the bond between reinforcement and concrete in the model is not plastically deformed the way it is in reality, which is a weakness in model. The bond in the model is elastic and the stiffness returns to its initial value if the difference in movement between concrete and reinforcement decreases again.

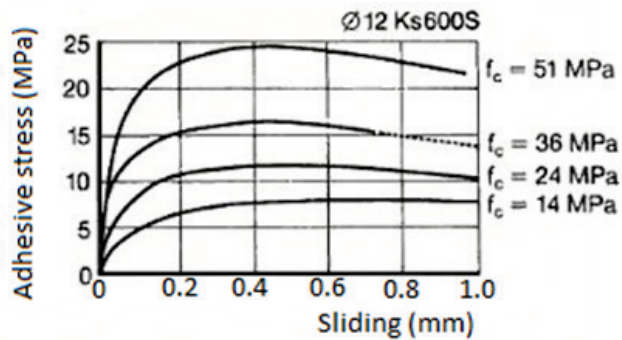


Figure 95 Bond – slip curves determined from pull-off testing with short bond length for Ks600S reinforcement with a diameter of 12 mm at four different concrete strengths (Berggren, 1965 presented in Tefpers & Törnwal, 1994)

Figure 96a shows the bond between reinforcement and concrete with the spring model. Just below the lower right hand corner of the door opening there is a plastic strain in the reinforcement inside the crack that has occurred in the model (and in reality). The right hand figure b shows the associated calculated slip between reinforcement bars and concrete.

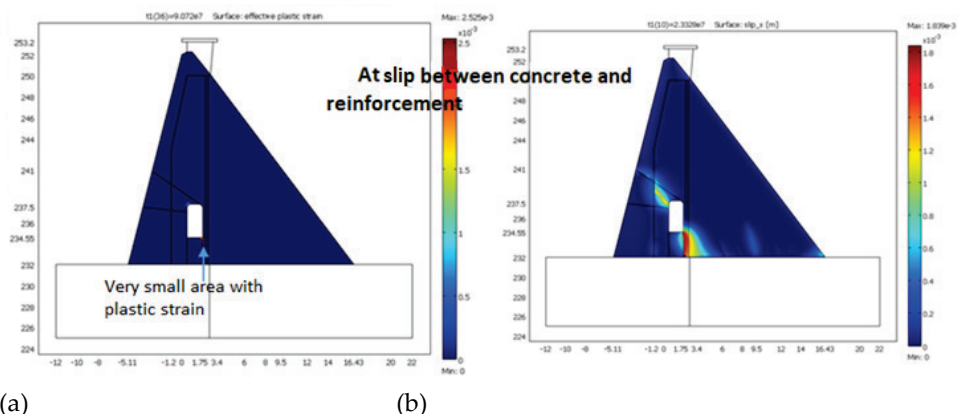


Figure 96 Study 2010: Important to understand what the bond between reinforcement and concrete looks like. (a) Plastic strain in the reinforcement just beneath the door opening with associated (b) slip between concrete and reinforcement

Figure 97 and Figure 98 show philosophically how reinforcement quickly can reach fatigue failure if it is completely fixed to the concrete, since the strain of the steel theoretically becomes very high just around the crack, as well as if load fluctuations occur, e.g. temperature fluctuations.

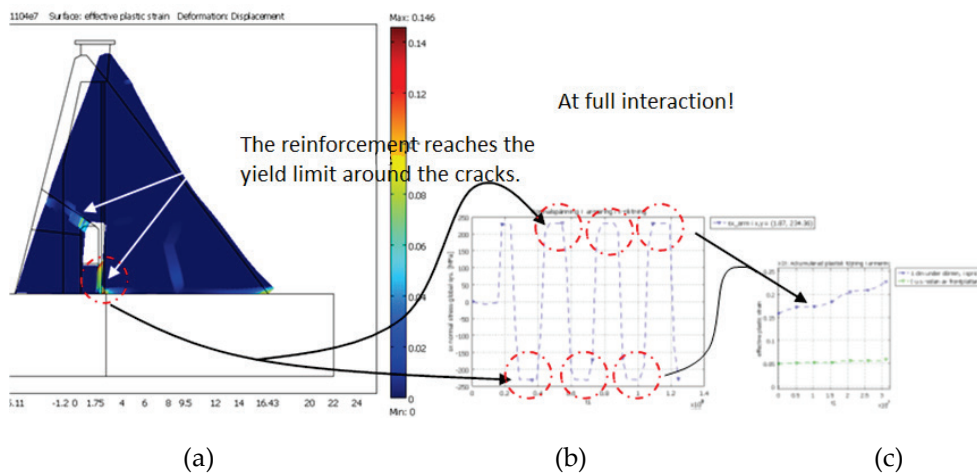


Figure 97 If the reinforcement has complete bond to the concrete, it reaches fatigue quickly at temperature and stress fluctuations.

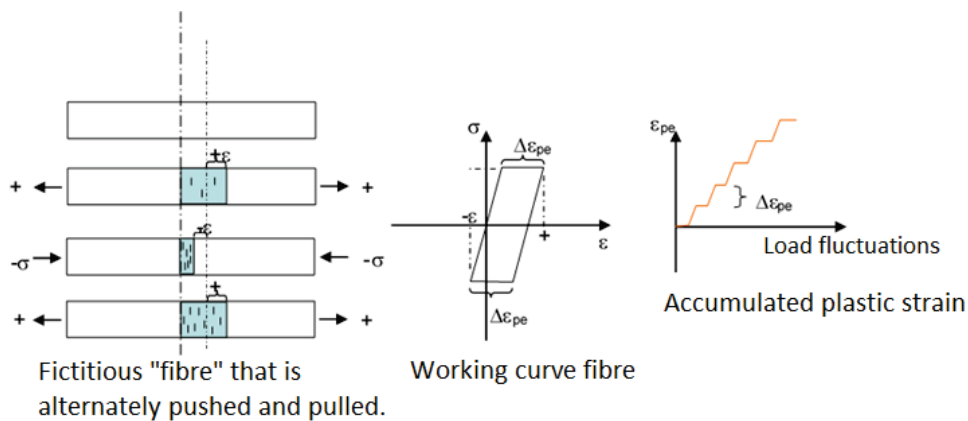


Figure 98 At many load fluctuations and to the concrete completely fixed reinforcement bar, the yield limit of the steel is theoretically reached quickly and leads to failure.

In the study 2010, the outdoor air and water temperatures were assumed, no measurements at the dam were available, after which the temperature distribution in the dam was calculated. With this among other things as a basis, a climate wall with a certain thickness of the insulation was proposed, in order to achieve a suitable temperature distribution over the year. By suitable here is meant a temperature which, in terms of calculation, varied between -3 and +11 °C during the winter and summer for a normal year, which entails a considerably smaller temperature variation than before the climate wall was built, leading to smaller movements and stresses on the concrete.

In 2016, a new study was conducted in which measured temperatures, crack movements, movements in the crest and pore water pressure were compared with calculated values, according to the fundamental process in Figure 99.

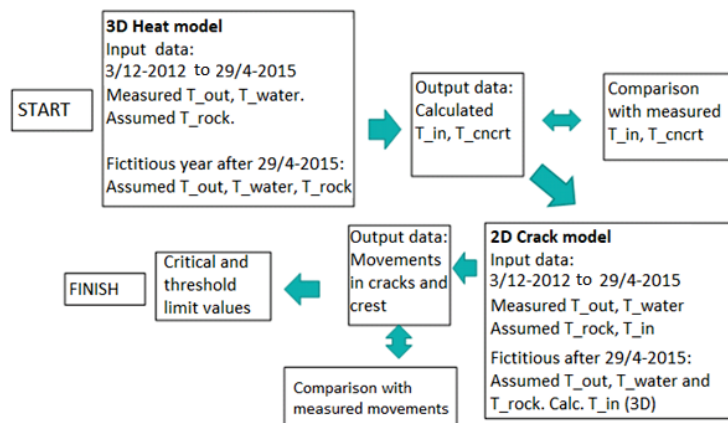


Figure 99 Study 2016: Calculation method at for analysis.

New calculations of the temperature distribution in the bedrock, concrete and indoor air were carried out in 2016. Input data for the boundary conditions in the calculation model were the measured temperatures of outdoor air and water that were carried out 2012-12-03 - 2015-04-29. Calculated temperatures of indoor air and concrete were then compared with measured values for the same period.

From the power house transformers, heat is supplied via a pipe (Figure 100) beneath the inspection gallery.

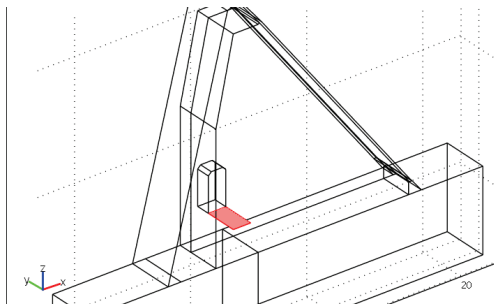


Figure 100 The dam is supplied with heat in reality and in the model from a pipe beneath the inspection gallery.

Figure 101 shows the measured temperature from three sensors that are mounted in the water at three different water depths in the reservoir at the monolith M38, which is located near the spillways. The measured values follow the outdoor temperature variations but more smoothly. The lowest and highest measured water temperature is approx. + 1.5 °C and + 24 °C respectively. The measured temperatures at all three depths are equal, which indicates that the water in the reservoir in front of the dam is strongly stirred by the water flow into the power house and sometimes to the spillways at discharge. It is also seen that the water temperatures follow the outdoor air surprisingly well, but more smoothly, the daily peaks are not included. The water temperature is roughly equal to the average temperature of the air.

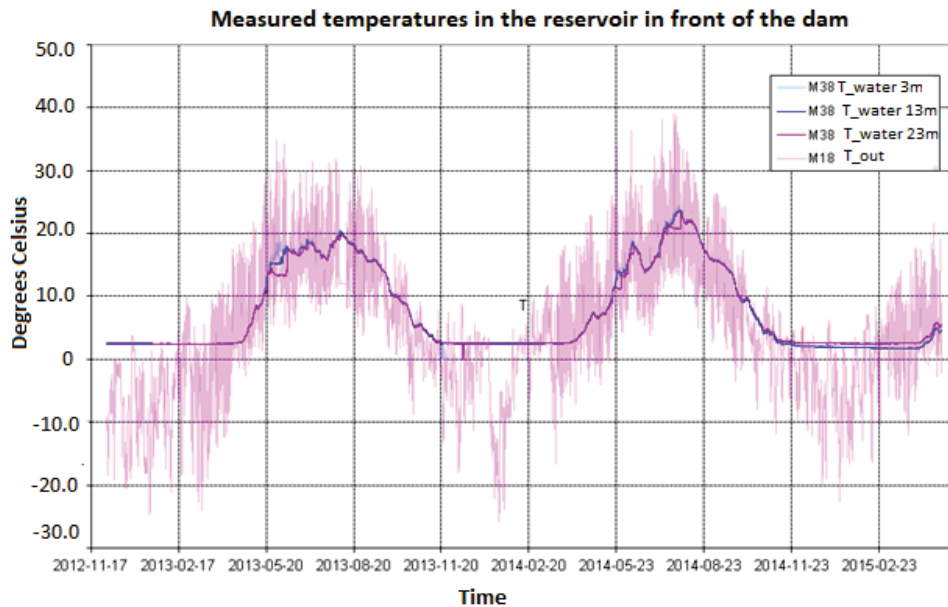


Figure 101 M38: Measured water temperature T11-T13. See the main document for position of sensors.

Figure 102 shows measured outdoor (T_{out}) and indoor temperatures (T_{in}) in air at the monolith M18 for the time period from 2012-12-03 to 2015-04-29. One can see that the indoor temperature is strongly smoothed compared to the outdoor temperature as a result of the new insulation wall. Before the new insulation wall was built, the concrete was outside the old climate wall, e.g. at T4, exposed to outdoor temperature with much larger temperature fluctuations, according to T_{out} .

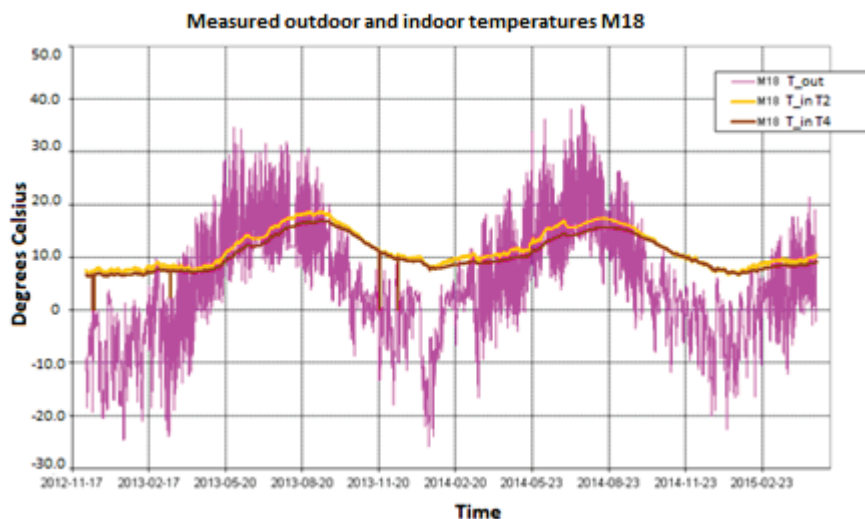


Figure 102 M18: Measured temperatures in indoor air T2 and T4 and outdoor air T5. See main document for position of sensors.

Figure 103 shows measured temperatures in air (T_{in}) and in concrete (T_{cnrt}) at the points T1-T4 (see main document). The temperatures at points 1 and 2, exactly

at the upstream side of the inspection gallery, are somewhat warmer than at points 3 and 4, which are located just above the rock surface fairly close to the insulation wall, which is realistic since the points 1 and 2 are located near the warm air channel in the inspection gallery and near the front slab, the temperature of which basically follows the water.

The temperature of the concrete, 0.5 m into the concrete, is basically the same as T_{in} , i.e. the temperature of the concrete follows the indoor air well on this time scale.

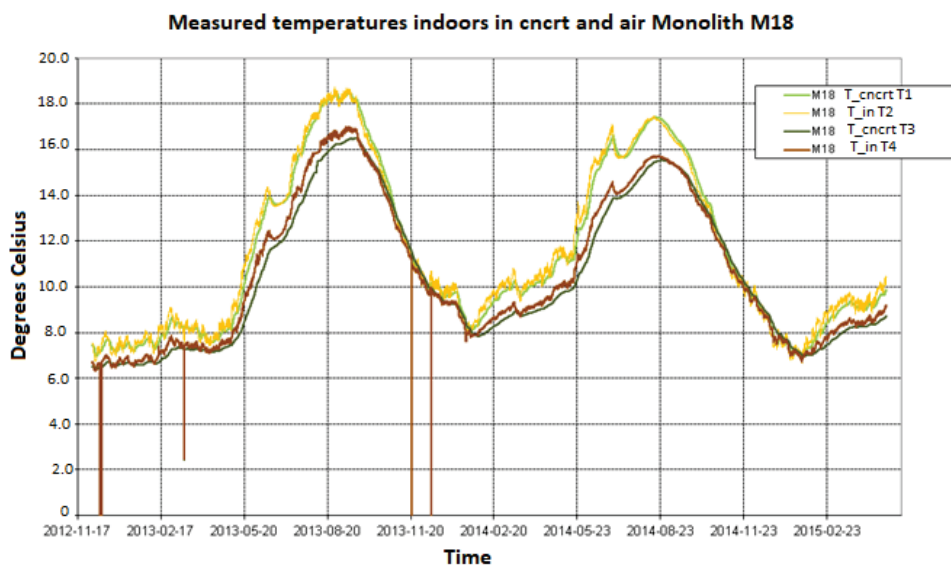


Figure 103 M18: Measured temperatures in concrete (0.5 m) T1 and T3, as well as indoor air T2 and T4. See the main document for position of sensors.

The temperature distribution in the concrete structure over time is calculated with the Comsol Multiphysic FEM program with transient solver.

The boundary conditions for the temperature model are shown in Figure 104 and Figure 105.

At all surfaces of concrete and new climate wall facing the outdoor air, the measured outdoor air M18_T5 is applied.

At the entire upstream side, beneath the upper water surface (uws)=maximum retention level (MRL), a water temperature is assumed according to Figure 105. During the fictitious year, the water temperature T_{water} is assumed to be 70% of the outdoor temperature T_{out} , except when T_{out} is less than zero, then T_{water} is + 4 °C. The use of 70% could be discussed when looking at Figure 10. Maybe T_{water} should have been set to about 80% of T_{out} instead.

Against the upper side of the rock surfaces, T_{rock} is set according to Figure 105, where the surface is assumed never to be colder than -4 °C due to snow that insulates.

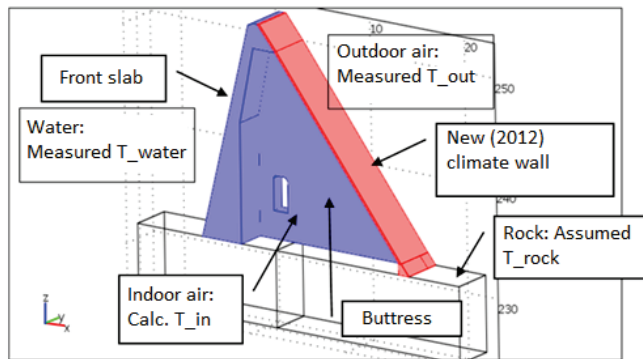


Figure 104 Geometry and material of model and different types of temperature.

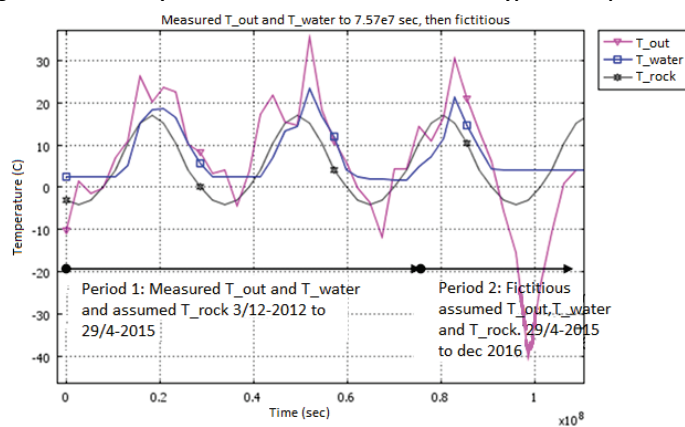


Figure 105 Measured temperatures in air (T_{air}) and water (T_{water}) against the monolith and that is used for the temperature calculation in the 3D model. T_{rock} is assumed temperature against the rock surface at the downstream side of the dam.

Figure 106 shows calculated temperatures inside the dam during the summer and winter of 2014, with measured temperatures in outdoor air and water as boundary conditions for the insulation wall and front slab.

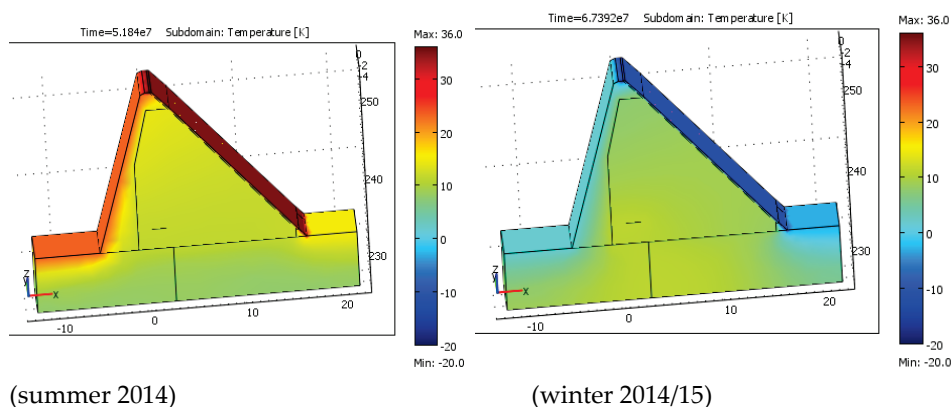


Figure 106 Calculated temperature of the dam for one summer and one winter. Heat 200 W/m^2 is supplied at $T_{in} < 4^\circ\text{C}$.

Figure 107 shows calculated and measured temperature at sensors M18_T2, at the inspection gallery. At red curve, 200 W/m² of the inspection gallery is assumed to be supplied during the first year (2013) but then only when $T_{in} < +4^{\circ}\text{C}$ thereafter. No added heat is assumed at the green line. It is seen that if heat is assumed in the calculation, the calculated T_{in} connects better with measured T_{in} , which is expected when heat is actually supplied along the inspection gallery.

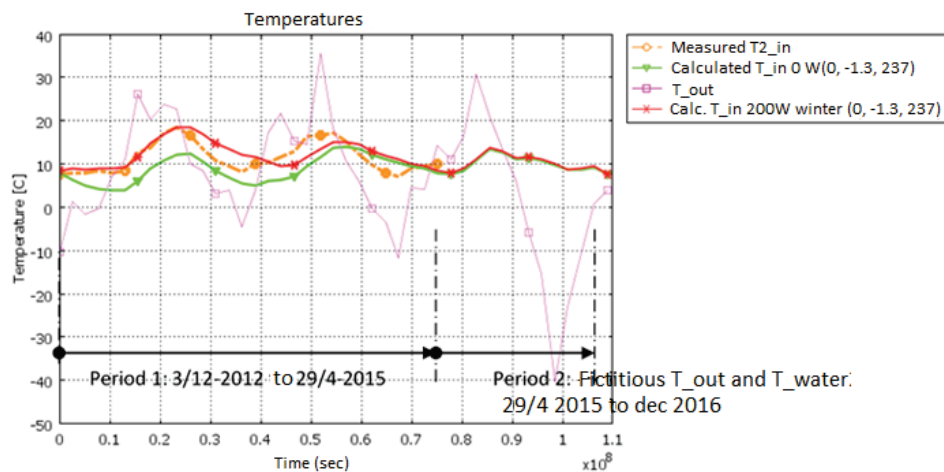


Figure 107 Calculated and measured indoor temperature at monolith M18 at sensor M8_T2_in, at the inspection gallery. In the calculation it is assumed that heat from the ventilation shaft beneath the gallery is turned on with 200 W/m² gallery at $T_{in} < +4^{\circ}\text{C}$.

Figure 118 shows that there is a very small difference between the calculated temperature in the indoor air and 0.5 m into the concrete, which also shown with measured values in Figure 12. In other words, the assumed heat conductivity and heat capacity of the concrete seem to fit well. Thus, the concrete is heated/cooled relatively quickly under the influence of surrounding air.

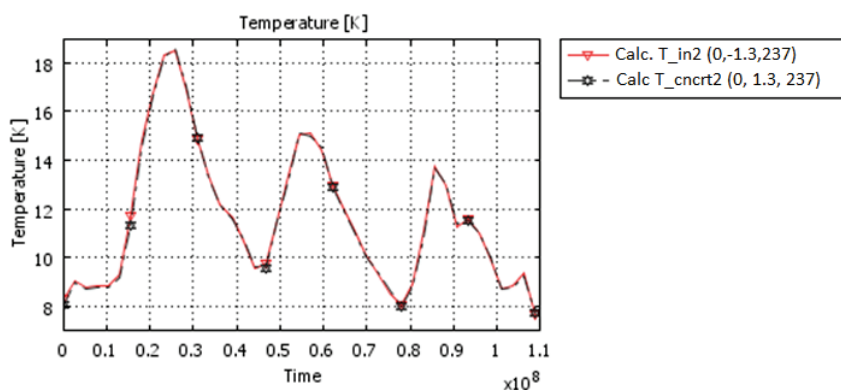


Figure 118 Calculated temperatures T_{in2} and T_{cnrc2}

In the following, the first measured movements of the monoliths M18 and M38 (Figure 93) are compared with calculated movements from a calculation model for a period 1, during 3/12-2012 to 29/4-2015 when measured values are present. Then,

movements are calculated for a subsequent period 2 with fictitious temperatures. Look for calculation times before and after $0.75 \cdot 10^8$ sec respectively in Figure 105.

Figure 119 shows how the crack motion in a fictitious crack is calculated. At the time t_0 , the crack sensor is assumed to be attached at two points on either side of the crack, (x_1, y_1) and (x_2, y_2) . At time t , the concrete is assumed to have deformed into a new position, whereby the crack sensor has followed into two new positions. The Pythagorean Theorem gives the length between the attachment points for the two different points in time and the difference is assumed to be caused by the crack movement. It should be noted that the absolute principal movement of the crack sensor is believed to occur due to a movement in the crack and not that the concrete on either side of the crack is stretching significantly. The attachment points should be placed slightly away from the visible crack as it is not known how the "crack" actually looks inside the concrete. It can be thought of as something of a crack zone. But as mentioned, the measured movement is calculated in the same point as in the calculation model, so the "crack movement" that is calculated should be relatively valid.

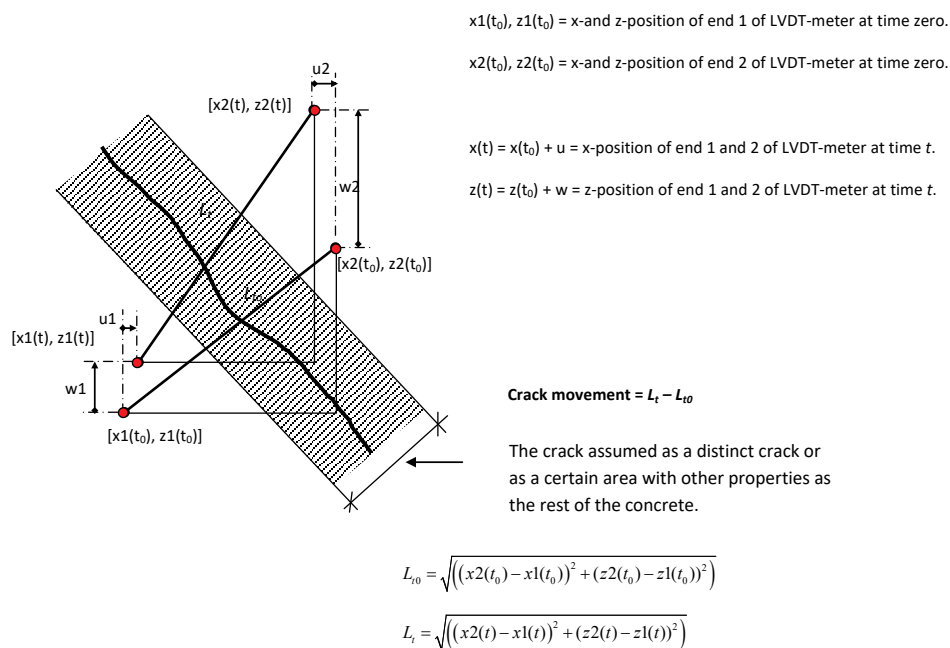


Figure 119 Methodology for estimating movements in a fictitious crack.

Since the upstream water surface lies quietly at the MRL, it is only temperature variations that cause the movement variations. No ice load is assumed because ice protection is available.

The temperature variations that are taken into account during period 1, 3/2-2012 to 29/4-2015, are partly measured water temperature T_{water} towards upstream side, partly assumed rock temperature T_{rock} , as well as measured indoor temperature T_{in} . The insulating wall completely covers the monolith so that no outdoor temperature T_{out} is assumed to affect the monolith. The bridge and the buttresses below the bridge are not included in the model.

For period 2, fictitious temperatures are assumed during a calculation year with maximum summer temperature + 32 °C and minimum winter temperature -43 °C, in order to investigate the influence on the movements during a possible and design significant year in the future. During this period, the assumed boundary conditions T_{water} , T_{out} and T_{rock} are applied, after which T_{in} is calculated in the 3D temperature model as seen above.

Figure 110 shows estimated deformation in summer before the new insulating wall was mounted. The dam bends in the upstream direction during the summer and downstream in the winter.

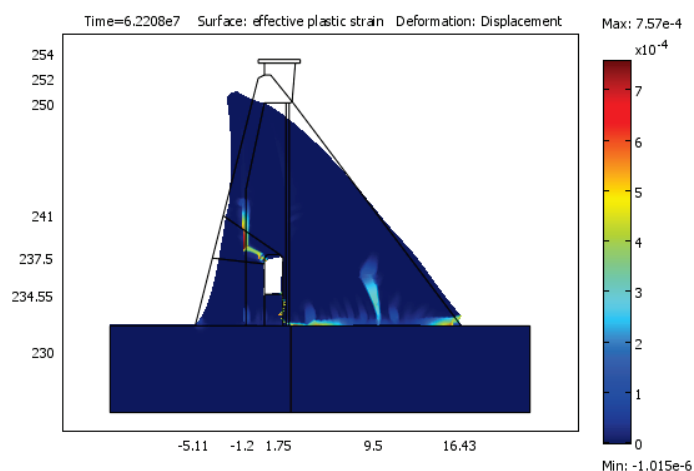


Figure 110 Deformation and plastic strains during a summer day before a new insulation wall was mounted.

Figure 111 shows the calculated deformation in summer after the new insulation wall was mounted in 2012. It is no longer as clear which way the dam bends, it is raised slightly as the warmer water and air expand the monolith upwards.

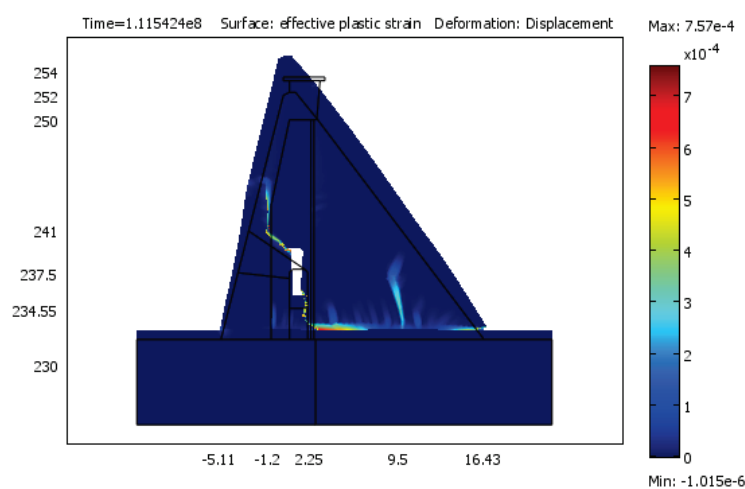


Figure 111 Deformation and plastic strains during the summer of 2014, after a new insulation wall had been mounted.

No further plastic strains, i.e. growth of cracks, is obtained in the calculations after the insulating wall was mounted autumn 2012.

In the calculated case, the water temperature during the period 3/12-2012 and 29/4-2015 has had the actual measured water temperature in front of the dam as input values.

Figure 113 shows the calculated movements in the crack at sensor S1 placed on the buttress, see Figure 112. The movement is a bit dependent on where along the calculated crack the sensor is assumed to be mounted, s1a, s1b or s1c, slightly different values are obtained for the calculated movements. At the location s1a, best correspondence with the measured values of the sensor S1 is obtained. According to photos, this mode corresponds best also for the real sensor. The calculated movement (blue line with blue squares) corresponds well with the measured one (red line) for Period 1, as long as measured values are present.

A little uncertainty remains as to how well cracked the front slab is in reality. The calculation gave that the front slab did not burst substantially, but instead the crack continues straight up into the buttress, which can be seen in the figure.

During Period 2, with fictitious assumed temperatures T_{out} and T_{water} , the calculated crack movement is shown with max. 0.20 mm and min. -0.06 mm in summer and winter respectively.

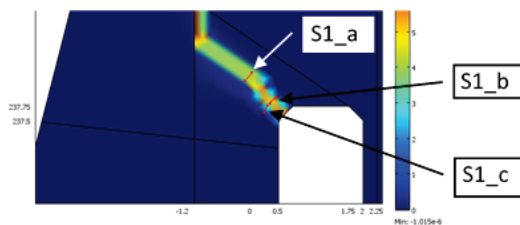


Figure 112 Points (red) where calculated values for sensor s1 are obtained.

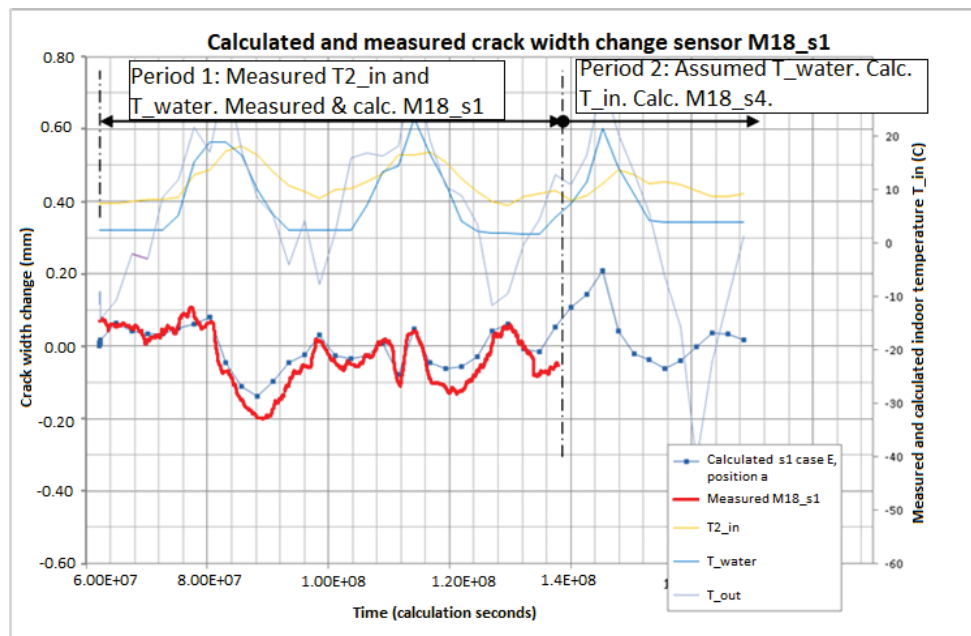


Figure 113 Calculated and measured movements. Temperatures included in the calculation are shown as information.

Since the calculation model can now be considered relatively valid, a calculation of the crack movements at sensor S1 before the new insulating wall was mounted in 2012 was also carried out. Figure 114 shows calculated crack movements at sensor s1 for an imagined extreme year, before the new insulating wall was mounted. The crack motion during an assumed extremely warm and cold summer and winter respectively and without the new insulating wall (blue line) may have had the order of magnitude of + 1.2/-0.2 mm, which is considerably more than the above calculated 0.20 and -0.06 mm with the new insulating wall (red line). The stresses must therefore have dropped significantly with the new insulation wall.

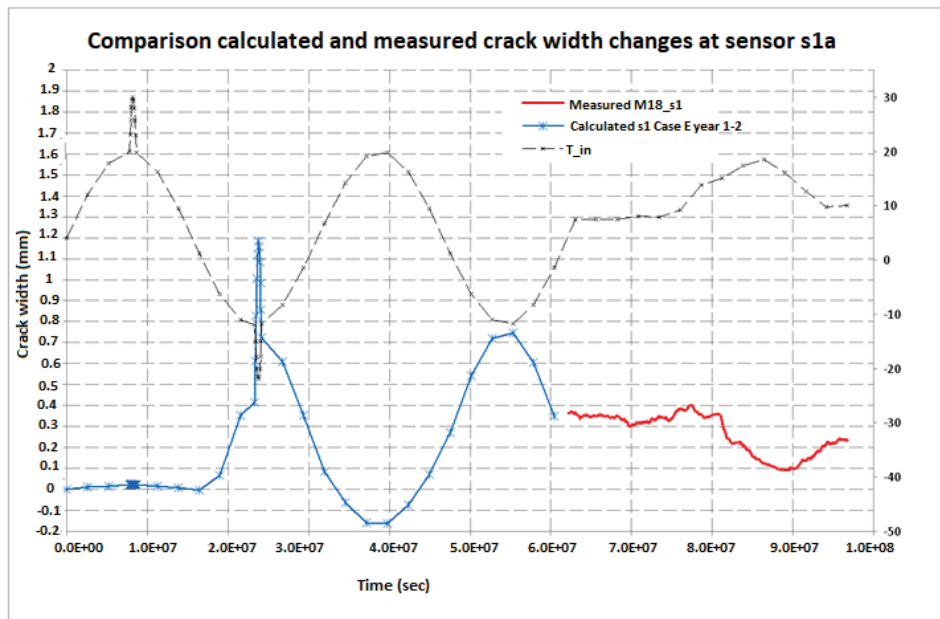


Figure 114 Calculated crack movement (blue line) at sensor s1 for a hypothetical T_{in} without a new insulation wall, compared to measured movement (red line) after a new insulation wall was mounted in 2012.

In the same manner the crack movements were calculated for sensors 2-5, see Figure 115-Figure 118, which gave a good correspondence to the measured values, however slightly dependent on where along the crack in the model it was measured, since the strain in the cracks is not distinct but varies slightly along the crack.

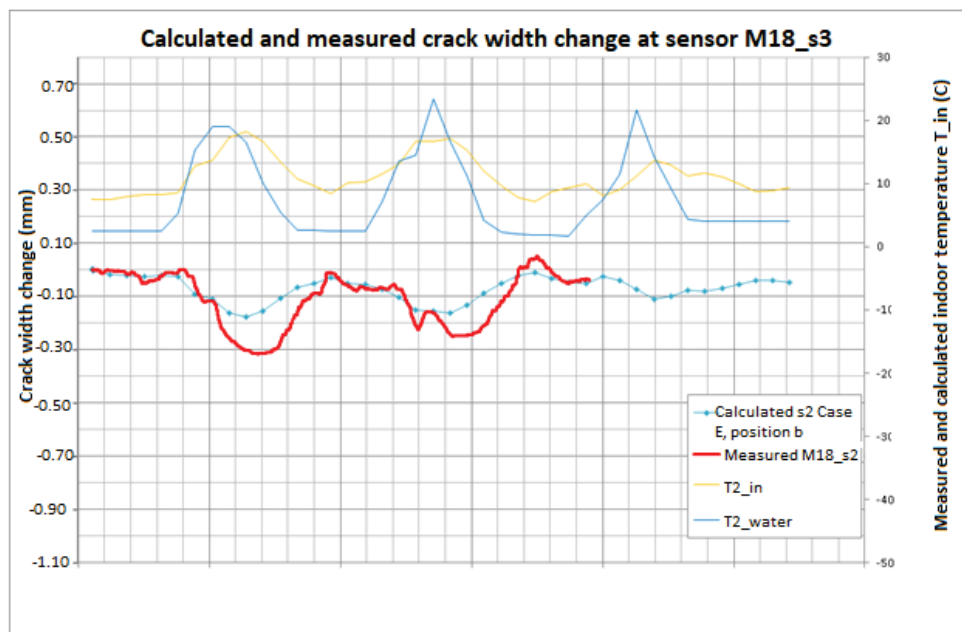


Figure 115 Study 2016: Calculated and measured movements. Temperatures included in the calculation are shown as information.

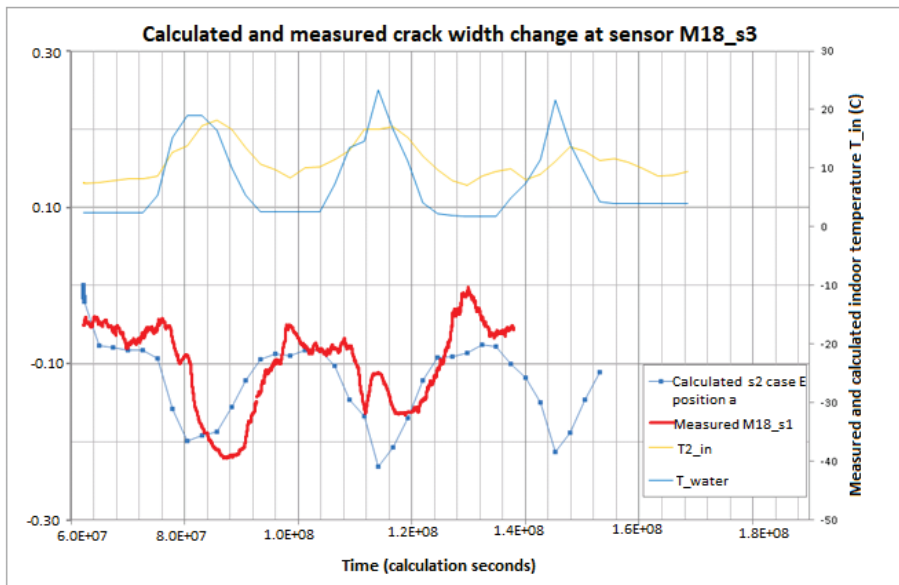


Figure 116 Calculated and measured movements. Temperatures included in the calculation are shown as information.

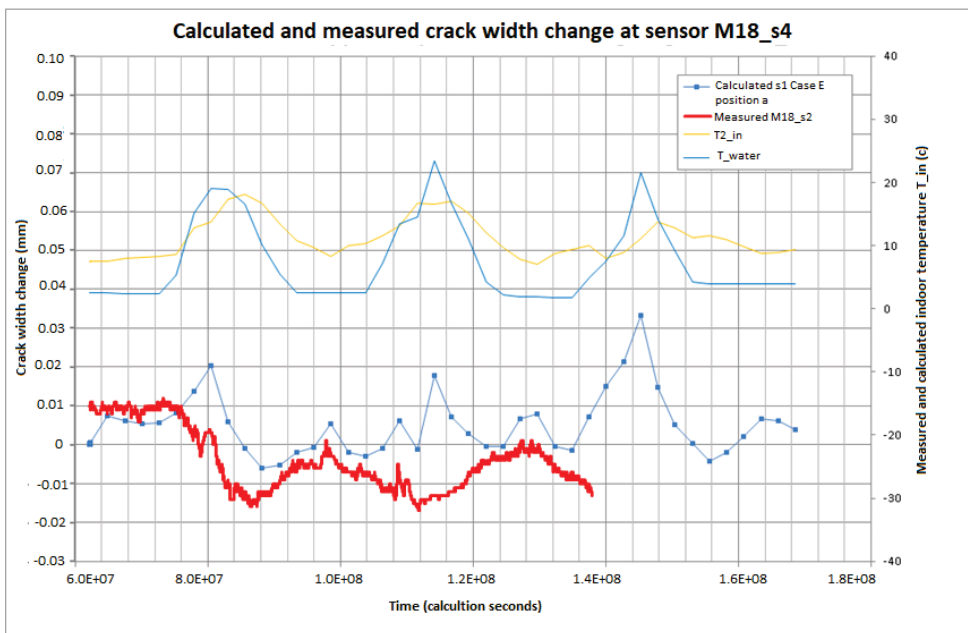


Figure 117 Calculated and measured movements. Temperatures included in the calculation are shown as information.

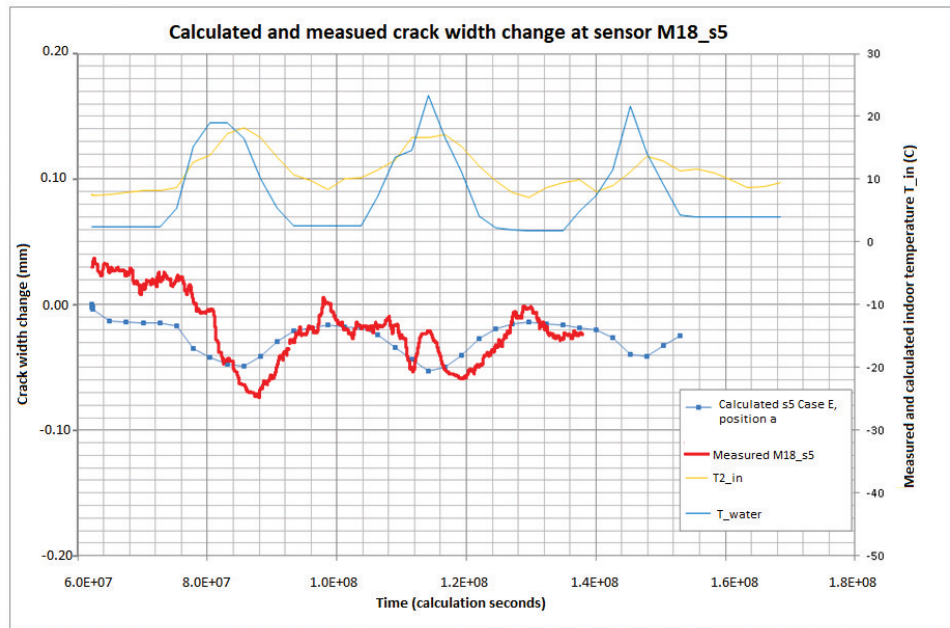


Figure 118 Calculated and measured movements. Temperatures included in the calculation are shown as information.

Figure 119 and Figure 120 show the calculated movements in the crack at the sensor S6 and respectively. S7 (Figure 121). They do not correspond well, which may be due to an overestimation of the calculated crack between monolith and rock. In reality, there may not be such a crack. Or maybe the sensor is not attached deep enough into the rock, so that the sensor and the part of the rock it is attached to actually follow the monolith, thus the sensor does not reflect the difference between the rock and the monolith.

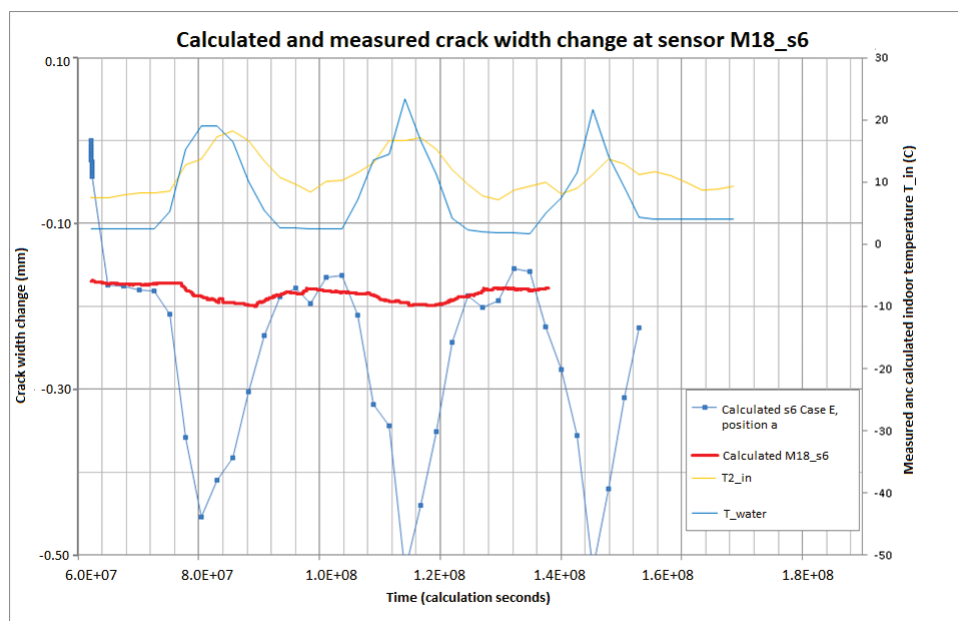


Figure 119 Calculated and measured movements. Temperatures included in the calculation are shown as information.

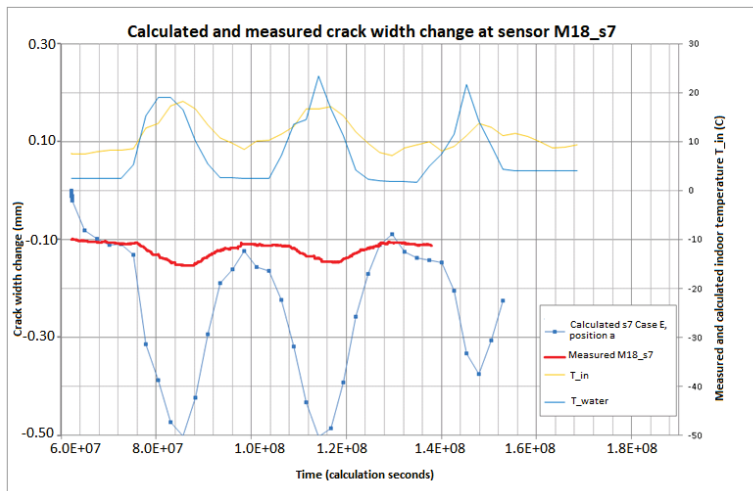


Figure 120 Calculated and measured movements. Temperatures included in the calculation are shown as information.

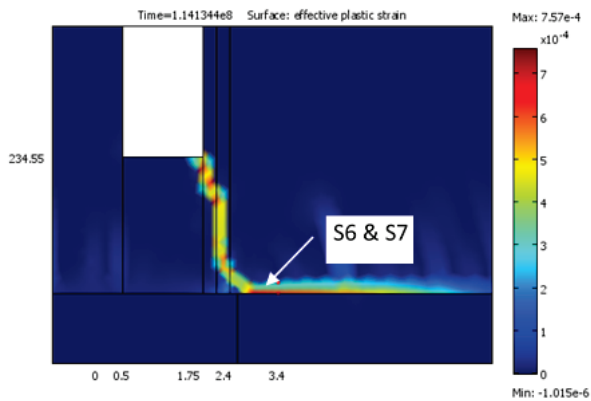


Figure 121 Points (red) where calculated values for sensor s6 are taken.

Figure 122 shows calculated (blue line with squares) crest movements before and after a new climate wall was mounted in 2012, as well as measured crest movements (red line) with the pendulum during the same period. It can be seen that calculated crest deflection corresponds well to measured values.

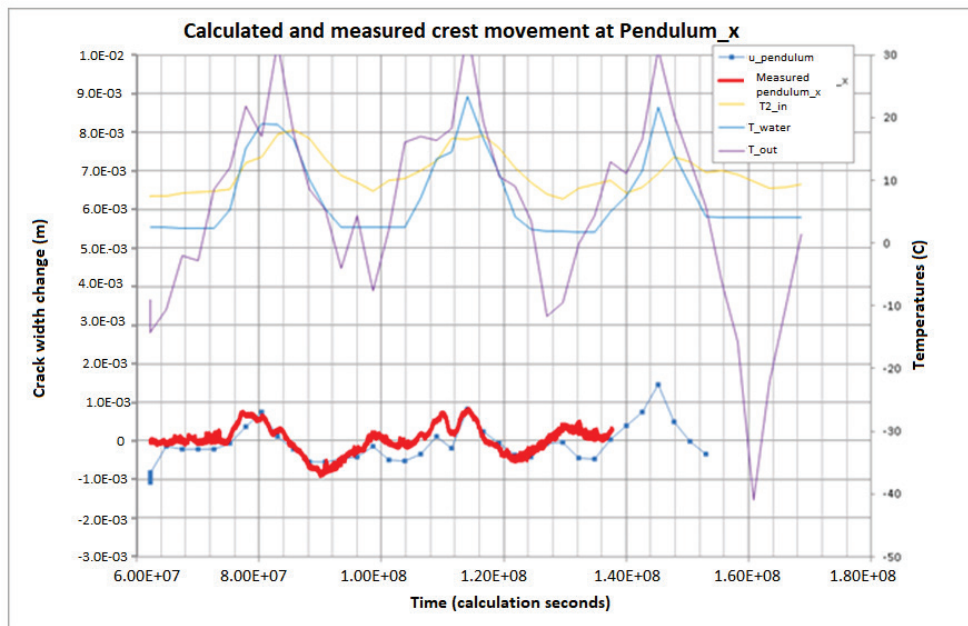


Figure 122 Measured (green line) and calculated (case A-E) crest movements and temperature on the inside of the climate wall.

Figure 123 shows calculated crest movements (blue line) in the direction of current during an extreme year, before the new insulating wall was mounted. The green line during Period 1 shows the same as the red line in Figure 122 at the same time period. The crest movement during an assumed extremely warm and cold summer and winter respectively without the new insulation wall may have been in the order of + 13/-5 mm, which is considerably more than the above calculated 1.5 and -0.5 mm with the new insulation wall and an extreme year. The stresses must therefore have dropped significantly with the new insulation wall.

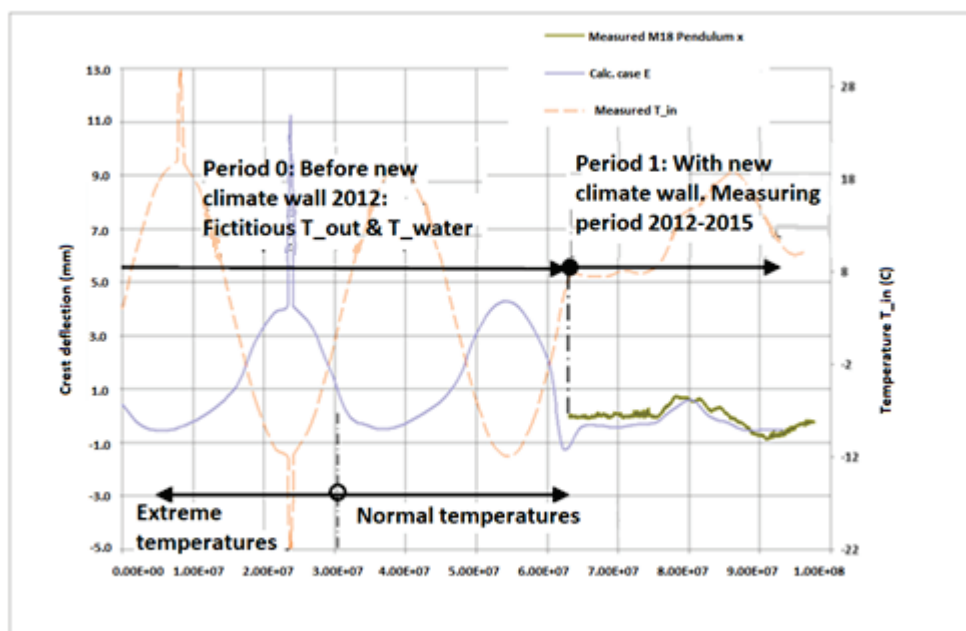


Figure 123 Measured (green line) and calculated (case E) crest movements Ekström (2014)

Figure 124 shows changes in the crest deflection at the various assumed ice loads 154, 200 and 300 kN/m. The values are not matched by values in RIDAS [3], [4], but are assumed to perform a sensitivity analysis. RIDAS [3], [4], says 200 kN/m. Here it is assumed that the ice load can attack during a heating phase on the late winter, e.g. at the calculation time 0.73×10^8 , 1.02×10^8 or 1.37×10^8 sec, see the dashed red rectangles in Figure 125. At most, there will be a difference of about 0.2 mm between 154 and 300 kN/m at the calculation time 1.57×10^8 sec.

Compared to calculated differences of 18 mm and 2 mm between summer and winter due to temperature movements, before and after a new insulating wall respectively, it is small and negligible. In other words, the ice load does not significantly affect the crest deflection, but it is temperature variations that in all essentials cause the crest to bend back and forth.

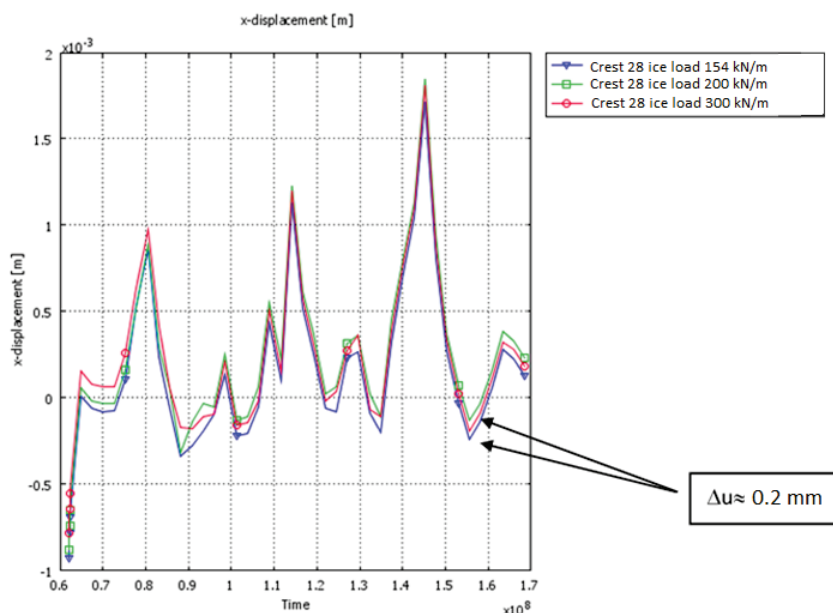


Figure 124 Calculated crest deflections in the x-direction (the direction of the current), at various assumed ice loads.

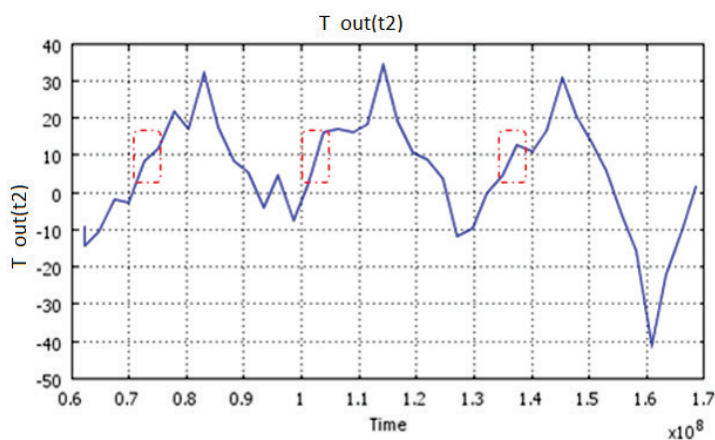


Figure 125 Measured outdoor temperatures years.

One way of analysing the cause is to perform a fracture mechanical calculation, which was carried out above.

Another way can be according to chapter 3.5.4 in the main document, with distinct cracks with special features inserted in the model.

A third way of assessing the safety of a cracked dam monolith can be to calculate the shear and normal stress in the intended crack planes, where cracks can be observed in reality and then compare with calculated shear capacity in the cracks according to "force transfer through joints" in BBK 04, section 3.11, which should be applicable in this context. This method is used in this section to estimate the risk of the cracked parts completely splitting, causing the monolith to lose some of its stability since there is no longer any interaction between the two parts.

The cracks are assumed to correspond to "rough surface" according to BBK 04, section 3.11. They are not believed to be so wide that the friction between the crack walls has been lost.

First, the stresses in the conceived crack plane in the FEM program are calculated, assuming completely linear elastic conditions, that is, "there are not really" any cracks and that no degradation of strength or E-modulus is found in the cracking area. This is a simplification but can be accepted when the cracks are not wide.

The calculated stresses in the crack plane are then compared analytically with the shear capacity in the crack plane, assuming "power transfer in joints" in BBK04 [6], section 3.11. If the calculated shear stresses exceed the capacity, there is a risk of continued cracking and a risk of reduced interaction in the crack plane. It is then assumed that there is a risk that the monolith no longer acts as an entire monolith, but divided into smaller parts. I.e.

- Calculate shear and normal stresses in the current crack plane assuming linear elastic material, i.e. no plastic damage model is used.
- Use equations force transfer through joints, rough surface in BBK04 [6].
- Shear stress > capacity according to BBK?
 - o Yes: Risk of further cracking and not completely monolithic behaviour of the pier.
 - o No: No greater risk of the above happening.

When calculating the stresses, it can be discussed how the monolith should be attached to the rock below, e.g. along overturning lines or fixed to the rock.

- a. The structure laid out on two lines as in stability calculations. This case overestimates the stresses in the crack plane.
- b. Design constructed and fixed to underlying bedrock. In this case, the rock volume is locked in its lower boundary in the model. This case underestimates somewhat the stresses in the cracks, because in reality the concrete may separate slightly from the rock at tensile stresses in between, and then the stresses in the pier may increase slightly.

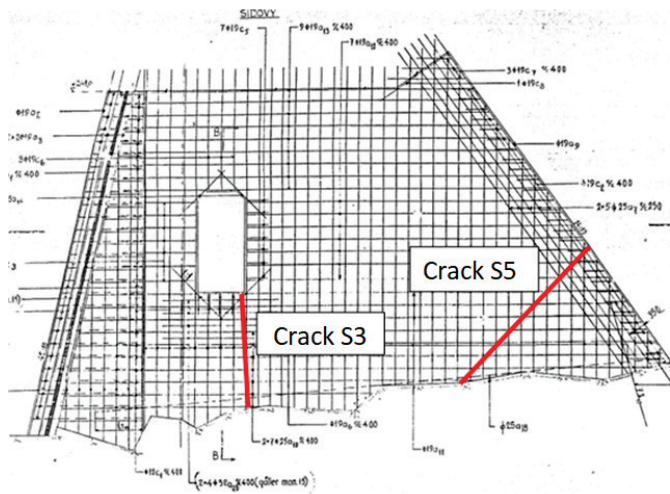


Figure 126 Reinforcement in monoliths 15-18 (drawing PL 01-007a, 1955).

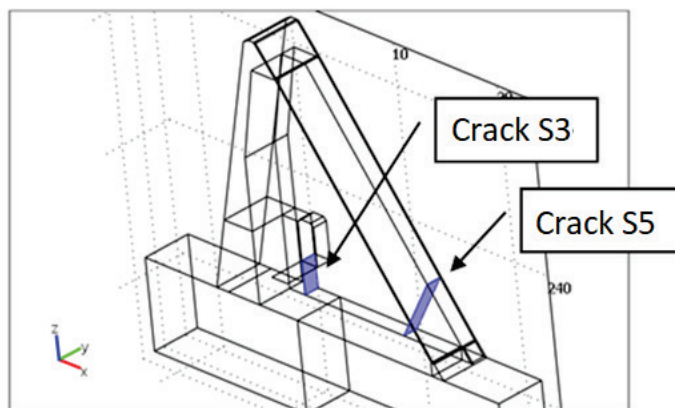


Figure 126 Cracks S3 and S5 In pier 1.

The following load cases were calculated in the linear-elastic 3D model:

- Load case LC1a (uws=MRL, ice load 200 kN/m and $T_{out}=+10^{\circ}\text{C}$) normal load case
- Load case LC1b (uws=MRL, ice load 200 kN/m and $T_{out}=+15^{\circ}\text{C}$) normal load case
- Load case LC14a (uws=MRL, $T_{out}=+33^{\circ}\text{C}$) Exceptional load case
- Load case LC14b (uws=MRL, $T_{out}=-43^{\circ}\text{C}$) Exceptional load case

At the studied cracks S3 and S5 (Figure 126 and Figure 127) the requirements were met, i.e. the shear stress capacity in the cracks exceeded the calculated shear stresses. Thus, the monolith, despite its observed cracks, can be said to constitute a monolith and does not affect the total stability calculated as a rigid body according to RIDAS [3], [4].

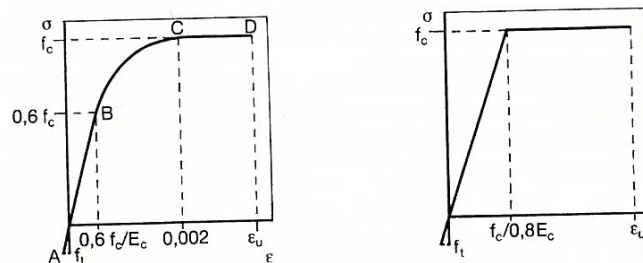
APPENDIX F – NON-LINEAR MATERIAL MODELS USED IN THE REFERENCE PROJECTS

CONCRETE

Tensioned concrete is fairly straight-line elastic up to failure where the limit strain ε_u is of the order of 0.1-0.2 ‰ (1-2·10⁻⁴) (Hillerborg, 1994). Nilsson (1983) states linear ratios up to about 70% of the tensile strength.

Compressed concrete has a much more curved, non-linear, stress curve up to maximum absorbable stress. The limit strain ε_u is then of the order of 2-3 ‰ (20-30·10⁻⁴). Straight-line conditions have up to 30 to 60 of the compressive strength. (Hillerborg, 1994).

Strength can e.g. be defined as the maximum compressive or tensile stress that can occur in a stress-deformation relation, e.g. according to Figure 128, which shows a uniaxial compressive stress state. As the load increases towards the strength (f_c), the system becomes unstable, the point of discontinuity, released energy becomes greater than the ability of the concrete to absorb this energy, the crack growth continues at a rapid rate and the material collapses. The point for this discontinuity, point C in the figure, for brittle materials such as concrete is analogous to the yield point for extensible, tough materials (Möller et al., 1994).



(a) Stress-strain for compressed concrete (b) Simplified stress-strain for compressed concrete

Figure 128 Stress-deformation curve for uniaxial compressive stress in concrete according to BBK (fig 13.2:20 in Hillerborg, 1994).

The strength of the concrete depends on several factors, e.g. inherent concrete properties such as water/cement ratios and water/air/cement ratios, cement type, admixture, aggregate type, maturity factor, curing conditions, casting direction and external influences such as temperature, temperature gradients, humidity condition and loading rate and loading duration, alternating loads, etc. The testing method and the shape and size of the test specimen also affect measured strength. The strength determined according to any standardized test method gives the potential strength of the concrete at 28 days (Möller et al., 1994). The real strength of the concrete in the existing structure is another because of the conditions during casting and curing differ and that the concrete has been able to cure for a long time.

The concrete may also have sustained damage during the operating phase, which has reduced the strength.

In reality, a multi-axial stress state usually exists. Pressure or tensile strength will then increase or decrease relative to the uniaxial strength. Figure 130 shows some experimental relationships developed by Kupfer et al. (1973). In the figure, it can be seen that with simultaneous compressive loading, the strength becomes higher while in the case of compression-tension or tension-tension, the relatively usable strength decreases. Figure 130 shows the same data but in stress-strain relationship.

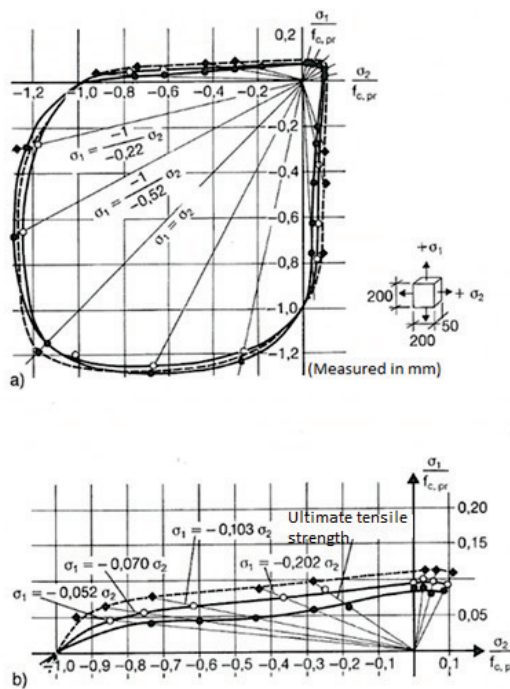


Figure 129 Strength in concrete at several strength levels at biaxial load according to Kupfer (1973), se fig 11.4:18 in Möller et al. (1994).

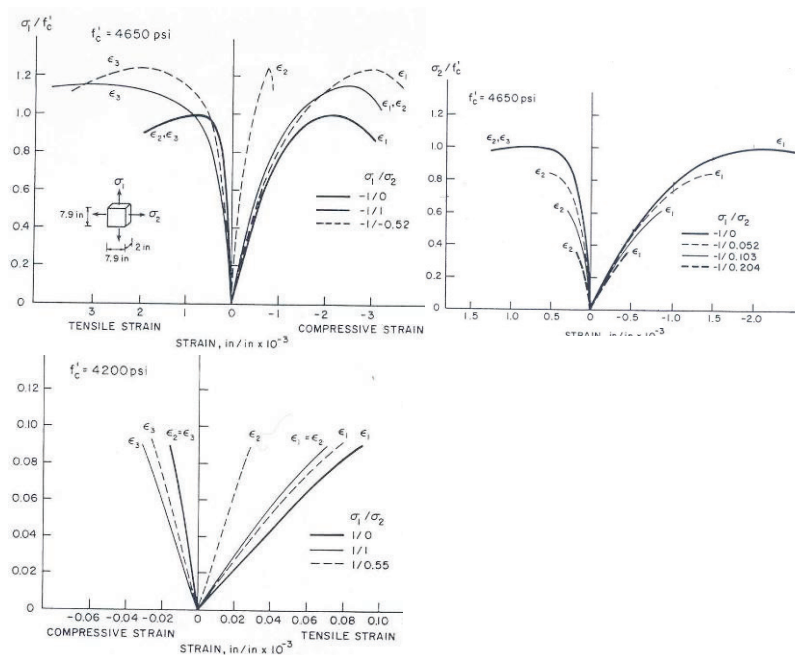


Figure 130 Stress-strain relation Kupfer et al. (1973).

Failure criteria for concrete can e.g. be (Möller et al., 1994):

1. Stress criteria with limits for principal stresses.
2. Strain criteria with limits for principal strains.
3. Energy criteria with limits for maximum total energy absorption.
4. Failure model criteria.

The material outside the fracture zone is still homogeneous and the strain ε is the same within adjacent parts. Increasing local deformation w occurs within the fracture zone, which is the total additional deformation of the fracture zone. This deformation cannot be stated as a relative deformation, but must be stated as an absolute deformation, e.g. in mm. One consequence of this is that there is no clear connection between σ and ε after the passage of the maximum point. A connection describes the σ - w -curve for the fracture zone and a correlation describes the σ - ε -curve for the remaining, non-cracked material. If the stresses are calculated on the assumption of continuum, some stress concentrations go towards infinity around the tips of the cracks. It is then not possible to use traditional solid mechanics, but fracture mechanical principles need to be used. (Hillerborg, 1994)

For tensioned concrete, the failure is initiated by the fact that micro-cracks begin to form mainly perpendicular to the tensile stress direction. The micro-cracks grow together into larger cracks, which eventually leads to failure. When forming the cracks, energy is released which must be absorbed by the remaining concrete, and for reinforced concrete also by the reinforcement. The more energy that can be absorbed, the tougher the material is.

For concrete under compression, the conditions are more complicated than for concrete under tension, because the compressive failure occurs during heavy cross-expansion and cracking in the stress direction.

For large and relatively thin structures, the failure is more of the brittle failure type since the large fracture energy released cannot be absorbed by the relatively thin concrete.

When casting large and rough structures such as dams, if necessary measures are not taken against this, cracks will occur during the cooling of the concrete. Surface cracks can occur if the temperature gradient between the surface and the interior of the concrete becomes too large. Through-going cracks can occur if the temperature gradient between the current design and the rock or the previously cast part becomes too large.

Cracking means that cross-sectional forces are redistributed to other concrete parts and/or to reinforcement, if such exists. The static system for all or part of the structure can thereby change and often deteriorate.

Cracks in dams usually mean poorer resistance to e.g. water penetration with consequent risk of leaching, frost damage or reinforcement corrosion. Experience values for acceptable crack width for self-healing are according to Lohmeyer (1984), reproduced in Petersson (1994), 0.15 mm for the water pressure gradient $\nabla P \leq 5$ m/m and 0.10 mm for $\nabla P \leq 10$ m/m.

REINFORCEMENT

Ks40 steel has often been used in the existing dams. This steel is hot rolled. For a hot-rolled rod Ks400, which is basically the same as Ks40, the working curve looks like the ones shown in Figure 131 a and b. The strain at the maximum failure load, the limit strain ε_{gr} , is about 16% for the Ks400s and the elongation at failure load, at the measuring lengths 10ϕ and 5ϕ , are 20 and 24% respectively (Tepfers & Törnwall, 1994).

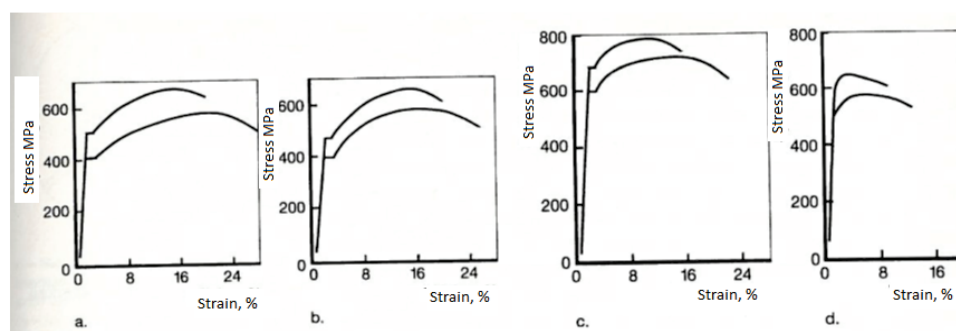


Figure 7.2:3 Typical minimum and maximum curves
a) Ks400S, ϕ 10mm. b) Ks400S, ϕ 25 mm. c) Ks600S, ϕ 16 mm. d) Ps50, ϕ 6 mm.

Figure 131 Typical minimum and maximum curves for steel reinforcement (Tepfers Törnwall, 1994)

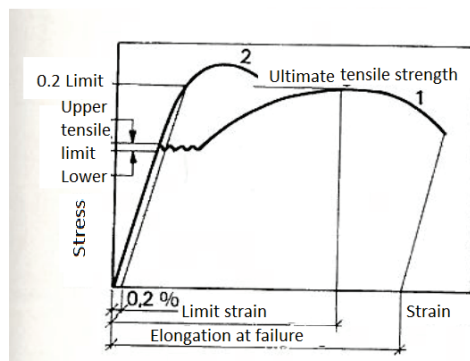


Figure 7.2:2 Stress-strain diagram for
 1. Hot-rolled bar
 2. Strain hardened bar

Figure 132 Conceptual working curve for steel reinforcement

The concrete, the rock and the reinforcement are modelled with flat stress models in this report. Especially for the reinforcement, this is a relatively rough simplification, but in the context it should be sufficient.

PLASTIC MATERIAL MODELS FOR CONCRETE

Basic plastic models such as Drucker-Prager can usually only be very rough approximations when it comes to load limit state analyses of concrete. The utility of plastic models in terms of concrete is actually very limited. Only for extremely high hydrostatic pressures, concrete has a plastic yield point. Instead, the concrete softens after having reached the maximum stress, which causes a localisation of material failures that is not simultaneous over a somewhat larger area. This means that there are effects of size, which is important for larger structures. Therefore, plastic yield conditions must be used together with realistic models for locating and propagating softening non-elastic zones, and they must be linked to certain characteristic lengths that are a material property (Jirásek & Basžant 2001).

Concrete is an anisotropic pressure-sensitive material with a much lower tensile than compressive strength. Main tensile stress exceeding the tensile yield limit causes formation and propagation of cracks in the same direction as the main tensile stress. Tensile cracks usually cause a breakdown of the E-modulus, the concrete "softens", which is not included in standard plastic deformation models, which, when unloaded, follow the initial E-modulus. Degradation of the E-modulus can be included in fracture mechanics or damage mechanics. The so-called "smeared crack models" can constitute a special type of damage model. Yield theoretical models can be used in monotonic increasing loads, provided that the energy release at cracking and the characteristic length are included in a good way. (Jirásek & Basžant 2001)

The deformation of the material within the fracture zone can only, as mentioned above, be stated as an absolute deformation and cannot be stated as a relative deformation. A trick that is often used in calculations is to use crack band models

where the fracture zone length w is related to a crack band width, h . After that the deformation w can be “smeared” across this width, and a fictitious strain is obtained

$$\varepsilon_{pl} = w/h \quad (1)$$

The larger h is, the steeper the slope of the downward working curve. The downward part of the curve must not be too steep, i.e. the element must not be made too big. The elastic energy released for each increase in strain within the element must be lower than that consumed. For the condition to be met, for the type of curve shown in Figure 134b, the following condition must be met:

$$h \leq \frac{2EG_F}{f_t^2} = 2l_{ch} \quad (2)$$

E = E modulus (Pa); G_F = fracture energy (Nm/m²); l_{ch} = the characteristic length of the material and is about 300 mm for normal concrete, which gives the upper limit of the size of the element. In practice, much smaller elements may need to be selected because the actual curve is significantly steeper than the slope of the linear approximation. In addition, elastic energy is released from other nearby elements. (Hassanzadeh, 2006)

The stress-strain relationship for a plastic, isotropic damage model can be written (Lee & Fenves, 1998):

$$\begin{aligned} \sigma &= (1-d)\sigma' \\ \sigma' &= (1-d)\mathbf{E}_0 : (\varepsilon - \varepsilon_{pl}) \end{aligned} \quad (3)$$

where d = degradation of the E-modulus (-); \mathbf{E}_0 = initial, “undamaged” E-modulus (Pa); ε = total strain (-); and ε_{pl} = plastic strain (-).

The failure criterion G_f for concrete should be calibrated against experimental data. This is not done in the current work. In practice, because the cracks formed up in the calculation models, there was no big difference if G_f varied.

Figure 133 shows a number of different theoretical failure criteria compared with experimental data in Jirásek & Basžant (2001).

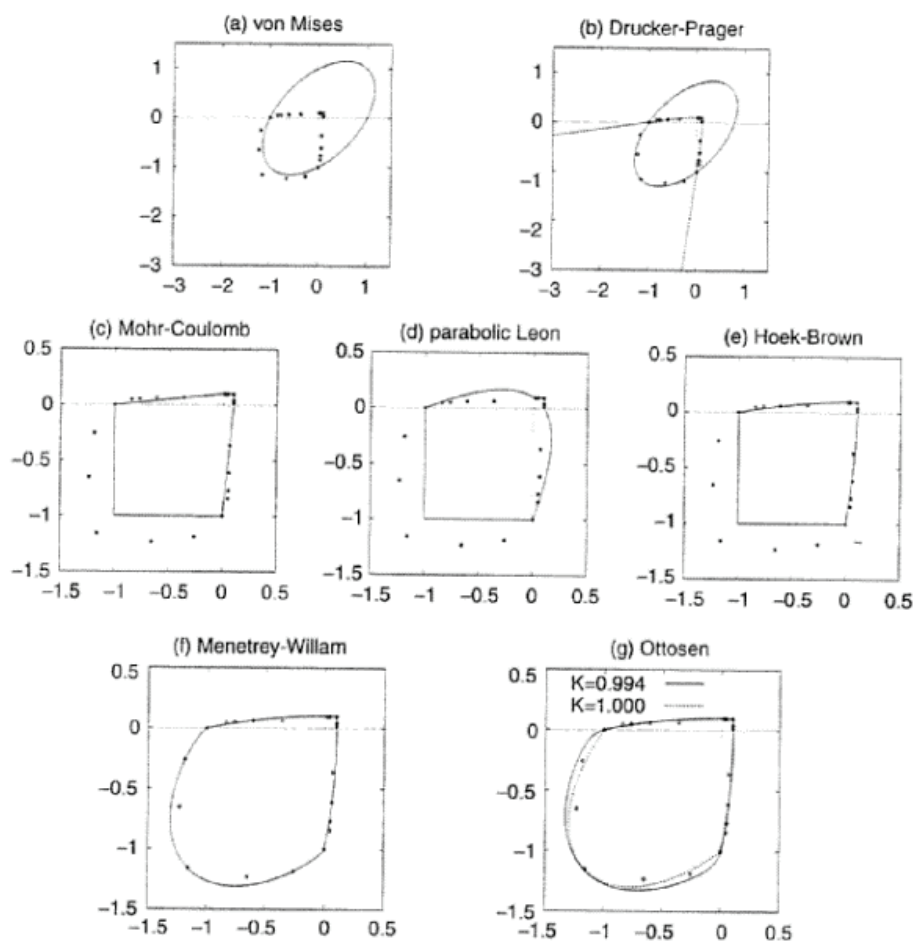


Figure 133 Biaxial failure envelopes of different yield criteria and plotted by Jirásek & Basžant (2001) in the normalised main stress plane (σ_1/f_c , σ_2/f_c) and compared with experimental data from Kupfer & Gerstle (1973).

Drucker-Prager's failure criterion is normally written as:

$$F = \alpha \cdot I_1 + \sqrt{J_2} \leq c_{tot} \quad (4)$$

$$I_1 = \sigma_x + \sigma_y + \sigma_z \quad (5)$$

$$J_2 = \frac{1}{2} \cdot (S_x^2 + S_y^2 + S_z^2) + \tau_{xy}^2 + \tau_{yz}^2 + \tau_{xz}^2 \quad (6)$$

$$\sigma_m = I_1/3 \quad (7)$$

$$S_x = \sigma_x - \sigma_m, \quad S_y = \sigma_y - \sigma_m, \quad S_z = \sigma_z - \sigma_m \quad (8)$$

F = comparative stress according to Drucker-Prager, Pa (1952); I_1 , J_2 = stress invariants; σ_x , σ_y , σ_z = normal stresses in x-, y- and z-direction; τ_{xy} , τ_{yz} , τ_{xz} = shear stresses in the different directions; and c_{tot} = current yield stress. For ideal plastic materials, c_{tot} is constant, and for softening materials, c_{tot} decreases with the current accumulated plastic strain.

By replacing I_1 and J_2 at maximum stress at uniaxial tension and uniaxial compression, the following is obtained (Jirásek & Bazant, 2001) for the Drucker-Prager condition:

$$\alpha = \frac{1}{\sqrt{3}} \cdot \frac{f_c - f_t}{f_c + f_t} \quad (9)$$

$$c_{tot} = \frac{2}{\sqrt{3}} \cdot \frac{f_c \cdot f_t}{f_c + f_t} \quad (10)$$

α , c_{tot} = material parameters, f_c and f_t are assumed to be the mean compressive strength and mean tensile strength, respectively. At $f_t/f_c \approx 1$, the expressions (2.12) - (2.18) provide a curve that is an ellipse. At smaller ratios, but above 0.1, the curve approaches Kupfer & Gerstler's data. For smaller ratios, ≤ 0.1 which is common for concrete, the curve goes towards infinity on the compressive side, a hyperbolic distribution, as can be seen in Figure 133b. The other models shown in Figure 133 (Mohr-Coulomb, parabolic Leon, Hoek-Brown, Menetrey-William and Ottosen) more closely connect to Kupfer & Gerstler's data.

One can re-write equation (4) with so-called Haigh-Westergaard coordinates (Jirazek & Bazant, 2001):

$$\alpha \cdot I_1 + \sqrt{J_2} = \alpha \sqrt{3} \cdot \zeta + \frac{\rho}{\sqrt{2}} \leq c_{tot} \quad (11)$$

Where

$$\text{(Jirazek \& Bazant, 2001, D.69)} \quad \zeta = \frac{I_1}{\sqrt{3}} \quad (12)$$

$$\text{(Jirazek \& Bazant, 2001, D.70)} \quad \rho = \sqrt{2 \cdot J_2} \quad (13)$$

A generalised expansion of equation (11) according to Jirazek & Bazant, 2001, eq. (21.7) is

$$c_1 \cdot \zeta + c_2 \cdot \rho \cdot r(\theta) + c_3 \cdot \rho^2 - 1 = 0 \quad (14)$$

Where the so-called *Lode angle* θ is written as

$$\cos 3\theta = \frac{3\sqrt{3}}{2} \cdot \frac{J_3}{J_2^{3/2}} \quad (15)$$

To get a good adaptation to the yield curves according to Figure 129 and Figure 133 (c)-(g), Ottosen (1977) suggested the following function of the Lode angle:

$$r(\theta) = \begin{cases} \cos\left(\frac{1}{3} \arccos(k_2 \cdot \cos 3\theta)\right) & \text{if } \cos 3\theta \geq 0 \\ \cos\left(\frac{\pi}{3} - \frac{1}{3} \arccos(-k_2 \cdot \cos 3\theta)\right) & \text{if } \cos 3\theta \leq 0 \end{cases} \quad (16)$$

For values of the variables c_1 , c_2 , c_3 and k_2 , Table 1 gives some suggestions according to the literature.

Table 1 Values from literature of the parameters c_1 - c_3 and k_2 in equation (2.22) and (2.24).

	CEB-FIP (1991) ¹⁾ s.361 2)	Ottosen (1977) ¹⁾ s.366	1) s. 366	1) s. 366	Tiecheng et al (2003)
c_1	$\frac{0.468}{\bar{f}_c \cdot k^{1.1}}$	$\frac{5.54}{\bar{f}_c}$	$\frac{5.8}{\bar{f}_c}$	$\frac{6.1}{\bar{f}_c}$	$\frac{3.20}{\bar{f}_c}$
c_2	$\frac{1.01}{\bar{f}_c \cdot k^{0.9}}$	$\frac{8.3}{\bar{f}_c}$	$\frac{8.04}{\bar{f}_c}$	$\frac{7.76}{\bar{f}_c}$	$\frac{11.74}{\bar{f}_c}$
c_3	$\frac{0.0556}{\bar{f}_c^2 \cdot k^{1.4}}$	$\frac{0.638}{\bar{f}_c^2}$	$\frac{1.29}{\bar{f}_c^2}$	$\frac{2.03}{\bar{f}_c^2}$	$\frac{1.28}{\bar{f}_c^2}$
k_2	$k_2 = 1 - 6.8(k - 0.07)^2$	0.98	0.994	1	0.980

1) Jirazek & Bazant (2001), 2) CEB-(FIP, 1991): (Jirazek) p.361: $k = \frac{\bar{f}_t}{\bar{f}_c}$

$$\text{(Jirazek) (21.12)} \quad \bar{f}_t = \sqrt{\frac{\bar{f}_c}{6895}} \cdot 6 \cdot 6895 = 498 \cdot \sqrt{\bar{f}_c} \quad (17)$$

$$\text{(Jirazek) (21.11)} \quad \bar{f}_t = \left(\frac{\bar{f}_c - 8}{10} \right)^{2/3} \cdot 1.40 \leq (\text{MPa}) \quad (18)$$

Instead, write equation (14) as

$$\begin{aligned} c_1 / \sqrt{3} \cdot I_1 + c_2 \cdot \sqrt{2} \cdot \sqrt{J_2} \cdot r(\theta) + c_3 \cdot 2 \cdot J_2 - 1 = \\ a \cdot I_1 + b \cdot \sqrt{J_2} \cdot r(\theta) + \frac{c}{f_c} \cdot J_2 - \bar{f}_c = 0 \end{aligned} \quad (19)$$

or expressed as a comparative stress F

$$F = a \cdot I_1 + b \cdot \sqrt{J_2} \cdot r(\theta) + \frac{c}{f_c} \cdot J_2 \leq \bar{f}_c \quad (20)$$

Where

$$\begin{aligned} a &= \frac{c_1}{\sqrt{3}} \cdot \bar{f}_c \\ b &= \sqrt{2} \cdot c_2 \cdot \bar{f}_c \\ c &= 2 \cdot c_3 \cdot \bar{f}_c \end{aligned} \quad (21)$$

That is, when the "comparative stress" F exceeds \bar{f}_c , the material begins to yield. In the case of deformation-hardening and deformation-softening material, the yield stress increases or decreases respectively after the plastic deformation begins. The right-hand side \bar{f}_c of equation (20) is therefore not constant but changes with the

plastic strain. It depends on the size of the strain and whether it is caused by tensile or compressive stresses. Here the yield stress is also referred to as c_{tot} .

Both the concrete and the bedrock are assumed in this work to be plastically deformed at a stress F according to equation (20) where a , b , and c are material parameters, here set to 3, 11 and 2. Compressive and tensile strength are assumed to be 25 and 2.5 MPa respectively. The elastic modulus $E = 30$ GPa, the cross-contraction number = 0.15. The fracture energy G_f is set to 140 N/m, but is varied, a little unrealistically, up to 200 N/m in some calculations, to obtain numerical convergence.

The concrete and the rock are assumed to soften after the stress limit F has been reached with a strength σ according to equation (22) and (b) in Figure 134, i.e. only for tensile failure and not for compressive failure. In this context, this is an acceptable simplification because the compressive stresses are so low relative to the compressive strength that compressive failure according to (a) does not occur. Concrete has about 10 times higher compressive strength than tensile strength in pressure.

$$\sigma = f_c \exp\left(-\frac{\varepsilon_{pe}}{\kappa_{2u}}\right) \quad (22)$$

where f_c = compressive strength (MPa), ε_{pe} = effective (accumulated) plastic strain (-); and κ_2 = factor for how fast the softening takes place (-).

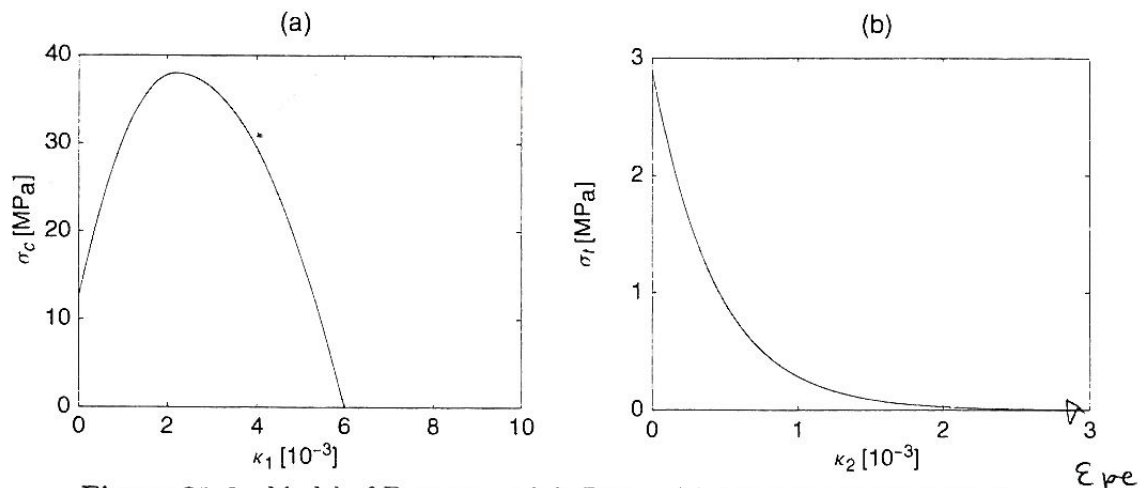


Figure 134 Model from Feenstra och de Borst (1996): a) compression hardening-softening, b) tension softening.

The E-modulus is assumed to be degraded to E_{damage} when the concrete softens, i.e. when unloading and reloading, the E-modulus is smaller than the original E_0 , see Figure 135. With each load that involves a larger accumulated plastic strain ε_{pe} , the E-module further decreases.

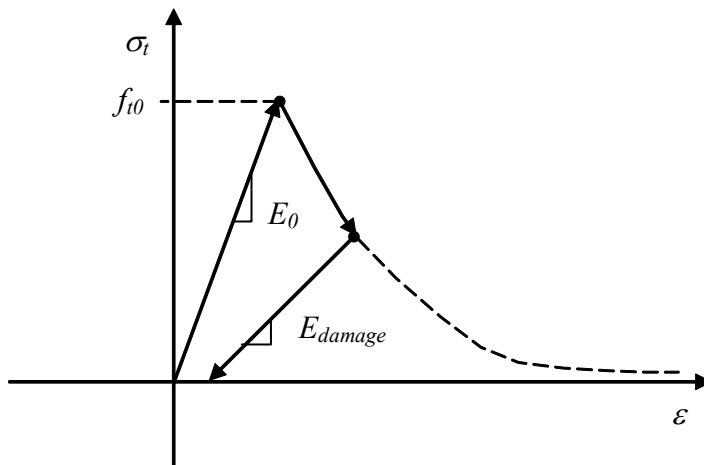


Figure 135 Assumed softening according to (eq. 2.30) and damaging of the E-modulus (ekv. 2.31).

The factor 10 000 has been used generally in the calculation cases, which is an adaptation to data from the literature.

$$E_{damage} = E_0 \cdot (-\exp(\epsilon_{pe} \cdot 10\,000)) \quad (23)$$

The reinforcement is believed to yield ideal-plastically when the von Mises stress in the layer symbolizing the reinforcement exceeds the design load-bearing capacity of $f_{yd} = 286$ MPa.

The exact bond between concrete and reinforcement is difficult to estimate. The more the reinforcement is attached to, "sticking together" with the concrete, the more it follows the stretching of the concrete. If the strain is then large, the strain of the reinforcement will also be large, as will the stress. This is especially true around the crack when the strain is concentrated to a short distance. If e.g. high and over the year changing stresses are achieved in the reinforcement there is a risk of fatigue failure eventually. If also yield in the steel is achieved, the reinforcement can theoretically break apart completely relatively quickly. In reality, the bars slide against the concrete when the force becomes high, see Figure 136.

Here the bond is assumed to follow a simplified model with linear elastic springs in the x and y directions (horizontally and vertically). The springs are assumed to soften with increasing slip between the concrete and the reinforcement. The springs in the x-direction are assumed to be connected according to

$$\text{Spring}_x = \text{Spring}_0 \cdot \exp(-\text{slip} \cdot \text{df_const}) \quad (24)$$

$$\text{Slip} = \text{abs}(u_2 - u) \quad (25)$$

where Spring_x = adhesive force between concrete and reinforcement in the x direction (N); Spring_0 = original adhesive strength (N); slip = slip between the concrete and the reinforcement (m); u, v = the movement of the concrete in the x and y directions; u_2, v_2 = the movement of the reinforcement in the x and y directions; and df_const = degradation coefficient (1/m). Springs in the y-direction are correspondingly adopted.

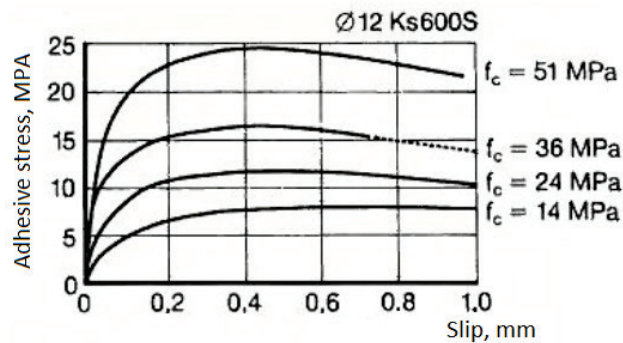


Figure 136 Bond – slip curves determined through tensile testing with short bond length for Ks600S reinforcement with the diameter 12 mm for 4 different concrete strengths (Berggren, 1965 presented in Tefers & Törnwal, 1994)

One disadvantage of the model Spring_x and Spring_y respectively is that it is elastic. If "slip" decreases again then Spring increases again, down to Spring₀ if slip becomes zero. In reality, the bonding is damaged to a lower value.

Another disadvantage is that for large slips, Spring decreases to an unrealistically low value, that is, the reinforcement takes too little load at large slip compared to reality.

REFERENCES:

- Hassanzadeh, M. (2006), "Spruckna betongdammar, översikt och beräkningsmetoder", kap. 2, Elforskrapport 06:29. (In Swedish)
- Hillerborg A. (1994), "Deformationer under last", ur Betonghandbok Material, Svensk Byggtjänst, Stockholm. (In Swedish)
- Jirásek M., Bazant Z.P. (2001), "Process zone resolution by extended finite elements", Fracture Mechanics of Concrete Structures", p. 805-808, Balkema, 2001.
- Kupfer H., Hilsdorf, K., Rusch H. (1969)
- J Lee, GL Fenves (1998), "Plastic-damage model for cyclic loading of concrete structures", Journal of engineering mechanics 124 (8), 892-900
- Nilsson L-G. (1983), "Konstitutiva teorier", Handboken Bygg Allmänna grunder kap. A19, LiberFörlag, Stockholm. (In Swedish)
- Möller & al. (1994), "Hållfasthet", ur Betonghandbok Material, Svensk Byggtjänst, Stockholm.
- Petersons N. (1994), "Sprickor", ur Betonghandbok Material, Svensk Byggtjänst, Stockholm.
- Tefers R., Törnwall B. (1994), "Armering", ur Betonghandbok Material, Svensk Byggtjänst, Stockholm.

STRUCTURAL SAFETY OF CRACKED CONCRETE DAMS

Here the goal has been to develop a Swedish guideline to define status and both current and future safety level for a cracked concrete dam with the purpose to create a uniform and reliable methodology for condition control and guidance for planning of measures.

Cracks and cracking in concrete dams can give a need to determine the current status from a dam safety perspective and an estimation on remaining service-life taking the cracks into consideration. A comparison between the current status and the formal requirements should be made.

Condition control is a prerequisite to define the current status and future development and to do this there is a need for knowledge on what type of cracks has occurred and the reason for cracking. To do this there is a need to combine observations, sampling, measurements and theoretical models and analysis.

A previous project within Dam Safety Interest Group (DSIG) resulted in a seven-step-method to analyze cracked concrete dams and the current work is taking this forward to adapt the methodology to Swedish conditions.

Energiforsk is the Swedish Energy Research Centre – an industrially owned body dedicated to meeting the common energy challenges faced by industries, authorities and society. Our vision is to be hub of Swedish energy research and our mission is to make the world of energy smarter!